A thesis submitted to

Department of Chemical and Biological Engineering

for the degree of

Doctor of Philosophy

Evaluation and characterisation of phenotypic

heterogeneity in Chinese Hamster Ovary cell

populations during long-term culture

Alejandro Fernández Martell

June 2015

Author's Declaration

I, Alejandro Fernandez Martell declare that I am the sole author of this thesis and that the research presented within is the result of my own efforts and achievements. I confirm that this work has not been submitted for any other degrees.

Abstract

The selection of CHO cell lines for manufacturing therapeutic proteins involves multiple screening steps of transfected cells that would meet industrial standards such as productivity and stability. This study is a starting point for the idea that cell line development could be improved if a reversed approach involving the selection of un-transfected cell with desirable growth characteristics is first implemented, followed by an accelerated genetic drift in a long-term sub-cultivation. To address this, the inherent cellular heterogeneity within an un-transfected parental CHO-S population was exploited by isolating 22 clonal CHO-S populations through two rounds of the limiting dilution cloning, followed by an accelerated genetic drift and directed evolution resulted from a continuous sub-cultivation (up to 220 generations), along with the cryopreservation of subpopulations approximately every 40 generations. The initial growth compassion exhibited positive correlations between the specific growth rate and generation number and between the peak of viable cell density and generation number. The fed-batch studies also showed that the integral of viable cell density (IVCD) performance can be enhanced along the long-term cultivation, but this was not necessarily improved with increasing generation number because clones were evolved to enhance the rate of biomass production and not to withstand severe environmental conditions typically found at mid- and late- stages of fed-batch cultivation.

Metabolic analyses showed that glucose and glutamine were rapidly metabolised to provide energy and intermediates for cell division, also showing that glutamine availability defines the duration of the exponential growth phase and that its depletion promotes a switch to a more efficient glucose usage tightly coupled to oxidative phosphorylation (OXPHOS) this in turn reduced glucose uptake and lactate production, and even switched to net lactate consumption. The lactate: glucose ratio in proliferating populations showed that glutamine was also metabolised to provide enough levels of NADPH for fatty acid biosynthesis and redox homeostasis, thus producing lactate given the down-regulation of pyruvic acid flux towards the tricarboxylic acid (TCA) cycle. The mitochondrial and glycolytic analysis along the long-term cultivation showed that clones reduced both metabolisms, whereas the analysis at exponential growth phase showed that populations with high proliferation rates present an elevated OXPHOS activity - supported by glutamine metabolism- and strong aerobic glycolysis -supported by glucose uptake-. Contrary, populations at stationary growth phase with high global IVCD performance presented a low respiratory metabolism, but efficiently couple to ATP production, to reduce a potential mitochondrial damage resulted from increments in the proton leakage across the inner mitochondrial membrane.

In conclusion, the work presented in this thesis exhibited the dynamic nature of CHO cell and revealed metabolic characteristics which enabled a cell to reach growth improvements. In the same context, the reversed strategy presented here generated a panel of 132 CHO cell variants with enhanced functional characteristic that meet industrial standards and therefore open a huge potential to increase our understanding of the nature of relevant cell lines with desirable metabolic and growth phenotypes.

Acknowledgements

To Sara, Gus and my parents

Table of Contents

List of Figures

List of Tables

Abbreviations

(•OH) Hydroxyl free radical

(acetyl-CoA) Acetyl coenzyme A

(AIF) Apoptosis-inducing factor

(ATP) Adenosine triphosphate

(BER) Base excision repair

(BER) Nucleotide excision repair

(BHK) Baby hamster kidney

(CHO) Chinese hamster ovary

(COS) African green monkey kidney

(DHFR) Dihydrofolate reductase

(DSBs) Double-strand breaks

(ETC) Electron transport chain

(FADH$_2$) Reduced flavin adenine dinucleotide

(GDH) Glutamate dehydrogenase

(GLS) Glutaminase

(GLUTs) Glucose transporters

(GMT) Mitochondrial glutamine transporter

(GPX) Glutathione peroxidase

(GR) Glutathione reductase

(GS) Glutamine synthetase

(GSH) Reduce glutathione

(GSSG) Oxidised glutathione

(GTP) Guanosine triphosphate

(H$_2$O$_2$) Hydrogen peroxide

(HEK-293) Human embryo kidney

(HIF-1) Hypoxia-inducible factor 1

(HR) Homologous recombination

(HT1080) Human fibrosarcoma

(IMM) Inner mitochondrial membrane

(IMS) Intermembrane space

(INN) International non-proprietary name

(IR) Ionising radiation

(IVCD) Integral of viable cell density

(LDH) Lactate dehydrogenase

(MMP) Mitochondrial membrane potential

(MMR) Mismatch repair

(MSX) L-methionine sulphoximine

(mTORC1) TOR kinase

(NADH) Reduced nicotinamide adenine dinucleotide

(NADPH) Reduced nicotinamide adenine dinucleotide phosphate

(Namalwa) Human lymphoma

(NHRJ) Non-homologous end joining

(NS0, SP2/0) Mouse myeloma cells

(O_2^-) Superoxide anion radical

(OMM) Mitochondrial membrane

(OXPHOS) Oxidative phosphorylation

(PDC) Pyruvate dehydrogenase complex

(PDH) Pyruvate dehydrogenase

(PDKs) Pyruvate dehydrogenase kinase

(PER-C6) Human retinal derived

(PFK) Phosphor-fructo-kinase

(PI3K) Phosphoinositide 3-kinase

(PPP) Pentose phosphate pathway

(PTMs) Post-translational modifications

(PYC) Pyruvate carboxylase gene

(ROS) Reactive oxygen species

(siRNA) Small interfering RNA

(Slc2a5) Fructose transporter gene

(SOD) Superoxide dismutase

(SSTs) Single-strand breaks

(TCA) Tricarboxylic acid

(TRXR) Thioredoxin reductase

(αKGDH) α-ketoglutarate dehydrogenase

"this page intentionally left blank"

Chapter 1

LITERATURE REVIEW

Chapter 1

Literature review

This chapter presents an overview of the biotechnological industry and the production of recombinant proteins using mammalian cell systems, introducing the importance of recombinant proteins for the pharmaceutical industry and the manufacturing processes using Chinese hamster ovary (CHO) cells, including cell expression system characteristics and their metabolic requirements. Finally, I describe the strategies implemented to enhance the overall CHO cell performance.

1.1 Biologics and the biopharmaceutical industry

Biologics or biopharmaceuticals are molecules with therapeutic importance produced by or obtained from biological sources, usually these molecules are produced using recombinant technologies in genetically modified organisms (Aggarwal 2008; Demain and Vaishnav 2009; Durocher and Butler 2009; Ferrer-Miralles et al. 2009; Walsh 2010b). Monoclonal antibodies, recombinant proteins, fusion proteins, cytokines, anti-coagulants, blood factors, growth factors, hormones, interferons, nucleic acids, recombinant vaccines and therapeutic enzymes are among the biologics that have been used to treat a large range of diseases. Biologics have seen a remarkable increase and acceptance in the pharmaceutical market because they have proven efficiency and safety for the treatment of cancer, cardiovascular diseases, respiratory disorders, transplantation, allergic diseases and autoimmune diseases. The notable advances in the "omics" disciplines (i.e., genomics, proteomics, metabolomics and transcriptomics) and the establishment of robust mammalian cell culture techniques have allowed the development of rapid and more precise diagnostics (Carlson 2011; Matasci et al. 2008) and opened a tremendous and attractive potential for developing a broad range of new therapeutic molecules with industrial relevance (Figure 1-1) (Kantardjieff et al. 2010).

Nowadays, a large range of novel biological molecules have been developed, prescribed and accepted in the therapeutic market (Table 1-1). Consequently, the pharmaceutical industry has witnessed significant changes in the drug development pipeline in effort to produce biologic products instead of chemical compounds for therapeutic purposes, shifting the industrial core from its original chemical synthesis to these novel biotechnological processes.

Since the last decade, recombinant proteins have dominated the therapeutic market with lucrative biological molecules exceeding $1 billion annual sales (Aggarwal 2008; Redwan 2007; Walsh 2010a) (Table 1-1). The enormous acceptance of biologics for therapeutic applications has notably increased their demand in the global market with more than 246 biological molecules approved in the in the United States and European Union, and with more than $140 billion in the annual revenue in 2014 (Walsh 2014). In 2010, was predicted that global market for biological molecules will increase between 7% and 18% annually over the subsequent 10 years (Hiller 2009; Walsh 2010a) and it was estimated that over 500 new biological drugs were in preclinical and clinical development (Durocher and Butler 2009; Walsh 2004). Several researches have also anticipated that a large number of new biological drugs will be developed as a result of the application of "omics" technologies combined with the vast information obtained from the ongoing sequencing of human genomes (McKown 2002; Walsh 2010b) and the CHO-K1 genome sequencing (Lewis et al. 2013; Xu et al. 2011). For example, the human genome has more than 25000 protein-coding genes, but these gene products undergo complex and variable post-translational modifications (PTMs), thereby resulting in an enormous amount of potentially functional proteins (Leader et al. 2008; Pray 2008). Consequently, the biotechnology industry's future looks promising due to the extraordinary opportunities to develop novel molecules with great biopharmaceutical potential (Aggarwal 2008; Goodman 2009).
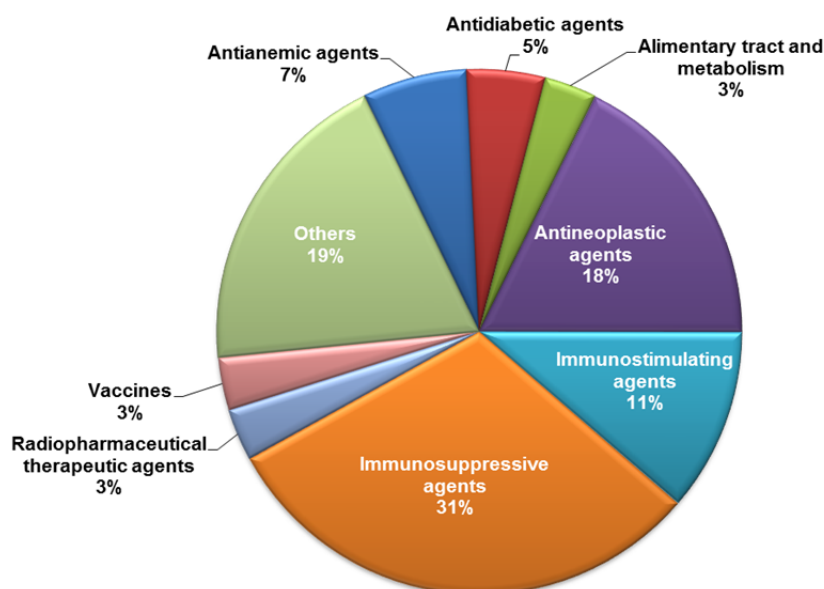
Figure 1-1 Biologic therapeutics market: proportion of biologics according to their approved therapeutic application in 2009. Data modified from Ferrer-Miralles et al. (2009).

Table 1-1 Best-selling biopharmaceutical products in 2014.

Product trade name (INN)	Expression system	Biological type	Sales value ($ billions)	Company
Humira (adalimumab)	CHO	Monoclonal antibody	10.7	AbbVie
Rituxan/MabThera (rituximab)	CHO	Monoclonal antibody	9.0	Biogen-Idec, Roche
Remicade (infliximab)	Murine myeloma	Monoclonal antibody	8.9	Janssen Biologics, Merck, Mitsubishi Pharma
Enbrel (etanercept)	CHO	Fusion protein	8.7	Amgen, Pfizer Takeda Pharmaceuticals
Lantus (insulin glargine)	*E. coli*	Protein	7.8	Sanofi
Avastin (bevacizumab)	CHO	Monoclonal antibody	7.1	Roche
Herceptin (trastuzumab)	CHO	Monoclonal antibody	6.9	Roche
Neulasta (pegfilgrastim)	*E. coli*	Protein	4.4	Amgen
Erbitux (cetuximab)	SP2/0	Monoclonal antibody	2.9	Merck, Eli Lilly Bristol-Myers Squibb
Epogen/Procrit/ Eprex/ESPO (epoetin alfa)	CHO	Protein	3.3	Amgen, Ortho, Janssen, Kyowa Hakko Kirin
Aranesp/Nespo (darbepoetin alfa)	CHO	Protein	1.9	Amgen, Kyowa Hakko Kirin
Neupogen (filgrastim)	*E. coli*	Protein	1.4	Amgen

Data adapted from "Biosimilars: 11 Drugs to Watch" (GEN 2014).

INN is international non-proprietary name.

1.2 Biological molecule expression systems: considerations and challenges

Since 1982 when the first biological recombinant molecule was approved for therapeutic proposes ("Humilin", rh-Insulin, Genentech-Eli Lilly), the biopharmaceutical industry has successfully developed and introduced a large number of biological molecules into the therapeutic market. Therefore is not surprising that the pharmaceutical industry is investing significant efforts to develop efficient expression systems, prokaryotic and eukaryotic, as well as cell-free expression systems for biologic manufacturing (Figure 1-2 and Table 1-2).
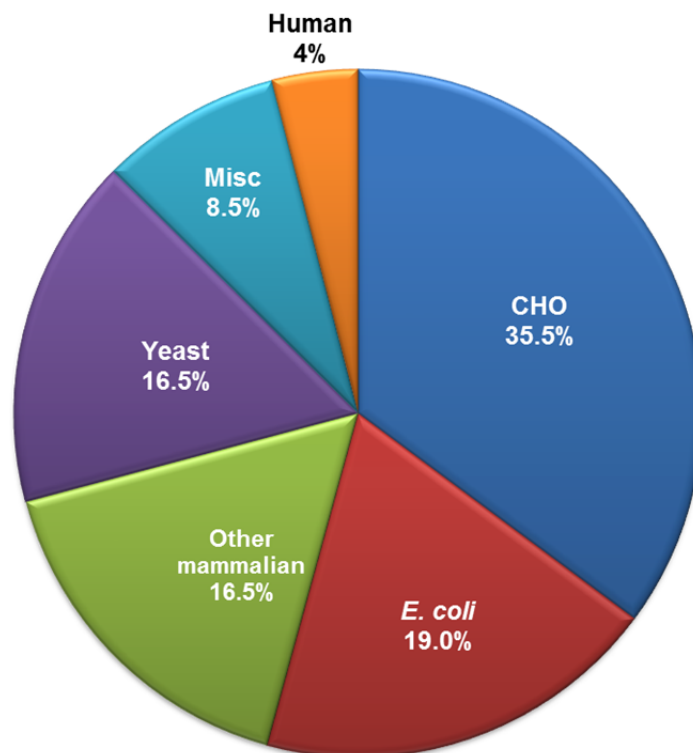
Figure 1-2. Proportion of biologics according to the expression host system used for production. Data modified from Walsh et al. (2014).

Escherichia coli and other prokaryotes are used as expression host systems for recombinant proteins, but their implementation for humanised protein manufacturing is still restricted mainly because their prokaryotic nature limits the processing of complex PTMs (i.e., glycosylation, acylation and phosphorylation) essential for humanised protein functions (Walsh and Jefferis 2006). Contrarily, eukaryotic organisms (i.e., yeast, plants, mammals and insects) are capable of performing complex protein

synthesis with correct folding and complete PTMs, particularly glycosylation (Barnes et al. 2000; Barnes et al. 2001; Walsh and Jefferis 2006; Wurm 2004). Consequently, eukaryotic cells have been chosen as the first option for manufacturing complex and functional human recombinant proteins (Figure 1-2).

PTMs are essential in many proteins because these modifications are associated with gene expression, gene regulation and transduction signalling, as well as protein localisation, stability, pharmacokinetic and activity (Walsh and Jefferis 2006; Webster and Thomas 2012). Among PTMs, glycosylation is the most common in human proteins with an estimated 50% of all human proteins glycosylated. Glycosylation is also considered the most complex PTMS due to their considerable heterogeneity (i.e., glycoforms) and large number of enzymatic reactions involved in the sequential modifications of the nascent glycoprotein through the endoplasmic reticulum and Golgi apparatus (Lauc et al. 2010; Walsh and Jefferis 2006; Wong 2005). These glycolytic modifications are associated with important metabolic processes (i.e., cell signalling, immune function, protein folding, localisation, degradation, secretion and transcription signalling) that maintain normal physiological processes. For example, incorrect glycolytic profiles are associated with cancer, diabetes and immunological and infectious disorders because an altered protein structure leads to changes in activity, cytotoxicity and immunogenicity that compromise their safety and function. Consequently, the regulation of specific-glycolytic profiles is vital for the organisms and for the therapeutic industry (Lauc et al. 2010; Walsh and Jefferis 2006) particularly because over 40% of the approved therapeutic proteins are glycosylated and many more proteins in development would be glycosylated (Walsh 2010a).

Although many PTMs are evolutionarily conserved and most of the eukaryotic cells are able to perform complex PTMs, the number and complexity of modifications differs from organism to organism (Walsh 2010a; Webster and Thomas 2012). These PTMs variations relate to the organism complexity, organisation and corresponding kingdom. As a result, taxonomy-associated PTMs may trigger undesirable effects in foreign organisms and would lead to heterogonous glycoproteins activities even if they share the same amino acid sequence. Therefore, although the same protein-coding gene can be expressed in different eukaryotic hosts (i.e., mammals, yeast, insects or plants) their protein product will be structurally and functionally different (Gomord et al. 2005; Webster and Thomas 2012). Taking this into account, the selection of an appropriate expression host systems is a critical decision that must be considered when expressing recombinant human proteins.

Table 1-2 Prokaryotic and eukaryotic expression host systems used for biological therapeutics production

Expression host systems

Bacteria: *Escherichia coli, Bacillus subtilis*

+ Easy cultivation	+ Human-like glycosylation possible by genetic engineering
+ Easy genetic manipulation	- Endotoxins (in *E.coli*)
+ High proliferation rates	- Lack of PTMs
+ Extensive characterisation	- Protein aggregation
+ High productivity	- Different codon usage (premature protein termination)
+ Low nutrient requirements	- Inclusion bodies for proteins > 60kDa

Chinese hamster: CHO, BHK

+ Human-like glycosylation	+ Efficient protein expression and secretion
+ Easy cultivation and adaptability	+ Proliferation in suspension cultures
+ Easy genetic manipulation	+ Long regulatory and safety approval records
+ Extensive characterisation	- Low productivities
+ Non-fucosylated proteins	- Complex media formulation
+ Growth in serum-free culture media	- Potential to propagate infectious agents

Human cells: HEK293, HT-1080, PerC6, HKB11, Namalwa

+ Human glycosylation	- High cost
+ Low immunogenic potential	- Complex media formulation
	- Potential to propagate infectious agents

Hybridomas

+ Human-like glycosylation possible by genetic engineering	- Immunogenic glycans
	- Potential to propagate infectious agents

Insect cells: *Spodoptera frugiperda, Trichoplusia ni*, MIMIC, SfSWT-3

+ Low cost	+ Human-like glycosylation possible by genetic engineering
+ Rapid production	- Low therapeutic protein bioactivity *in vivo*
-Short half-life of recombinant proteins	- Potentially immunogenic glycans

Murine myelomas: NS0, SP2/0

- Immunogenic glycans	- Potential to propagate infectious agents

Plants: *Lemna minor*, carrot cells, tobacco plants

+ Inexpensive cultivation	- Large outdoor field scale production
+ Easy cultivation	- Low productivities
+ Lack of human pathogens	- Non-human-type glycosylation
+ Possible human-like glycosylation by genetic engineering strategies	- Potentially immunogenic glycans (a1,3-fucose)
	- Regulatory concerns for GMO cultivation

Transgenic animals: rabbit, goat

- Immunogenic glycans	- Potential to propagate infectious agents

Yeasts: *Pichia pastoris, Hansenula polymorpha, Saccharomyces cerevisiae*

+ Easy cultivation	+ Adequate for non-glycosylated proteins
+ Easy genetic manipulation	+ Growth in chemically defined media
+ High productivity	+ Human-like glycosylation possible by genetic engineering
+ Inexpensive cultivation	- Potentially immunogenic glycans (N-linked and O-linked)
+ Robust cell systems	

Cell-free expression systems

+ Expression of toxic proteins	- Low yield
+ Protein folding	- Incomplete and few PTMs
+ Inexpensive and rapid production	- Protein aggregation

Expression systems along with recognised advantages (+) and disadvantages (-). Data modified from Demain and Vaishnav (2009), Durocher and Butler (2009), Ferrer-Miralles et al.(2009) and Endo and Sawasaki (2006).

The production of recombinant proteins is commonly performed on empirical basis (Hacker et al. 2009; Matasci et al. 2011) with typical challenges that continue to be weaknesses for the biopharmaceutical industry since its origins (i.e., low recombinant protein production rates, low cell growth rates, high environment sensibility, medium complexity and genetic and phenotypic cell line heterogeneity) (Barnes et al. 2000). Currently, the biological processes used for manufacturing recombinant proteins are much more efficient and regulated than the first biological productions performed in 1980's. However, the industry seeks to develop a universal manufacturing platform that overcomes problems and would be compatible with any kind of recombinant protein (Walsh 2010a).

Today we are far from reaching this desirable system due to the structural complexity of recombinant proteins and the metabolic, phenotypic and genetic diversity of the expression systems. These inherent features restrain the use of a unique expression system and encourage the use and development of specific host systems to meet the structural requirements that the novel recombinant proteins demand. Therefore, cell line engineering, next-generation sequencing, glycoengineering, microarrays, real time PCR, transfection technologies and vector design are some of the "omics" technologies that together with an optimised cell culture media (i.e., controlled nutrient feeding and synthetic media formulation) and controlled culture environment (i.e., pH, temperature, osmolarity and oxygen supply) have been extensively implemented to obtain larger protein expression quantities (1 to 2 g L^{-1} yield commonly achieved) and high cellular densities (20 x10^6 cells mL^{-1} commonly reached) at reduced production costs in order to meet the increasing biological molecule demand (Jayapal et al. 2007).

1.3 Mammalian cell lines and CHO cells

Mammalian cells are the most widely used expression system for the production of biological molecules, among these the African green monkey kidney (COS), baby hamster kidney (BHK), Chinese hamster ovary (CHO), human embryo kidney (HEK-293), human retinal derived (PER-C6), human fibrosarcoma (HT1080), human lymphoma (Namalwa), mouse myeloma (NS0, SP2/0) and hybridomas are commonly used for recombinant protein production. However, about 60-70% of the licenced therapeutics and the majority of proteins under development are expressed in CHO cells (Durocher and Butler 2009; Jayapal et al. 2007; Li et al. 2010; Matasci et al. 2008; Walsh 2014), essentially because CHO cells offer advantages such as manufacturing

more complex biological molecules such as bi-specific antibodies, humanised monoclonal antibodies and Fc-fusion proteins with human-type glycosylation, phosphorylation and carboxylation PTMs and also exhibiting a proper secretory signal pathway for efficient gene-product secretion (Barnes et al. 2000; Meleady 2007; Page 1988; Wurm 2013). Additionally, their extensive characterisation, easy cultivation, adaptability to synthetic environments, susceptibility to foreign DNA integration and their long regulatory and safety approval records have positioned CHO cell lines as the leading mammalian host cell line for safe biological therapeutic production (Durocher and Butler 2009; Jayapal et al. 2007).

As mentioned previously, we are far away from developing a universal host platform or an ideal CHO cell line for efficient recombinant protein production. Therefore, the industry is still using multiple mammalian cell lines, each with advantages and limitations, to overcome expression and process drawbacks. Fortunately, there are many strategies can be implemented to generate more applicable knowledge with respect to cellular metabolism for understanding how cell growth and gene expression are synchronized and regulated within the host systems, and for understanding the environment effects (i.e., nutrient availability, culture operation conditions, dissolved oxygen, pH, osmolarity and temperature) over the cell performance, which are necessary for developing fully controlled, predictable and robust biotechnological processes.

1.4 Phenotypic heterogeneity in CHO cells

The original CHO cell line was developed in 1957 as an immortal cell line from a Chinese hamster (*Cricetulus griseus*) primary cell culture (Tjio and Puck 1958). Since then, numerous functional CHO cell lines have been generated by exploiting the intrinsic nature of CHO cells as immortalised cells and by applying a large number of genetic engineering strategies (Hacker et al. 2009). Through time, all these strategies have considerably altered the CHO genome, leading to large differences in its karyotype in comparison with the original Chinese hamster karyotype (Deaven and Petersen 1973; Derouazi et al. 2006). These cumulative genomic aberrations have allowed the development of thousands of CHO cell lines with notably different metabolic and physiologic characteristics such as CHO-K1, CHO-K1SV (GS-KO), CHO-DG44 (DHFR$^{-/-}$), CHO-S (suspension cell lines), DUKX-B11 (DHFR$^-$) (Wurm 2013).

The phenotypic plasticity in CHO cells is attributed to their inherent and useful genetic instability (Barnes et al. 2006; Derouazi et al. 2006; O'Callaghan et al. 2010), which constantly causes rearrangements in the genome to evolve functional phenotypes to survive, proliferate and adapt in the constantly changing synthetic environments (Sinacore et al. 2000). These genomic rearrangements also provide an important source of cell variability that can be harnessed to isolate more efficient and robust derived CHO cell lines, for example cell lines able to assemble complex recombinant proteins (Dinnis et al. 2006; O'Callaghan et al. 2010), extend the cellular viability over fed-batch regimes (Prentice et al. 2007), reach high cellular densities (O'Callaghan et al. 2010; Prentice et al. 2007) and grow in synthetic and hostile environments (Schumpp and Schlaeger 1992; Sinacore et al. 2000; Sunley et al. 2008).

Understanding the biological mechanisms underlying the phenotypic diversification is essential to identify the changes in genetic and phenotypic characteristics that drive the acquisition of varied functional features. Consequently, multiples approaches such as karyotyping (Deaven and Petersen 1973; Derouazi et al. 2006), genome sequence (Lewis et al. 2013; Xu et al. 2011) and chromosomal structure analysis (Derouazi et al. 2006; Yoshikawa et al. 2000) have been studied to elucidate the phenotypic heterogeneity in CHO cells.

It is clear that the phenotypic heterogeneity in CHO cells provides innumerable opportunities to select improved CHO cell lines with industrial capabilities, but also generates an unpredictable and uncontrollable cellular behaviour that arises from the loss of gene function (Bergoglio et al. 2002), chromosomal aberrations (Derouazi et al. 2006), metabolic and enzymatic dysfunction (Jackson and Loeb 2001) and epigenetic alterations (Sandoval and Esteller 2012). These undesirable effects are commonly observed during the manufacturing of recombinant proteins, resulting in the loss of recombinant genes (Barnes et al. 2001; Beckmann et al. 2012; Hammill et al. 2000; Jun et al. 2006; Kim et al. 1998), the decline in transgene mRNA levels (Chusainow et al. 2009; O'Callaghan et al. 2010), the emergence of non-productive cells during culture (Bae et al. 1995) and by-product accumulation (Altamirano et al. 2004; Chen et al. 2001; Gorfien et al. 2003).

Studies have identified important variations between and within populations' growth parameters, demonstrating that CHO cells exhibit high genetic instability rates which result in a constant appearance of subpopulations with varied phenotypic traits (Barnes et al. 2006; Davies et al. 2012; Kim et al. 1998). In the same context, clonal variation between and within populations measured in terms of metabolic profiles

(Bailey et al. 2012; Beckmann et al. 2012; van Berkel et al. 2009) and cell performance (Heinrich et al. 2011; Prentice et al. 2007; Yoon et al. 2004) have also been observed as the result of changes in culture strategies such as feeding regimen and cultivation mode (i.e., batch, fed-batch and perfusion). In general, these studies have emphasised the unpredictable and random genetic heterogeneity within CHO populations that causes the appearance of multiple phenotypes within populations, even in short time periods after being derived from a single cell (e.g., 20-25 cell generations) (Barnes et al. 2006; Kim et al. 1998; Kromenaker and Srienc 1994; Pilbrough et al. 2009).

Several studies have used measurements of growth rate, productivity, transgene copy number and transgene stability in presence and absence of selective pressure to evaluate the cellular genetic heterogeneity (Bailey et al. 2012; Barnes et al. 2006; Davies et al. 2012; Pilbrough et al. 2009; Yoshikawa et al. 2000). For example, Yoshikawa et al. (2000) revealed a correlation between the chromosomal localisation of the transgene and the cell line stability in terms of recombinant gene expression, showing that in stable cell lines the recombinant gene is inserted near the telomeric region whilst in unstable cell lines the gene is inserted in non-telomeric regions. These results also showed that the constant and random genomic heterogeneity leads to the appearance of non-, low-, mid- and high-producing cells throughout the manufacturing processes. Similarly, Davies et al. (2012) and Pilbrough (2009) demonstrated that CHO cells extensively vary in terms of productivity, proliferation rate, cell performance and cell size with increasing generation number. Additionally, Davies et al. (2012) found a significant functional variability within the CHOK1SV population in the ability of a clone to create new cell biomass from supplied precursors (up 1.5-fold)

In general, CHO cells are well known for their inevitable genetic heterogeneity (O'Callaghan and James 2008; Pilbrough et al. 2009). Nonetheless, it is important to recognise, especially in the context of functional characteristics, that the genetic heterogeneity provides a tremendous source of cell-to-cell variability that must be harnessed to increase the range of functional phenotypes able to endure industrial processes such as resisting stress conditions to survive in synthetic environments and reaching high cellular densities and productivities (O'Callaghan and James 2008). Therefore, combining the genetic heterogeneity with genetic and non-genetic strategies (i.e., cell selection, cell adaptation and cell evolution, genetic and metabolic engineering) may increase significantly the chances for generating a vast number of sub-clones with desirable phenotypes, but to achieve this goal a large range of knowledge that enables us to surpass obstacles and bottlenecks in cell line development is still necessary.

Several cancer models can increase our understanding of the causes of heterogeneity and help us to identify more effective approaches to exploit CHO cell-to-cell variability. For example, the clonal evolution theory (Figure 1-3) holds that genetic variability within a population confers selective growth advantages, allowing individual clones to out-compete others by developing a superior functional phenotype and thus allowing its expansion (Greaves and Maley 2012; Nowell 1976). In the same context, the cancer stem cell model must be evaluated to identify whether the heterogeneity arises from genetic or epigenetic factors (Shackleton et al. 2009). Taking into account these models, I suggest that the cellular heterogeneity observed in CHO cells constantly arises from genetic mechanism such as mutations (i.e., beneficial or deleterious) and from extrinsic and intrinsic factors that co-exist in culture (i.e., age and stage of culture, cell growth stage, metabolic fluxes, osmolality, temperature) causing environmental fluctuations, and the latter triggering epigenetic modification that contribute to the acquisition of phenotypic changes (Merlo et al. 2006; Pilbrough et al. 2009). Therefore, in this research is suggested that minimising culture fluctuations by growing the cells under environment with a low environmental stress (e.g., not nutrient limitation, low toxic by-product accumulation and low-osmolarity) the (i) clonal variation within a population would be reduced and (ii) non-limiting environments would promote the selection of cell lines with desirable growth and protein manufacturing characteristics.
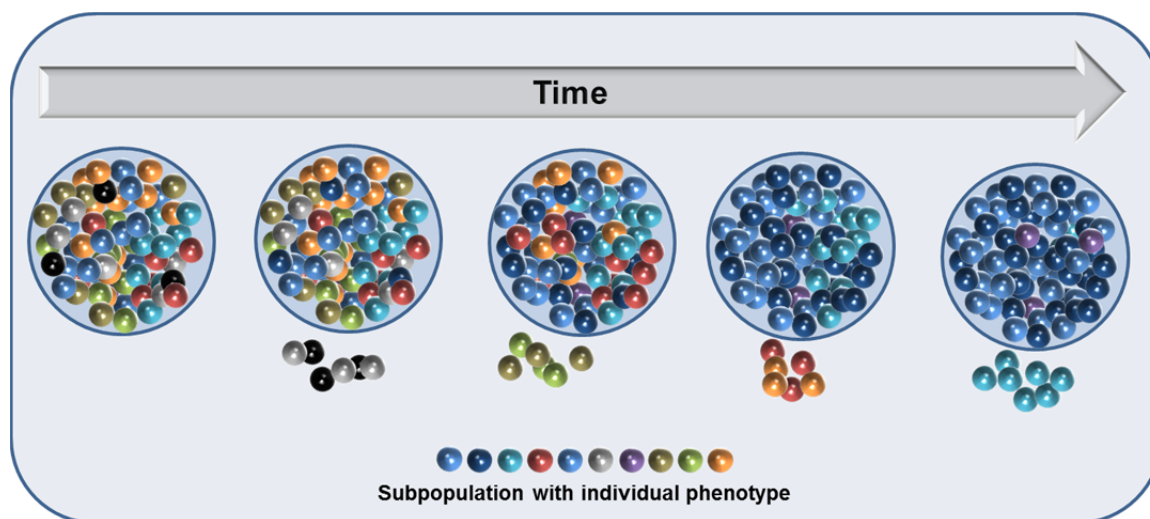
Figure 1-3 Simplified clonal evolution model. The different coloured circles represent cell subpopulations with phenotypic differences accumulated through successive mutations. At early stages of cell culture several subpopulations coexist, but throughout extended sub-cultivation some subpopulations become extinct, some coexist and others become dominant. The expanding subpopulations represent superior phenotypes.

1.5 Nutritional requirements in CHO cells

CHO cells need a complex medium that contains glucose, glutamine, vitamins, amino acids, growth factors, hormones, trace metals and salts for their optimal cell performance. Consequently, multiple attempts to increase productivity, cell density and culture longevity have been achieved through media optimisation and the development of synthetic media and supplements which support elevated metabolic requirements, enhance the biological processes and satisfy with the increasing nutritional demands of bioprocess' scale-up (van der Valk et al. 2010). Nowadays, there are a large variety of media formulations for CHO cells, e.g., CD-CHO™, CD OptiCHO™, CD FortiCHO™, Ex-Cell™ CD CHO, ProCHO™, PowerCHO™, BalanCD™ CHO Growth A, Cellvento™ CHO-100, HyClone™ SFM4CHO™ and HyClone CDM4CHO™, that have improved the overall cellular performance of CHO cell lines (Reinhart et al. 2013). However, to attain further improvements in cell culture, these media formulations are usually accompanied with additional nutrient supplementations (e.g., ActiCHO™ Feed A and B, CHO CD EfficientFeed™ A and B, CHO Feed Bioreactor, BalanCD™ CHO, FunctionMAX™ and Zap-CHO™) throughout the culture to prevent depletion of important nutritional compounds, especially in the mid- and late-stages of the fed-batch cultivation (Prentice et al. 2007; Xing et al. 2009).

An unbalanced feeding strategy may generate undesirable side effects such as increased osmolarity, by-product generation and metabolic deregulations. Therefore, to attain improved cell performance the feeding strategies must be optimised with respect to cell specific productivity and/or viable cell density (Xing et al. 2009). Although significant progresses for developing more efficient feeding strategies have been developed, these approaches are still performed on empirical basis, which limits the understanding of CHO metabolism and misrepresents their nutritional requirements therefore causing suboptimal performances and batch-to-batch inconsistencies (Altamirano et al. 2004; Gorfien et al. 2003).

During recombinant protein production, the cell viability, product quality and protein titter are usually affected by the accumulation of cellular by-products such as lactate and ammonia. To reduce their toxic effects, several implemented strategies are dedicated to maintain a low by-product accumulation by growing cells in controlled environments, especially in low glucose and glutamine concentrations (Altamirano et al. 2000; Altamirano et al. 2004; Chen et al. 2001; Cruz et al. 1999; Kurano et al. 1990; Lao and Toth 1997). These strategies are usually performed in fed-batch and perfusion systems, which permit better control of essential nutrient concentrations and reductions in by-product accumulation resulting in increments in cell viability, growth performance

and product titter (Altamirano et al. 2004; Chen et al. 2001; Gorfien et al. 2003). From these culture modes, the fed-batch system has been extensively used in biological processes due to its simplicity and flexibility. However, it is important to note that these culture strategies only minimise by-product side effects by maintaining low concentrations throughout the culture, without eliminating their generation.

Fed-batch operations consist in adding, either continuously or semi-continuously, controlled concentrations of essential nutrients such as glucose and glutamine to avoid nutrient depletion, reduce inhibitory growth effects of by-products, maintain an active metabolism and meet the nutritional cellular demands for survival, proliferation and biomolecule production (Altamirano et al. 2004; Chen et al. 2001; Gorfien et al. 2003; Mulukutla et al. 2012) (Figure 1-4). This supplementation is usually performed on basis of growth rate, glucose or glutamate consumption, by-product accumulation and productivity data, providing essential metabolites which makes possible to control growth parameters including specific growth rate and culture growth phases, as well as to increase the longevity of the culture and reach high cellular densities, viabilities and productivities (Chu and Robinson 2001).
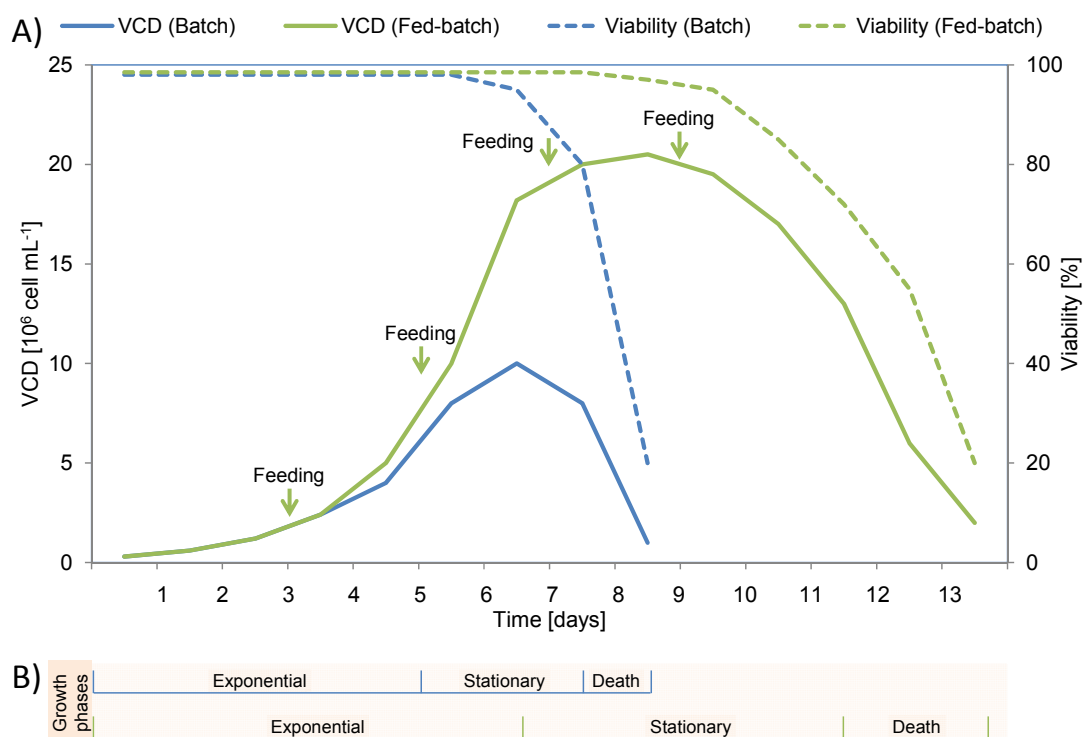
Figure 1-4 Typical growth curves illustrating fed-batch improvements between batch and fed-batch culture. The blue and green lines represent the growth parameters for batch and fed-batch cultivation through culture, respectively. The solid lines represent VCD, dotted lines cellular the cellular viability and the green arrows represent the feeding addition. (B) Improvements in the cell growth phases between batch and fed-batch culture.

Given the metabolic differences among CHO cell lines and the genetic constructs, a fed-batch optimisation must be carried out to obtain optimal growth and productivity performance. An inefficient nutrient feeding strategy generates an unbalance in the metabolism which may lead to apoptosis or unpredictable cellular performance which jeopardises the quality, stability and structure of recombinant glycoproteins. In addition, an inefficient feeding strategy results in suboptimal growth characteristics (e.g., μ. VCD peak and viability) affecting the Integral of Viable Cell Density (IVCD), a routinely indicator of cell line performance used to compare the cell performance among different cell lines, and therefore impacting the volumetric productivity (Kumar et al. 2009). For that reason, it is not surprising that low productivities and detrimental growth performance along fed-batch cultures are usually associated to an ineffective feeding strategy (Fan et al. 2014; Ozturk et al. 1992; Yang and Butler 2000).

Most improvements in fed-batch cultures have been obtained by monitoring glucose and glutamine consumption and lactate production, mainly because these molecules are the principal carbon and nitrogen sources and by-product metabolite along a culture, respectively (Altamirano et al. 2000; Altamirano et al. 2004; Gorfien et al. 2003; Legmann et al. 2011). Other fed-batch strategies replacing the carbon source with slowly-metabolised molecules (e.g., fructose, galactose and glutamate) have been implemented. For example, Altamirano et al. (2000) showed that the substitution of glucose with galactose and glutamine with glutamate improved the culture longevity, reduced lactate and ammonia formation, and reduced the cell culture osmolarity. This approach resulted in IVCD improvements between 116 and 150% and suggested that the low by-product accumulation and osmolarity were the result of a slow metabolism and transport of glutamate and galactose, respectively. This glucose substitution was also associated with the negative effect in proliferation rates as galactose is metabolised slowly. Finally, these negative effects were compensated with positive effects in cell viability, productivity and culture longevity (Altamirano et al. 2000; Altamirano et al. 2004). Other approaches showed that the glycolytic metabolism and by-product formation can also be controlled by alternating carbon sources such as galactose and fructose during the productive phase (Legmann et al. 2011). Through combination of these findings, volumetric productivities of up to 10 g L^{-1}, cellular densities of 20 x10^6 cells mL^{-1} and longer fed-batch culture between 10 and 12 days have been reported (Jayapal et al. 2007; Kim et al. 2013), therefore these accumulative data strongly suggests that even greater improvements in cell performance can still be achieved by improving the feeding strategies and media composition.

1.6 CHO cells metabolism and cellular engineering

Cellular metabolism comprehends a set of biochemical reactions within the cells required for the maintenance of life. These biochemical reactions are classified as catabolic (molecule breakdown) and anabolic (molecule construction) which together produce all the energy and precursors needed for the cells to grow, proliferate, respond to stimuli and maintain their structural integrity (Nelson and Cox 2013).These biochemical reactions involve highly regulated metabolic pathways such as glycolysis, glutaminolysis, tricarboxylic acid (TCA) cycle, electron transport chain (ETC), oxidative phosphorylation (OXPHOS), gluconeogenesis, fatty acid β-oxidation, urea cycle and pentose phosphate pathway (PPP), which respond according to the energetic demands and the physiological status of cells i.e., cell growth, cell division and senescence.

Put simply, cellular metabolism is the process through which living organisms obtain energy in the form of adenosine triphosphate (ATP) through glucose oxidation. However, cells are open systems that continually interact with their environment and therefore changing their metabolism in response to internal and external stimulus and making the cellular metabolism a complex phenomenon (Kim et al. 2006; Papandreou et al. 2006). A clear example is observed during recombinant protein manufacturing processes, where cells are constantly down- and up-regulating metabolic pathways in function of nutrient availability (e.g., carbohydrates, amino acids and lipids), environmental stimuli (e.g., temperature, pH, dissolved oxygen, osmolarity, inhibitors, pro- and anti-apoptotic proteins) and growth stage (e.g., exponential, stationary and death growth phases), or even switching between metabolite production and consumption (e.g., lactate metabolism). These coordinated changes throughout cultivation involve mechanisms that regulate gene expression that may lead to phenotypic variations in terms of cell size, cell protein content and metabolite transporter expression (Nelson and Cox 2013).

The phenotypic and metabolic variation described above needs to be avoided in the biotechnology industry to develop robust production methods. The current production processes have minimised cellular variation by optimising and standardising the culture stages, which should promote a quick proliferation rate at the early stage of the cultivation in order to attain a satisfying viable cell density for recombinant protein production, then followed by a production phase characterised by slow proliferation rates over extended periods of time to maintain and elevated cellular viability and biomass accumulation which together increase the product yield (Altamirano et al. 2000). The conjunction of both metabolic states is not only essential to meet the energetic demands and minimise cellular variation, but also crucial to minimise the by-

product production and promote its consumption (Ahn and Antoniewicz 2012; Altamirano et al. 2000; Chen et al. 2001; Kurano et al. 1990; Lao and Toth 1997).

Despite multiple efforts to standardise production processes CHO cells still present many metabolic challenges that lead to an unbalanced metabolism, characterised by large glucose and glutamine consumption with large by-product production (i.e., lactate and ammonia) (Ahn and Antoniewicz 2012; Chen et al. 2001; Kurano et al. 1990; Lao and Toth 1997; Ozturk et al. 1992). The undesirable by-product accumulation are usually minimised by maintaining low glucose concentrations (Cruz et al. 1999; Kurano et al. 1990; Wong et al. 2005; Zhang et al. 2004), utilising alternative carbon sources (Altamirano et al. 2000; Altamirano et al. 2004; Gorfien et al. 2003; Kim et al. 2013; Legmann et al. 2011; Wilkens and Gerdtzen 2011), optimising the culture environment (Kantardjieff et al. 2010; Luo et al. 2012; Rodriguez et al. 2005; Yoon et al. 2004) and regulating gene expression (Dorai et al. 2009; Kim et al. 2006; Kim and Lee 2007b; Paredes et al. 1999; Zhou et al. 2011).

Genetic engineering strategies have also been implemented to improve cell culture performance particularly by reducing by-product accumulation. Dorai et al. (2009) showed that cellular viability, peak of viable cell density and global IVCD were improved by over-expressing either individual or multiple anti-apoptotic genes such as Bcl-2Δ, Bcl-XL, E1B-19K and XIAPΔ. This strategy allowed significant improvements in product titter (up to 180%) and reductions in lactate production (up to 80%), and also demonstrated that over-expressing anti-apoptotic genes switched the lactate metabolism from production to consumption. Similarly, Kim and Lee (2007b) found that down-regulating the lactate dehydrogenase A (LDH-A) via siRNA reduced lactate production (up to 79%) and increased glucose uptake (up to 87%), however this strategy did not improve the specific productivity. To improve the productivity, Zhou et al. (2011) down-regulated LDH-A and pyruvate dehydrogenase kinase (PDKs) in CHO cells by siRNA resulting in notable increments in productivity and antibody titter (up to 75% and 68%, respectively) without negative effects in cell growth or product quality. The PDK down-regulation reduced its inhibitory effects on pyruvate dehydrogenase (PDH) therefore increasing the intracellular ATP content and reducing lactate accumulation (up to 90%). A similar strategy was implemented in CHO cells by Paredes et al. (1999), reducing the ammonia accumulation by over-expressing the glutamine synthetase (GS) gene and reducing the lactate accumulation by down-regulating the glucose transporter (GLUT1) and α-enolase via antisense RNA technique. This strategy also resulted in improved cell culture longevity, slow glucose consumption and low glutaminolytic and glycolytic metabolism.

1.6.1 Glucose metabolism

Glucose is the primary source of energy and a key molecule for living organisms. To meet the energy requirements, glucose is transported across the cell membrane by glucose transporters (GLUTs), followed by its oxidation into pyruvate through glycolysis and then either oxidised into CO_2 through the TCA cycle or reduced to lactic acid by the lactate dehydrogenase enzyme (LDH). These metabolic pathways generate ATP and energetic intermediates such as NADH (reduced nicotinamide adenine dinucleotide) and $FADH_2$ (reduced flavin adenine dinucleotide) that fuel the metabolism. Additionally, glucose can be metabolised through the PPP for nucleotide and aromatic amino acid biosynthesis and to obtain other indispensable energetic intermediates for fatty acid biosynthesis such as NADPH (reduced nicotinamide adenine dinucleotide phosphate) (Koopman et al. 2013), (Figure 1-5).

Glycolysis is considered as the main metabolic pathway for cells because it is the entry point for the breakdown of glucose and other carbohydrates, which leads to ATP and other intermediates for macromolecule biosynthesis. Glycolysis is highly regulated at different levels, starting with the glucose uptake across the cellular membrane and until its interconnection with other metabolic pathways (Amoedo et al. 2013). The glycolytic flux yields two ATP molecules that are used for biosynthesis, two molecules of NADH that can be oxidised in the mitochondria or during lactate formation, and two pyruvic acid molecules that can be oxidised to CO_2 via the TCA cycle or reduced to lactate (Adekola et al. 2012; Koopman et al. 2013) (Figure 1-5).

In aerobic conditions, pyruvic acid is subsequently transported to the mitochondrial matrix and converted to acetyl coenzyme A (acetyl-CoA) by the PDH, yielding one molecule of CO_2, NADH and acetyl-CoA, which then feed the TCA cycle to complete the carbon oxidation. During the TCA cycle, acetyl-CoA is oxidised into two molecules of CO_2, three molecules of NADH, one molecule of $FADH_2$ and one molecule of GTP. Then, the NADH and $FADH_2$ generated are fed into the ETC to create an electrochemical proton gradient across the mitochondrial membrane that drives ATP synthesis through the conversion of ADP to ATP by the ATP synthase. The complete glucose oxidation under aerobic conditions yields up to 36 ATP molecules per glucose molecule (Gatenby and Gillies 2004; Koopman et al. 2013).
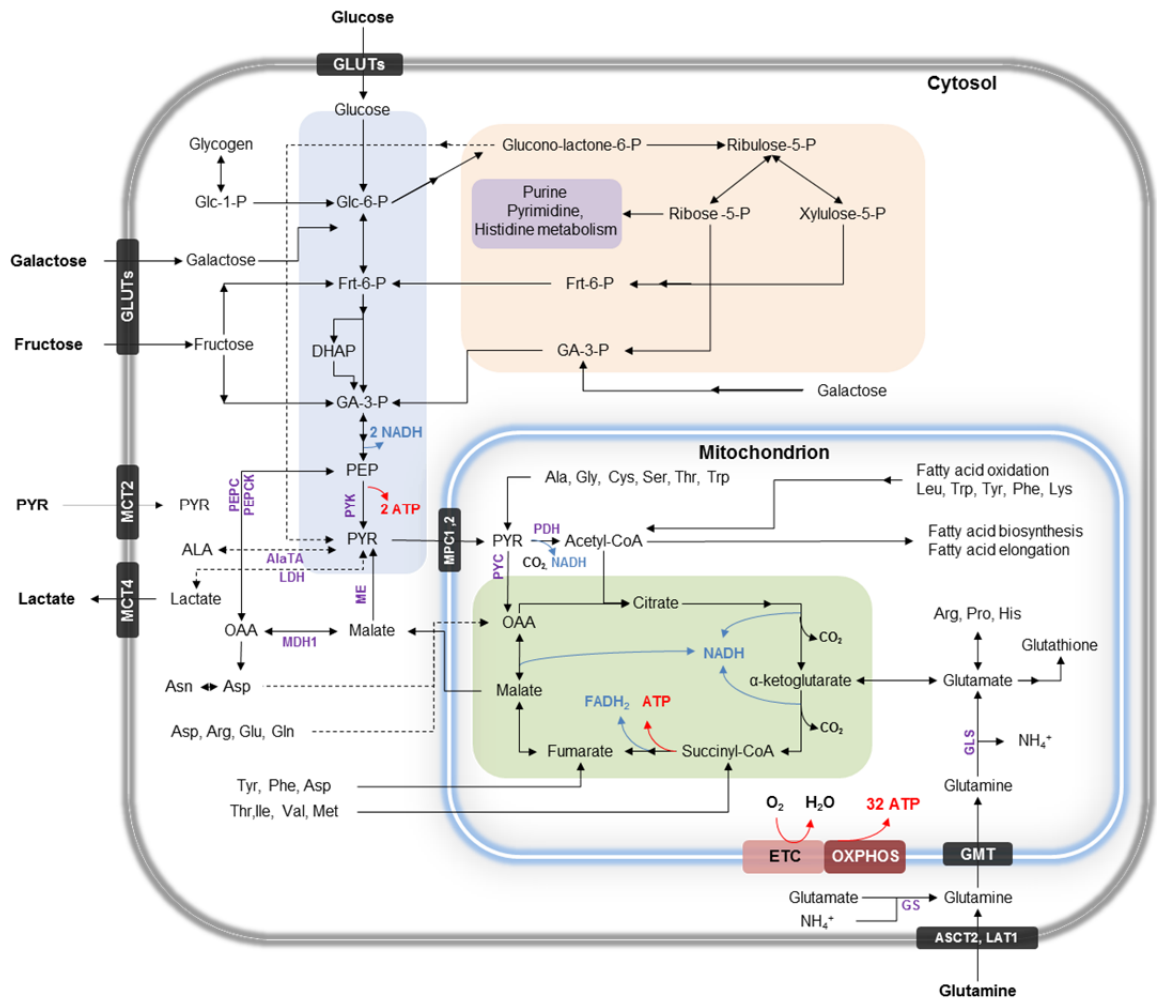
Figure 1-5 Typical mammalian cell metabolism for energy production. Firstly, glucose enters the cells through glucose transporters (GLUTs) and is oxidised through the glycolytic pathway (blue filled box) into two pyruvate (PYR), two ATP and two NADH molecules. PYR is then shuttled into the mitochondria and immediately converted to acetyl-CoA with the release of NADH and CO_2. The acetyl-CoA is oxidised through the TCA cycle (green filled box) to form 2 CO_2, 1 $FADH_2$, 3 NADH and 1 GTP molecules. Later, the electron carrier molecules (NADH and $FADH_2$) generated in glycolysis and the TCA cycle transfer electrons to the final electron acceptor (O_2) via the ETC. Finally, the proton gradient generated across the mitochondrial membrane leads to the conversion of ADP to ATP via OXPHOS. Alternately, PYR can be converted to lactate and other carbon sources (e.g., such as fructose, galactose, glutamine, fatty acids and other amino acids) that feed either glycolysis or the TCA cycle. The diagram also shows alternative entry points for different carbohydrates and amino acids along the metabolic pathways. Enzymes: pyruvate kinase; PYK, alanine transferase; AlaTA, lactate dehydrogenase; LDH, phosphoenolpyruvate carboxylase; PEPC, phosphoenolpyruvate carboxykinase; PEPCK, malic enzyme; ME, malate dehydrogenase; MDH1, pyruvate carboxylase; PYC, pyruvate dehydrogenase; PDH, glutamine synthetase; GS, glutaminase ; GLS.

In hypoxic conditions, the pyruvic acid can be reduced to lactic acid by the LDH to restore the levels of NAD+/NADH and maintain the ATP production. Therefore, under these conditions glycolysis becomes the main source of ATP, giving a fast source of energy, but an inefficient metabolism with only two ATP molecules per glucose molecule (Gatenby and Gillies 2004; Kim et al. 2006; Papandreou et al. 2006; Vander Heiden et al. 2009).

The incomplete glucose oxidation described above is a common defect observed in cancer cells in which they prefer to use the glycolytic pathway as the main source of energy that fuels the cell metabolism even under aerobic conditions (Gatenby and Gillies 2004; Warburg 1956), suggesting that cells have undergone important metabolic and physiologic changes that cause down-regulation of pyruvic acid flux from glycolysis to the TCA cycle (Diers et al. 2012) and potentially denoting mitochondrial damage. The bond between pyruvic acid and mitochondrial metabolism involves a critical enzymatic step catalysed by the multi-enzyme pyruvate dehydrogenase complex (PDC), which consists of three enzymes: pyruvate dehydrogenase (PDH, E1 domain), dihydrolipoyl transacetylase (E2 domain) and dihydrolipoyl dehydrogenase (E3 domain). The enzymatic complex converts pyruvate to acetyl-CoA, which enters the TCA cycle. PDC has been shown to be highly regulated by PDK activity through the phosphorylation of E1 domains of the PDC, resulting in PDC inhibition and subsequent reduction in the transport of pyruvate to the TCA cycle (Kim et al. 2006; Young 2013; Zhou et al. 2011).

Several studies in cancer and CHO cells have demonstrated that deficiency or inhibition of PDH results in an abnormal glucose metabolism, which is characterised by high glycolytic fluxes and high lactate accumulation (Kim et al. 2006; Papandreou et al. 2006; Zhou et al. 2011). Consequently, several strategies have been implemented to overcome this features. For example, Zhou et al. (2011) improved the shuttle of pyruvate into the TCA cycle by down-regulating the PDK activity via siRNA, observing that PDK-deficient cell lines significantly reduced the lactate accumulation (up to 90%) and efficiently coupled glycolysis and the TCA cycle.

Studies have demonstrated that hypoxic conditions also inhibit the PDH activity by activating the hypoxia-inducible factor 1 (HIF-1). Kim et al. (2006) found that HIF-1 increases the glycolytic flux and promotes lactate production by over-expressing glycolytic genes and up-regulating PDK to suppresses the TCA cycle. Additionally, they revealed that HIF-1α rescued cells from hypoxia-induced apoptosis by promoting the pyruvate transport from the mitochondria to the cytosol to be subsequently reduced to lactate in an effort to regenerate NAD+/NADH levels and attenuate reactive oxygen

species (ROS) production. Similarly, Papandreou et al. (2006) showed that PDK can be regulated by inhibiting HIF-1, observing that HIF-1-deficient cancer cells exhibited higher rates of mitochondrial respiration and lower PDK activity than HIF-1 cancer cells, thereby they suggest that PDK can be down-regulated even under hypoxic conditions by inhibiting HIF-1. Together, Kim et al. (2006) and Papandreou et al. (2006) concluded that under hypoxic conditions HIF-1 (i) stimulates the expression of glucose transporters and glycolytic enzymes in an effort to meet the energetic requirements via glycolysis, (ii) inhibits PDH activity by up-regulating PDK, which blocks the pyruvate flux to the TCA cycle to avoid the generation of ROS and (iii) promotes the conversion of pyruvate to lactate by overexpressing LDH to restore the levels of NAD+/NADH and continue with the energy production via glycolysis.

In addition, cancer studies have proven that an elevated glucose contributes to tumour progression. This research found that this behaviour is promoted by the over-expression of glucose transporters (i.e., GLUT1, GLUT4 and GLUT9) and glycolytic enzymes (Adekola et al. 2012; Macheda et al. 2005). Consequently, some strategies have tried to reduce this metabolism with enough success, for example successfully reduction in sugar uptake has been achieved by down-regulating the GLUT1 (Paredes et al. 1999) or GLUT5 (Wlaschin and Hu 2007) transporter.

1.6.2 Lactate metabolism

Lactate is derived from pyruvate reduction by LDH, a homo- or hetero-tetramer enzyme consisting of A and B subunits encoded by the LDHa and LDHb genes, respectively. In CHO cells LDH exists as LDH-A and LDH-B tetramer, being LDH-A the most important isoenzyme because it catalyses the reaction under anaerobic conditions (Jeong et al. 2001) and maintains the NAD+ levels for glycolytic ATP production during aerobic glycolysis and under hypoxic conditions (Kim and Lee 2007b; Zhou et al. 2011).

Lactate is considered an undesirable by-product during cell culture resulted from the truncated metabolism of glucose and other carbohydrates (Altamirano et al. 2004; Chen et al. 2001; Legmann et al. 2011; Ozturk et al. 1992; Paredes et al. 1999; Zhang et al. 2004). However, lactate production is also used as an important cellular metabolic strategy to restore the levels of NAD+/NADH to maintain the ATP production which is essential to survive and proliferate under hypoxic conditions by maintain an active glycolytic metabolism (Kim et al. 2006; Papandreou et al. 2006; Zhou et al. 2011). Therefore, lactate build-up is a critical consideration that must be controlled

during recombinant protein manufacturing because its accumulation causes cell culture acidification which alters protein structures and threatens the cell metabolism resulting in significant reductions of the overall cell culture performance and recombinant protein production (Ahn and Antoniewicz 2012; Lao and Toth 1997). For example, Ozturk et al. (1992) reported that lactate levels above 20 mM inhibit the cell growth and antibody production CHO cells. The culture acidification at medium and large production scales is neutralised by alkali addition, resulting in an increased osmolarity that declines productivity and cell growth performance (Li et al. 2010; Luo et al. 2012; Xing et al. 2009; Zhou et al. 2011). Thereby, slow rates of lactate production levels and a switch from lactate production to consumption are desirable characteristics in CHO cell lines (Luo et al. 2012).

Different strategies have been proposed to decline lactate formation in order to improve cell growth and productivity, for example down-regulating the LDH (Chen et al. 2001; Jeong et al. 2001; Kim and Lee 2007b), down-regulating PDK (Kim et al. 2006; Zhou et al. 2011), manipulating sugar transporters (Paredes et al. 1999; Wilkens and Gerdtzen 2011; Wlaschin and Hu 2007), optimising the culture nutrient feeding strategy (Altamirano et al. 2004; Cruz et al. 1999; Rodriguez et al. 2005; Wilkens and Gerdtzen 2011; Zhang and Robinson 2005) and optimising the culture environment (Kim and Lee 2007a; Yoon et al. 2004) have proved efficacy.

To reduce the negative effects of high LDH activity, Kim and Lee (2007b) down-regulated LDH-A, resulting in notable decreases in its activity and in the glucose uptake (up to 89% and 87%, respectively). However, this strategy did not improve the specific productivity, growth rate and the interconnection between glycolysis and the TCA cycle. This low cell performance was related to the lower LDH-A activities, which limited the NAD+ regeneration for ATP production via glycolysis and consequently limited the energetic capacity of the cells. Similar studies were performed by Zhou et al. (2011), but to improve the conversion of pyruvate to acetyl-CoA they also down-regulated the PDK activity to allow the pyruvate progression to the TCA cycle. The down-regulation of PDK and LDH activities resulted in a notable decrease in glucose uptake and lactate production with important improvements in productivity. These studies also showed that reductions in PDK expression levels improve the shuttle of pyruvate into the TCA cycle by maintaining an active PDC activity throughout the culture and stimulating the metabolic switch from lactate production to consumption.

Diverse genetic engineering strategies have also been implemented in CHO cells with optimistic results. Wilkens and Gerdtzen (2011) transfected CHO cells with both the fructose transporter gene (Slc2a5) and the pyruvate carboxylase gene (PYC), and

cultivated the cells in presence of both glucose and fructose in an effort to reduce the lactate production and increase the carbon supply to the TCA cycle. Their findings showed that over-expressing the fructose transporter (GLUT5) and PYC enzyme notably improved the specific growth rate (between 1.6 and 2.25 fold change) and enhanced cell culture longevity. These findings were accompanied by important reductions in lactate production when cells were grown under low glucose concentration and fructose supplementation. Additionally, transfected cells also exhibited an improved glucose metabolism that was characterised by slow glucose uptake and high pyruvic acid fluxes into the TCA cycle. Similarly, Paredes et al. (1999) improved the glycolytic metabolism by down-regulating the glucose transporter (GLUT1) and the α-enolase enzyme, finding that targeting GLUT1 and α-enolase significantly reduced the glucose uptake, decreased lactate accumulation and extended the culture longevity.

Although genetic strategies have seen remarkable improvements in lactate metabolism control, it is known that genetic modifications may increase even more the genetic instability within cells, affecting the cell culture performance and product quality during long-term production and making even more complex the production processes for manufacturing recombinant proteins at the industrial scale. Consequently, several non-genetic strategies designed on empirical basis and previous findings have been implemented to reduce these problems. For example, maintaining low concentrations of glucose throughout cultivation has shown enormous improvements in cell growth performance and product quality and quantity with notable reductions in lactate accumulation (Ahn and Antoniewicz 2012; Altamirano et al. 2000; Altamirano et al. 2004; Lao and Toth 1997; Zhang et al. 2004). In the same context, the utilisation of alternative carbon sources such as galactose and fructose have also seen satisfactory results in the overall cell culture performance (Altamirano et al. 2000; Altamirano et al. 2004; Gorfien et al. 2003; Legmann et al. 2011; Wilkens and Gerdtzen 2011).

1.6.3 Glutamine metabolism

Glutamine has a central importance in the cell metabolism, being extensively used as a precursor for protein, amino sugar, cofactor, purine, pyrimidine and ATP synthesis (Amoedo et al. 2013; Barnes et al. 2000; Pochini et al. 2014). Additionally, glutamine is a key metabolite that maintains the cell functionality, including important biological processes such as gene expression regulation, gluconeogenesis, redox potential maintenance (via GSH/GSSG ratio), pH homeostasis, anaplerotic carbon

supply for the TCA cycle, NH_3 release and NADPH generation for the maintenance of the mitochondrial membrane potential and integrity (Barnes et al. 2000; Pochini et al. 2014; Wise and Thompson 2010).

In mammalian cells, glutamine is a non-essential amino acid synthesised endogenously from glutamate and ammonia by the GS, then transported into the mitochondria and coupled to the energy flux. However, in cancer cells, including CHO cells, the biosynthetic glutamine machinery results insufficient to meet the proliferation demands, making necessary the integration of exogenous glutamine to survive. To address this dependence, cancer cells must efficiently assimilate exogenous glutamine using several membrane transporter families, which include system AlaSerCys Transporter 2 (ASCT2), L-type amino acid transporters (LAT1, LAT2), system N/A amino acid transporters (SNAT1, SNAT2, SNAT3, SNAT5, SNAT7, B0AT1) and the mitochondrial glutamine transporter (GMT) (Bode 2001; Pochini et al. 2014). From these, the over-expression of ASCT2 and LAT1 has been associated with tumour growth and progression (Kyriakopoulos et al. 2013; McGivan and Bungard 2007).

Different studies have identified the glutamine addiction of cancer cells as necessary for maintaining the functionality of bidirectional mitochondrial transporters such as SLC7A5 and SLC3A2, which exchange glutamine for other amino acids to increase the intracellular amino acid concentration. Amino acid accumulation, but in special of leucine, induces the TOR kinase (mTORC1) activity, an essential pathway that regulates cell growth, cell proliferation, cell size, gene transcription and protein synthesis and degradation (Fumarola et al. 2005; Pochini et al. 2014; Wise and Thompson 2010). In addition, glutamine breakdown provides important anaplerotic carbon sources for the TCA cycle to maintain ATP production and also is used to synthesise amino acids, lipids, nucleic acids and cofactors (Amoedo et al. 2013). In order to maintain an elevated glutaminolytic metabolism with high proliferations, cancer cells up-regulate the glutaminase (GLS) enzyme, activate RAS and Myc oncogenes and inactivate the P53 function (Amoedo et al. 2013; Vander Heiden et al. 2009).

Although an elevated glutamine catabolism is necessary for cancer cells, studies in CHO cells have demonstrated that glutamine addiction results in undesirable ammonia accumulation in the culture environment during recombinant protein manufacturing processes, which notably decreases cell growth, cell metabolism and glycoprotein quality (Altamirano et al. 2000; Altamirano et al. 2004; Gawlitzek et al. 1998; Kim et al. 2013; Lao and Toth 1997; Ozturk et al. 1992; Wong et al. 2005). Glutaminolysis involves two enzymatic reactions, the first catalysed by GLS which converts glutamine to ammonia and glutamate, and the second catalysed by glutamate

dehydrogenase (GDH) which converts glutamate to ammonia and α-ketoglutarate, the latter is immediately incorporated into the TCA cycle to produce energy for cell growth. The intensive glutaminolytic metabolism observed in cancer cells is usually resulted from GLS overexpression, as a consequence several anti-cancer strategies have been focused in inhibiting the GLS activity to control cancer metabolism (Zhao et al. 2013).

Ammonia accumulation is critical and must be controlled in biological production because it indirectly triggers cell acidification, which alters the internal cellular structures and disrupts the electrochemical gradient (Cruz et al. 2000), having detrimental effect on cell growth. Ozturk et al. (1992) reported a 50% decline in viable cell density at levels between 2 to 10 mM in CHO cells studies. However, other studies reported that a cell line specific sensibility to ammonia sensibility, for example Lao et al. (1997) did not observe a decline on cell growth or productivity when up to 10 mM ammonia was added to CHO cultures. The unwanted detrimental effects caused by ammonia have been reduced by implementing a large number of strategies. For example, notable reductions in ammonia build-up have been achieved by controlling glutamine availability (Altamirano et al. 2004; Cruz et al. 1999; Kim et al. 2013; Kurano et al. 1990; Lee et al. 2003; Wong et al. 2005) and by substituting glutamine for asparagine (Christie and Butler 1999; Henry and Durocher 2011), pyruvate (Genzel et al. 2005; Kim et al. 2013), wheat gluten hydrolysate (Kim et al. 2013), glutamate (Altamirano et al. 2004; Hong et al. 2010; Janke et al. 2011), glutamine containing dipeptides (Kim et al. 2013), threonine, proline and glycine (Chen and Harcum 2005). In the same context, several genetic engineering strategies have been implemented to develop more robust CHO cell lines with reduced ammonia levels. For example, down-regulating the LDH-A activity (Chen et al. 2001; Kim and Lee 2007b; Zhou et al. 2011), expressing urea cycle enzymes (Chung et al. 2003; Park et al. 2000), over-expressing pyruvate carboxylase (Bollati Fogolin et al. 2004; Fann et al. 2000; Henry and Durocher 2011; Kim and Lee 2007c) and using the GS-gene expression system (Barnes et al. 2000; Barnes et al. 2001; Cockett et al. 1990).

Metabolic analyses have also been widely performed to characterise cultures with elevated glutaminolytic metabolism. Kyriakopoulos et al. (2013) analysed the global amino acid metabolism of CHO cells, especially by monitoring the regulation of 40 amino acid transporters during the exponential, stationary and dead cell growth phases in a batch culture of non-producing and producing CHO cells. These studies revealed notable differences in the induction of amino acid transporters along the culture, with significant increases during the stationary phase when amino acid concentrations decline. Similarly, the protein-producing cell lines up-regulated the

majority of amino acid transporters throughout the culture, probably to increase the amino acid reserve for recombinant protein assembly. Interestingly, leucine and branched-chain amino acid transporters (SLC43A2) and glutamate and aspartate transporter (SLC1A2) were significantly up-regulated, indicating that these transporters may be linked to recombinant protein production. These studies also revealed that the five amino acid transporters associated with glutathione (i.e., slc1a4, slc6a9, slc1a2, slc7a11 and slc3a2-slc7a11) were up-regulated during the stationary phase to increase the intracellular amino acid uptake. By comparing the protein-producing and non-producing cell lines, significant metabolic differences were observed, for example, the protein-producing cell lines were more metabolically efficient, exhibiting higher proliferation rates and lower lactate and glycine production rates than the null cell lines. On the other hand, the consumption rate of methionine, isoleucine, leucine, phenylalanine, tryptophan and lysine varied significantly between cell lines, being much higher in the null cell line. With respect to glutamine production, the protein-producing cell lines exhibited higher production.

Finally, one of the most important approaches to reduce ammonia accumulation during recombinant protein production has been attained by implementing the GS-gene expression system developed by Lonza-Celltech. This platform involves the expression of exogenous GS enzyme to allow cell growth in glutamine-free media with reduced ammonia build-up in culture. This system also allows the selection of multi-copy transfected clones and the recombinant-gene amplification through L-methionine sulphoximine (MSX) supplementation, an inhibitor of GS activity (Barnes et al. 2000). Although the GS-systems have been successfully implemented in CHO cell lines with notable improvements in cell culture performance (e.g., IVCD, μ, VCD), their efficiency is markedly reduced due to the endogenous GS activity in CHO cells. For overcoming this limitation a GS-knockout CHO cell line was developed (CHO-K1SV, Lonza) (Barnes et al. 2000).

1.6.4 Warburg effect

In normal conditions glucose is metabolised through glycolysis and the TCA cycle for energy generation through the ETC and OXPHOS. However, cancer cells exhibit a different glucose metabolism to fuel cellular processes that is not completely coupled to the TCA cycle and OXPHOS, being more dependent on aerobic glycolysis and glutaminolysis (Vander Heiden et al. 2009; Zhao et al. 2013). The Warburg effect or "aerobic glycolysis" is a metabolic change characterised by the preference of glucose

fermentation over its oxidation through OXPHOS even when oxygen is abundant (Amoedo et al. 2013). This feature is not exclusive of cancer cells and was first described in the 1920's by Otto Warburg. His studies compared the rate of lactate production and oxygen consumption in normal and cancerous tissue, finding that both produced similar amounts of ATP, however, cancer cells produced higher amounts of lactic acid whilst normal cells showed higher respiration rates. These observations demonstrated that cancer cells prefer the lactate pathway over OXPHOS as the main energy source (Warburg 1956).

Studies have suggested that cancer cells embrace aerobic glycolysis as the main energy source to rapidly meet the increasing energetic and metabolite requirements to proliferate. An intensive cell biomass production requires a fast metabolism able to increase the cellular protein content, replicate the genome and synthesise biomolecules in short time periods (Garber 2006; Gatenby and Gillies 2004; Kim et al. 2006; Papandreou et al. 2006; Zhao et al. 2013). Cancer cells also require over-express key enzymes (i.e., hexokinase (HK), phospho-fructo-kinase (PFK), PYK-isoform M and LDHA), activate signalling pathways (i.e., phosphoinositide 3-kinase (PI3K), myc and AKT) and up-regulation glucose transporters (GLUT 1, GLUT 3 and GLUT 4) (Vander Heiden et al. 2009; Zhao et al. 2013). Evidences also suggest that aerobic glycolysis provides growth advantages under hypoxic environments (Gatenby and Gillies 2004). Likewise, an environmental acidification, resulted from lactic acid accumulation, offers additional growth advantages because cancer cells exhibit mechanisms that protect them from acidified environments (Gatenby and Gillies 2004; Kim et al. 2009; Webb et al. 2011), and lastly acidified environments enhance cancer progression by encouraging protease release, which decreases cell adhesion and thus favours metastasis (Stock and Schwab 2009; Webb et al. 2011).

Despite the low energetic efficiency of aerobic glycolysis, CHO cells can meet their intensive energetic request because the ATP production via glycolysis is 100x times faster than via OXPHOS (Bartrons and Caro 2007), and because aerobic glycolysis supplies enough metabolites for nucleic acid and lipid synthesis (Vander Heiden et al. 2009; Zhao et al. 2013). However, the large lactate quantities generated from this metabolism are detrimental for CHO cell performance. By today, few approaches to modulate the Warburg effect have been implemented in CHO cells, but cancer studies strongly indicate that a regulation of the Warburg effect may lead to efficient cell culture processes (Bartrons and Caro 2007; Kim and Lee 2007b; Nijsten and van Dam 2009; Papandreou et al. 2006), therefore the Warburg effect is an inherent characteristic of CHO cells that must be considered in cell line development.

1.7 Mitochondria: (dys) functional mitochondrial respiration

The mitochondrion is a specialised organelle that performs indispensable metabolic and energetic processes for maintaining an optimal cellular performance. Considered as the cellular horsepower, the mitochondria produce the majority of energy and metabolic intermediates, and regulate key cellular phases such as apoptosis, cell division, cell growth, homeostasis, gene expression and ROS production (Bereiter-Hahn et al. 2008; Cadenas and Davies 2000). In addition, mitochondria possess their own genome (mDNA) and perform specific and independent biological processes such as mitochondrial fusion and fission, mDNA replication and transcription, and mitochondrial protein synthesis (Bereiter-Hahn et al. 2008; Detmer and Chan 2007). As a result, these complex organelles require a strict regulation and coordination to support and interconnect all biochemical processes (Nicholls and Ferguson 2013).
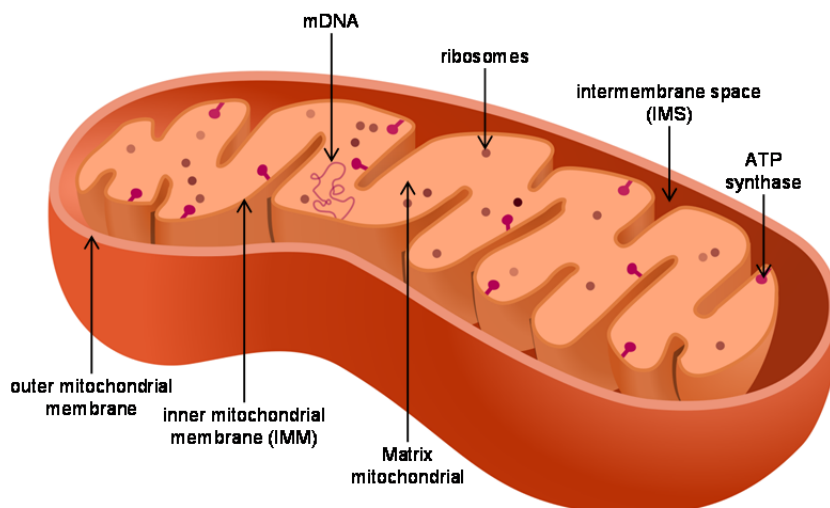
Figure 1-6 Mitochondrial structure.

Mitochondria are dynamic structures consisting of outer and inner double phospholipid membranes, intermembrane space (IMS) and matrix, which together maintain their functionality, integrity and communication with the cytosol (Detmer and Chan 2007; Gabriel et al. 2007; Vogtle et al. 2012) (Figure 1-6). The outer mitochondrial membrane (OMM) controls the metabolite and ion flux between the cytosol and the IMS, defines the boundaries and interactions with the cytosol, maintains the mitochondrial homeostasis and controls the permeability of small and large molecules (up to 5000 daltons) (Vander Heiden et al. 2000). The OMM also

releases pro-apoptotic proteins such as cytochrome C, smac/diablo, HTRA2/omi, apoptosis-inducing factor and endonuclease G through Bcl regulators when its integrity is compromised (Susin et al. 1999; Vander Heiden et al. 2000). The inner mitochondrial membrane (IMM) is more impermeable to the transport of large molecules and ions to maintain a proton gradient across membrane, which later is used for ATP synthesis via ATP synthase. The IMM contains all the essential enzymes involved in mitochondrial respiration and ATP production, as well as the proteins for large-biomolecule exchange between the matrix and the IMS (Bereiter-Hahn et al. 2008)(Bereiter-Hahn et al. 2008)(Bereiter-Hahn et al. 2008)(Bereiter-Hahn et al. 2008). The mitochondrial matrix contains mDNA, ribosomes and enzymes involved in the TCA cycle. The IMS is involved in the modification and transport of metabolites and proteins from the cytosol for the TCA cycle, ETC and OXPHOS (Gabriel et al. 2007; Vogtle et al. 2012), as well as involved in the transit of pro-apoptotic molecules and maintenance of protein redox homeostasis by preventing their oxidation (Vogtle et al. 2012).

For the above mentioned reasons, mitochondria are crucial and their failure can result in apoptosis or pathologies such as cancer and ageing (Koopman et al. 2013; Valko et al. 2007). Consequently, mitochondria evolved a complex, but efficient regulatory metabolism which strictly coordinates a large number of metabolic and signalling pathways and restricts molecule exchange across the membrane to avoid catastrophic consequences.

1.7.1 Mitochondrial respiration and mitochondrial membrane potential

Mitochondrial respiration represents the more efficient cellular metabolism in terms of ATP production, coupling the TCA cycle, the ETC and the OXPHOS pathways. This aerobic process comprises a set of biochemical reactions performed in the IMM that transfer electrons from NADH and $FADH_2$ to O_2, the final acceptor, through a series of enzymatic complexes (complex I, II, III, and IV of the ETC) and electron carriers (ubiquinone/coenzyme Q and cytochrome c) yielding one water molecule and pumping protons to the IMS (Nicholls and Ferguson 2013). This electrochemical proton gradient across the IMM, also known as mitochondrial membrane potential (MMP), is used by OXPHOS to generate ATP through the F_0F_1 ATP synthase complex. In addition, the MMP generated by the ETC is essential for metabolite and ion exchange across the IMM and for maintaining the mitochondrial integrity and functionality (Koopman et al. 2013).

1.7.2 Reactive oxygen species and oxidative stress

Reactive oxygen species are molecules containing oxygen with elevated reactive chemical properties. Among these species, the superoxide anion radical (O_2^-), hydrogen peroxide (H_2O_2) and hydroxyl free radical (·OH) have a notable biological importance (Klaunig et al. 2010; Pelicano et al. 2004). ROS production is a normal cellular process during mitochondrial respiration, it is estimated that between 4-5% of the oxygen consumed is converted to ROS, being the O_2^- the principal molecule (Kim et al. 2009; Klaunig and Kamendulis 2004). The O_2^- specie is the result of an inadequate mitochondrial respiration, mainly from the electron leakage that occurs in the ETC complex I and III that directly reduces O_2 to O_2^- (Cadenas and Davies 2000; Jastroch et al. 2010; Maynard et al. 2009). This ROS molecule is then converted to H_2O_2 by superoxide dismutase (SOD) and it can further react to be converted into ·HO (Cadenas and Davies 2000; Klaunig and Kamendulis 2004).

ROS can also be generated endogenously by peroxisomes (Klaunig and Kamendulis 2004) and by the α-ketoglutarate dehydrogenase (αKGDH) (Koopman et al. 2013), or exogenously by ionising radiation (IR), toxins and chemicals (Maynard et al. 2009; Pelicano et al. 2004). Therefore, resulting in a constant threats that must be eliminated from the cells in form of H_2O through antioxidant enzymes such as catalase, glutathione reductase (GR), glutathione peroxidase (GPX) and thioredoxin reductase (TRXR) (Koopman et al. 2013) and by non-enzymatic molecules such as catechins, glutathione (GSH), vitamin E and vitamin C (Cadenas and Davies 2000; Klaunig and Kamendulis 2004; Pelicano et al. 2004) to maintain a normal cellular metabolism.

1.8 Oxidative stress

Oxidative stress is the unbalance between the ROS production and its elimination, being a common pathology widely observed in cancer cells (Klaunig and Kamendulis 2004). This pathology arises from deficiencies and inactivation of antioxidant enzymes, as well as from oncogenic signals, mitochondrial damage and an elevated cellular metabolism (Benhar et al. 2001; Pelicano et al. 2004). These dysfunctions results in significant increments in ROS levels which cause cellular damage and promote more ROS levels within the cells which consequently will damage the genomic DNA, therefore ROS usually results in constant alterations in the DNA sequence and structure (Ames 1983; Bereiter-Hahn et al. 2008; Jackson and Loeb 2001; Klaunig and Kamendulis 2004) that lead to mutations with consequences such as apoptosis, cellular heterogeneity, drug sensitivity, gene deregulation, genetic

instability, metabolic dysfunction, necrosis, protein malfunction, uncontrolled cellular proliferation and carcinogenesis (Bereiter-Hahn et al. 2008; Cadenas and Davies 2000; Jackson and Loeb 2001; Klaunig and Kamendulis 2004; Klaunig et al. 2010; Pelicano et al. 2004).

Increased ROS levels possess other detrimental effects as they can affect the protein integrity by catalysing amino acid chain oxidation and peptide cleavage (Cadenas and Davies 2000; Pelicano et al. 2004) which jeopardise the membrane integrity by increasing lipid peroxidation (Klaunig and Kamendulis 2004; Pelicano et al. 2004) and mitochondrial fragmentation (Bereiter-Hahn et al. 2008) and (Bereiter-Hahn et al. 2008)(Bereiter-Hahn et al. 2008)(Bereiter-Hahn et al. 2008)endangering the energy supply through the inactivation of mitochondrial enzymes involved in the TCA cycle, OXPHOS and the ETC (Bereiter-Hahn et al. 2008; Cadenas and Davies 2000; Klaunig and Kamendulis 2004) and compromising the mitochondrion function by generating defects in mDNA which lead to mutations and malfunctions in the translated mitochondrial proteins (Beckman and Ames 1999; Bereiter-Hahn et al. 2008).

1.8.1 Oxidative DNA damage

The genome is continuously subject to alterations in its chemistry and sequence as a result of a large variety of signals and stressors (Ames 1983; Bandyopadhyay et al. 2010; Friedberg 2003; Loeb 1989; Schmitt et al. 2010). These cellular stressors can be generated either endogenously or exogenously. In the first group, ROS and the alkylation, depurination and deamination of cytidine are important source of oxidative DNA damage (Ames 1983; De Bont and van Larebeke 2004) whereas in the second group DNA-damaging agents such as chemicals, viruses and ionisation radiations (Loeb 1989; Maynard et al. 2009; Miller 1978; Paques and Haber 1999), as well as environmental factors such as high temperature and pH (Friedberg et al. 2006) are included. In addition, this DNA modifications can also result from errors during homologous recombination, DNA replication and DNA repair (Friedberg 2006).

DNA damage is unavoidable and it is estimated that more than 20000 DNA damaging events occur daily in each cell, being the endogenous agents responsible for the majority (Beckman and Ames 1997; De Bont and van Larebeke 2004; Schmitt et al. 2010). This threat leads to multiple DNA lesions, such as single-strand breaks (SSTs), double-strand breaks (DSBs), mismatches, base or sugar damage and DNA-DNA and DNA-protein crosslinks (Friedberg 2006; Helleday et al. 2007; Maynard et al. 2009). To protect themselves from these damages, cells evolved DNA repair mechanisms such

as base excision repair (BER), nucleotide excision repair (NER), mismatch repair (MMR), homologous recombination (HR) and non-homologous end joining (NHEJ) for recognising and repairing specific DNA damage (Lange et al. 2011; Maynard et al. 2009; Zhou and Elledge 2000). Otherwise, accumulated DNA damage may results in apoptosis or irreversible mutations leading to carcinogenesis and genetic instability (Helleday et al. 2007; Jackson and Loeb 2001; Maynard et al. 2009; Miller 1978; Singer and Kusmierek 1982). The fidelity of DNA repair mechanisms is extremely high, ensuring low mutation rates on the order of 10^{-10} mutations per nucleotide per cell per generation (Baer et al. 2007; Jackson and Loeb 2001). In addition to the DNA repair fidelity, cells possess DNA-damage tolerance mechanisms that allow them to survive in the presence of DNA-polymerase blocking lesions (Chang and Cimprich 2009; Maynard et al. 2009).

The most catastrophic oxidative damage events is when $\cdot$OH reacts with the sugar moiety of DNA causing single and double strand breaks, or reacts with the double bond of pyrimidines (C_5-C_6) modifying bases. From these, DSBs are considered the most common, toxic and deleterious type of DNA lesions in organisms, however, DSBs are also important to control some biological processes that maintain the heterogeneity among organisms (Helleday et al. 2007). For example, during meiosis the recombination between homologous chromosomes is mediated by an intentional and temporal DSB (Helleday et al. 2007).

The absence or improper DSB repair allows chromosomal aberration accumulation over time leading to loss of heterozygosity and increasing genomic instability, carcinogenesis and cellular death (Bonner et al. 2008; Helleday et al. 2007; Paques and Haber 1999; Pastwa et al. 2003). To alleviate DNA breaks, cells can directly ligate the two DNA ends through the NHEJ process (Helleday et al. 2007; Pastwa et al. 2003) or through HR by using homologous DNA sequences from the undamaged sister chromatid as template to re-synthesise damaged DNA or the missing sequence at the break site (Paques and Haber 1999; Schofield and Hsieh 2003; Takata et al. 1998).

1.9 Long-term evolution: genetic instability and genetic drift plasticity

Genetic instability is the set of events that facilitate the acquisition of unscheduled alterations across the genome, and it results from deficiencies in DNA repair pathways (Lengauer et al. 1998; Loeb 2001; Pavelka et al. 2010) and chromosomal segregation (Cahill et al. 1999; Thompson et al. 2010). Genetic instability is widely observed in

cancer cells (Michor 2005; Negrini et al. 2010) as well as in CHO cells (Davies et al. 2012; Derouazi et al. 2006; O'Callaghan and James 2008; Wurm 2013) causing the fixation of beneficial and deleterious mutations through time, affecting the global phenotype and defining the population fitness (Stich et al. 2010).

Data suggests that CHO populations' inherent genetic instability may confer selective growth advantages (Barnes et al. 2006; Davies et al. 2012; Jones and Baylin 2007; Nowell 1976; Silander et al. 2007; Stich et al. 2010). For example, beneficial mutation may result in higher cellular densities and increments in the culture longevity as a result of the acquisition of tolerance to environmental stressors usually encounter at late stages in a fed-batch culture (e.g., osmolarity and toxic by-product levels). This latent growth advantages may be translated in higher IVCD performances, and therefore in greater protein quantities at larger-scale. For example, assuming two cultures with equal specific productivity and a difference of 1 x10^6 cells ml^{-1} in cell density between both cultures at stationary growth phase, the one with the greater cell density would yield ~6.5% more products. For that reason, harnessing genetic instability to identify subpopulations with selective growth advantages, such as higher cell densities in culture and elevated IVCD, is essential to isolate improved clones able to significantly increase volumetric productivity, particularly at large-scale processes.

Combining the effects of genetic instability with natural selection, directed evolution and genetic drift processes in synthetic environments may accelerate evolution and adaptation of populations (Beckmann et al. 2012; Hallatschek et al. 2007; Stich et al. 2010). Linking together, these evolutionary steps may confer specific fitness advantages in the long-term by enhancing existing functions or inducing new functions (Jones and Baylin 2007; Nowell 1976; Stich et al. 2010), therefore phenotypes with high tolerance to by-product accumulation, osmolarity and synthetic environments can be obtained (Schumpp and Schlaeger 1992; Sinacore et al. 2000; Sunley et al. 2008). Genetic drift allows individual cells to out-compete other subpopulations and dominate the population over time as a result of small random sampling events along subculture which generate randomness and fluctuations in allele frequencies and also increase the level of homozygosis of populations because along repetitive cycles of cell sampling/ expansion a low allele/gene frequency becomes more common. Genetic drift is a constant feature of mammalian cell culture with a potential to define the population's fitness during routine and extensive subculture when only a small proportion of population is expanded (Torsvik et al. 2014). Studies have demonstrated that this phenomenon lead to significant improvements in growth phenotype (Beckmann et al. 2012; Davies et al. 2012; Torsvik et al. 2014). For example,

Beckmann et al. (2012) observed significant increments in peak of viable cell density (up to 82%) and specific exponential growth (up to 23%) by subjecting cells into a long-term cultivation (>400 generations). Similarly, Davies (2012) measured the genetic drift effects of a panel of CHO-K1SV clones along 55 generations, observing median increments in µ of 0.0031 h^{-1} per generation. Unfortunately, these studies not reported their IVCD performance along increasing generations, but the results seem to indicate that IVCD performance was also improved at some extent. Numerous reports within the literature have demonstrated that genetic drift also has the potential to completely reshape a population by spontaneously fixing subpopulation with altered metabolism (Hallatschek et al. 2007; Loeb 2001), which eventually may develop a new population that not represents its original phenotypic patterns.

As mentioned above, CHO cells have accumulated a large number of mutations and chromosomal aberrations across time (see section 1.4), developing an innate genetic instability which has diversified their original phenotypic and genetic characteristics (Wurm 2013). Consequently, we suggest that the inherent genetic instability within CHO cells and genetic drift can be used as a motor to drive evolution and provide cell lines with fitness advantages for the production of recombinant proteins (Chandhok and Pellman 2009; Gresham et al. 2008; Pavelka et al. 2010; Polakova et al. 2009; Selmecki et al. 2008).

1.10 Project overview

Given the evidences generated from previous research that demonstrated that the dynamic genetic heterogeneity within of CHO cell may improve functional characteristic in CHO populations and from those researches that have suggested the benefits of implementing directed evolution in cell line development for manufacturing relevant cell lines with desirable metabolic and growth characteristics that meet industrial standards, we design this research project as a starting point to improve the cell development processes by implementing a reversed approach involving the selection of un-transfected cell lines with desirable growth characteristics.

This research allow us to harness the inherent cellular heterogeneity within an un-transfected parental CHO-S population by isolating 22 clonally-derived CHO-S populations through two rounds of the limiting dilution cloning, followed by an accelerated evolution through genetic drift and directed evolution in a chemically defined media (Chapter 3). This project was followed by an initial compassion of phenotypic heterogeneity within a panel of 22 clone CHO-S cell lines along an

extended sub-cultivation (up to 220 generations; Chapter 3), then by extensive cell growth performance (Chapter 4) and metabolic (Chapter 5) assessments under fed-batch mode to evaluated whether the metabolic and phenotypic characteristics were conserved or improved throughout the long-term cultivation. Finally, given the significant differences in cell growth and metabolic activity at exponential and stationary growth phases, we studied the mitochondrial and glycolytic activity at both growth phases to evaluated (i) whether the phenotypic differences among clones are the cause or the consequence of the mitochondrial metabolism and (ii) whether a functional mitochondria result in cell lines with desirable and enhanced phenotypes (Chapter 6).

Chapter 2

MATERIALS AND METHODS

Chapter 2
Materials and methods

2.1 Mammalian cell culture

2.1.1 Routine mammalian cell maintenance

In this study, a set of 22 clonally-derived CHO-S cell lines were isolated from a donor parental CHO-S cell line (Life Technologies, Paisley, U.K.) and cultivated in CD CHO medium (Life Technologies, Paisley, U.K.) supplemented with 8 mM L-glutamine (Life Technologies, Paisley, U.K.) unless otherwise mentioned. CHO-S cells were routinely cultured in 125 mL vent-capped Erlenmeyer shake flasks (Corning, Surrey, U.K.) using 20 mL of glutamine supplemented CD CHO medium. Cells were sub-cultured every 3-4 days during the mid-exponential growth phase and inoculated at densities of 2-3 x 10^5 cells mL^{-1}. Cells were incubated at 37°C, 140 rpm, under 5% (v/v) CO_2 atmosphere in an orbital-shaking incubator (Inforst AG, Bottmingen/Basel, Switzerland). Measurements of cell density and cell viability were performed by trypan blue exclusion method using an automated cell counter. For this method, a sample of 550 µL of cell culture was loaded onto the Vi-CELL XR cell viability analyser (Beckmann Coulter, High Wycombe, UK).

2.1.2 Cryopreservation

Prior to cell cryopreservation CHO-S cells were sub-cultured in a 250 mL vent-capped Erlenmeyer shake flask (Corning, Surrey, U.K.) using 50 mL of glutamine supplemented CD CHO medium. Cells with high viability (≥95%) were seeded at densities of 2.5-3.5 x 10^5 cells mL^{-1}, incubated at 37°C, 140 rpm, under 5% (v/v) CO_2 atmosphere in an orbital-shaking incubator for 3 days. After the incubation, cell density and viability were measured using the trypan blue exclusion method using a Vi-CELL XR cell viability analyser according to the manufacturer instructions. The cells were then harvested and centrifuged at 200 g for 5 minutes, and then re-suspended in cold glutamine supplemented CD CHO medium containing 10% (v/v) DMSO (Sigma-Aldrich, Haverhill, U.K.) at densities of 6-7 x 10^6 cells mL^{-1}. 1.5 mL aliquots were dispensed into 1.8 mL Nunc Cryogenic vials (Thermo Scientific Nunc, Loughborough, U.K.). The vials were placed in a -20°C freezer for 4 hours, then transferred into a -70°C freezer overnight and finally transferred into liquid nitrogen for long term storage in a cryostat (Statebourne, Washington Tyne & Wear, U.K.).

2.1.3 Cell revival

Cryogenic vials were removed from liquid nitrogen storage and thawed for 1-2 minutes in a 37°C water bath. Once thawed, cells were transferred into 15 mL conical tubes containing 5 mL of cold fresh CD CHO medium and centrifuged at 200 g for 5 minutes. The cell pellet was then transferred and re-suspended in a 125 mL vent-capped Erlenmeyer shake flask using 20 mL of warm glutamine supplemented CD CHO medium. Cells were incubated at 37°C, 140 rpm, under 5% (v/v) CO_2 atmosphere in an orbital-shaking incubator. Cell density and viability were assessed by Trypan blue exclusion method using a Vi-CELL XR cell viability analyser. Before performing an experiment, cells were sub-cultured at least three times to restore optimal cell performance.

2.2 Clonal CHO-S cell line generation and characterisation

2.2.1 Cell cloning by limiting dilution cloning

To evaluate the inherent genetic heterogeneity found in the parental CHO-S population, 22 clonally-derived CHO-S cell lines were isolated from the parental CHO-S cell line through two rounds of limiting dilution cloning (LDC). Prior to single-cell isolation, the donor cell line (parental cell line) was subcultured three times in glutamine supplemented CD CHO medium at the initial cell density of 0.2×10^6 cells mL^{-1}. Cell density and viability were measured at the mid-exponential growth phase by trypan blue exclusion as described above. Then, 1×10^6 cells were harvested and serially diluted in warm glutamine supplemented CD CHO medium to a final cell density of 3.33 cells mL^{-1}. Finally, 150 µL of cell suspension were dispensed into each well of a 96-well culture plate (Thermo Scientific Nunc, Loughborough, U.K.). The plates were incubated at 37°C, in a 5% (v/v) CO_2 atmosphere for 21 days in a static incubator (Thermo Scientific Heracell, Loughborough, U.K.). After 24 hours of incubation, the plates were visually inspected in an inverse microscope to identify wells with single cells. Once identified, plates were returned into the static incubator. After 48 hours of incubation, the presence of single colonies was confirmed by visual observations using an inversed microscope. At day 15, half the volume of conditioned medium was replaced with fresh glutamine supplemented CD CHO medium in those wells containing a single colony.

To increase the probability of monoclonality, a second round of LDC was performed using single colonies form the first LDC round. For this, the number of cells

in single colonies were counted using an inversed microscope and diluted in glutamine supplemented CD CHO medium to a final cell density of 3.33 cells mL^{-1}. Then, the LDC procedures were performed as mentioned above. The probability of monoclonality after two LDC rounds was 0.97, calculated as described in section 2.5.2.

After two LDC rounds, single colonies were scaled-up in 24-well plates (Thermo Scientific Nunc, Loughborough, U.K.), followed by their expansion in 6-well plates (Thermo Scientific Nunc, Loughborough, U.K.) and 75 cm^2 cell culture flasks (T75 flask; Corning, Surrey, U.K.). Finally, clones were expanded in 125 mL Erlenmeyer shake flasks until sufficient cells were produced for cell banking and experimentation. Master cell banks were generated when high viability (≥95%) was reached. For this project, at this point, the generation number and passage number were reset to zero and one, respectively.

2.2.2 Long-term cell culture maintenance

To promote the acquisition of improved cellular capabilities, clones were subjected to a long-term cultivation (up to 220 generations) in 50 mL vent-capped cultiflask disposable bioreactors (Sartorius AG, Göttingen, Germany) using 5 mL of glutamine supplemented CD CHO medium. Cells were sub-cultured at initial densities of 2.5-3.5 x 10^5 cells mL^{-1} every 4 days and incubated at 37°C, 170 rpm, under 5% (v/v) CO$_2$ atmosphere in an orbital-shaking incubator. Cell samples (subpopulations) were cryopreserved at approximately 0, 40, 80, 120, 160 and 200 generations.

2.2.3 Fed-batch experiments

Prior to fed-batch experiments, cells were sub-cultured four times as mentioned in the Routine mammalian cell maintenance section (section 2.1.1). Then, fed-batch cultures were inoculated with densities of 2-3 x 10^5 cells mL^{-1} in 125 mL vent-capped Erlenmeyer shake flasks using 25 mL of glutamine supplemented CD CHO medium. Cells were incubated at 37°C, 140 rpm, under 5% (v/v) CO$_2$ atmosphere in an orbital-shaking incubator. Daily, cell density, cell viability and average cell diameter were assessed using 550 μL samples. Also, 180 μL samples were centrifuged at 200 g for 5 minutes to obtain the supernatant, which was stored at -20°C for glucose, lactate, glutamine, and glutamate quantification. CHO CD EfficientFeed™ B (Life Technologies, Paisley, U.K.) was used as nutrient supplement to meet the nutritional demands and maintain optimal cell growth performance during the fed-batch culture. A

multi-day supplementation of 10% (v/v) CHO CD EfficientFeed™ was fed at days 3, 5, 7 and 9. Fed-batch was terminated when cell viability dropped below 60%. Specific growth rate and integral of viable cell density was calculated according to Chusainow et al. (2009) (see section 2.5.3).

2.3 Mitochondrial bioenergetics

2.3.1 Measurement of oxygen consumption and extracellular acidification rates

Oxygen consumption rate (OCR) and extracellular acidification rate (ECAR) were measured using the cell metabolic analyser Seahorse XF24 (Seahorse Biosciences, North Billerica, MA, USA). Prior to experimentation, cells were sub-cultured four times in 125 mL vent-capped Erlenmeyer shake flasks (Corning, Surrey, U.K.) using 20 mL of glutamine supplemented CD CHO medium. Cells at mid-exponential growth phase were sampled on day 2 post-subculture to assess cell density and viability. Then, 2×10^6 cells were centrifuged at 200 g for 5 minutes and the cell pellet was re-suspended in fresh glutamine supplemented CD CHO medium at final density of 1.2×10^6 cells mL^{-1}. 100 µL aliquots were dispensed into 3 wells of a XF24 Tissue Culture Plate (Seahorse Biosciences, North Billerica, MA, USA) previously treated with 50 µL of 22.4 µg mL^{-1} BD Cell-Tak cell and tissue adhesive (BD Biosciences, Oxford, U.K.). The plate was incubated at 37°C, under 5% (v/v) CO_2 atmosphere in a static incubator for 30 minutes to allow cell attachment. Two plates were required, one for glycolysis and one for mitochondrial evaluation. After incubation, cells were inspected using an inversed microscope to confirm cell attachment. Conditioned CD CHO media was then removed and replaced with either 600 µL of un-buffered XF media supplemented with 2 mM L-glutamine at pH 7.4 for glycolysis evaluation or 600 µL of un-buffered XF media supplemented with 2 mM L-glutamine and 16.74 mM glucose at pH 7.4 for mitochondrial respiration evaluation. The plates were then incubated for 30-45 minutes at 37°C in a CO_2 free incubator to allow temperature and pH equilibration before transferring to the XF24 analyser. The seahorse XF24 extracellular analyser was run using an 8 minute cyclic protocol (mix for 3 minutes, wait for 2 minutes and measure for 3 minutes) in triplicate. After either measuring the basal OCR or the basal ECAR, the cells were sequentially treated with 83.33 mM glucose, 11.25 µM oligomycin and 1 M 2-deoxy-D-glucose (2-DG) to give a final concentration of 10 mM glucose, 1.125 µM oligomycin, 100 mM 2-DG during the glycolysis analysis or sequentially treated with 10 µM oligomycin, 11.25 µM carbonyl cyanide p-[trifluoro-methoxy]-phenyl-hydrazone (FCCP) and 12.5 µM

rotenone/antimycin A to give a final concentration of 1 µM oligomycin, 1.25 µM FCCP and 1 µM rotenone/antimycin A during the mitochondrial analysis.

For the glycolysis analysis the Seahorse injection ports were loaded as follows:

- Port A: 81.8 µL of 83.33 mM glucose pH 7.4 (glycolysis inducer)
- Port B: 75.4 µL of 11.25 µM oligomycin (ATP synthase inhibitor)
- Port C: 84.2 µL of 1 M 2-DG pH 7.4 (glucose analogue, glycolysis inhibitor)

For the mitochondrial analysis the Seahorse injection ports were loaded as follows:

- Port A: 66.7 µL of 10 µM oligomycin (ATP synthase inhibitor)
- Port B: 74.1 µL of 11.25 µM FCCP (ETC accelerator)
- Port C: 82.3 µL of 12.5 µM Antimycin A / Rotenone (ETC inhibitors)

2.4 Analytical methods

2.4.1 Metabolite analysis

Glucose, lactate, glutamine and glutamate concentration were quantified at different time points of the fed-batch culture (i.e., 2, 3, 5, 7, 9 and 11 days) using a Cedex bio analyser (Roche Diagnostics Ltd., West Sussex, U.K.). The Cedex bio analyser uses hexokinase method for glucose determination, lactate oxidase method for lactate, glutaminase for glutamine and glutamate oxidase for glutamate determination. Prior to measurements, the Cedex analyser's probe was cleaned with 1 ml of ISE deproteiniser (Roche Diagnostics Ltd., West Sussex, U.K.) and conditioned with 0.75 ml of Activator (Roche Diagnostics Ltd., West Sussex, U.K.). Then, two-point calibration were performed for glucose, lactate, glutamine and glutamate assays, followed by a quality control check to ensure the integrity of the whole measuring system by measuring and comparing the known concentration of the controls (Roche Diagnostics Ltd., West Sussex, U.K). Finally, 150 uL of cell-free supernatant samples, previously collected at days 2, 3, 5, 7, 9 and 11 of the fed-batch culture, were thawed for 15 minutes at 4°C and measured in duplicate on a Cedex bio analyser according to the manufacturer instructions.

2.4.2 Protein content assay

Protein content was determined using Pierce BCA Protein Assay Kit (Thermo Scientific, Surrey, U.K.) according to the manufacturer instructions. For each sample, 2.5×10^6 cells were pelleted and then washed with 0.8 mL PBS, centrifuging at 200 g for 5 minutes at 4°C. Cells were lysed using 1 mL of RIPA buffer (Thermo Scientific, Surrey, U.K.) supplemented with Halt Protease Inhibitor Cocktail 1% [v/v] (Life Technologies, Paisley, U.K.), centrifuging at 14000 g for 15 minutes and the supernatant was collected and stored at -20°C until protein analysis. The protein concentration was measured at 570 nm using a PowerWave™ spectrophotometer plate reader (BioTeK, Bedfordshire, U.K.). The blank background fluorescence was subtracted from each reading to give relative protein content. The protein concentration was determined using a standard curve provided in the Pierce BCA Protein Assay Kit.

2.5 Equations

2.5.1 Colony forming efficiency

The colony forming efficiency (C.E.) was calculated using the following equation:

$$C.E.\,(\%) = \frac{number\ of\ single\ colonies}{Total\ number\ of\ inoculated\ wells} x100$$

2.5.2 Probability of monoclonality

The probability of monoclonality using LDC was calculated according to Coller and Coller (1983) using the following equations:

Probability of monoclonality for a single LDC round

$$\text{P(clonality)} = \frac{\text{P}(1)}{(\,1 - \text{P}(0)\,)} = \frac{S}{R}$$

Probability of monoclonality for two repetitive LDC rounds

$$\text{P(clonality)} = y + x + \frac{Aa}{2} + \frac{Ab}{3} + \frac{Ac}{4} + \frac{Ad}{5} \ldots$$

$$+ \frac{Ba}{4} + \frac{Bb}{9} + \frac{Bc}{16} + \frac{Bd}{25} \ldots$$

$$+ \frac{Ca}{8} + \frac{Cb}{27} + \frac{Cc}{64} + \frac{Cd}{125} \ldots$$

Where:

$P(clonality) = probability\ that\ a\ given\ well\ in\ the\ Plate\ 2\ contains\ only\ a\ single\ clone$

$$y = \frac{S}{R}\ for\ the\ second\ subcloning$$

$$x = \frac{S}{R}\ for\ the\ first\ subcloning$$

$$A = \frac{fraction\ of\ wells\ in\ 2nd\ subcloning\ containing\ 2\ cells}{fraction\ of\ wells\ in\ 2nd\ subcloning\ showing\ any\ growth} = \frac{P(2)}{(1-P(0))} = \frac{2}{R^A}$$

$$B = \frac{fraction\ of\ wells\ in\ 2nd\ subcloning\ containing\ 3\ cells}{fraction\ of\ wells\ in\ 2nd\ subcloning\ showing\ any\ growth} = \frac{P(3)}{(1-P(0))} = \frac{3}{R^B}$$

$$C = \frac{fraction\ of\ wells\ in\ 2nd\ subcloning\ containing\ 4\ cells}{fraction\ of\ wells\ in\ 2nd\ subcloning\ showing\ any\ growth} = \frac{P(4)}{(1-P(0))} = \frac{4}{R^C}$$

$$D = \frac{fraction\ of\ wells\ in\ 2nd\ subcloning\ containing\ 5\ cells}{fraction\ of\ wells\ in\ 2nd\ subcloning\ showing\ any\ growth} = \frac{P(5)}{(1-P(0))} = \frac{5}{R^D}$$

$$a = \frac{fraction\ of\ wells\ in\ 1st\ subcloning\ containing\ 2\ cells}{fraction\ of\ wells\ in\ 1st\ subcloning\ showing\ any\ growth} = \frac{P(2)}{(1-P(0))} = \frac{2}{R^a}$$

$$b = \frac{fraction\ of\ wells\ in\ 1st\ subcloning\ containing\ 3\ cells}{fraction\ of\ wells\ in\ 1st\ subcloning\ showing\ any\ growth} = \frac{P(3)}{(1-P(0))} = \frac{3}{R^b}$$

$$c = \frac{fraction\ of\ wells\ in\ 1st\ subcloning\ containing\ 4\ cells}{fraction\ of\ wells\ in\ 1st\ subcloning\ showing\ any\ growth} = \frac{P(4)}{(1-P(0))} = \frac{4}{R^c}$$

$$d = \frac{fraction\ of\ wells\ in\ 1st\ subcloning\ containing\ 5\ cells}{fraction\ of\ wells\ in\ 1st\ subcloning\ showing\ any\ growth} = \frac{P(5)}{(1-P(0))} = \frac{5}{R^d}$$

These equations used Poisson distribution methods for describing the cell distribution in micro-titre plates in single or repetitive rounds of sub-cloning

2.5.3 Cell growth

Cell growth, specific growth rate, doubling time and generation number were calculated using the following equations.

Specific growth rate (μ):

$$\mu = \frac{Ln\left(\frac{X_1}{X_0}\right)}{t_1 - t_0}$$

Doubling time (dt):

$$dt = \frac{Ln(2)}{\mu}$$

Generation number (GN):
$$GN = \frac{Ln\left(\frac{X_1}{X_0}\right)}{Ln(2)} = \frac{\mu(t_1 - t_0)}{Ln(2)}$$

Integral of viable cell density (IVCD):
$$IVCD = \frac{(X_1 - X_0)(t_1 - t_0)}{Ln\left(\frac{X_1}{X_0}\right)} = \frac{(X_1 - X_0)}{\mu}$$

Specific metabolic rate (qMet):
$$qMet = \frac{(Met_1 - Met_0)((X_1 - X_0)(t_1 - t_0)}{Ln\left(\frac{X_1}{X_0}\right)} = \frac{Met_1 - Met_0}{IVCD_1 - IVCD_0}$$

Integral of cellular protein accumulation (ICPA):
$$ICPA = \frac{(PrC_1 - PrC_0)((X_1 - X_0)(t_1 - t_0)}{Ln\left(\frac{X_1}{X_0}\right)} = \frac{PrC_1 - PrC_0}{IVCD_1 - IVCD_0}$$

Cell volume
$$\text{Cell volume} = \frac{4}{3}\pi \frac{\text{cell diameter}}{2}$$

Where:

   t_0 and t_1 is the time at time points 0 and 1, respectively

   X_0 and X_1 is the viable cell density at time points 0 and 1, respectively

   PrC_0 and PrC_1 is the cellular protein content at time points 0 and 1, respectively

   Met_0 and Met_1 is the metabolite concentration at time points 0 and 1, respectively

2.5.4 Standard error of the mean

The standard error of the mean (SEM) was used to express the mean of data in the form of the mean ± SEM.

$$SEM = \frac{(x - m)^2}{n(n - 1)}$$

Where:

   x is the observed value

   m is the arithmetic mean of n observations

   n is the number of independent observations

n-1 is the number of degrees freedom

Chapter 3

EXPLOITING THE PHENOTYPIC HETEROGENEITY IN CHINESE HAMSTER OVARY CELL POPULATIONS AND EVOLVING GROWTH CHARACTERISTICS DURING LONG-TERM CULTURE

Chapter 3

Exploiting the phenotypic heterogeneity in Chinese Hamster Ovary cell populations and evolving growth characteristics during long-term culture

This chapter introduces the procedures employed to harness the genetic heterogeneity within CHO-S cell populations, followed by a cell expansion and a routinely long-term sub-cultivation to improve the cells' fitness (e.g. high specific growth rate and VCD) and gain insight into the dynamic mechanism of genetic instability and genetic drift in CHO cells.

3.1 Background

The production of biopharmaceuticals using mammalian cell systems has been widely expanded in the last decades, being CHO cells the preferred mammalian expression system at industrial scale (Wurm 2004), mainly because they can easily be genetically manipulated to produce complex recombinant glycoproteins with correct folding and safe therapeutic applications, and because of their robust growth performance and adaptability to synthetic environments. Since their origins, CHO cells have been exposed to multiple physical and genetic manipulations that have increased their genomic instability, leading to cumulative mutations (Derouazi et al. 2006; Torsvik et al. 2014) and developing a large number of derived CHO cell lines with varied phenotypes such as CHO DG44, CHO-K1, CHO-K1SV, CHO-S, and DUKX-B11. Throughout this time, CHO cells evolved beneficial characteristics that allowed them to adapt, proliferate, resist and survive in synthetic environments (Gillies et al. 2012), but also developed detrimental features that increased their genetic instability leading to unpredictability in terms of cell growth (Barnes et al. 2006), recombinant protein productivity (Barnes et al. 2001; Beckmann et al. 2012; Chusainow et al. 2009) and protein quality (van Berkel et al. 2009).

The undesirable characteristics have been extensively studied. For example, cytogenetic studies revealed that CHO cells have accumulated a large number of chromosome aberrations such as amplification, deletion, translocation, aneuploidy and polyploidy since their origins. These aberrations moulded a wide range of genomic mutations and drove significant changes in morphology and metabolism among derived-CHO cell lines (Deaven and Petersen 1973; Derouazi et al. 2006). This

genomic instability has been widely used to develop numerous industrial CHO cell lines with optimal growth performances and desirable gene-production characteristics (Barnes et al. 2006; Prentice et al. 2007; van Berkel et al. 2009). However, cell line development processes still present limitations, mainly because CHO cells have unstable and unpredictable cellular behaviours which make costly, labour-intensive and time-consuming the identification and selection of improved phenotypes (O'Callaghan and James 2008; Pilbrough et al. 2009). Therefore, the likelihood of isolating an ideal CHO cell line with desirable industrial characteristics is extremely low due to poor understanding of genetic drift and the heterogeneous evolution along increasing generations. Several studies have analysed the global cellular metabolism of improved cell lines (Chusainow et al. 2009; Kyriakopoulos et al. 2013; Legmann et al. 2011; Luo et al. 2012) and the phenotypic variation throughout cultivation (Barnes et al. 2006; Beckmann et al. 2012; Davies et al. 2012; Heinrich et al. 2011) to identify metabolic and phenotypic characteristics that allow the selection of cell lines with desirable characteristics. These studies have demonstrated that a low glucose and glutamine consumption (Altamirano et al. 2004; Cruz et al. 1999; Kim et al. 2013; Kurano et al. 1990; Lee et al. 2003; Wong et al. 2005), lactate-metabolism shift (Dorai et al. 2009; Mulukutla et al. 2012; Zagari et al. 2013) and an elevated TCA cycle activity (Papandreou et al. 2006; Wilkens and Gerdtzen 2011; Zhou et al. 2011) are the most important metabolic characteristics associated with cell growth and productivity improvements in fed-batch cultures.

The mammalian cell culture is continually subjected to genetic drift effects as a result of extensive sub-cultivation (Torsvik et al. 2014). Studies have demonstrated that routine sub-cultivation drives significant improvements in cell growth performance (Beckmann et al. 2012; Davies et al. 2012; Torsvik et al. 2014), but reduce productivity (Beckmann et al. 2012; Chusainow et al. 2009). Beckmann et al. (2012) observed that elevated cell passage number significantly improved growth characteristics as a result of increments in glucose utilisation, over-expression of glycolytic enzymes (i.e., PYK, phosphoglycerate mutase 1; PGAM-1, and phosphoglycerate kinase 1; PGK-1) and up-regulation of non-ER anti-stress proteins. These studies also revealed that an extended cultivation promotes recombinant-gene loss even under selective pressure, leading to notable reductions in heavy and light chain transcripts. These data showed that over long-term cultivation cells acquired a more robust phenotype and become more glycolytic, providing higher tolerance to environmental stress and producing ATP rapidly, this robustness supports higher cell densities and proliferation rates.

The accumulated data suggests that the inherent genetic instability within CHO populations confer adaptive advantages (Jones and Baylin 2007; Nowell 1976; Silander et al. 2007; Stich et al. 2010) and together with the random genetic drift may shape the genetic pool and allow individual cells to out-compete other subpopulations and gradually dominate the whole population. Indeed, by combining the genetic instability and genetic drift in synthetic environments, populations may undergo beneficial mutations (Stich et al. 2010) as higher selection pressures may confer specific fitness characteristics in the long-term such as high tolerance to lactate and ammonia (Schumpp and Schlaeger 1992), osmolarity (Liu et al. 2010; Sunley et al. 2008), hypothermia (Sunley et al. 2008), synthetic environments (Sinacore et al. 2000), and attain high cell densities (Prentice et al. 2007). However, it cannot be ignored that these evolutionary mechanisms may also lead to completely altered phenotypic characteristics (Hallatschek et al. 2007; Loeb 2001), resulted from deleterious mutations (Stich et al. 2010; Torsvik et al. 2014) that may increase even further the genetic instability (Jones and Baylin 2007).

As mentioned before, CHO cells exhibits an enormous phenotypic heterogeneity mainly because they have been exposed to genetic instability, epigenetic changes, natural selection and genetic drift over many years, accumulated a vast number of mutations which have generated an enormous potential isolate superior phenotypes capable to withstand biopharmaceutical processes, proliferate at high cell densities and produce large quantities of recombinant proteins (O'Callaghan and James 2008).they

3.2 Chapter aims

In this chapter, I investigated two hypotheses, (i) that the inherent genetic instability within a donor CHO-S population can be exploited to generate cell lines with improved growth characteristics and (ii) that genetic drift and directed evolution will promote better growth phenotypes. Thereby, I suggest that:

(i)   The inherent cellular heterogeneity present in a parental CHO-S population can be exploited through basic cloning techniques, allowing the isolation of multiple clonally-derived cell lines with desired and relevant manufacturing characteristics such as maximal specific growth rate and improved integral of viable cell density.

(ii)   The extent of phenotypic heterogeneity among clonal CHO-S cell lines can be reduced by accelerating the random genetic drift through a continuous and extended sub-cultivation.

(iii)   Genetic drift will favour the dominance of fast-growing subpopulations, significantly improving the overall cell performance throughout the long-term subculture.

The aim of this chapter is to present an approach to harness the inherent phenotypic heterogeneity within a donor CHO-S cell line to produce functional sub-clones with relevant industrial capabilities by using the traditional limiting dilution cloning (LDC) technique and by accelerating the genetic drift selection through a routine and prolonged sub-cultivation. Additionally, I aimed to (i) characterise differences in morphology, in terms of cell size, and growth behaviour of 22 clonally-derived cell lines and compare them to the parental CHO-S population, (ii) study the genetic drift effects in growth patterns and cellular heterogeneity through long-term cultivation and (iii) compare the adaptation rates of isolated clonal populations, especially to the agitated conditions of the culture. Finally, I aimed to identify characteristics that could improve screening methodologies for selecting subpopulations with enhanced and relevant phenotypes.

3.3 Chapter objectives

To address the chapter aims, the objectives were to:

i) Isolate a panel of clonally-derived CHO-S cell lines from a donor parental CHO-S population.

ii) Characterise the clone's growth behaviour along the extended cultivation.

iii) Generate a set of subpopulations at different time points of the long-term cell cultivation.

iv) Assess and compare the genetic drift effects in growth performance among clonal CHO-S cell lines during the long-term cultivation.

v) Examine and compare cell growth profiles among and within clonal cell lines along the extended culture.

vi) Quantify the level of phenotypic heterogeneity within and between clones along the extended culture.

vii) Identify clones with enhanced phenotypic characteristics such as maximal specific growth rate (μ), higher peak of viable cell density and fast rate of adaptability.

3.4 Results

3.4.1 Harnessing the phenotypic heterogeneity of a donor parental CHO-S population

The cellular heterogeneity within a donor parental CHO-S population was assessed using a strategy linking two approaches: harnessing and exploiting the phenotypic heterogeneity within the donor CHO-S population and evolving cell phenotypes through accelerated genetic drift and directed evolution through long-term cell culture in a chemically defined media (Figure 3-1). (i) To exploit the phenotypic abundance within the parental CHO-S population, clonally-derived cell lines were isolated through two LDC rounds, and (ii) to evolve improved phenotypic characteristics, clonally derived CHO cell lines underwent an accelerated genetic drift and directed evolution as a result of a continuous sub-cultivation (up to 220 generations) in a chemically defined media. Finally, to assess phenotypic variations among and within clonal CHO-S cell lines during the long-term sub-cultivation, cell samples were cryopreserved approximately every 40 generations (identified as "subpopulations") for subsequent experimentation. In addition, for enabling further comparisons and minimise environmental stress variations, all clones were sub-cultivated using the same batch media, supplements and culture conditions.

After the first LDC round, only 22 wells were identified as single colonies from a total of 1920 wells seeded, giving a cloning efficiency of 1.15% with a probability of monoclonality of 0.771, indicating that almost three out of four colonies were monoclonal. This data agrees with other studies that found that a single round of cell cloning does not guaranty the monoclonality of the colonies (Barnes et al. 2006). For that reason, a second round of LDC was performed (Figure 3-2B), at this point the probability of monoclonality for repetitive rounds of cell cloning was 0.97, ensuring monoclonality.

For the purpose of these studies, the generation and passage number of the generated clones' master cell banks were reset to "zero" and "one", respectively, to enable future comparisons between clones and trace phenotype evolution throughout the long-term sub-cultivation.
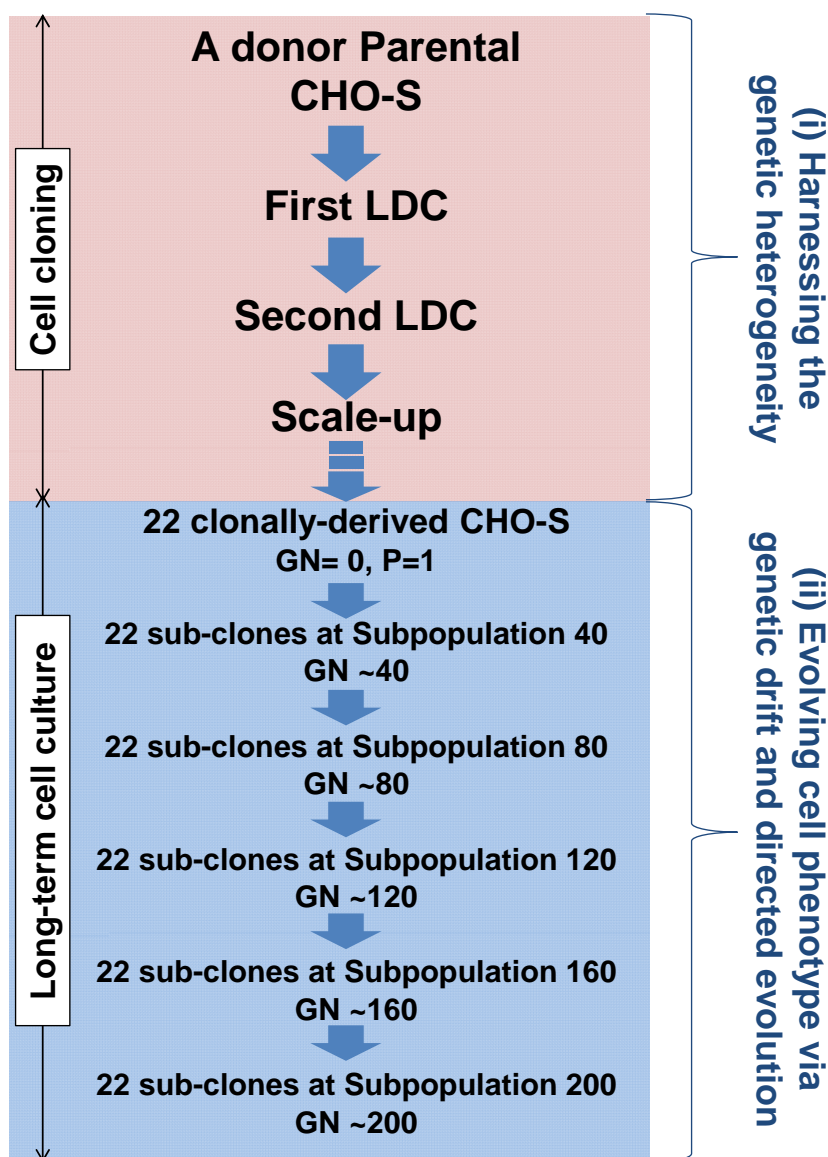
Figure 3-1 Strategy to (i) harness and exploit the phenotypic heterogeneity within a donor CHO-S population and (ii) evolve cell phenotypes through accelerated genetic drift and directed evolution through long-term cell culture in a chemically defined cell culture media. The diagram indicates the strategy for cell cloning, scaling-up and long-term cultivation. Parental CHO-S cells were subjected to two rounds of LDC, scale-up and transfer from static to agitated incubation and finally sub-cultured in a long-term regime for up to 220 generations. For each clone, cell growth performance along the culture was analysed and subpopulations were cryopreserved approximately every 40 generations. A total of 6 subpopulations per clone were cryopreserved at generations 0, 40, 80, 120, 160 and 200.
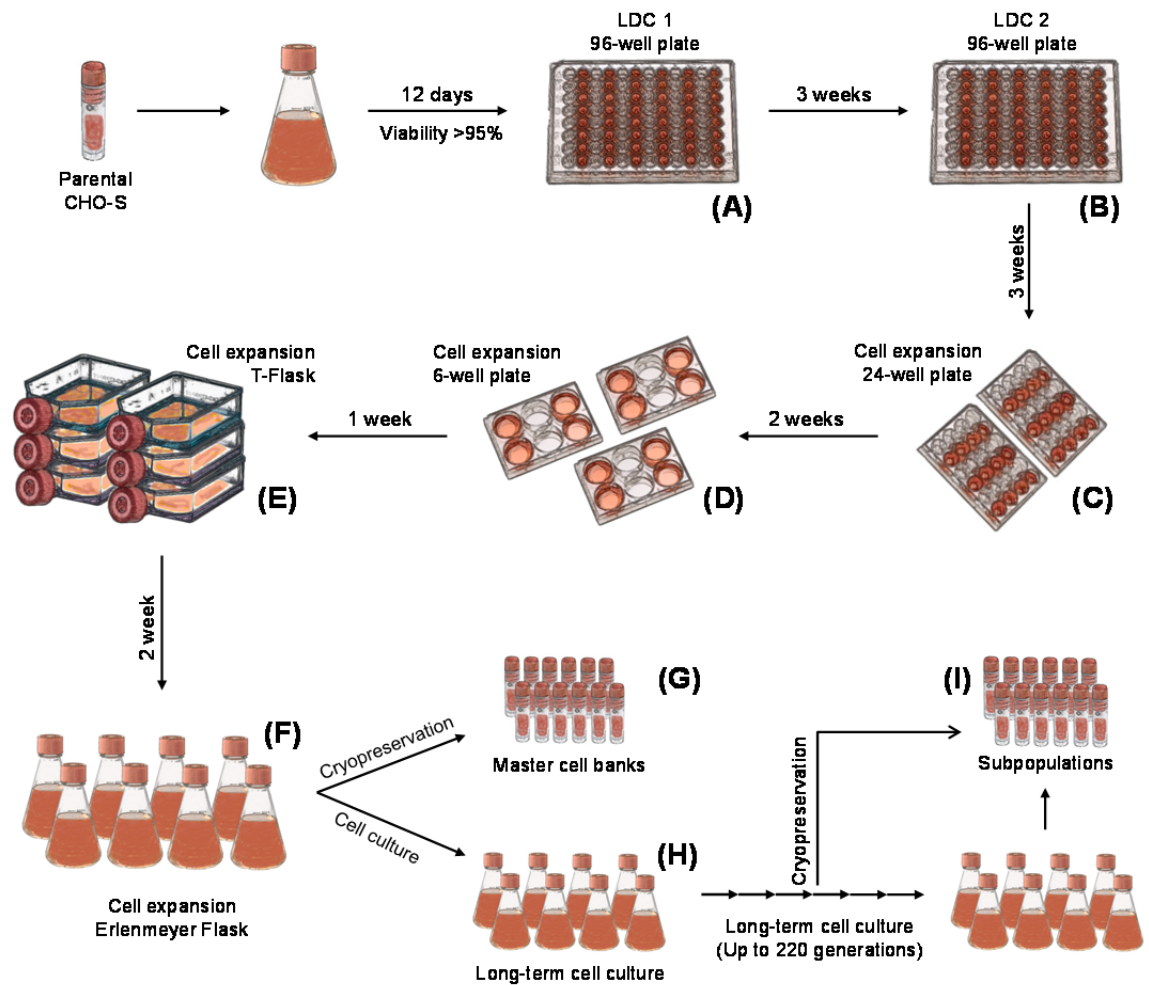
Figure 3-2 Schematic representation of the cell cloning strategy. 22 clonally-derived CHO-S cell lines were isolated from a donor parental CHO-S population through two rounds of limiting dilution cloning in CD CHO medium supplemented with 8 mM L-glutamine at densities of 0.5 cells per well (A-B). Wells that exhibited single cell colonies were gradually scaled-up into larger cell culture vessels, from 96-well plates to T-75 flasks in a static incubator (B-E). Then, the clones were scaled-up to 125 mL Erlenmeyer flasks and incubated in a shaking incubator until high cell viability was achieved (F). Finally, master cell banks were created for every clonally-derived CHO cell line and cryopreserved in liquid nitrogen (G). Also, each clone was sub-cultivated at 190 rpm and 37°C under 5% (v/v) CO_2 atmosphere for up to 220 generations in 125 mL Erlenmeyer flasks containing CD CHO medium supplemented with 8 mM L-glutamine (H). Every 40 generations, subpopulations were cryopreserved (I).

The second part of the proposed strategy was designed to evaluate whether cell lines can develop superior phenotypes by subjecting them to long-term cultivation and to characterise the growth behaviour resulted from the genetic instability and genetic drift along cultivation. This strategy consisted in routinely propagating the 22 CHO-S clones under agitated conditions for up to 220 generations with a four-day subculture regime to ensure constant exponential cell growth during the whole cultivation (Figure 3-1 and Figure 3-2H). To enable further intra and inter clonal comparisons, cell samples or subpopulations were harvested and cryopreserved every 40 generations (Figure 3-2I), giving six subpopulations per clone (i.e., at ~ 0, 40, 80, 120, 160 and 200 generations) and a total of 132 subpopulations with varied growth and metabolic characteristics.

At first glance, it was observed that the growth behaviour throughout the extended cell cultivation was clearly separated in two phases, being the first an adaptation phase between zero and 50 generations, characterised by low growth rates (median $\mu < 0.031$ h^{-1}) and random fluctuations in μ resulted from transferring the cells from static to agitated environment (Figure 3-3A). The second phase defined as evolution phase characterised by gradual increments in proliferation rates and significant reductions in cellular heterogeneity with increasing generation number (Figure 3-3A). The high phenotypic heterogeneity observed in the clonal CHO-S cell lines clearly indicates substantial differences among populations, which arises from genetic, epigenetic and selection factors and supports the hypothesis that cell lines with varied cell growth characteristics can be isolated from a donor population (Figure 3-3). This observed data also agrees with previous studies which found an intrinsic cellular heterogeneity among clonally-derived CHOK1SV (Davies et al. 2005) and NS0 (Barnes et al. 2006) populations.

The extent of cellular heterogeneity within each clone and between them was evaluated using specific growth rate as indicator of phenotypic heterogeneity (Figure 3-3B and Figure 3-3C). Comparing the distribution ranges in μ along the whole cultivation (Figure 3-3B), clones 1, 10, 11, 13, 16, 19 and 22 were the most stable cell lines over the long-term cultivation, whilst clones 6, 7, 8, 15, 18 and 20 were by far the most heterogeneous cell lines. The slightly right-skewed box plot data in Figure 3-3B also suggests that CHO-S clones tended to improve the growth characteristics with increasing generation number.
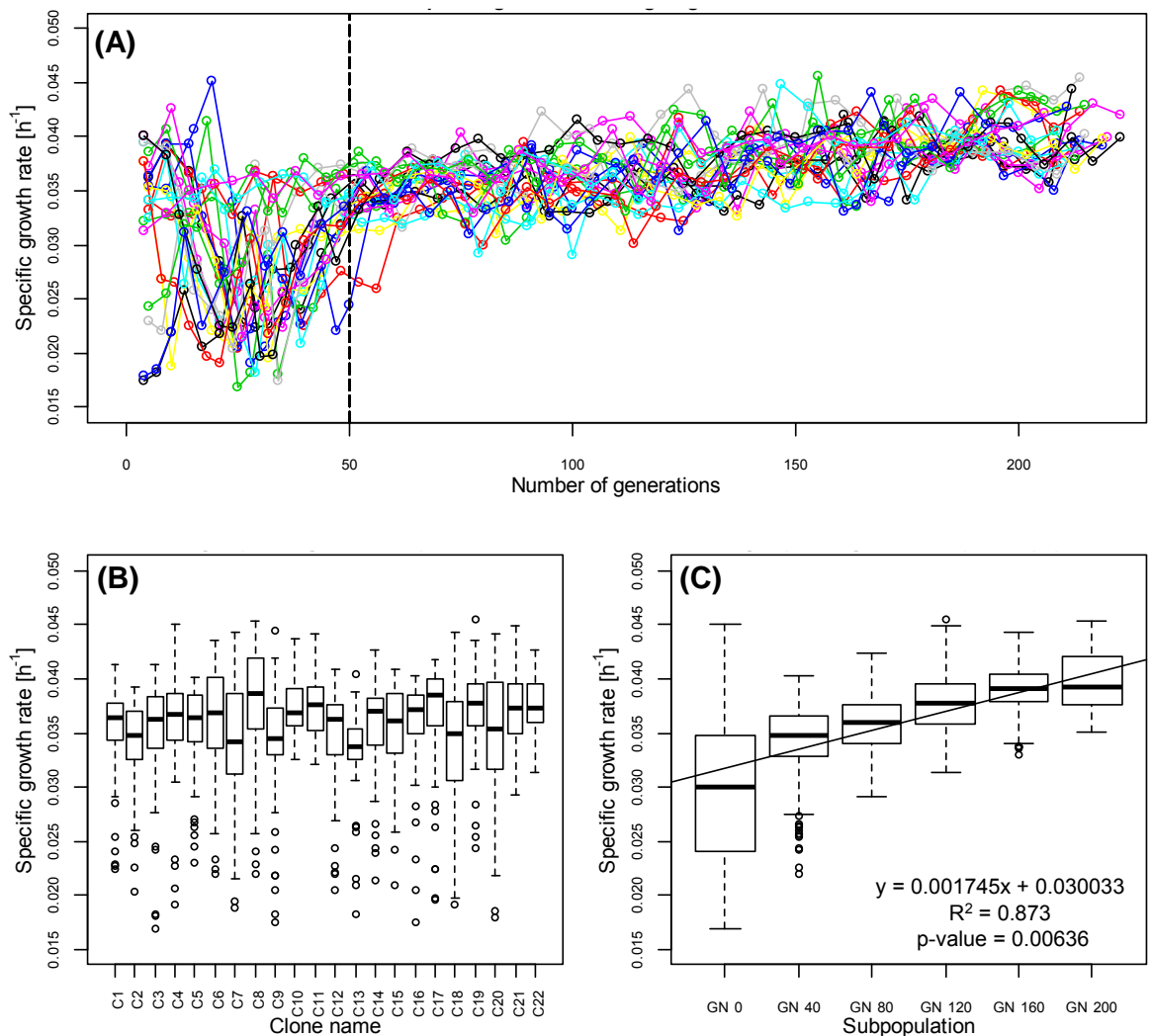
Figure 3-3 Specific growth rate patterns for 22 clonally-derived CHO-S cell lines along long-term culture. Clones were grown in Erlenmeyer flasks for up to 220 generations to characterise their growth phenotype. Specific growth rates were calculated using the viable cell density at the beginning and end of each passage (A). Then, the extent of growth heterogeneity along long-term cultivation was analysed for each individual clone (B) and for all 22 clones classified into subpopulations (C). The overall rate of change in μ along subpopulations was calculated as the linear regression of the median of the observed cell growth rate values for each subpopulation. "Subpopulation 0" groups generations 0 to 39, "subpopulation 40" groups generations 40 to 79, "subpopulation 80" groups generations 80 to 119, "subpopulation 120" groups generations 120 to 159, "subpopulation 160" groups generations 160 to 199 and "subpopulation 200" groups generations 200 to up to 220.

For enabling further comparisons, the μ data was divided into 6 subpopulations with the intention that each subpopulation would represent the time point at which cells were cryopreserved along the long-term culture regime. Therefore, μ data was separated in "subpopulation 0" grouping data from generations 0-39, "subpopulation 40" grouping generations 40-79, "subpopulation 80" grouping generations 80-119, "subpopulation 120" grouping generations 120-159, "subpopulation 160" grouping generations 160-199 and "subpopulation 200" grouping generations 200-up to 220.

Grouping the data of all clones by subpopulations confirmed that clones continuously improved their growth phenotype and reduced their heterogeneity (Figure 3-3C) and demonstrated that the age of the clones (i.e., 0, 40, 80 160 or 200 generations) had an effect on μ (two-way ANOVA, $p<0.0001$, F=166.17). Also, Tukey's test corroborated the significant μ differences between all the subpopulations, but except between subpopulations 160 and 200 (Tukey's test, $p>0.05$). Moreover, the large distribution range at subpopulation 0 indicates that clones tended to increase their heterogeneity in order to develop fitness to the agitated environment whilst the reduced distribution on the subsequent subpopulations showed a tendency to reduce heterogeneity over time. In addition, the left-skewed data in subpopulation 0 indicates that slow-growing phenotypes were the dominant populations at early generations.

The linear regression in Figure 3-3C shows a positive and strong correlation between growth rate and subpopulations with accumulative generations (R-squared=0.873, n=6, p-value=0.0064), supporting that growth phenotypes were improved over increasing generations with an overall average rate of change in μ of 0.00176 h^{-1} per subpopulations or 4.5×10^{-5} h^{-1} per generation. Moreover, the plateau observed between subpopulations 160 and 200 indicates that clones may have a maximum possible μ supported for the glutamine supplemented CD CHO media under the selected conditions (e.g., 170 rpm in 5 mL cultiflask disposable bioreactor) and probably clones started to reach their maximum and stable μ after 160 cell generations.

A slightly negative correlation between the extent of μ heterogeneity and subpopulations with accumulative generations can be observed in Figure 3-3C, being this reduction more evident from subpopulations 0 to 40 with a 66% of reduction in the overall heterogeneity, thus confirming the existence of an adaptation phase at subpopulation 0. This data was followed by a modest but significant reduction in cellular heterogeneity (between 2 and 27.8%) from subpopulations 40 to 160, suggesting that these reductions resulted from genetic drift. Finally, the maintenance of the μ median (~0.039 h^{-1}) from subpopulation 160 to 200 suggest that clones may have converged to a maximum μ under these cultivation environment, but the significant

increase in μ heterogeneity (69%) from subpopulation 160 to 200 suggest that cell populations still attempted to acquired better growth rates, but probably these populations with potential for higher μ were not become dominant as they demanded different nutritional demands (e.g., amino acid) which were not constantly provided by the supplemented CD CHO media (Huang 2009).

3.4.2 Long-term cultivation improved the growth characteristics in clonal CHO-S cell lines

To test the hypothesis that clones exhibited notable differences in their growth patterns over increasing generations, the extent of cellular heterogeneity within each clone was evaluated using the accumulated data from their respective six subpopulations (Figure 3-4). At first glance, it seems that all cell lines increased their specific growth rate and significantly reduced their growth rate heterogeneity with increasing generation number. Being clones 10, 11, 21 and 22 those populations that exhibited a substantially lower initial heterogeneity and maintained their low heterogeneity throughout cultivation, whereas clone 6 was the most heterogeneous population during the whole extended cultivation. The box and whisker plots also confirmed the existence of elevated phenotypic variability among clones, particularly at subpopulations 0 with growth rates ranging from 0.017 h^{-1} to 0.045 h^{-1} for clones 3 and 4, respectively. The subsequent subpopulations narrowed the heterogeneity, reaching the smallest difference in μ at subpopulations 200, being clone 12 (0.035 h^{-1}) and clone 11 (0.045 h^{-1}) the slowest and fastest growing cell lines, respectively.

The observed reductions in phenotypic heterogeneity from subpopulations 0 to 200 were highly variable, observing global decreases from 42.9% for clone 9 to 95.0% for clone 3 (Figure 3-4). The majority of the clones (15 out of 22 clones; clones 1, 2, 3, 4, 5, 7, 8, 12, 13, 14, 16, 17, 18, 19 and 20) showed considerable reductions in growth rate heterogeneity (>80%), whilst six clones (clones 6, 9, 11, 15, 21 and 22) presented reductions between 42.9 and 71%. From the 22 clones, only clone 10 increased its heterogeneity along the long-term cultivation, displaying two separate growth performances throughout cultivation. The first was a steady phase from subpopulations 0 to 80, characterised by low growth heterogeneity and high proliferation rates and the second stage was a heterogeneous phase from subpopulations 120 to 200, characterised by notable increments in growth heterogeneity, but without decreases in the mean growth rate. This observed behaviour in clone 10 probably resulted from two causes, the first cause resulted from the intrinsic genetic instability which fixed a spontaneous non-beneficial mutation altering the growth homeostasis of the population

and the second cause as the result of genetic drift which modified the stablished growth rate equilibrium through the random sampling of a non-dominant subpopulation, this random genetic competition has been documented in bacteria and yeast populations (Hallatschek et al. 2007). The observed unbalance derived in increased phenotypic heterogeneity in succeeding generations until the "new-fixed" subpopulation would become extinct, coexist or become dominant (Greaves and Maley 2012; Hallatschek et al. 2007; Nowell 1976). Both possibilities mentioned above are conceivable because populations carry accumulated mutations with potential to change the phenotype at any moment (Torsvik et al. 2014) and because the random sampling can change the equilibrium of a population by fixing subpopulations with varied physiological characteristics.

Another important finding can be observed during the evolution phase, in which most of the clones eventually exhibited a plateau. The plateau is more notable in clones with initial high growth rates (Figure 3-4, clones 3, 4, 10, 14, 15, 16 and 21) corroborating that clonal cell lines have a maximum μ possible in the glutamine supplemented CD CHO media cultivation implemented for this study.

For each clone, the average rate of change in μ was calculated as the slope of the linear regression of the growth rate values between 0 and up to 220 generations. Using the slope values, clones 7, 8, 9, 18 and 20 exhibited the largest rates, between 6.5×10^{-5} and 8.0×10^{-5} h^{-1} per generation, with a global improvement in μ between 0.013 and 0.016 h^{-1} along 200 generations. On the other hand, clones 4, 10, 16, 21 and 22 exhibited the smallest rates of change, observing increments in μ between 2.6×10^{-5} and 3.4×10^{-5} h^{-1} per generation and giving global improvements between 0.0052 and 0.0068 h^{-1} after 200 generations (Figure 3-4). As expected, the initially slow-growing clonal populations reached the highest rates of change in μ, whereas clones with the lowest rates change in μ presented smaller improvements. This data suggest that populations with slow changes rates in μ exhibited agitation-adapted phenotypes from their isolation, thus showing less heterogeneous populations, except for clone 7.
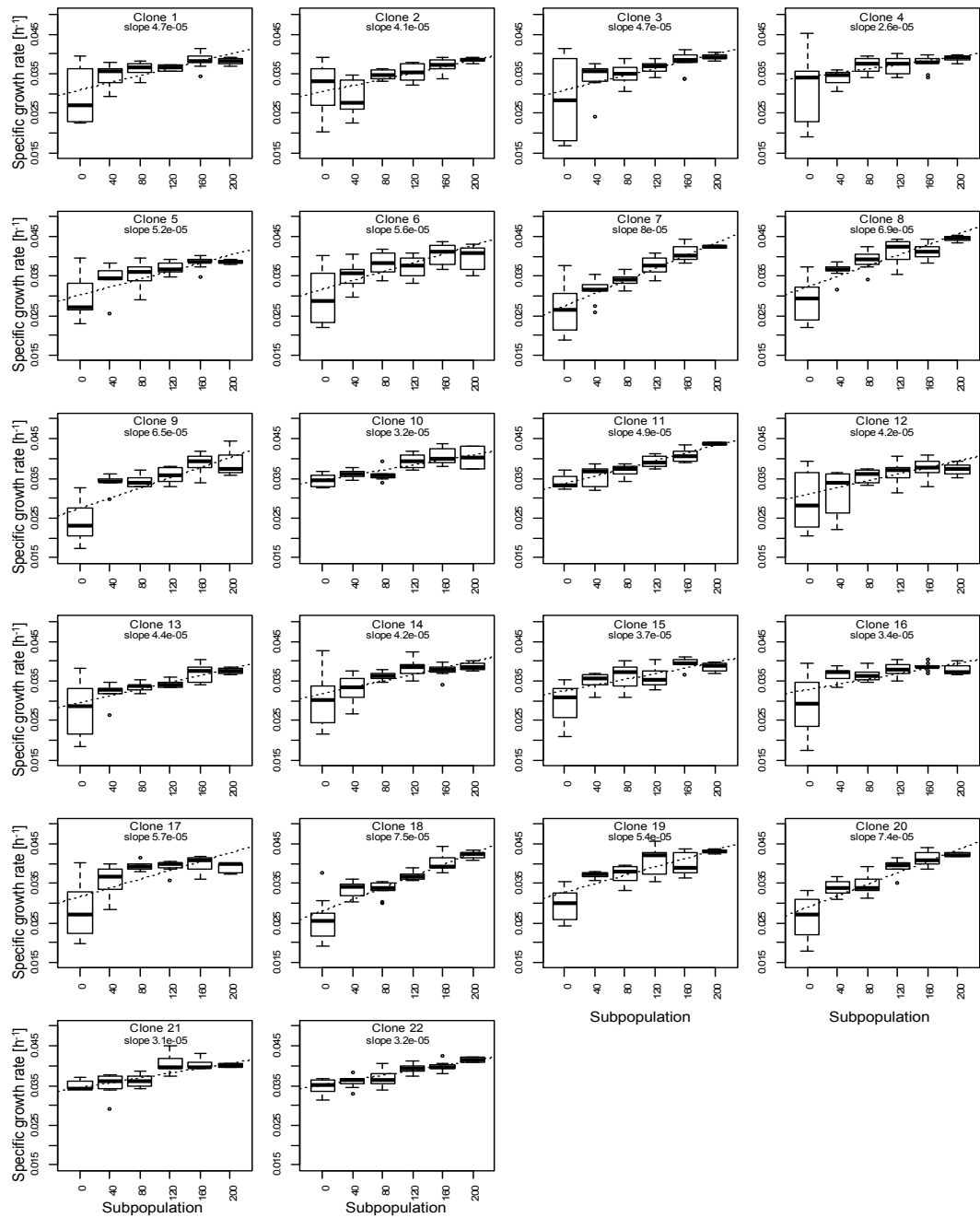
Figure 3-4 Growth rates for 22 LDC clonally-derived CHO-S populations at different time points along long-term culture. Cell growth rate was measured every 4 days and grouped into 6 subpopulations: subpopulation 0 (generations 0-39), subpopulation 40 (generations 40-79), subpopulation 80 (generations 80-119), subpopulation 120 (generations 120-159), subpopulation 160 (generations 160-199) and subpopulation 200 (generations 200-up to 220). The bottom and top of the box represent the 25th and 75th percentiles, the line within the box the median, error bars indicate the 0th and 100th percentiles and dots are outliers. Slope values are the rate of change in µ [h^{-1} per generation].

59

Comparing clones 4 and 7, the ones with the lowest and highest rate of change in μ, respectively, a ~3.0 fold difference was observed. Interestingly, both clones exhibited large growth heterogeneity at subpopulation 0, however, the right-skewed distribution and the high μ median (0.034 h^{-1}) at subpopulation 0 for clone 4 (Figure 3-4) suggested notable improvements in its growth rate within few generations, whilst the low μ median (0.026 h^{-1}) at subpopulation 0 for clone 7 indicated gradual μ improvements. Consequently, this data suggests significant differences in the rate of acquisition of improved cellular performance among individual clones.

3.4.3 Analysis of adaptation phase of clonal CHO-S cell lines during long-term subculture

In order to test the hypothesis that clones exhibited differences in the period of adaptation to agitated conditions, the residual values of the linear regression showed in Figure 3-4 were plotted against generation numbers to identify the extent of deviation from the estimated μ values (Figure 3-5). This data clearly separates the adaptation and evolution phases and shows that the clones were highly variable, ranging from non-adaptation period (clones 10, 11, 20 and 21) to up to 56-generations (clone 2). Additionally, this analysis showed that majority of the clones became adapted between 28 and 44 generations (13 out of 22 clones; clones 1, 3, 4, 5, 6, 7, 8, 13, 14, 15, 16, 17, and 18).

To compare adaptability among clones, the average residual value for the first 56 generations, corresponding to the longest adaptation period observed (clone 2), was used. The average μ variability distribution (Figure 3-6) confirms that clones 10, 11, 21 and 22 were by far the most adapted populations (with low μ variability rate ≤0.0002 h^{-1} gen^{-1}), whilst the most least adapted were clones 3, 4, 6, 16 and 17 which increased their mutation rate in order to develop growth advantages to resist shearing stress and pressure forces produced by agitated environments, therefore exhibiting elevated μ variability rates, ranging between 0.0013 and 0.0017 h^{-1} gen^{-1}.

To evaluate whether the large heterogeneity described in clone 6 at mid and late long-term generations resulted from incomplete adaptation (section 3.4.2; Figure 3-4), a residual analysis of the proliferation rate was performed (Figure 3-5-clone 6). The results show that clone 6 had an adaptation period of 36 generations and suggesting that the increments in heterogeneity at mid- and late-subpopulations was the result of a fixed mutation within population around generation 80 that caused an unbalance in the subsequent generations.
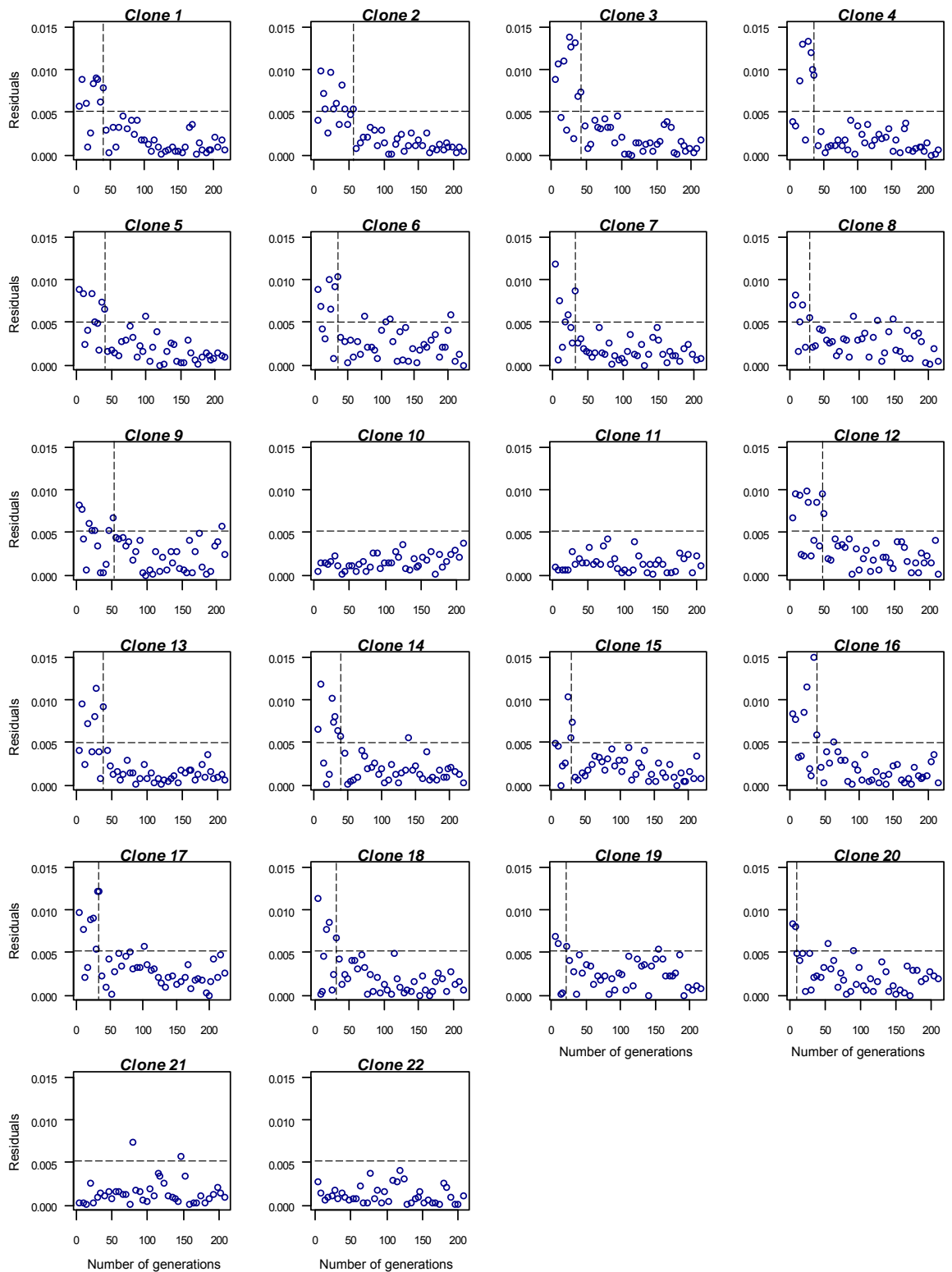
Figure 3-5 Growth deviation from the estimated µ values for 22 LDC clonally-derived CHO-S populations during long-term cultivation. The vertical dot lines represent the time point at which cells became adapted to agitated environments and the horizontal lines represent the stability threshold.

Average variability in µ during adaptation phase [hr⁻¹gen⁻¹]
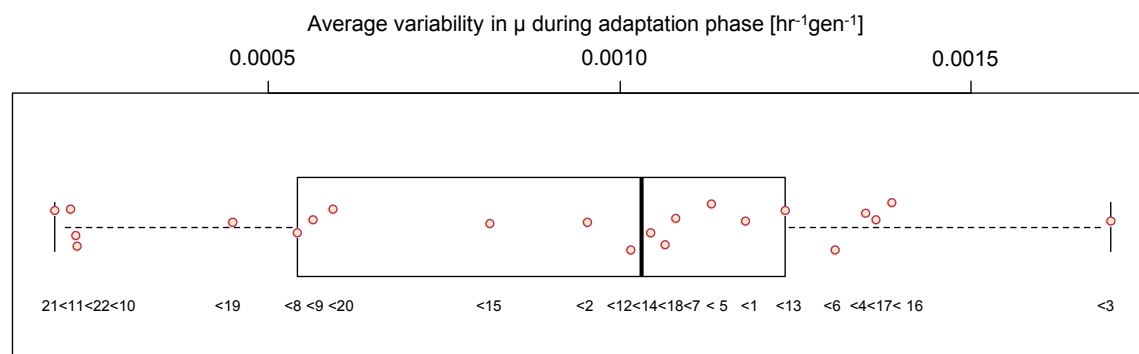
Figure 3-6 Average variability in µ [hr^{-1} gen^{-1}] for 22 clonally derived CHO-S cell lines during the adaptation phase of a long-term subculture regime (initial 56 generations). The left and right of the box represent the 25th and 75th percentiles, the line within the box the median, the whisker the 0th and 100th percentiles and dots the outliers.

In this analysis was suggested that the average variability in µ can be used as a measure of stability among clones because unstable populations exhibited higher variability in µ rates (Figure 3-6). These results are clearly associated with the constant fluctuations in proliferation rates along increasing generations until the appearance and dominance of adapted subpopulations that out-compete other unfitted subpopulation. Therefore, this data shows that unstable clones continuously generated growth characteristics to increase the likelihood of proliferating and surviving in the new environments, indicating that unstable clones increased up to 8.5 fold their phenotypic heterogeneity to cope with the agitated environment and that 13 out of 22 clones exhibited elevated variability (>0.0010 h^{-1} gen^{-1}) indicating that the majority of the clones were not completely adapted to growth under agitated environments, and thus unstable populations are required to increase their mutation rate frequency to adapt and proliferate.

3.4.4 Analysis of evolution phase of clonal CHO-S cell lines during long-term subculture

The evaluation of cell growth improvement during the evolution phase of the long-term subculture was performed by analysing the rate of change in µ after the adaptation period. In this phase, observed improvements in µ commonly result from genetic drift, as seen for other long-term subculture regimes (Davies et al. 2012). For each clone, the average rate of change in µ was calculated as the slope of the linear regression of the growth rate values observed during the evolution phase (generations

57 to up to 220). Using the slope values (Figure 3-7), clones 7, 8, 11, 18, 20 and 21 exhibited greater enhancement in μ, between 4.7×10^{-5} h^{-1} gen^{-1} (clone 21) and 7.3×10^{-5} h^{-1} gen^{-1} (clone 7), also indicating that the genetic drift affected these populations higher. On the other hand, genetic drift improvements were lower for clones 1, 4, 12, 14, 16 and 17 with values ranging between 9.31×10^{-7} h^{-1} gen^{-1} (clone 17) and 2.1×10^{-5} h^{-1} gen^{-1} (clone 4).

Comparing the rate data obtained for the adaptation and evolution phases (Table 3-1), clones 10, 11, 19, 21 and 22 exhibited short adaptation periods (<28 generations), elevated rates of change in μ during the evolution phase (3.75-5.04×10^{-5} h^{-1} gen^{-1}) and rapidly reached 200 generations (between 155 and 159 days of continuous sub-cultivation). This data clearly indicates that since their isolation these clones were the most robust, more resistant to agitated environments and least heterogeneous populations. Contrary, clones 3, 4, 6, 13, 16 and 17 required longer time periods to develop fitness to the agitated environment (between 36 and 44 generations) and to reach 200 generations (up to 177 days). In addition, these unstable cell lines exhibited low rates of change in μ during the evolution phase.

The heterogeneous and prolonged adaptation processes observed in unstable populations also increased the complexity and unpredictability of cultures because the populations were continuously changing their growth phenotype in response to the dynamic appearance and decline of phenotypes. It is thought that this active and dynamic heterogeneity in unstable populations is associated with the absence of functional genetic traits that would favour the resistance to stress conditions (Davies et al. 2005). As a consequence, these populations were forced to evolve resistant phenotypes to survive and proliferate in the presence of shear stresses and pressure forces produced by agitated cultures. On the other hand, stable populations probably inherited functional phenotypic characteristics that allowed them to resist shearing stress and easily get accustomed to the agitated environment. Considering these findings, the data here presented supports the hypothesis that clones are genetically and phenotypically different despite being obtained from the same parental CHO-S population and also confirms that by harnessing the cellular heterogeneity is possible to isolate stable cell lines able to resist specific culture environments such as media and culture conditions, and probably have improved manufacturing capabilities.

Table 3-1 Summary of the adaptation and evolution phases of 22 clonally-derived CHO-S cell lines during a long-term subculture regime

Clone	Rate of μ variability in adaptation phase h⁻¹ gen⁻¹ (Rank)	Rate of change in μ in evolution phase x10⁻⁶ h⁻¹ gen⁻¹ (Rank)	Duration of adaptation phase Generations (Rank)	Period to reach 200 generations Days (Rank)
Clone 21	0.0002 (1)	4.70 (6)	0 (1)	155 (2)
Clone 11	0.0002 (2)	5.04 (4)	0 (1)	157 (3)
Clone 22	0.0002 (3)	3.49 (11)	0 (1)	157 (4)
Clone 10	0.0002 (4)	3.75 (9)	0 (1)	155 (1)
Clone 19	0.0004 (5)	3.88 (8)	20 (6)	159 (6)
Clone 8	0.0005 (6)	4.77 (5)	28 (7)	159 (5)
Clone 9	0.0006 (7)	4.15 (7)	52 (20)	174 (20)
Clone 20	0.0006 (8)	6.69 (2)	12 (5)	169 (15)
Clone 15	0.0008 (9)	2.89 (14)	32 (8)	168 (14)
Clone 2	0.0010 (10)	3.36 (12)	56 (22)	172 (16)
Clone 12	0.0010 (11)	1.96 (19)	52 (20)	172 (18)
Clone 14	0.0010 (12)	2.05 (18)	40 (13)	168 (13)
Clone 18	0.0011 (13)	6.40 (3)	36 (9)	173 (19)
Clone 7	0.0011 (14)	7.26 (1)	36 (9)	177 (22)
Clone 5	0.0011 (15)	2.75 (16)	40 (13)	167 (9)
Clone 1	0.0012 (16)	1.93 (20)	40 (13)	168 (11)
Clone 13	0.0012 (17)	3.74 (10)	40 (13)	174 (21)
Clone 6	0.0013 (18)	2.91 (13)	36 (9)	162 (8)
Clone 4	0.0014 (19)	2.16 (17)	40 (13)	168 (12)
Clone 16	0.0014 (21)	1.47 (21)	40 (13)	167 (10)
Clone 17	0.0014 (20)	0.93 (22)	36 (9)	161 (7)
Clone 3	0.0017 (22)	2.86 (15)	44 (19)	172 (17)
Median	**0.00105**	**3.43**	**36**	**168**

The rate of μ variability was calculated during the adaptation phase (generations 0 to 57) and the rate of change in μ was calculated as the slope of the linear regression of the growth rate values observed during the evolution phase (generations 57 to up to 220). The value in parenthesis indicates the rank of each parameter; the blue and red values are the top 7 and bottom 7, respectively.

Average rate of change in μ during evolution phase (hr⁻¹ gen⁻¹)
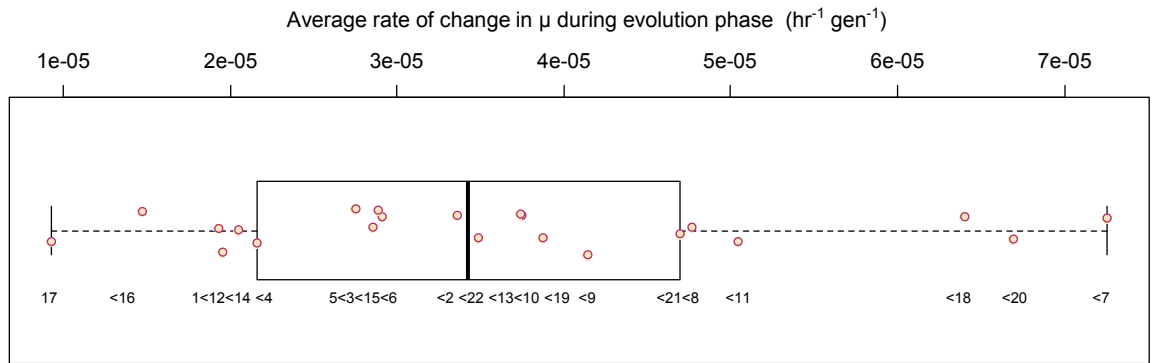
Figure 3-7 Average rate of change in μ [hr^{-1} gen^{-1}] for 22 clonally derived CHO-S cell lines during the evolution phase of a long-term subculture regime (generations 57 to up to 220). The left and right of the box represent the 25th and 75th percentiles, the line within the box the median, the whisker the 0th and 100th percentiles and dots the outliers.

3.4.5 Growth patterns among clonal CHO-S populations over long-term culture

To test the hypothesis that phenotypic heterogeneity observed in the 22 clonal cell lines also affected other growth characteristics, measurements of cell size (Figure 3-8A), viable cell density (Figure 3-8B) and cell viability (Figure 3-8C) were performed during each passage. The collected data was plotted to identify the extent of variation among clones, corroborating that the 22 clones were highly variable among them and within them along the long-term cultivation (Figure 3-8). Grouping each growth parameter by subpopulations (i.e., 0, 40, 80 160, or 200 generations) it was possible to observe that the age of the clones had an effect on cell size (two-way ANOVA, $p<0.01$, F=3.79), VCD (two-way ANOVA, $p<0.0001$, F=75.33), and cell viability (two-way ANOVA, $p<0.0001$, F=29.47).

The large cell viability and cell size heterogeneity during adaptation phase clearly validate that the majority of the clones did not exhibited a fully adapted phenotype to agitated conditions and consequently cells enhanced their genetic instability to accumulate more phenotypic cellular diversity with growth advantages that allowed them to survive and proliferate under agitated conditions (Greaves and Maley 2012). On the other hand, the high cellular viabilities and cell size stabilisation (between 15 and 16 μm) during evolution phase confirms that clones developed phenotypes able to survive to the agitated environment and corroborates that populations underwent genetic drift, resulting in adapted phenotypes with low inter-heterogeneity.

Altogether, this data shows the feasibility for harnessing the genetic heterogeneity within CHO cells to isolate cell lines with varied cell growth

characteristics and the possibility to improve cellular robustness through an accelerated genetic drift. Likewise, these observations agree with previous studies that exhibited the intrinsic variability in cell growth performance among clonal cell lines in CHOK1SV (Davies et al. 2005) and NS0 (Barnes et al. 2006) cells.
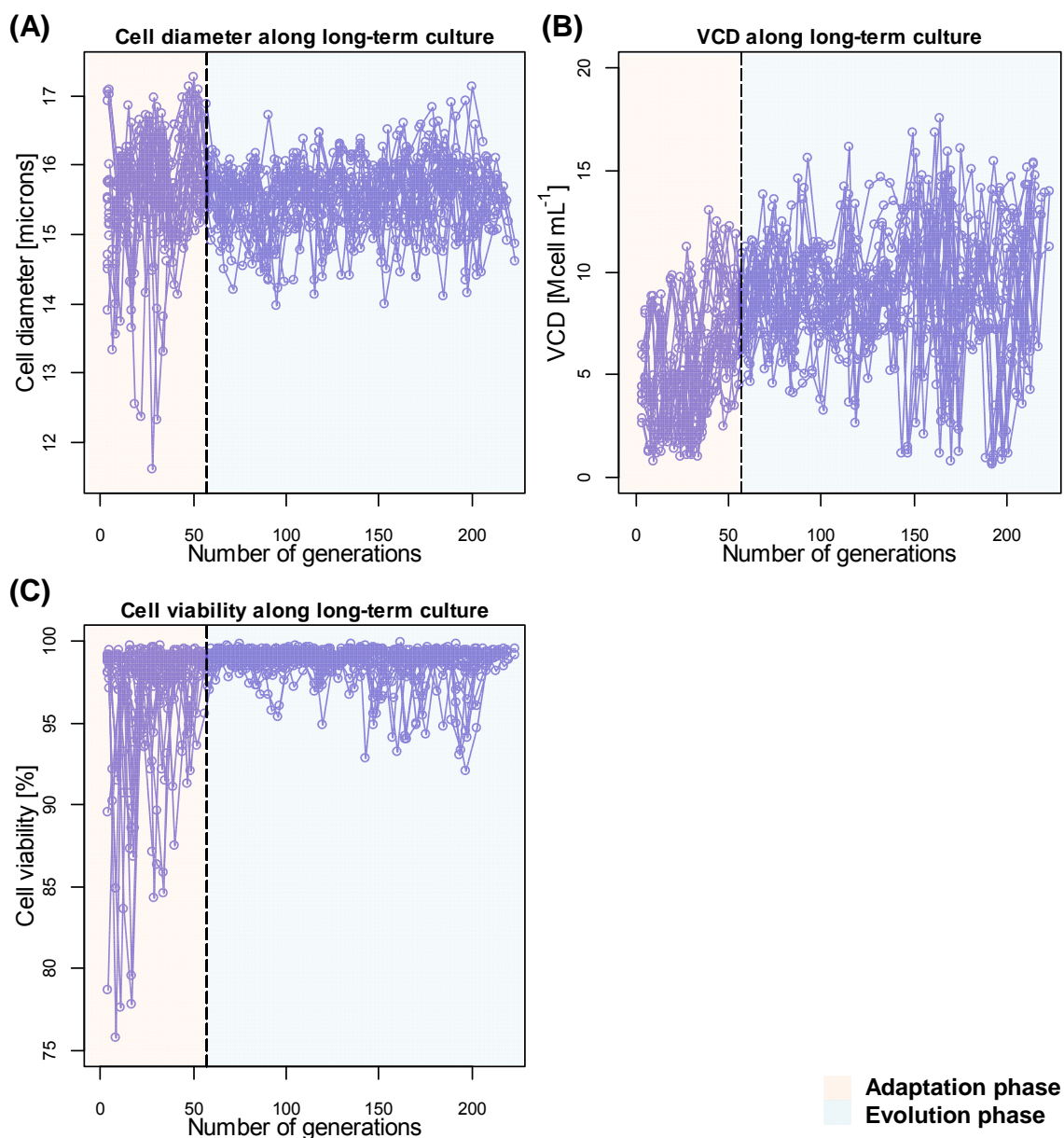
Figure 3-8 Cell growth characteristics for 22 LDC clonally-derived CHO-S cell lines during long-term culture. Clones were grown in agitated conditions for up to 220 generations to characterise their growth phenotype. Average cell diameter (A), viable cell density (B) and cell viability (C) were monitored every four days using a Vi-CELL XR cell viability analyser. The patterns consist of an initial adaptation phase (generations 0-56), followed by an evolution phase (generations 57-220).

3.4.6 Clonal CHO-S cell lines at mid- and late-generations of long-term cultivation improved their growth phenotype

The degree of divergence in growth rates between the parental population and clonal CHO-S cell lines along long-term cultivation was assessed (Figure 3-9). In general was observed that all clones at subpopulations 0 and 40 showed lower μ rates than the parental population (between 0.67 to 1 fold change), whilst some clones at subpopulations 80 and 120 started to exhibit higher growth rates than the parental population (up to 1.11 fold changes), and by subpopulations 160 and 200 all clones exhibited growth advantages (up to 1.2 fold changes). It is important to emphasise that the growth performance of the parental population was monitored only during three passages and not along an extended culture to avoid significant alteration on its phenotype because the goal of this project was to assess whether the growth performance of the isolated clones improved with respect to the parental population.

Using 0.031 to 0.038 h^{-1} (LifeTechnologies 2007) as values of reference for comparing the average proliferation rates among the clonal CHO-S populations, it can be observed that at the beginning of the long-term cultivation 17 out of 22 clones exhibited detrimental μ performances (<0.031 h^{-1}; "subpopulation 0"; Figure 3-9), being clones 2, 10, 11, 21 and 22 those with μ values within the mentioned limits. The analysis described in Figure 3-9 also shows that clones fell within the μ limits when they became adapted to the agitated environment (between 40 and 80 generations; "subpopulation 40"). Once adapted, clones started to exhibit proliferation rates above the reference μ limits (>0.038 h^{-1}; clones 6, 8 and 17 at "subpopulation 120") and eventually the majority of them (16 out of 22 clones at "subpopulation 160" and 19 out of 22 clones at "subpopulation 200") attained superior growth rates.

Comparing the overall cell growth performance, viable cell density and average cell diameter during the evolution phase (Table 3-2), clones 6, 8, 11, 17, 19, 21 and 22 were the cell lines that exhibited the fastest growth rates over the whole evolution phase, whereas clones 2, 3, 9, 12, 18 and 13 exhibited the slowest growth performance. When the average VCD was compared the clones 4, 7 8, 11, 17, 19 and 20 were the cell lines that exhibited higher VCD during the whole evolution phase, whilst the lowest VCD were observed in clones 2, 3, 5, 9, 12 and 13. Using the same analogy for the average cell diameter, clones 10, 13, 16, 21 and 22 were the clones with elevated cell diameter during the whole evolution phase, whilst the lowest diameter were observed in clones 2, 8, 6, 17 and 19.
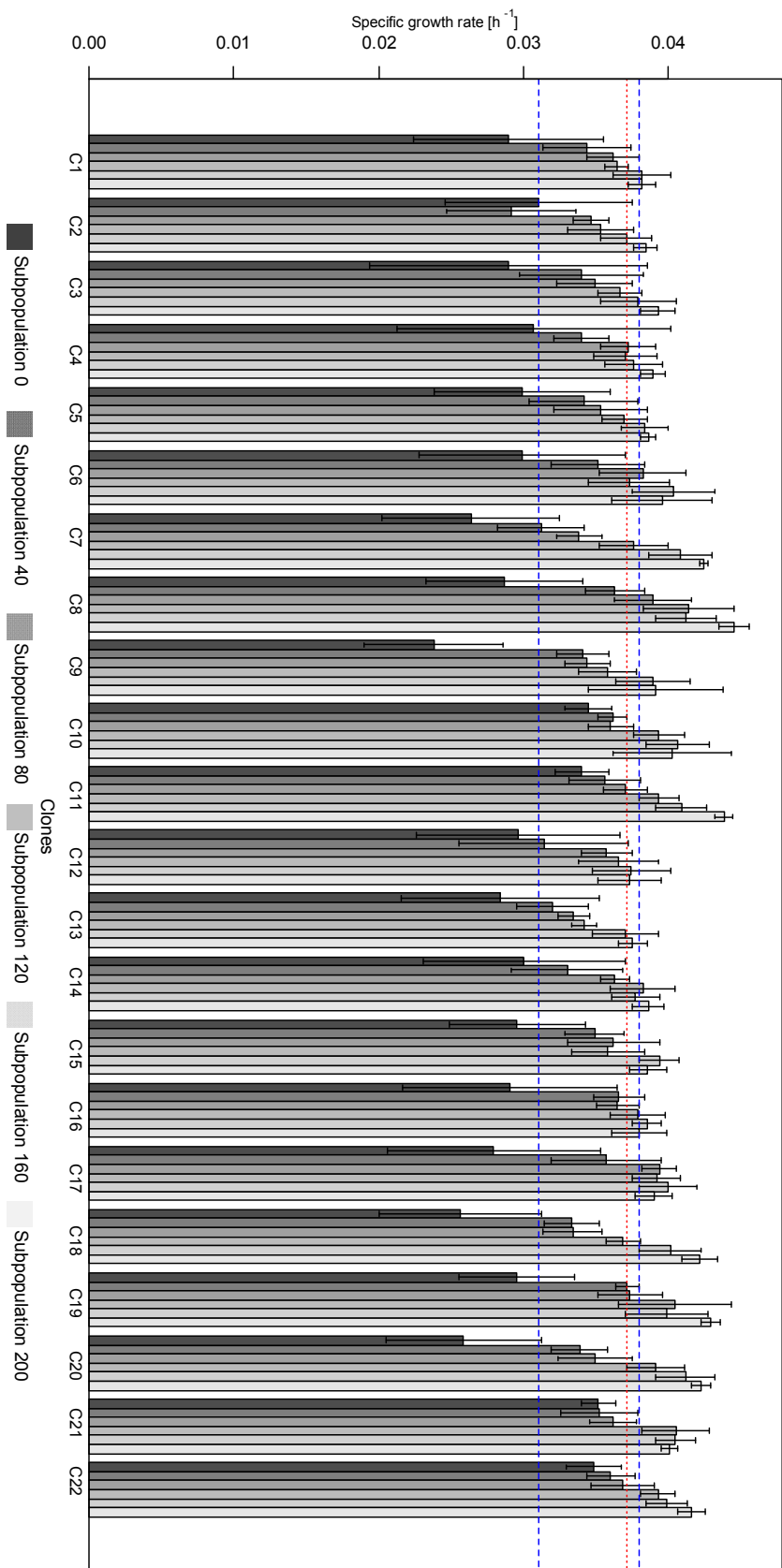
Figure 3-9 Specific growth rate for 22 clonally-derived CHO-S cell lines at six stages of the long-term subculture: Subpopulation 0 (generations 0 to 39), subpopulation 40 (generations 40 to 79), subpopulation 80 (generations 80 to 119), subpopulation 120 (generations 120 to 159), subpopulation 160 (generations 160 to 199) and subpopulation 200 (generations 200 to up to 220). The mean value and standard deviation (error bars) was calculated from accumulated growth data during 39 generations. The red dotted line represents the specific growth rate reached by the parental population and the blue dashed line the inferior and superior values reported for CHO-S cells.

Table 3-2 Average specific growth rate (μ), viable cell density (VCD) and cell diameter for 22 clonally-derived CHO-S cell lines and parental CHO-S population (PAR) during the evolution phase of a long-term subculture.

Clone	Specific growth rate $[h^{-1}]$ Mean ± sd (Rank)		VCD $[10^6$ cells mL$^{-1}]$ Mean ± sd (Rank)		Size [Microns] Mean ± sd (Rank)	
Clone 8	0.0402 ± 5e-04	(1)	11.6 ± 0.6	(1)	15.1 ± 0.1	(1)
Clone 19	0.0392 ± 5e-04	(2)	10.4 ± 0.6	(3)	15.3 ± 0.1	(5)
Clone 17	0.0392 ± 4e-04	(3)	10.6 ± 0.6	(2)	15.3 ± 0.1	(4)
Clone 11	0.0386 ± 5e-04	(4)	9.7 ± 0.5	(4)	15.6 ± 0.1	(17)
Clone 6	0.0384 ± 5e-04	(5)	9.1 ± 0.6	(9)	15.3 ± 0.1	(3)
Clone 21	0.0384 ± 5e-04	(6)	8.8 ± 0.5	(14)	15.7 ± 0.1	(18)
Clone 22	0.0384 ± 4e-04	(7)	9.1 ± 0.5	(10)	16.0 ± 0.1	(22)
Clone 10	0.0383 ± 5e-04	(8)	9 ± 0.5	(11)	15.8 ± 0.1	(21)
Clone 20	0.0377 ± 7e-04	(9)	9.4 ± 0.6	(5)	15.6 ± 0.1	(16)
Clone 16	0.0376 ± 4e-04	(10)	8.8 ± 0.5	(15)	15.8 ± 0.1	(20)
Clone 14	0.0373 ± 4e-04	(11)	8.9 ± 0.4	(12)	15.6 ± 0.1	(15)
PAR	**0.0371 ± 6e-04**	**(12)**	**7.5 ± 0.2**	**(21)**	**16.2 ± 0.01**	**(23)**
Clone 15	0.0371 ± 5e-04	(13)	9.3 ± 0.6	(8)	15.5 ± 0.1	(11)
Clone 4	0.0371 ± 3e-04	(14)	9.4 ± 0.5	(7)	15.5 ± 0.1	(10)
Clone 5	0.0370 ± 4e-04	(15)	8.1 ± 0.5	(19)	15.6 ± 0.1	(14)
Clone 1	0.0370 ± 3e-04	(16)	8.9 ± 0.4	(13)	15.5 ± 0.1	(9)
Clone 7	0.0369 ± 7e-04	(17)	9.4 ± 0.6	(6)	15.5 ± 0.1	(8)
Clone 18	0.0368 ± 7e-04	(18)	8.7 ± 0.5	(16)	15.5 ± 0.1	(7)
Clone 3	0.0368 ± 4e-04	(19)	8.6 ± 0.4	(17)	15.6 ± 0.1	(13)
Clone 12	0.0365 ± 3e-04	(20)	8.3 ± 0.5	(18)	15.6 ± 0.1	(12)
Clone 9	0.0363 ± 5e-04	(21)	8 ± 0.4	(20)	15.5 ± 0.1	(6)
Clone 2	0.0357 ± 4e-04	(22)	7.4 ± 0.4	(22)	15.3 ± 0.1	(2)
Clone 13	0.0348 ± 4e-04	(23)	6.7 ± 0.4	(23)	15.8 ± 0.1	(19)
Average	**0.0375 ± 1e-03**		**8.9 ± 1.1**		**15.6 ± 0.2**	

The mean value and standard deviation were calculated using the experimental data collected between generations 57 and 200 for the clones (1-22) and during three passages for the parental cell line (PAR). The value in parenthesis indicates the rank of each parameter; the blue and red values are the top 7 and bottom 7, respectively.

Table 3-2 also exhibited that the cell growth characteristic measured during the whole evolutionary phase were highly variable. For example, the viable cell density ranged between 6.7 x 10^6 and 11.6 x 10^6 cells mL^{-1} with a mean slightly superior than the parental cell populations (8.9 and 7.5 x 10^6 cells mL^{-1}, respectively). Similar results were observed in the proliferation rates and cell diameter fluctuating between 0.035 and 0.040 h^{-1} with a mean of 0.0375 ± 0.001 h^{-1} and between 15.1 and 16.2 microns giving an average of 15.6 ± 0.2 microns. In addition, when the 22 clonal CHO-S cell lines were compared with the parental population (Table 3-2), it was observed that 10 clones improved their average proliferation rates (up to 0.040 h^{-1}), 9 exhibited similar growth rates (~0.037 h^{-1}) and 3 reduced their growth performance (up to 0.035 h^{-1}). In the same context, from the 22 clones, 20 (90% of the clones) exhibited higher average VCD, one showed similar average VCD and one displayed lower average VCD (7.4 x 10^6 cells mL^{-1}). From clones with improved VCD, it was seen that the majority of them exhibited a measurement of VCD between 8.6 and 9.4 x10^6 cells mL^{-1}. On the other hand, the cell diameter measurements showed that the parental population are by far the biggest cells (16.2 microns cell diameter). These drops in cell diameter among the clones may suggest that these derived cell lines developed a more efficient metabolism and probably they required to produces of less biomolecules to proliferate.

3.4.7 Clonal CHO-S populations reduced their cell volume during evolution phase

To identify any association between cell diameter and proliferation rate, the values were ranked and compared in Table 3-2. The data show that the majority of faster-growing clones (e.g., clones 6, 8, 17 and 19) exhibited a smaller cell size, suggesting the existence of a negative correlation. Previous experiments reported that cell size, either measured as cell diameter, volume, mass or protein content, correlates with cell growth and productivity (Davies et al. 2012; Kim et al. 2001). For example, Davies (2012) found that CHOK1-SV cell size and protein content inversely correlated with proliferation rate (Davies et al. 2012). A contrary, results were observed by Dreesen and Fussenegger (2011) finding a positive correlation between cell size and cell growth and productivity through mTOR over-expression.

To corroborate whether exist any correlation between cell size and proliferation rates, a Pearson's correlation was performed, showing a negative, but weak correlation between cell diameter and specific growth rate (PPMCC r^2= -0.2874, n=22; Figure 3-10A). It can be suggested that this weak association resulted from the mere fact that clones became more robust over increasing generation as a result of adaptation and

evolution processes. In order to validate these findings, the average cell size data collected for all the 22 clones during the long-term sub-cultivation was analysed as subpopulations (subpopulations 0, 40, 80, 120, 160 and 200; Figure 3-10B. however, the global analysis did not exhibited significant changes over the extended cultivation, probably indicating that CHO-S cells may have mechanisms that regulate cell size

The analysis of cell variability among subpopulation agreed with the previous analysis (see section 3.4.3), showing that subpopulation 0 exhibited the greatest variation, which was caused from a continuous appearance of fitted and non-fitted phenotypes within population to cope with agitated environments. Also, indicating a significant reduction of 30% in cell size variability during the transition from adaptation to evolution phase and not significant changes along the whole evolution phase (Figure 3-10B). The extent of phenotypic heterogeneity observed among clones confirmed that the donor population contains a mixture of phenotypes. This analysis also agrees with previous research that found a substantial clone specific variation in cell size, measured as cell volume and cell protein biomass, among clonal CHOK1SV populations (Davies et al. 2012).
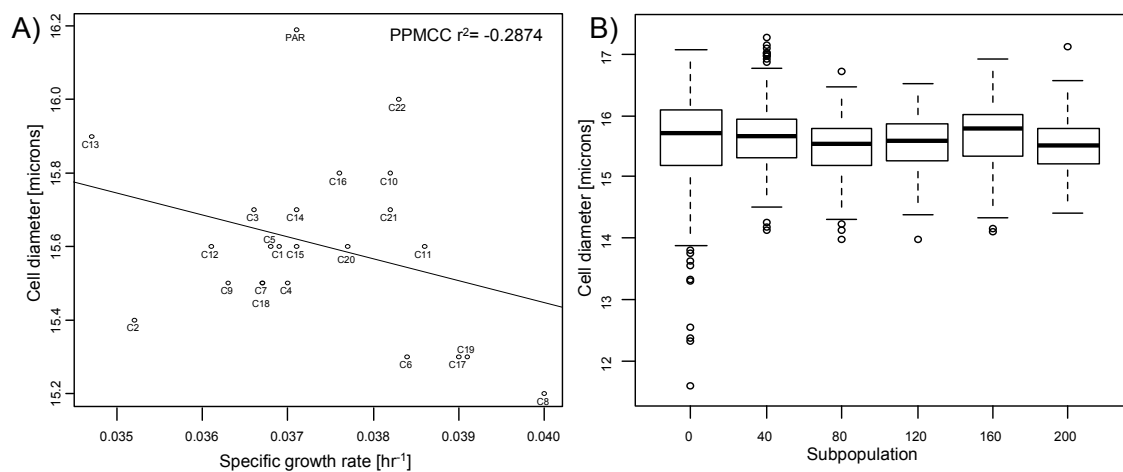
Figure 3-10 Cell size for 22 clonally-derived CHO-S populations along long-term culture. For each clone, during the long-term cultivation, growth parameters were measured every 4 days for up to 220 generations. The relationship between average values for cell diameter and specific growth rate for the whole long-term cultivation (A) and cell diameter values grouped into subpopulations 0 (generations 0-39), 40 (generations 40-79), 80 (generations 80-119), 120 (generations 120-159), 160 (generations 160-199) and 200 (generations 200-220) (B) are shown. The bottom and top of the box represent the 25th and 75th percentiles, the line within the box the median, error bars indicate the 0th and 100th percentiles and dots are outliers.

The comparison between the average cell growth and proliferation rates along the adaptation phase seem to indicate that clones 6, 8, 17 and 19 have the best cell growth phenotypes as these faster-growing cell lines required less cellular protein content to survive and proliferate whereas clone 13 the lower phenotype is observed in clone 13 as present poor growth performance and large cell size. However, it is important to note that these findings only gave preliminary and general trend of the clones' diversity; to make a convincing conclusion further data analysis were carried out and described in chapter 4, 5 and 6.

3.5 General discussion

The phenotypic heterogeneity among clonally-derived CHO-S cell lines observed in this chapter supports the hypothesis that CHO populations contain a substantial degree of phenotypic heterogeneity which can be harnessed to obtain cell lines with desirable characteristics by implementing robust techniques such as cell cloning. The data also confirms that CHO cell populations always increase their phenotypic heterogeneity at initial stages of subculture despite being generated from a single cell and constantly interact with their surroundings in order to adapt and proliferate. Similar behaviour have previously been reported by Barnes et al. (2006) and (Davies et al. 2012) suggesting that the high genetic instability within populations result in a constant appearance of subpopulations with varied phenotypic characteristic along the culture. The data presented in this chapter confirm that clonal populations are dynamic systems and thus clonal populations are non-identical, leading to unpredictable cellular responses during cell line development processes.

The strategy implemented in this chapter was designed to explore the phenotypic variation within parental populations by using the limiting dilution cloning methodology to generate cell lines and to evaluate the stability of these populations along long-term culture by routinely sub-culturing the isolated clones for up to 220 generations. In this strategy the LDC was chosen as the primary method for creating clonal derivatives of CHO-S cells owing to its simple operation, low cost and low technical requirements that have positioned it as the most common method for screening production cell lines. This cell cloning method involves a large cellular dilution that can mislead the estimation of monoclonality due to single cells being undetected during the verification of single cell colonies (Underwood and Bean 1988). Therefore, to increase the chances of obtaining monoclonal colonies two LDC rounds are usually performed. It is important to note that the proposed strategy showed in this chapter is not limited to the implementation of

LDC as the unique technique for exploiting the vast phenotypic variation within CHO populations. Contrary, I suggest that coupling this strategy with automated or semi-automated clone screening technologies such as fluorescence-activated cell sorting (FACS) systems, ClonePix FL (Life Technologies) or Cell Metric^{TM} CLD (Solentim) can significantly increase the feasibility of this strategy, and thus accelerate the selection processes to exploit even more the great cellular diversity in CHO populations. For example, FACS systems can be used to isolate and enrich populations with determined physiological or functional criteria (e.g., protein content, glycoform patterns and cellular content) by labelling specific proteins, then measuring fluorescence from each cell and lastly sorting them into specific collection tubes or well-plates(Lai et al. 2013).

The considerable variation between the isolated clones exhibited in this chapter, strongly agrees with previous studies which elucidated the phenotypic variation in derivative CHO cell lines such as in CHO DG44 (Chusainow et al. 2009; Kim et al. 1998), CHO DP-12 (Beckmann et al. 2012), GS-CHOK1SV (Davies et al. 2012), GS-CHO (Bailey et al. 2012) and NS0 (Barnes et al. 2006) populations. These studies showed that mammalian cell populations consist of a mixture of subpopulations with different cell performances which mould the overall cell performance. Additionally, they also suggested that CHO populations are constantly evolving beneficial characteristics (e.g. high specific growth rates, elevated cell densities, efficient protein synthesis and resistant phenotypes) that allow them to acquire competitive phenotypes. Although CHO cells present high heterogeneity and this inherent genetic trait cannot be eliminated, this study and previous studies in CHO and NS0 cells have provided evidence that the heterogeneity level can notoriously be reduced by accelerating genetic drift (Barnes et al. 2006; Davies et al. 2012). Moreover, the findings presented in this work showed that the genetic drift cannot ensure the low heterogeneity along culture because CHO cells have a greater ability to unpredictably change their overall performance as the result of multiple changes in their genome or regulation in response to extrinsic factors which are translated as beneficial and non-beneficial phenotypic variation which alters the populations' balance.

Although it is clear that the phenotypic variation may result from mutation(s) across the genome, the implementation of genomic analysis such a karyotyping (Derouazi et al. 2006; Worton et al. 1977) and genomic sequencing (Lewis et al. 2013; Xu et al. 2011) for characterising the genetic and phenotypic heterogeneity has not been widely used due to the inherent genetic instability within CHO cells imposing genomic restrictions and increasing the complexity of data analysis between and within populations. This inherent complexity occurred as a result of the genetic instability arise

from cell lines and even clonal cell lines having undergone a large number of mutations across time, making them unique (Lewis et al. 2013). Therefore, none of these genomic analytical approaches have given a complete picture of variations at the whole genome level. Cytogenetic examination carried out by Derouazi et al. (2006) and Worton et al. (1977) exhibited that derivative CHO cell lines underwent extensive chromosomal aberrations since their origins (i.e., aneuploidy, translocations and deletions) confirming that CHO cell's karyotypes not only differed from the normal Chinese hamster karyotype, but also differed from one population to another. These accumulated genomic aberrations observed in CHO cell lines clearly constrained the identification of any correlation between the degree of chromosomal instability and populations' stability.

The large genetic differences among individual cells makes genomic characterisation of a whole population harder; therefore many researchers have preferably used global phenotypic characteristics of the whole population such as cell growth, productivity and glycosylation patterns as markers for the identification and semi-quantification of genetic heterogeneity (Barnes et al. 2006; Chusainow et al. 2009; Davies et al. 2012; Kim et al. 1998). In this study I used the growth rate heterogeneity as indicator of genetic heterogeneity, finding that the large heterogeneity observed at early generations probably resulted from the initial loss of phenotypic characteristics during clonal cell line generation, which previously had allowed them to resist mechanical stressors such agitation and cell shearing. These findings clearly suggest that the environmental conditions used during cell cloning and cell expansion were not optimal for the long-term incubation conditions the cells would encounter, probably because single colonies modified their original phenotypic status to become adapted to static environment and thus becoming less resistant to mechanical stress. The subsequent transfer of the clonal cell lines to the agitated environment triggered and enhanced the inherent genomic instability which resulted in an enormous phenotypic heterogeneity within populations. The fact that some clones did not exhibit adaptation periods suggest that they preserved heritable genetic characteristic that promoted their easy adaptation to agitated environments. Contrary, it can be suggested that heterogeneous populations may have silenced or lost some heritable mechanical-resistant genetic characteristics, which previously allowed them to survive in shaking environments, triggering and enhancing their "mutator phenotype" in an effort to cope with the mechanical environmental stressor and proliferate under agitated environment.

It can be suggested that the observed heterogeneity at early stages of the long-term cultivation was not only derived from the inherent genetic instability (genetic

mutations). In fact, previous observations have suggested that epigenetic factors as well as many physical, chemical and biological factors that co-exist in culture (i.e., age and stage of culture, cell growth stage, environmental conditions, metabolic flux, osmolality, temperature, characteristic of the cells) contribute to the acquisition of phenotypic changes (Merlo et al. 2006; Pilbrough et al. 2009). Other studies have suggested that cell background status (i.e., size, cell density, growth rate, growth phase and resistance to stressors) is determinant in the acquisition of phenotypic heterogeneity (Ryall et al. 2012). Together, these epigenetic, genetic and background factors make up and define the phenotype of populations.

The early long-term stage data analysis strongly agrees with other studies which analysed the cell growth performance of derived cell lines as marker of heterogeneity, in special after three consecutive rounds of LDC (Barnes et al. 2006), demonstrating that NS0 populations consist of mixture of multiple phenotypes in culture which vary from population to population and confirming that inherent genetic instability cannot be supressed, therefore clonally-derived cell lines must be considered as heterogeneous populations even if multiple rounds of cell cloning are performed. In addition, the mid- and late-long-term data also agrees with Davies et al. (2012) who demonstrated that populations acquire fitness advantages through accelerated genetic drift. The collected data along the long-term cultivation also evidenced that CHO cells exhibit regulatory mechanisms that maintain the heterogeneity within boundaries to avoid extreme phenotypic characteristics such as elevated proliferation rates that may risk the cell integrity by not meeting the nutritional demands. Therefore, the supplemented CD CHO media may set the boundaries for specific cell growth values, also establishing a maximum proliferation rate for each of the 22 clonally derived CHO-S cell lines.

The highest growth heterogeneity observed for the majority of the clonal cell lines during the adaptation phase clearly indicated that changes in the culture environment triggered adaptive pathways to develop phenotypic traits that contribute to cellular fitness. However, the mechanisms that define the population's adaptation rate in new culture environments are mostly unknown. Ryall et al. (2012) suggested that the initial cellular heterogeneity and culture background are determinants to develop cellular fitness during the transition into new environments. Ha et al. (2011) suggested that epigenetic factors also provide mechanisms that increase the variability among and within populations by modifying the gene expression and cell growth. In the same context, other researchers have demonstrated that high genetic instability results in beneficial and deleterious mutations through time, affecting the cellular metabolism

which leads to phenotypic variability throughout the culture (Barnes et al. 2006; Davies et al. 2012; Kim et al. 1998).

The data here presented shows that the 22 clonal derivatives CHO-S cell lines exhibited diverse adaptation periods ranged from 0 to 56 generations, and only four clones (clones 10, 11, 21 and 22) exhibited optimal growth characteristics at generation 0 and also displayed lower heterogeneity during the extended cultivation. On the other hand, the rest of the clones exhibited sub-optimal growth performance at generation 0 and thus required to evolve beneficial growth characteristic to cope with the environmental stressor, ranging their adaptation periods from 12 to 56 generations. These findings support that change in culture environments trigger cellular heterogeneity, but also suggest that the cellular ability to acquire beneficial growth features depended on inherited genetic and epigenetic traits and from the cellular background stablished before the environmental transition.

Analysis of the adaptation rates exhibited that the CHO-S clones with sub-optimal growth performance were the most genetically unstable populations and therefore they required to accumulate a large number of beneficial mutations which later were observed as large adaptation periods and elevated phenotypic heterogeneity, whereas the genetically stable populations exhibited optimal and stable growth characteristics with shorter or even absent adaptation periods. Building on these results, this work suggested that phenotypically stable clonal CHO-S cell lines are present within parental populations and probably inherited growth advantages to resist the mechanical stress, while unstable populations probably silenced or lost those features, leading to cellular stress that limited their rapid adaptability to agitated environments. Considering that the phenotypic heterogeneity results from accumulated mutations, the μ variability observed for stable and unstable populations indicated that unstable populations increased their mutator phenotype up to 8.5 fold in an effort to survive, compared with genetically stable populations.

The examination of cell specific growth rates during the evolution phase (subpopulations 40, 80, 120, 160 and 200) clearly agrees with previous works which observed that clonal populations enhanced their growth performance when subjected to a continuous and extended cultivation (Beckmann et al. 2012; Davies et al. 2012). It is plausible to suggest that improvements in proliferation rates during the evolution phase could be attributed to genetic drift during each subculture, which intentionally favoured a constant and random selection of the fast-growing phenotypes that would dominate the population. The constant dominance of faster growing populations during the mid-exponential growth phase supports this hypothesis, indicating that the best

fitted subpopulations have higher probabilities to be picked up and expanded in the subsequent sub-cultivation. On the other hand, clonal evolution theory may also explain why clonal cell lines continuously improved their growth phenotype. This theory suggests that cell genetic variability within a population confers selective growth advantages that allow individual clones to out-compete (Greaves and Maley 2012; Nowell 1976). Therefore, is probable that during the extended cultivation the fast-growing subpopulations gradually increased their population size and progressively minimised or inhibited the population size of slow-growing subpopulations.

Although it was observed that genetic drift notably reduced the cellular heterogeneity, its effects on each population depended on intrinsic factors such as cellular diversity, doubling times, metabolic efficiency and level of genetic instability, and from extrinsic factors such as population's size, sampling volume and sampling frequency (Merlo et al. 2006). Together, these factors have the potential to completely reshape and reduce the diversity of one population by modifying the rates of fixation and loss of phenotypes in culture. Consequently all clones exhibited differences in the levels of growth heterogeneity throughout the long-term cultivation. The data presented in this chapter also corroborated that the phenotypic heterogeneity cannot be eliminated and that phenotypic heterogeneity can arise unexpectedly at any time of the cultivation by a random selection event that fixes a non-beneficial mutation.

Analysis of cell growth during the late long-term cultivation stage (subpopulations 160 and 200) revealed that clonal cell lines reached a near-maximum growth rate between the generations 160 and 220. Similar observations using anti IL-8-antibody-producing CHO DP-12 (clone#1934, ATCC CCL-12445) resulted from the work performed by Beckmann et al. (2012), observing that subpopulations SP165 and SP420 (denoting 165 and 423 days of cultivation, respectively) attained a near-maximal growth rate when cell samples from the long-term cultivation were cultivated in bioreactor systems. However, when the same samples were cultivated in shaking flasks, SP420 cells still improved their proliferation rates and even reached higher cell densities in culture. These findings suggest that the bioreactor strategy limited the overall performance of the long-term cell samples, probably because the bioreactor cultivation was performed using a non-optimised culture strategy. Thus, their findings corroborate that cell culture environment is a key player that moulds the growth behaviour and imposes proliferation rate boundaries to cell populations, and also exhibit that through culture environment optimisation (i.e., feeding strategy, nutrient availability, by-product accumulation, temperature and osmolarity) the μ boundaries can be increased.

Chapter 4

HETEROGENEOUS CELL GROWTH PERFORMANCE IN CLONAL DERIVATIVES OF CHO-S CELLS DURING FED-BATCH CULTURE

Chapter 4

Heterogeneous cell growth performance in clonal derivatives of CHO-S cells during fed-batch culture

This chapter introduces the procedures employed to culture 22 clonally-derived CHO-S cell lines at early-, mid- and late-generations under fed-batch regimen, corresponding to generations 0, 80 and 200, respectively, followed by assessments of their growth characteristics during the fed-batch cultivation. Altogether, this methodology allows us to gain insight into growth dynamics within CHO cell populations and identify optimal growth performance among the clonally-derived CHO-S populations.

4.1 Background

The fed-batch cultivation is the preferred culture mode for recombinant protein production, allowing the control of indispensable nutrients such as glucose and glutamine to avoid nutrient depletion, and reducing the inhibitory growth effects of by-products by minimising their formation and accumulation (Altamirano et al. 2004; Chen et al. 2001; Gorfien et al. 2003; Mulukutla et al. 2012). In addition, fed-batch cultures make possible to control growth parameters such as the specific growth rate and culture growth phases, as well as to increase the longevity of the culture and achieve high cell densities, viabilities and productivities (Chu and Robinson 2001). In fed-batch cultivation the nutrients are added either continuously or semi-continuously in an attempt to maintain an active metabolism and meet the nutritional cellular demands for survival, proliferation and biomolecule production. Given the metabolic differences among CHO cell lines and incorporated genetic constructs, fed-batch optimisation must be carried out to obtain optimal growth and productivity performance. Inefficient nutrient feeding strategies generate unbalance in the metabolism which may lead to apoptosis or unpredictable cellular performance which jeopardises the quality, stability and structure of recombinant glycoproteins; it is not surprising that low culture performances observed in fed-batch cultures are usually associated to an ineffective feeding strategy (Fan et al. 2014; Ozturk et al. 1992; Yang and Butler 2000).

During fed-batch cultures, the populations exhibit five growth phases: lag, exponential, deceleration, stationary and dead phases. The lag phase is a stage of adaptation to the new culture environment in which cells rearrange their metabolism to proliferate. This phase is usually short in recombinant production processes due to

cells being previously acclimatised to the cultivation conditions using the same media composition and culture environment, inoculating with cells at the mid-exponential growth phase also accelerates the transition into the following phase. The second stage corresponds to exponential growth, occurring when cells have been accustomed to the culture environment and the nutrient availability is not limited thus rapid proliferation is promoted. The deceleration phase follows when some of the essential nutrients are depleted (e.g., glutamine and glucose) or some by-products reach toxic levels, then cells rearrange their metabolism in order to meet their energetic requirements to survive, resulting in a gradual decrease of their proliferation rates.

The stationary phase is the most important phase during the production of recombinant proteins because cells switch their metabolism to produce secondary metabolites such as antibodies. The ability of a culture to remain viable over extended time periods is a determinant factor that needs to be considered during recombinant protein production processes as longer periods imply higher volumetric productivities. In this growth phase, cells are metabolically active, but they minimise or even arrest their proliferation rates as a result of environmental changes such as essential nutrient depletion, elevated by-product build-up and osmolarity (Al-Rubeai and Singh 1998; Cotter and Alrubeai 1995). It has been suggested that phenotypic traits within populations play an important role during the stationary growth phase, for example beneficial growth traits permit cells to resist and/or tolerate elevated environmental stressors and remain viable over extended periods whereas cells with low tolerance levels compromise the cellular integrity in short time periods and trigger cell death.

Cell death may occur by three mechanisms: necrosis, autophagy and apoptosis. Necrosis occurs when elevated stress in the environment generates a physical cellular damage on the cell membranes which results in membrane rupture and release of cytoplasmic content (Arden and Betenbaugh 2004; Laken and Leonard 2001). On the other hand, autophagy is a programed cellular death resulting from the exhaustion of essential nutrients triggering the reutilisation of internal biomolecules to meet the cellular metabolic demand (Levine 2005; Lum et al. 2005). Finally, apoptosis or programmed cell death is a controlled physiological mechanism responding to changes in the culture environment such as nutrient deprivation, by-product accumulation, oxygen limitation and hyperosmotic conditions (Laken and Leonard 2001; Vives et al. 2003) and to endogenous events such as the cytochrome C release from the mitochondria and/or incomplete protein synthesis, folding and glycosylation in the endoplasmic reticulum (Arden and Betenbaugh 2004; Laken and Leonard 2001). Together, the death stimulus activate signalling cascade events that lead to notorious

changes in morphology (e.g., DNA condensation and fragmentation, cellular shrinkage, membrane bulging and apoptotic-bodies formation) and finally cell death (Arden and Betenbaugh 2004; Cotter and Alrubeai 1995).

As mentioned above CHO cells are highly sensitive to changes in the culture environment and the fed-batch cultivation offers a rapid solution for minimising variations during production processes through monitoring the culture environment and controlling the cell growth characteristics (Laken and Leonard 2001). Taking into account the phenotypic heterogeneity among CHO populations, it is suggested that the assessment of growth performance during fed-batch cultures will permit to identify clonal populations with superior growth characteristics such as high tolerance to environmental stress, ability to reach elevated cellular densities, rapid proliferation rates and survival over extended culture periods. Additionally, fed-batch studies enable the evaluation of detrimental growth characteristics acquired during the long-term culture strategy used to generate the studied clones (see chapter 3).

4.2 Chapter aims

In this chapter, I investigated two hypotheses: (i) that the inherent genetic instability within a donor CHO-S population generated a panel of 22 clonal CHO-S cell lines with varied range of growth patterns such as elevated IVCD and tolerance to environmental stressors, and (ii) that during the adaptation and evolution phase clones diverged significantly from their initial growth status by acquiring beneficial and/or detrimental growth characteristics along the culture. Thereby, I suggest that:

(i)   The inherent cellular heterogeneity present within the parental CHO-S population permitted the isolation of clonally-derived cell lines with desired and relevant manufacturing characteristics such as elevated specific growth rate and IVCD.

(ii)   The panel of 22 clonally derived CHO-S cell lines would exhibit remarkable differences in the growth performance (i.e., variable IVCD, peak VCD, µ and cell size) at their different subpopulations along the long-term regimen (i.e., early, mid-, and late-subpopulations, corresponding to generations 0, 80 and 200, respectively).

(iii)   The panel of 22 clonally derived CHO-S cell lines at early-subpopulations would exhibit a poor growth performance such as low viable cell densities, short fed-batch periods and slow proliferation rates, followed by notable

improvements in these growth parameters as the result of the adaptation and evolution phases that underwent each clonal CHO-S cell line during the long-term culture regime.

The aim of this chapter is to reveal the phenotypic variability among the panel of 22 clonally-derived cell lines with regards to their phenotypic stability along long-term culture regime (i.e., early, mid-, and late-subpopulations for each clone, corresponding to generations 0, 80 and 200, respectively), overall growth performance (i.e., IVCD, peak VCD, µ and cell size) and their proposed potential (i.e., for recombinant protein production or cell line development). Additionally, I aimed to identify, characterise and classify the cellular performance for 66 differently aged clonal CHO-S subpopulations, corresponding to three subpopulations for each clone at generations 0, 80 and 200, respectively, under fed-batch regimen to generate a panel of clonal CHO-S cell lines with relevant industrial capabilities or potential such as protein production processes and further cell line development processes. Finally, I aimed to identify the growth parameters that make cell lines with industrial relevance in order to improve screening methodologies to facilitate the selection of relevant phenotypes and recognise growth traits that permit to optimise biopharmaceutical processes.

4.3 Chapter objectives

To address the chapter aims, the objectives of the work presented here were to:

i)   Identify the optimal feeding strategy that permits an elevated integral of viable cell density among the clonally-derived CHO-S cell lines.

ii) Evaluate the cell growth performance under optimised fed-batch culture for a set of 22 clonally-derived CHO-S cell lines at their early-, mid-, and late-subpopulations.

iii) Asses and compare the effect of long-term subculture regimen in the cellular growth performance among the clonally-derived CHO-S cell lines.

iv) Identify clones with enhanced growth characteristics such as maximal specific growth rate (µ) and superior IVCD and peak VCD.

v)   Identity clones with phenotypic stability in terms of low variability in IVCD, peak VCD, µ and cell size throughout the early-, mid- and late-subpopulations.

vi) Identify the changes in the growth parameters that led to inferior or enhanced IVCD.

4.4 Results

For achieving optimal cell growth performance during fed-batch studies, a multi-day supplementation strategy was optimised using CHO CD EfficientFeed™ B as nutrient supplement. The feeding strategy that supported the highest VCD peak and IVCD growth performances was selected as the optimal strategy. The optimised fed-batch culture consisted in growing CHO-S cells at initial density of 2-3 x 10^5 cells mL^{-1} in 25 mL CD CHO media supplemented with 8 mM L-glutamine with a multi-day supplementation of 10% (v/v) CHO CD EfficientFeed™ B on days 3, 5, 7 and 9. The cultures were incubated in an orbital-shaker incubator at 37°C, 170 rpm, under 5% (v/v) CO_2 atmosphere and ended when cell viability dropped below 60%. In addition, to ensure consistency between cultures, clones were grown using same media and nutrient supplement batch.

Apart of the CD CHO media Fed-batch optimisation, an alternative fed-batch strategy was attempted, involving cultivation in CD FortiCHO™ Medium (Life Technologies, Paisley, U.K.) instead of CD CHO medium. However, when CD FortiCHO was used as basal media, IVCD values were lower than those observed with CD CHO medium. Studies have described that CD FortiCHO promotes better growth performance (Barrett et al. 2012), but the fed-batch optimisation performed here suggested that for achieving a top performance clones must be fully adapted to CD FortiCHO culture environment before carrying out the optimisation processes or even they should have been isolated using CD FortiCHO media. The fed-batch optimisation involving CD FortiCHO were performed after 5 cellular passages in CD FortiCHO, being the first three passages in a combination of CD CHO: CD FortiCHO media (50:50, 30:70 and 10:90, respectively) to allow a gradual and faster adaption. The passages 4 and 5 were carried out in 100% CD FortiCHO to allow full adaptation, however the optimisation data suggested that clones 4 and 10 did not develop fully-adapted populations and thus longer periods of adaptation were likely required (data not shown). Therefore, the implementation of CD FortiCHO medium as an option for the fed-batch strategy basal media was discarded because longer adaptation periods would also lead to dramatic changes in the original phenotypic profile of the clones.

For this set of experiments it was hypothesised that by growing cells under an optimised fed-batch regimen, clones with superior growth phenotype and adaptability would resist better the environmental conditions encountered during the cultivation, particularly in the late fed-batch culture stages. As a result, clones with superior growth performance and phenotypic characteristics would reach elevated cell densities and cell viability over the entire culture period. Additionally, because previous experiments

performed on the clones indicated that genetic drift improved their growth characteristic over increasing generations (chapter 3), the fed-batch cultivation was used to investigate if such improvements were maintained when cells were exposed to the environmental stress generated during this cultivation mode (i.e., fed-batch cultivation) after cell revival.

For each of 22 clones, a set of three subpopulations (early-, mid- and late-subpopulations, corresponding to generations 0, 80 and 200, respectively) generated from a long-term subculture regime were selected and grown in fed-batch culture in glutamine supplemented CD CHO media. It is theorised that each subpopulation represents a specific evolutionary time point along the long-term cultivation (see chapter 3). In that sense, the early-subpopulations (generation 0) represent cells during the adaptation phase, mid-subpopulations (generation 80) represent cells at the beginning of the evolution phase and late-subpopulations (generation 200) represent the evolved phenotypes.

For the fed-batch cultures presented here, the viable cell density, cell diameter and cell viability was monitored daily, followed by the calculation of the specific growth rate and cumulative IVCD. The growth performance during fed-batch cultivation was characterised and compared with the parental population to corroborate that improved cell phenotypes can be generated by harnessing the genetic instability in a parental population, and that such derived populations maintain the improved phenotype after cryopreservation and cell revival. Finally, in order to facilitate the identification of the clones along the long-term culture, the name of each subpopulation was derived from the clone number and the time point at the moment in which the subpopulation sample was cryopreserved. For example, "clone 1-early" is the original subpopulation of the clone 1 generated before starting the long-term sub-culture (generation 0), "clone 1-mid" is a subpopulation of the clone 1 cryopreserved after ~80 generations and "clone 1-late" is a subpopulation cryopreserved after ~200 generations.

4.4.1 Evaluating the maximal viable cell density among clonally-derived CHO-S cell lines during fed-batch culture

The previous experiments described in chapter 3 exhibited that clonal populations derived from the same parental population were highly variable among and within them. To test the hypothesis that clones exhibited notable differences in their growth patterns over increasing generations, fed-batch studies using subpopulations at early (generation 0), mid (generation 80) and late (generation 200) stages of the long-

term subculture were performed for each clone. The ANOVA analysis (Figure 4-2A) revealed that the age of the clones (i.e., 0, 80 or 200 generations) had an effect on VCD (two-way ANOVA, $p<0.005$, F=6.61) and the Tukey's test showed significant VCD differences between early- and mid-subpopulation (Tukey's test, $p<0.0001$) and early- and late- subpopulation (Tukey's test, $p<0.0001$).

Comparing the peak of viable cell density obtained during the fed-batch cultivation (Figure 4-1) it can be observed that values were highly variable among and within clones, ranging between 10.76×10^6 cells mL^{-1} for clone 22-Late and 26.71×10^6 cells mL^{-1} for clone 11-Mid. In addition, it was observed that the majority of subpopulations tested (58 out of 66) acquired significant differences with respect to the parental cell line (17.73×10^6 cells mL^{-1}). Analysing in detail these changes, the data shows that 16 out of the 22 clones at early subpopulations enhanced their VCD peak. However, only for clones 7, 9 and 19 the improvements observed were statistically significant (Student's T-test, p<0.05). Similarly, 21 out of the 22 clones at the mid- and late-subpopulations exhibited increments, but only the changes for 12 mid- and 14 late-subpopulations were statistically significant (Student's T-test, $p<0.05$). From the 22 clones, clones 12, 13, 16, 17, 18, 20 and 21 gradually improved the peak viable cell density with increasing generation number obtained from the long-term cultivation during the fed-batch culture. Contrary to this behaviour, clone 9 gradually declined the ability to reach higher cellular densities with increasing generation number, however its values were still higher than the observed for the parental population (1.23, 1.04 and 1.05 fold change at early-, mid- and late-subpopulations, respectively). On the other hand, clones 3 and 10 exhibited improvements from early to mid-subpopulations without significant changes in the late-subpopulations, whereas clones 1, 4, 5, 6, 11 and 22 improved their mid-subpopulations, but decreased at late-subpopulations, probably indicating changes within population structure generated from the genetic drift. Finally, clones 7, 14, 15 and 19 only increased their late-subpopulation peak VCD with respect to the values observed for each clone at early-subpopulations.

To analyse the overall peak VCD trend among subpopulations the data was grouped according to subpopulations irrespective of individual clones, this analysis showed that clones tended to significantly improve their VCD peak with increasing generation number (two-way ANOVA, $p<0.003$, F=6.6), exhibiting overall improvements of 7 and 15% at mid- and late-subpopulations, respectively. Moreover, the Tukey's test showed that the differences between early- and mid- subpopulations and also between early- and late-subpopulations were statistically significant (Tukey's $p<0.02$ and $p<0.005$, respectively), in contrast, no significant differences were

observed between mid- and late-subpopulations (Tukey's *p*>0.9). The data also displayed that, overall, the mean VCD peak values for early-, mid- and late-subpopulations were greater than the value obtained for the parental population by 7, 21 and 23%, respectively (Figure 4-2A).
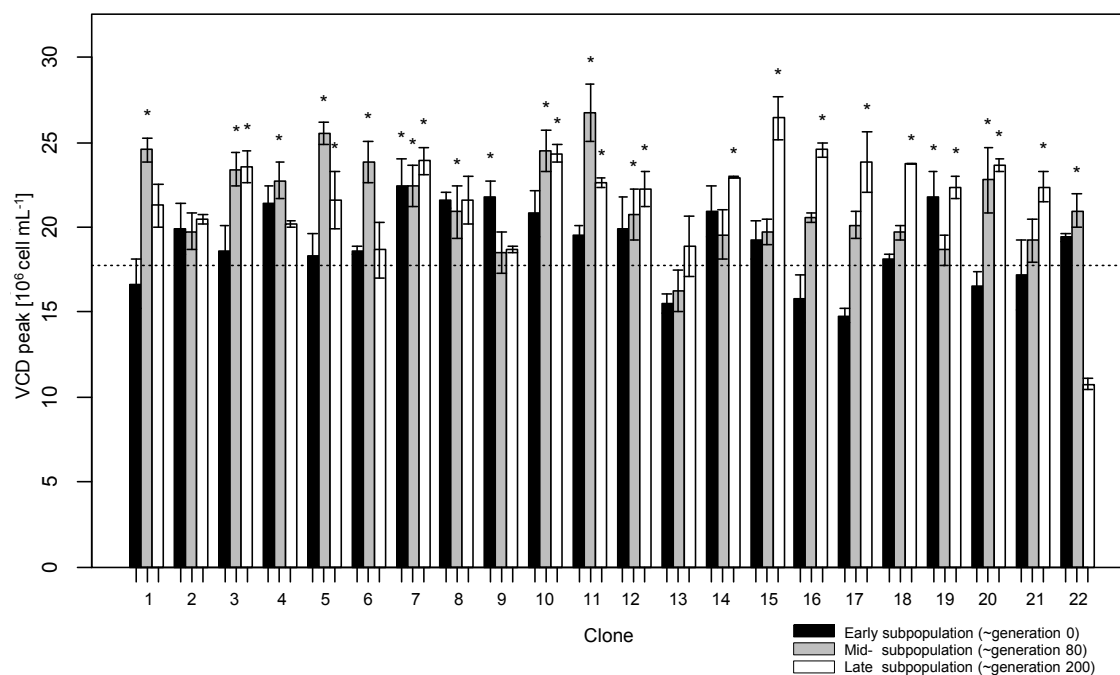
Figure 4-1 Peak of viable cell density for 22 clonally-derived CHO-S cell lines during fed-batch culture. For each clone, early-, mid- and late-subpopulations generated from a long-term subculture regime, corresponding to generations 0, 80 and 200, respectively, were grown in fed-batch culture in CD CHO media supplemented with 8 mM L-glutamine and maintained at 37°C, 170 rpm, under 5% (v/v) Catmosphere until culture viabilities dropped below 60%. During the culture, 10% (v/v) CHO CD EfficientFeed™ was fed at days 3, 5, 7 and 9. The viable cell density was evaluated during the fed-batch culture and the highest value is the peak of viable cell density. The mean and standard deviation were calculated from duplicate fed-batch cultures. The * denotes a significant difference between subpopulation and parental cell line values (Student's T-test, *p*<0.05). The dotted line indicates the peak of viable cell density reached by the parental population.
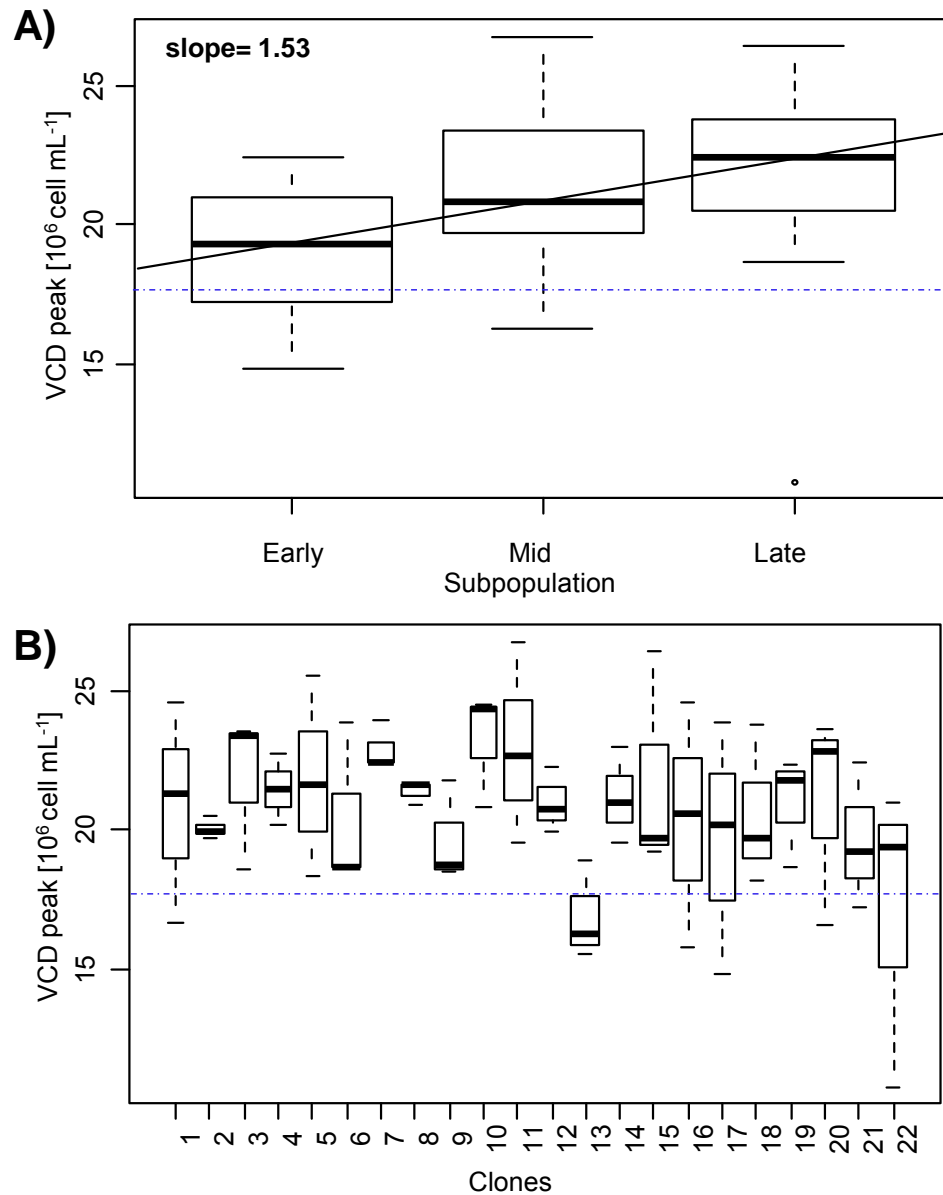
Figure 4-2 Peak viable cell density patterns for 22 clonally-derived CHO-S cell lines during fed-batch culture. Cells were grown in fed-batch culture in CD CHO media supplemented with 8 mM L-glutamine and maintained at 37°C, 170 rpm, under 5% (v/v) CO_2 atmosphere until culture viabilities dropped below 60%, during the culture 10% (v/v) CHO CD EfficientFeed™ was fed at days 3, 5, 7 and 9. Viable cell density was assessed daily and the maximum value for each clone is reported as the peak of viable cell density. For each clone, early-, mid- and late-subpopulations generated from a long-term subculture regime, corresponding to generations 0, 80 and 200, respectively, were evaluated and grouped according to long-term culture stage (A). Also, the obtained values for early-, mid- and late-subpopulations for each of the 22 clones are presented (B). The blue dotted line indicates the peak of viable cell density of the parental population and the diagonal black line represents the regression line which is accompanied by the slope value.

Clones at early subpopulation showed VCD peak values in the range of 14.78 to 22.39 $\times 10^6$ cells mL^{-1} with a mean of 19.03 $\times 10^6$ cells mL^{-1}. Clone 7 was the population that displayed the highest peak of viable cell density at this early-subpopulation, maintaining similar maximal density value at mid-subpopulation and enhancing its capacity in the late-subpopulation (1.07 fold changes). Contrary, clone 17 showed the lowest VCD peak among clones at the early subpopulation, but exhibited greater improvements at mid- and late-subpopulations (1.36 and 1.61 fold changes, respectively). Among the clones with low peak of VCD at early-subpopulations, clone 13 showed the lowest improvements in subsequent subpopulations (5 and 22% increments at mid- and late-subpopulations, respectively) and was the unique clone with two out of three subpopulations having lower VCD peak values than the parental population (Figure 4-1).

Using the variation range of VCD peak values for each clone's subpopulations as indicator of phenotypic stability (Figure 4-2B), it was observed that clones 2, 4, 7, 8 and 12 were the most stable clones, whereas clones 1, 5, 16, 17 and 22 showed large variability for the long-term cultivation derived cell populations. The data also showed that the stable clones exhibited better VCD performance than the parental line since early subpopulations, indicating that probably this clones inherited beneficial traits which prevented increments in genetic heterogeneity, and probably this slight enhancement in VCD peak, observed at mid- and late-subpopulations, resulted from genetic drift. On the other hand, the phenotypically unstable populations (clones 1, 5, 16 and 17) exhibited low VCD peak performance at early subpopulations and notable improvements at mid- and late-subpopulations, it can be suggested that this cellular behaviour observed at early subpopulations was the result of their high phenotypic heterogeneity with an elevated proportion of cells that inherited deleterious phenotypic traits which limited their growth in agitated culture environments triggering to suboptimal performances (see chapter 3), the enhancements observed at mid- and late-subpopulations resulted from beneficial growth characteristics acquired during the adaptation phase and evolution phase leaded for genetic drift (see chapter 3).

It is important to note that clones with stable populations along increasing generations (clones 2, 4, 7, 8 and 12) not exhibited significant changes in maximum viable cell density among early-, mid- and late-subpopulations (Student's T-test, $p > 0.05$; data not shown), however, it is expected that these clones differ significantly in other growth parameters (e.g., μ and IVCD) and in their metabolic activity (e.g., glucose consumption and lactate production). To gain more insight into the clonal variability among and within clones, these growth parameters are analysed in the next sections.

4.4.2 Fed-batch cultivation revealed that clonally-derived CHO-S cell lines improved their specific growth rate throughout the long-term cultivate regimen.

To evaluate if the differences in µ described along the long-term cultivation (see chapter 3) were conserved after cell revival and during the fed-batch cultivation, and to compare if the findings observed with the peak of VCD evaluation (section 4.4.1) were replicated by analysing a different growth parameter, the specific growth rate at mid-exponential growth phase was used as indicator of phenotypic change. It is important to note that the specific growth rate at mid-exponential growth phase was measured before starting with EfficientFeed™ B feeding, which allows for comparison with long-term cultivation derived data (chapter 3).
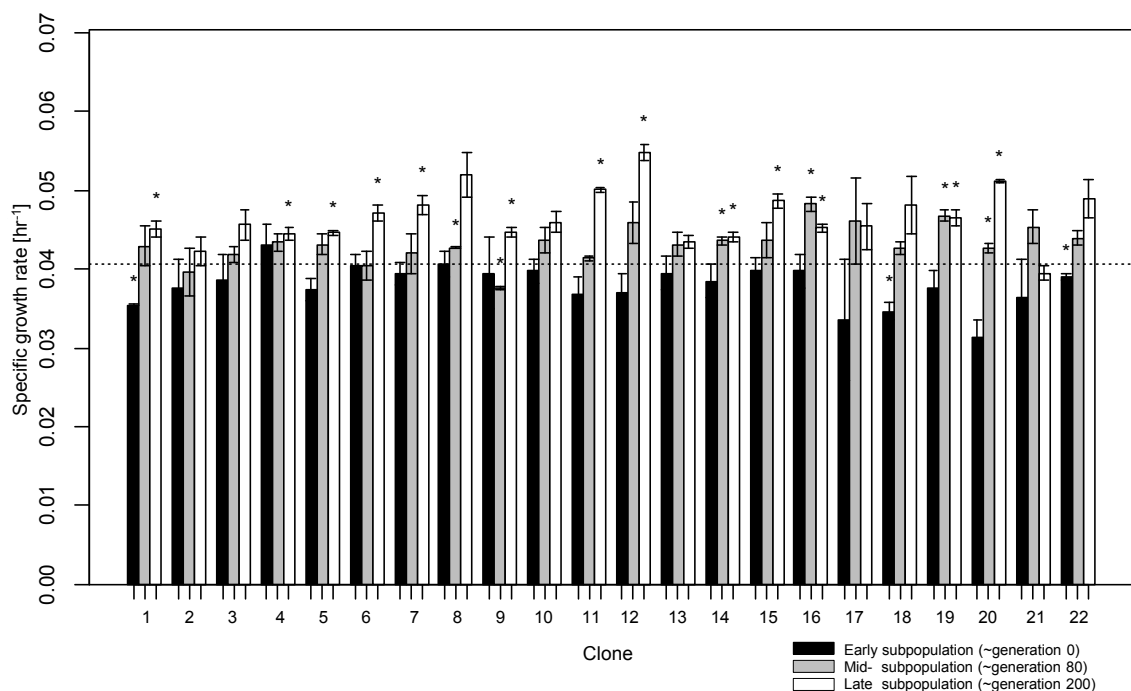
Figure 4-3 Specific growth rate at mid-exponential growth phase for 22 clonally-derived CHO-S cell lines during fed-batch culture (before starting the feeding scheme). For each clone, early-, mid- and late-subpopulations generated from a long-term subculture regime, corresponding to generations 0, 80 and 200, respectively, were grown in fed-batch culture in CD CHO media supplemented with 8 mM L-glutamine and maintained at 37°C, 170 rpm, under 5% (v/v) CO_2 atmosphere until culture viabilities dropped below 60%. During the culture 10% (v/v) CHO CD EfficientFeed™ was fed at days 3, 5, 7 and 9. The mean value and standard deviation were calculated from duplicate fed-batch cultures at the mid-exponential growth phase prior to initiation of feeding scheme. The * denotes a significant differences between subpopulation and parental cell line values (Student's T-test, $p < 0.05$). The dotted line indicates the specific growth rate reached by the parental population.
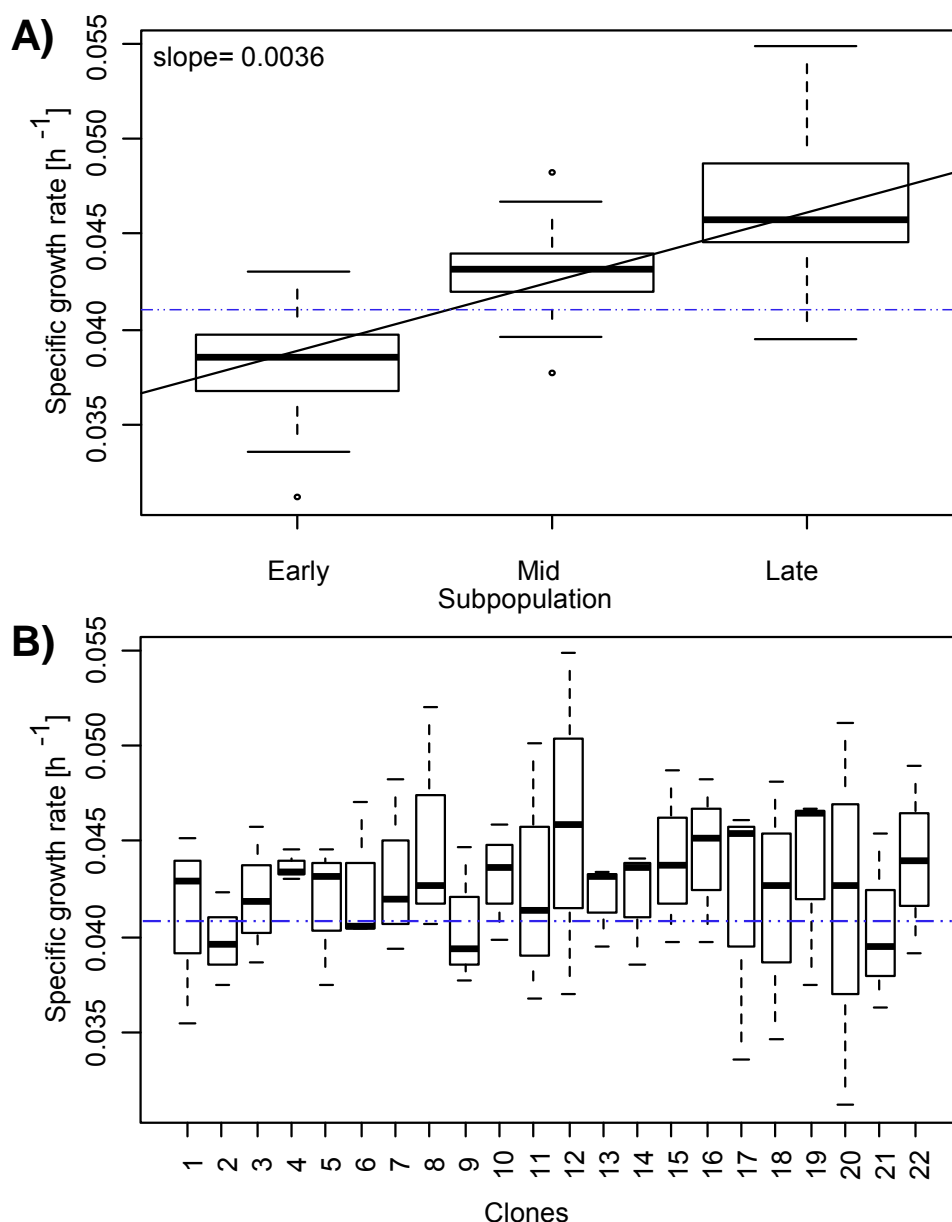
Figure 4-4 Specific growth rate patterns at mid-exponential growth phase for 22 clonally-derived CHO-S cell lines during fed-batch culture (before starting the feeding scheme). Cells were grown in fed-batch culture in CD CHO media supplemented with 8 mM L-glutamine and maintained at 37°C, 170 rpm, under 5% (v/v) CO_2 atmosphere until culture viabilities dropped below 60%, during the culture 10% (v/v) CHO CD EfficientFeed™ was fed at days 3, 5, 7 and 9. For each clone, early-, mid- and late-subpopulations generated from a long-term subculture regime, corresponding to generations 0, 80 and 200, respectively, were evaluated and grouped according to long-term culture stage (A). Also, the obtained values for early-, mid- and late-subpopulations for each of the 22 clones are presented (B). The blue dotted line indicates the μ value of the CHO-S parental line and the diagonal black line represents the linear regression line which is accompanied by the slope value.

The ANOVA analysis revealed that the age of the clones (i.e., early-, mid- or late-subpopulations) had an effect on μ (two-way ANOVA, $p<0.0001$, $F=51.57$) and the Tukey's test confirmed that the three subpopulations showed significant differences between them (Tukey's test, $p<0.0001$). The comparison of the mid-exponential specific growth rate observed among the 22 clones during the fed-batch cultivation (Figure 4-3) also showed that clones were highly variable in terms of specific proliferation rates observing values between 0.031 h^{-1} for clone 20-early and 0.055 h^{-1} for clone 12-late. Comparing the growth rate with respect to the parental population was observed that around 60% of subpopulations improved their growth performance, being more notorious at late subpopulations where 21 out of 22 clones exhibited improvements (up to 1.34 fold change), followed by the mid-subpopulations were 19 out of 22 clones showed higher proliferation rates (up to 1.18 fold change). Contrasting results were observed at early subpopulations, at which the majority of the clones (21 out of 22) showed lower proliferation rates than the parental population (decreases of up to 23%). These results agree with the findings observed during the long-term cultivation (chapter 3), confirming that early subpopulations exhibited suboptimal performance as the result of their lower capacity to grow in agitated environments. A Student's T-test analysis showed that only 43% of all the observed μ improvements were statistically significant (Student's T-test, $p<0.05$).

Further analysing the μ improvements between and within clones, 13 out of 22 clones (clones 1, 2, 3, 5, 7, 8, 10, 11, 12, 15, 18, 20 and 22) gradually improved their proliferation rates from early to late subpopulations, three clones (clones 4, 6 and 9) improved μ only in the late-subpopulations and the remaining six clones (clones 13, 14, 16, 17, 19 and 21) also improved μ at mid- and late-subpopulations, but showed the highest μ value at mid-subpopulations (Figure 4-3). From clones that exhibited gradual improvements along subpopulations, clone 20 showed the highest improvements, being 37% and 64% at mid- and late- subpopulations, respectively. Contrarily, clone 2 exhibited the lowest improvements with 6 and 13% at mid- and late-subpopulations, respectively. On the other hand, the late subpopulation of clone 12 exhibited the greatest proliferation rate (0.0548 hr^{-1}) and also showed regular increments along subpopulations (24 and 48% at mid- and late- subpopulations, respectively).

The degree of divergence in the growth rate at mid-exponential growth phase within subpopulations derived from a long-term cultivation was assessed during fed-batch culture (Figure 4-4A), observing notable difference within subpopulations. The general observations were that clones evolved better growth characteristics over time, being the differences between all subpopulations statistically significant (two-way

ANOVA, $p < 0.00001$, F=51.6; Tukey's test, $p < 0.001$ between subpopulations). The results were µ improvements of 14% and 24% at mid- and late-subpopulations, respectively, when compared to the corresponding early subpopulation. In addition, these findings corroborate the long-term cultivation results (see chapter 3), in which clones improved their growth performance with increasing generation number.

Furthermore, the comparison between the subpopulations µ median values and the µ of the parental population showed that early subpopulations were less fitted than the parental cell line with an average decline of 7% in their proliferation rates. In contrast, mid- and late-subpopulations enhanced their µ performance around 6 and 15% with respect to the parental line, respectively. The assessment of variability within clones' µ was used to measure the stability along increasing generations (Figure 4-4B). The majority of the clones exhibited large intra-variations (21 out of 22 clones). Among cell lines, clone 4 was by far the most stable population with growth rates from 0.043 to 0.045 hr^{-1}. In contrast, clones 8, 11, 12, 17, 18 and 20 were the most unstable populations with ranges from 0.031 to 0.055 hr^{-1}. The proliferation rates observed for clone 4 were notably higher than the parental population µ value (6, 7, and 9% at early-, mid- and late- subpopulations, respectively) and also notably higher than the rest of the clones at early-subpopulations, suggesting that the low variability in clone 4 was the result of the inherited beneficial growth traits which allowed it to proliferate without generating drastic changes in its phenotype. On the other hand, the high variability observed in the unstable populations suggest that during the long-term culture and particularly during the adaptation phase (see chapter 3) the clones must have evolved better growth characteristics to resists agitated conditions and they still were improving their proliferation rates during the evolution phase until reaching a maximal µ.

4.4.3 Evaluating the global integral of viable cell density among clonally-derived CHO-S cell lines during fed-batch cultivation

For this study, the IVCD was chosen as main indicator of cell line performance, because the integral of viable cell density is recurrently used to compare the average growth performance among different cell lines because is a key factor that determines the overall yield performance during recombinant protein production (Kumar et al. 2009). The IVCD is calculated as the area under the curve when the VCD is plotted against the culture and it represents the "cumulative cell time" which can be easily compared among cultures to identify cell lines that exhibit better cellular responses to environmental stressors and environmental factors that are commonly encountered

during the recombinant protein production. Therefore, IVCD is commonly used as indicator of growth performance and defined as essential measurement in all biotechnological processes that involve biologic production due to greater IVCD results in higher volumetric recombinant proteins titters, for example assuming two cultures with equal specific productivity, the one with the greater IVCD would yield more product (Pörtner 2007). In addition, IVCD is employed to calculate fundamental parameters such as the specific productivity and the rates of metabolite consumption and production along the culture. Therefore, although the 22 isolated clonally derived CHO-S cell lines presented here do not express any recombinant gene, the IVCD measurements can be employed to identify cell lines with great potential for producing recombinant proteins and for other studies involving cellular mechanisms in biogenesis and chemical sensibility.

As seen for other parameters (sections 4.4.1 and 4.4.2), the accumulated IVCD at the end of fed-batch culture exhibited considerable variations within and between clones (Figure 4-5), between 1417 x 10^6 cells h mL^{-1} (clone 13-mid) and 4207 x 10^6 cells h mL^{-1} (clone 11-mid). By comparing the subpopulations' IVCD performance with respect to the parental performance, it was observed that the majority of the clones (18 out of 22 clones) exhibited statistically significant changes on at least two of the three evaluated subpopulations (Student's T-test, $p<0.05$). Interestingly, clone 13 was the unique clonal CHO-S cell line that exhibited inferior cellular performance than the parental population along the three subpopulations, showing 6, 33 and 18% lower IVCD at early-, mid- and late-subpopulations, respectively.

Assessing the global IVCD behaviour along subpopulation, the ANOVA analysis revealed that the age of the clones (i.e., 0, 80 or 200 generations) had no effect on IVCD (two-way ANOVA, $p>0.05$, F=1.68), however to characterised their IVCD performance clones were fit one of five categories, clones that (i) significantly improved both mid and late subpopulations, (ii) enhanced only at mid-subpopulations, (iii) enhanced only at late subpopulations, (iv) did not change across subpopulations and (v) showed inferior performance at mid- and late-subpopulations. The data analysis showed that clones 4, 12, 17, and 19 fell in the first group with increments between 6 and 141%. Among these, clones 17 and 19 exhibited gradual improvements in IVCD along increasing generations and clones 4 and 12 exhibited the greater improvement at mid-subpopulations (1.15 and 1.38 fold changes, respectively). In addition, the data showed that clones 17 and 19 were the most unstable populations over time with improvements in IVCD between 7 and 141% along subpopulations. In contrast, clones

4 and 12 exhibited a more stable population over time with IVCD enhancements between 6 and 38%.
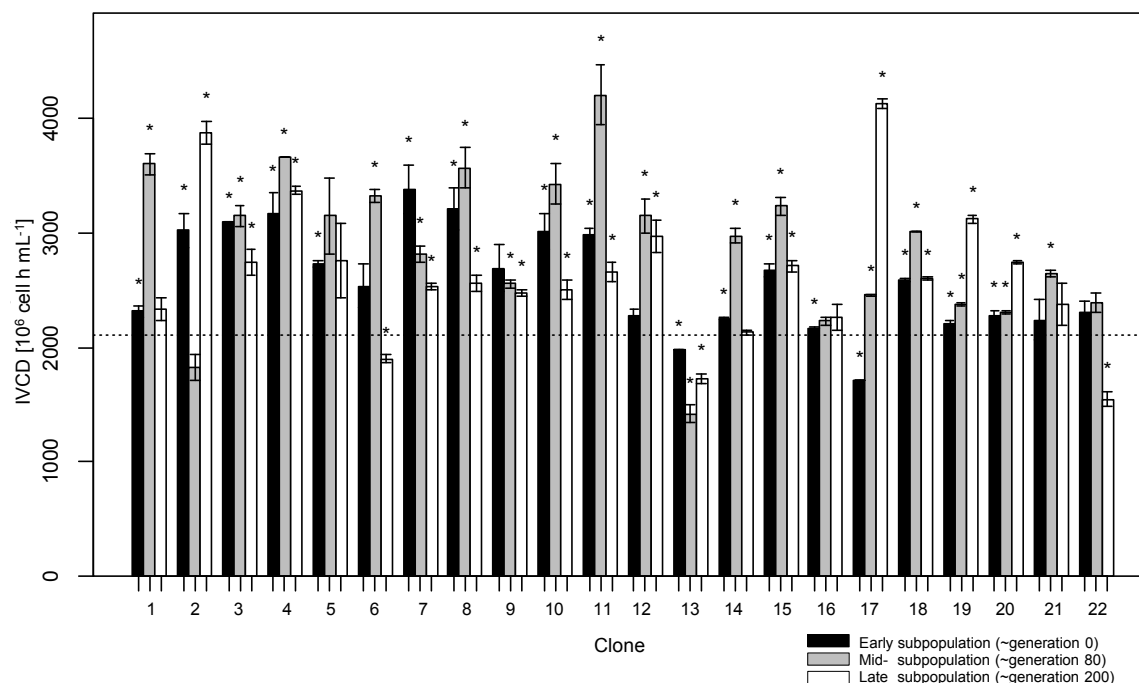
Figure 4-5 Global integral of viable cell density at the end of a fed-batch culture (IVCD60) for 22 clonally-derived CHO-S cell lines. For each clone, early-, mid- and late-subpopulations generated from a long-term subculture regime, corresponding to generations 0, 80 and 200, respectively, were grown in fed-batch culture in CD CHO media supplemented with 8 mM L-glutamine and maintained at 37°C, 170 rpm, under 5% (v/v) CO_2 atmosphere until culture viabilities dropped below 60%. During the culture 10% (v/v) CHO CD EfficientFeed™ was fed at days 3, 5, 7 and 9. The mean value and standard deviation were calculated from duplicate fed-batch cultures. The * denotes a significant difference between subpopulation and parental cell line values (Student's T-test, $p<0.05$). The dotted line indicates the global integral of viable cell density reached by the parental population at the end of the culture.

Clones 1, 3, 5, 6, 8, 10, 11, 14, 15, 18, 21 and 22 integrated the second and largest group, showing the enhancement up to 56% at mid-subpopulations and decrements of up to 33% at late subpopulations. From this group, clones 3, 5, 15, 18 and 21 showed stable growth behaviour, whereas clones 1, 6, 8 and 11 displayed by

far an unstable growth performance. The third group, presenting their maximal improvement at late-subpopulation, was integrated by clones 2 and 20. However, clone 20 exhibited a similar behaviour at early and mid-subpopulations and a slightly improved IVCD at the late-subpopulation (20%), whilst clone 2 showed a dramatic decrease at its mid-subpopulation (0.6 fold change) that recovered at late-subpopulation (1.28 fold change). The fourth group was integrated by clones 9 and 16, which exhibited the most stable IVCD behaviour across generations with no significant changes across subpopulations for both clones. Finally, the last group, integrated by clones 7 and 13, showed significant reductions at mid- and late-subpopulations (between 13 and 29%).

Grouping the IVCD performance for all the clones and classifying it into early-, mid- and late-subpopulations (Figure 4-6A) showed that IVCD was highly variable within subpopulations however no statistical difference between subpopulations was observed (two-way ANOVA, $p>0.05$, F=1.7). In addition, it can be observed that the clones, except for Clone 13, exhibited superior IVCD performances than the parental population (Figure 4-6B). Analysing the mid-subpopulations it can be observed that the IVCD were highly variable, ranging from 1417 to 4207 x 10^6 cells hr mL^{-1}, and that in general these subpopulations reached higher IVCD performance. On the other hand, late-subpopulations showed the lowest IVCD variability, observed as a small IVCD interquartile range, suggesting that over increasing generations most of the clones did not enhance their IVCD performance and indicating that late-subpopulations tended to converge into narrower IVCD boundaries. The inability of the clones to improve IVCD on their late-subpopulations seems to be a result of the evolution strategy, as late-subpopulations were evolved to increase their biomass production and not for tolerating the severe environmental conditions encountered at mid- and late- stages of fed-batch culture such as by-product accumulation, nutrient limitation and high cellular densities during the long-term cultivation that originated the differently-aged clones. Consequently, late-subpopulations were not able to resist and responded satisfactory to environmental stressor found at the stationary growth phase of the fed-batch culture

The variability observed within clones at different generations was also highly irregular (Figure 4-6B), being clones 1, 2, 6, 8, 11 and 17 those with unstable phenotype in terms of IVCD, and clones 16 and 9 the most stable populations among all the clones, with changes in IVCD values below 5% along the early-, mid- and late-subpopulations.
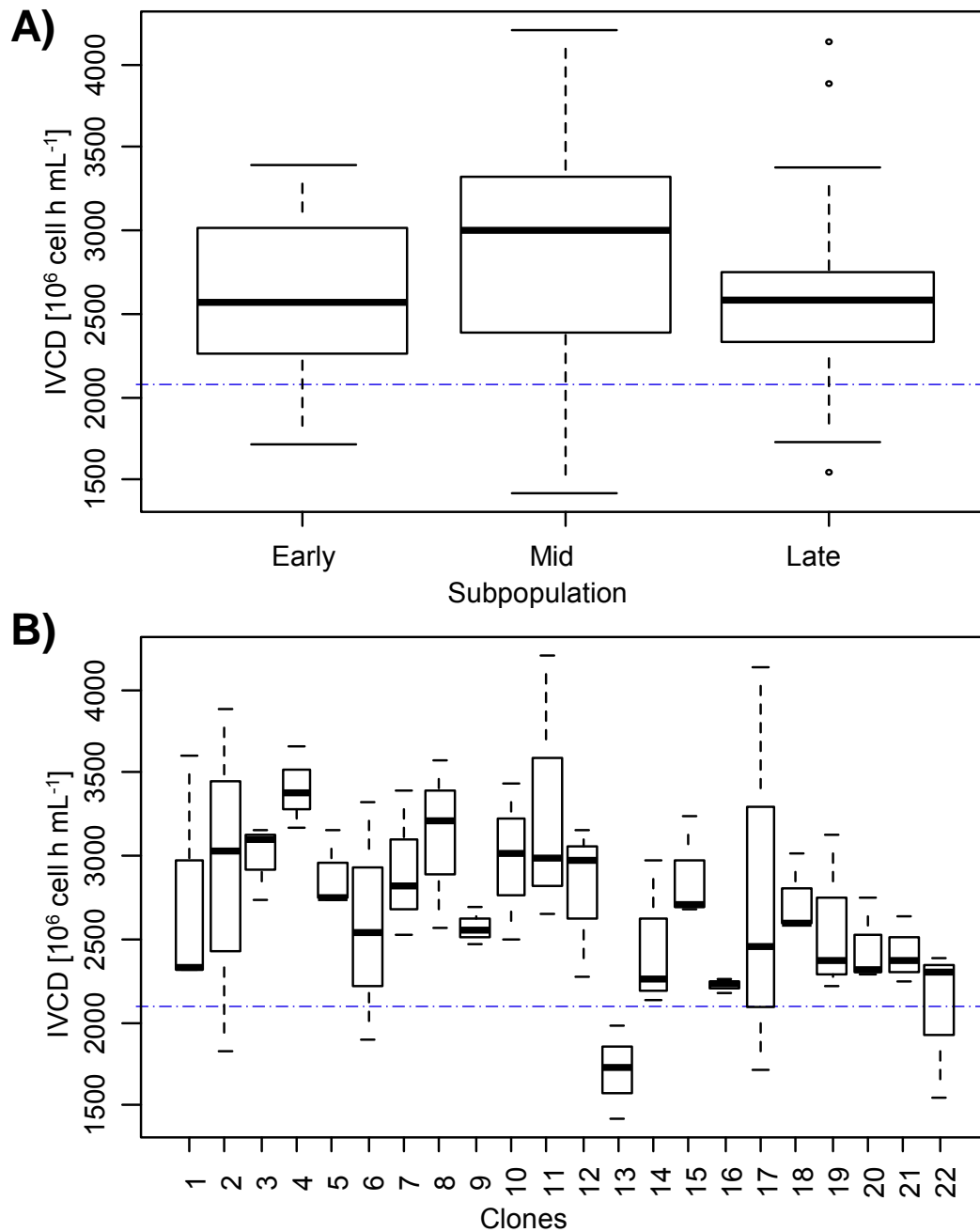
Figure 4-6 Global integral of viable cell density patterns at the end of a fed-batch culture for 22 clonally-derived CHO-S cell lines. Cells were grown in fed-batch culture in CD CHO media supplemented with 8 mM L-glutamine and maintained at 37°C, 170 rpm, under 5% (v/v) CO_2 atmosphere until culture viabilities dropped below 60%, during the culture 10% (v/v) CHO CD EfficientFeed™ was fed at days 3, 5, 7 and 9. For each clone, early-, mid- and late-subpopulations generated from a long-term subculture regime, corresponding to generations 0, 80 and 200, respectively, were evaluated and grouped according to long-term culture stage (A). Also, the obtained values for early-, mid- and late-subpopulations for all 22 clones are presented (B). The blue dotted line indicates the IVCD value for the CHO-S parental line.

4.4.4 Comparison of the cell diameter and growth characteristics among clonally-derived CHO-S cell lines during fed-batch cultivation

Previous experiments have reported that cell size, either measured as cell diameter, volume, mass or protein content, plays an important role in cell growth and productivity during recombinant protein production processes (Davies et al. 2012; Kim et al. 2001). Dreesen and Fussenegger (2011) showed that the increases in cell size and cell protein content (through mTOR over-expression) positively correlates with cell growth and productivity. Similarly, Kim et al (2001) found a positive correlation between cell size and productivity. Therefore, to evaluate if the observed variability in other growth parameters evaluated for the clones generated for this study (sections 4.4.1, 4.4.2 and 4.4.3) was correlated to changes in cell size, the average cell diameter of populations was measured by image analysis using a Vi-CELL XR cell viability analyser during the routine cell counting, but for this analysis mid-exponential growth phase measurements were selected as the most representative due to at this growth stage the culture media have low osmolarity and the cells exhibit their near maximal metabolic and growth capacity.

To test the hypothesis that clones reduced their cell volume along the long-term culture regime (see chapter 3), the ANOVA analysis was performed using the cell diameter measurement at mid-exponential growth phase (day thee) to allow comparison with the finding showed in chapter 3. The ANOVA revealed that the age of the clones (i.e., 0, 80 or 200 generations) had an effect on cell size (two-way ANOVA, $p<0.03$, F=4.14; Figure 4-7B), being significant the transition from early- to mid-subpopulations (Tukey's test, $p<0.05$; Figure 4-7B). This data allows us to hypothesise that evolved phenotypes, and thus faster-growing cells, required less cellular protein content to survive and proliferate in the agitated environment.

Moreover, as expected the cell diameter between and within clones was highly variable, ranging from 15.04 microns for clone 8-late to 17.53 microns for clone 22-late (Figure 4-7A). This data also agrees with that of previous researchers that found substantial clone specific variation in cell size, measured as cell volume and cell protein biomass, among clonal CHOK1SV populations (Davies et al. 2012). However, the comparison of the average cell diameter for clones at each subpopulation with respect to the parental cell line showed no statistically significant changes. In contrast, comparisons in cell size along increasing generations showed that the differences of clones 13, 16, 19 and 22 between early and late subpopulations and for clone 20 between mid and late subpopulations were statistically significant (Student's T-test, $p<0.05$).
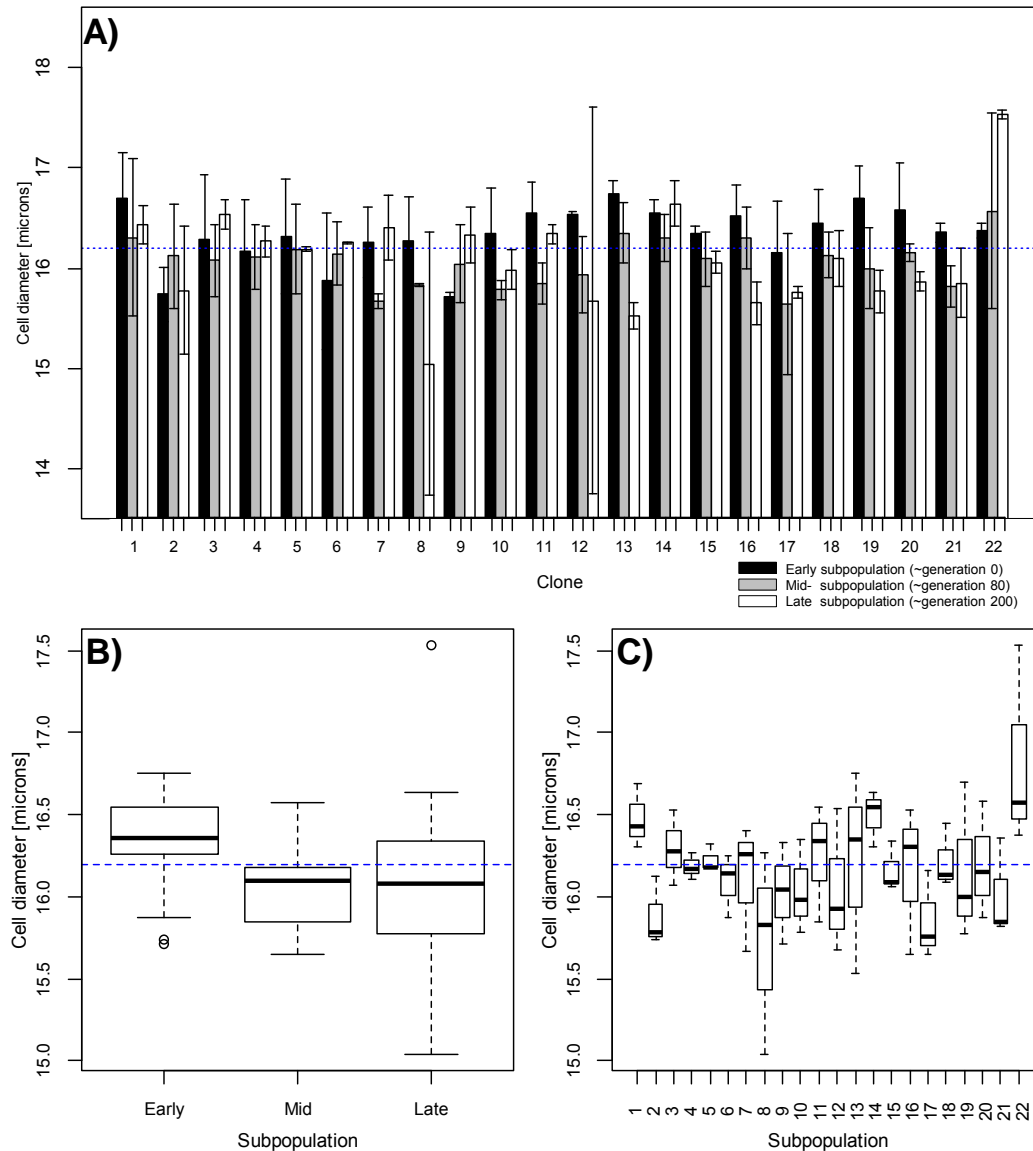
Figure 4-7 Average cell diameter at mid-exponential growth phase for 22 clonally-derived CHO-S cell lines during fed-batch culture. Cells were grown in fed-batch culture in CD CHO media supplemented with 8 mM L-glutamine and maintained at 37°C, 170 rpm, under 5% (v/v) CO_2 atmosphere until culture viabilities dropped below 60%, during the culture 10% (v/v) CHO CD EfficientFeed™ was fed at days 3, 5, 7 and 9. (A) The mean and standard deviation were calculated from duplicate fed-batch cultures at the mid-exponential growth phase prior to initiation of feeding scheme. The * denotes a significant differences between subpopulation and parental cell line values (Student's T-test, $p<0.05$). For each clone, early-, mid- and late-subpopulations generated from a long-term subculture regime, corresponding to generations 0, 80 and 200, respectively, were evaluated and grouped according to long-term culture stage (B). Also, the obtained values for early-, mid- and late-subpopulations for all 22 clones are presented (C). The blue dotted line indicates the average cell diameter value for the CHO-S parental population.

The analysis of the general cell diameter trend among subpopulations (i.e. early, mid- and late subpopulations, irrespective of clones; Figure 4-7B) indicated that clones significantly reduced their cell size from early to mid-subpopulation (Tukey's test, p<0.05) with no significant changes in cell size value from mid- to late-subpopulations (Tukey's test, p>0.96). Interestingly, the cell size variability observed among clones notably increased at late-subpopulations and resembles the μ heterogeneity observed at late subpopulations (section 4.4.2, Figure 4-4), suggesting that the differences in growth rates and cell sizes have some degree of correlation. Additionally, the intra-clonal comparison showed that cell size values for clones 4, 5 and 15 remained constant along subpopulations whereas the observed values for clones 8, 12, 13, 16, 19 and 22 notably changed with increasing generation number (Figure 4-7C).

To identify if the cell diameter exhibited some extent of correlation between the growth parameters observed during fed-batch cultivation, the relationship between cell size and VCD peak, specific growth rate and integral of viable cell density were also examined (Figure 4-8). The correlation revealed that variations in cell size were negatively correlated with specific growth rate (PPMCC r = -0.304, p-value < 0.02, n = 67; Figure 4-8A), integral of viable cell density (PPMCC r = -0.357, p-value < 0.01, n = 67; Figure 4-8B) and peak of viable cell density (PPMCC r = -0.304, p-value < 0.001, n = 67; Figure 4-8C). Although these correlations were moderate, it is evident that the smallest cell lines, in terms of average cell diameter, exhibited better (i.e., higher) growth characteristics (i.e., VCD peak, μ and IVCD) and probably would lead to higher volumetric product yield if transfected for productive processes. This moderated correlations also agrees with previous observations that found that CHOK1-SV cell size and protein content inversely correlated with proliferation rate (Davies et al. 2012).

Taking into account that the cell size is an indirect measure of protein content (Davies et al. 2012), the data allows us to hypothesise that faster-growing cell lines require less cellular protein content to survive and proliferate. Therefore it can be suggested that smaller cells are more efficient than bigger cells due to their lower synthesis requirements for cell biomass reduce their energetic and metabolite requirements. Further analyses, in particularly for evaluating the production of recombinant protein must be performed in order to hold that cell size measurements can be used as an indicator of metabolism efficiency and/or cellular productivity for recombinant proteins and to complement the findings of improved proliferation rates with smaller cell size.
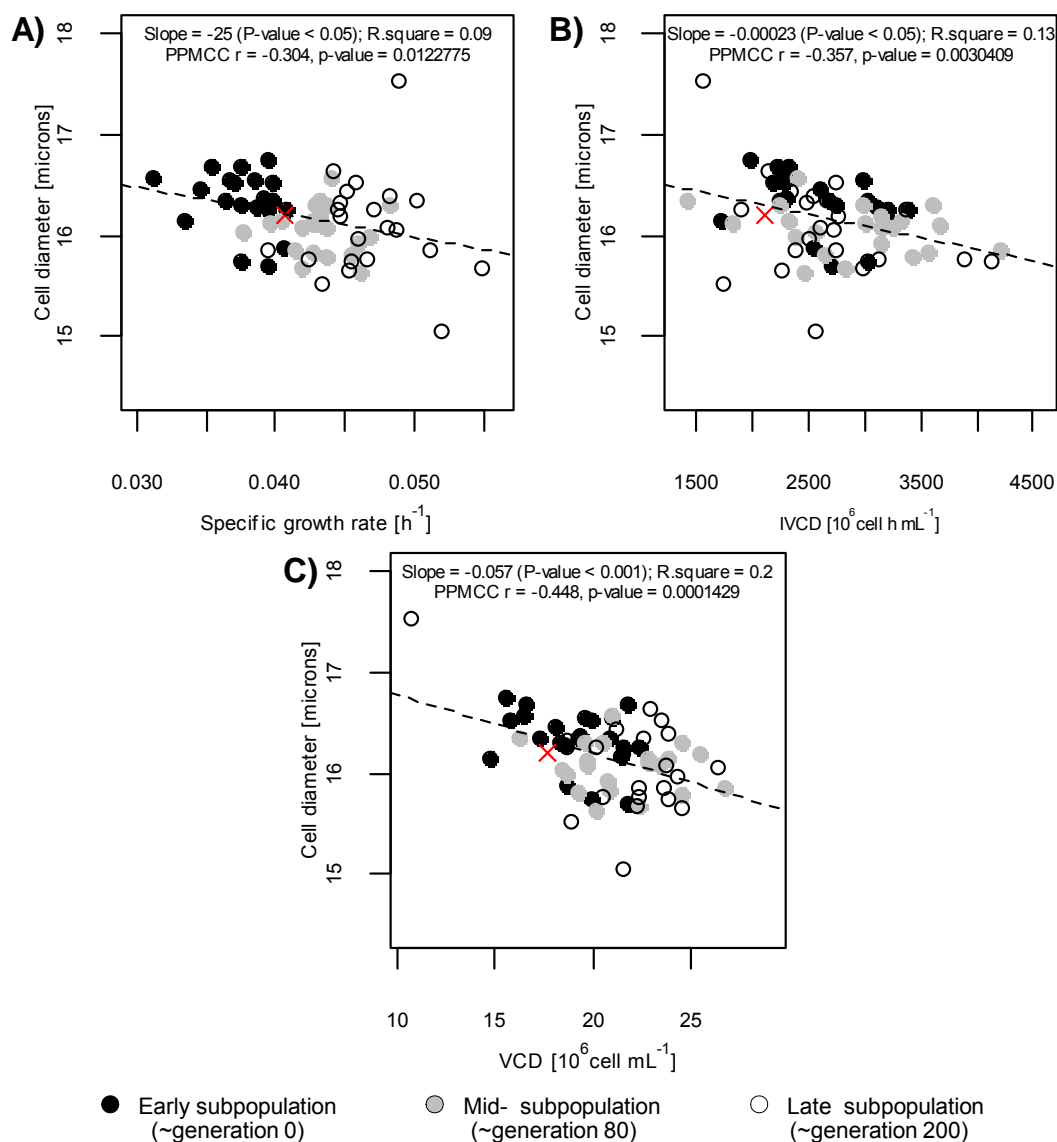
Figure 4-8 Relationship between the average cell diameter and growth characteristics during fed-batch culture for 22 clonally-derived CHO-S cell lines. Cells were grown in CD CHO media supplemented with 8 mM L-glutamine and maintained at 37°C, 170 rpm, under 5% (v/v) CO_2 atmosphere until culture viabilities dropped below 60%. During the culture 10% (v/v) CHO CD EfficientFeed™ was fed at days 3, 5, 7 and 9. Pearson correlation between (A) the cell diameter mid-exponential growth phase and specific growth rate at mid-exponential growth phase (PPMCC r = -0.304, *p*-value < 0.02, n = 67), (B) the cell diameter at mid-exponential growth phase and integral of viable cell density (PPMCC r = -0.357, *p* -value < 0.01, n = 67) and (C) the cell diameter at mid-exponential growth phase and peak of viable cell density (PPMCC r = -0.304, *p* -value < 0.001, n = 67). The black, grey and white circles represent clones at the early, mid- and late stages of the long-term subculture (i.e. generations 0, 80 and 200), respectively. The parental cell line is represented by a red "x" in the plot.

4.4.5 Cell volume normalisation did not show significant improvements in the growth parameter

Previous studies in using CHO cells have observed markedly differences in the cellular performance between populations with varied cell size. For example, Dreesen and Fussenegger (2011) showed that increases cell size and protein content of cells correlated positively with cell growth and productivity. Similarly, Kim et al (2001) also found stable populations exhibited higher cell size and productivities. Therefore, it can be suggested that the observed differences in cell size (i.e., cell diameter, volume, mass, or protein content) may mislead the growth parameters particularly when comparisons between cell lines are performed. Therefore in this section I suggest that the normalisation of growth parameters with respect to the cell size would improve the comparison between clones by reducing the cell size variability effects among clones. For this analysis, the normalised growth parameters for each clone were calculated as follow: GPN =GP/ (Ø population / Ø parental), where the GPN is the normalised growth value, GP is the growth value, Ø population and Ø parental are the populations and parental cell lines' diameter, respectively.

To evaluate if this cell size normalisation improved any correlation between the growth parameters, the relationships between the global IVCD and μ, the global IVCD and VCD peak, and the VCD peak and μ before normalisation (Figure 4-9A, Figure 4-9B and Figure 4-9C, respectively) and after normalisation (Figure 4-9D, Figure 4-9E and Figure 4-9F, respectively) were analysed. This comparison that normalised data slightly improved the correlations. For example, the Pearson' between the IVCD and VCD peak increased from 0.567 (PPMCC p-value < 0.00001, n = 67) to 0.603 (PPMCC p-value < 0.00001, n = 67) after the normalisation, between the VCD peak increased. However, the ANOVA analysis revealed that the differences between the normalized and non-normalized data were not significant (two-way ANOVA; IVCD peak p>0.05, F=0.013; VCD peak, p>0.05, F=0.026; and μ p>0.05, F=0.03).

Moreover, this data showed that the IVCD performance cannot be estimated by using the exponential data (e.g., specific growth rate; Figure 4-9A; PPMCC p-value > 0.09, n = 67) as this measurement represent a difference metabolic status of the cells. In contrast, using a growth parameter from stationary data (e.g., VCD peak; Figure 4-9B; PPMCC p-value > 0.567, n = 67) notable increased the likely to predict the IVCD performance of the clones as both parameter were obtained under similar culture environments such as nutrient depletion and hyper-osmolarity.

Finally, Figure 4-9A exhibits the µ values of the early-, mid- and late-subpopulations are clearly separate (Figure 4-9A).
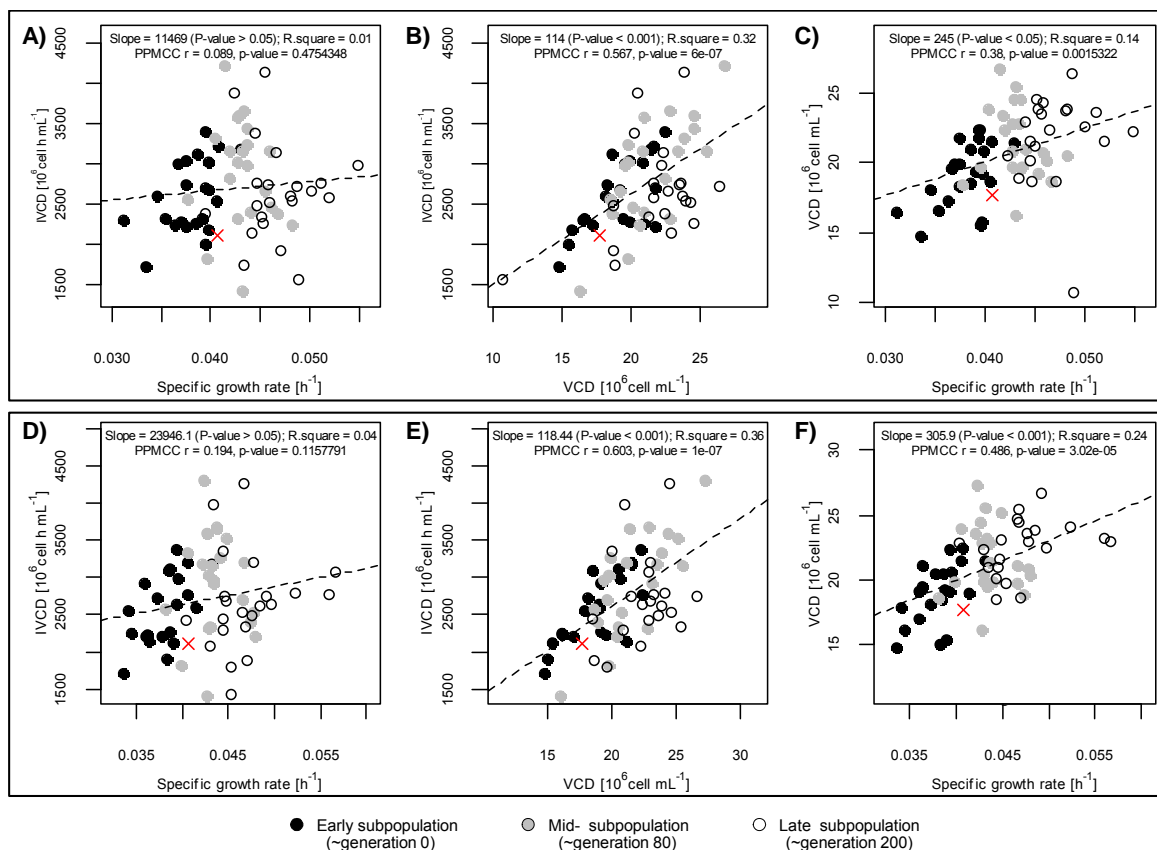
Figure 4-9 Relationship between growth parameters before and after normalisation for 22 clonally-derived CHO-S cell lines. Cells were grown in CD CHO media supplemented with 8 mM L-glutamine and maintained at 37°C, 170 rpm, under 5% (v/v) CO_2 atmosphere until culture viabilities dropped below 60%. During the culture 10% (v/v) CHO CD EfficientFeed™ was fed at days 3, 5, 7 and 9. Pearson correlation between integral of viable cell density and specific growth rate before (A) and after (D) cell size normalisation, between integral of viable cell density and peak of viable cell density before (B) and after (E) cell size normalisation, and between and peak of viable cell density and specific growth rate before (C) and after (F) cell size normalisation, The black, grey and white circles represent clones at the early, mid- and late stages of the long-term subculture (i.e. generations 0, 80 and 200), respectively. The parental cell line is represented by a red "x" in the plot.

4.5 General discussion

The optimised fed-batch process performed for this study allowed optimal growth performance among the clones by supplementing a defined concentration of CHO CD EfficientFeed™ B that permitted elevated IVCD at the end of the cultivation. In this strategy, nutrient supply was provided as a predetermined volume/concentration based on estimated energetic requirements for all clones, rather than supplied to meet individual metabolic demands based on the specific assessments of particular media components for each individual clone. This approach is widely implemented during cell line development processes because it allows us to enhance cell growth, minimise fluctuations in the culture environment and standardise the fed-batch processes among cell variants. In addition, the fed-batch strategy utilised here minimised the cell sampling volume required, not doing so would reduce the culture volume, would increase the risk of contamination, and would likely destabilise the populations in particular at early stages of the fed-batch culture when populations are more vulnerable to genetic drift effects (Campos and Wahl 2009).

Estimating the metabolic requirements in fed-batch cultures has important benefits at laboratory scale (e.g., shake flask cultures) because it decreases the cell sampling along the culture, thus reducing the genetic drift effects and also preventing reductions in the size of low allele/gene frequencies which would lead to population bottlenecks that eventually would reduce genetic diversity and the rate of mutation/phenotypic fixation within these populations (Campos and Wahl 2009; Gordo and Dionisio 2005). Since the optimisation process described in this chapter was performed using clones 4 and 10 at "subpopulation 120" (μ values of 0.037 and 0.040 h^{-1}, respectively), which exhibited growth rates within and above the reference μ limits. The implementation of these clones during the optimisation ensure that the feeding strategy would be enough to satisfy the metabolic demand for the whole range of μ values observed among the clonal CHO-S cell lines

The elevated growth variability exhibited by CHO-S cells, derived from the long-term subculture (see chapter 3), during fed-batch cultivation remained elevated for all growth parameters (i.e., specific growth rate, VCD peak and IVCD), indicating that genetic and epigenetic changes constantly occurred within cells leading to detrimental characteristics that moulded their phenotypic status (Bergoglio et al. 2002; Derouazi et al. 2006; Sandoval and Esteller 2012). The results presented here confirm that CHO populations tended to improve their growth characteristics with increasing generation number. However, the variation observed in IVCD, VCD peak and cell size did not show a consistent pattern throughout the subpopulations (i.e., early (0), mid (80) and

late (200) generations), mainly because these parameters are the result of a combination of different environmental conditions (e.g., nutrient availability, hyper-osmolarity and by-product built-up) that occur over the fed-batch culture (Al-Rubeai and Singh 1998; Jardon et al. 2012). For example, in general μ exhibited a gradual improvement over increasing generations whereas IVCD did not exhibit a defined pattern (two-way ANOVA, *p*>0.05, F=1.68).

The variation among growth parameters patterns clearly indicated that the culture stages, but mainly stationary and cell-death phases were determinant to define the observed VCD peak and IVCD trends, as clones were evolved to increase growth rates under non-limiting growth conditions (e.g., nutrient abundance and low by-product built-up) and not evolved to resist the elevated environmental stressors commonly observed at such stages (e.g., nutrient depletion and toxic by-product levels). The non-limiting growth conditions silenced a large number of genes involved in cellular protection against environmental variations that are required at mid- and late stages of fed-batch culture (e.g., Bcl-2), as consequence, this loss of gene expression triggered diverse cellular responses to overcome environmental stressors, such as lactate and ammonia concentration, thus leading to phenotypic diversity within CHO populations.

As expected, μ patterns during the fed-batch culture remained similar to those observed in the long-term cultivation (see chapter 3), mainly because in both cases the μ was calculated at mid-exponential growth phase when there are no nutrient limitations and environmental stressors are lower. In contrast, the VCD peak and IVCD patterns were highly variable because clones were not evolved to resist environmental stressors such as nutrient depletion, by-product toxicity and hyper-osmolarity commonly found during the stationary and death phases of a fed-batch culture (Wuest et al. 2012). Therefore, although late-subpopulations (i.e., clones at 200 generations) exhibited higher proliferation rates, they did not necessarily reach the highest cellular densities when faced to unusual environmental challenges.

Here can be suggested that the phenotypic variation among subpopulations was promoted by their inherent "mutator phenotype" of CHO cells, usually characterised by an inefficient DNA repair mechanism that generate random point mutations (Loeb 2001; O'Callaghan and James 2008; Venkatesan et al. 2006), and from epigenetic factors that triggered constant fluctuations in gene expression along time (Flatscher et al. 2012; Lao and Toth 1997; O'Callaghan and James 2008; Yang and Butler 2000). The cell culture media and incubation settings clearly defined environmental conditions, leading epigenetic changes, such as histone deacetylation and DNA methylation, affecting chromatin accessibility at transcriptions sites, and therefore inducing gene

silencing (Flatscher et al. 2012; O'Callaghan and James 2008; Wurm 2004). It is suggested that the inherence of epigenetic mechanisms of gene regulation were determinant to define which genes would be expressed in subsequent generations (Barnes and Dickson 2006; Flatscher et al. 2012; Sandoval and Esteller 2012). Both hypotheses, genetic and epigenetic factors, provide a feasible explanation to the phenotypic heterogeneity observed because the long-term cultivation was designed to promote a continued proliferation in a synthetic environment in order to promote mutations or gene silencing over time. In addition, an alternative hypothesis for this heterogeneity among growth patterns can be associated with genetic drift as this was an important source of evolution throughout the long term cultivation by randomly selecting rapid growth phenotypes, regardless of their metabolic and genetic status

During the evolution phase, clones accumulated beneficial growth characteristics such as elevated μ, however none of the subpopulations were exposed to nutrient limitation, toxic by-product accumulation and hyper-osmolarity which are commonly found during production processes and in the current experiment during late stages of the fed-batch culture. Therefore, when populations were cultured under fed-batch mode the clones exhibited different responses during the stationary and death phases, which in general led to the observed variability among clones. A major exposure to environmental perturbations during the long-term cultivation would be an interesting characteristic that may have led to better growth patterns at late generations. Therefore, this study suggests that evolving phenotypes under constant environmental stress would improve the stress response in the cells leading to significantly better growth performance (e.g., high IVCD and elevated osmolarity tolerance). This alternative approach has been performed previously, Prentice et al. (2007) evolved DG44 cell lines cells capable of surviving in severe environmental conditions and reaching elevated cell densities and IVCD performances without jeopardising the productivity in the cells. Their approach allowed constant perturbations in the environment that resulted in better cellular response with significant improvements in the growth performance of the CHO cell lines.

It is important to emphasise that clones employed in the studies here reported did not express any recombinant protein because the aims of this project were to evaluate improvements in growth performance over increasing generations without the burden of an additional genetic construct and to develop a panel of CHO-S cell lines with improved and varied growth characteristics. As mentioned before, IVCD is a key factor that determines the overall yield performance during recombinant protein production, thus by producing a set of derived CHO-S cell lines with optimal IVCD performance

indirectly the titters of recombinant proteins will be improved (Pörtner 2007). Previous long-term sub-cultivation studies have used recombinant antibody expressing CHO cell lines, but their aims have been to evaluate the transgene stability over extended culture to characterise and identify changes in the genome and transcriptome that lead to the loss of recombinant protein expression (Bailey et al. 2012; Barnes et al. 2001; Chusainow et al. 2009; Kaneko et al. 2010).

The previous experimentation (see chapter 3) revealed that the early subpopulations (generations 0-57 of the long-term cultivation) exhibited an adaptation phase which was characterised by a large heterogeneity among clones. Interestingly, when these cells were revived and cultured under fed-batch regimen, they exhibited lower variability among them. This drastic change in the cellular behaviour after cell revival suggests significant changes in the growth phenotype for the clones at early-subpopulations. This indicates that cryopreservation and subsequent cell revival acted as strong selective forces, removing those phenotypes with low resistance to cryopreservation and slow-growth proliferation rates and favouring those phenotypes that exhibited faster recovery rates.

The comparison of specific growth rates obtained during the long-term and fed-batch cultures for each clone at generations 0, 80 and 200, also revealed that after cell revival all clones improved significantly their proliferation rates (33, 19 and 16% for clones at early-, mid- and late-subpopulations, respectively). As expected the improvements were observed at early-subpopulations, confirming that the cryopreservation/cell revival cycle selected the most fitted populations and removed those with low adapted phenotype. Moreover, it can be suggested that the 10% (v/v) of the cryoprotectant, dimethyl sulfoxide (DMSO), may be toxic for some populations thus increasing the selection effects within the population. However, this hypothesis seems unlikely because DMSO concentrations between 5 and 10% (v/v) have no demonstrated detrimental effects (Barnes et al. 2003). To investigate if the DMSO in fact acts as selector, analyses of the cell cycle and apoptosis after cycles of exposure to DMSO could be performed.

Moreover, analysing the global effects in µ after cell revival, the data shows that the global improvements observed at early-generations were equivalent to those µ enhancements observed after 120 generations in the long-term cultivation. Therefore this accumulated data seems to corroborate that cycles of cryopreservation-cell revival accelerate genetic drift within CHO-S populations and also presents it as an alternative strategy to improve growth characteristics in CHO-S cell lines.

Further, comparisons between fed-batch culture and the long-term cultivation indicated that after cell revival (in fed-batch experiments) late-subpopulations (i.e., cell lines after 200 generations) enhanced their growth rates. Interestingly, these were significantly higher than the rates obtained during the long-term cultivation. This finding reveals that the maximal µ values reached by clones between 160 and 200 generations during the long-term cultivation were not defined and/or restricted only by the culture media as mentioned in chapter 3, in fact the data suggest that cell cryopreservation/cell revival plays as selective pressure by removing unstable phenotypes with poor growth rates and fixing stable subpopulation with optimal phenotypes able to proliferate after cell revival. These growth improvements after cell revival (fed-batch experiments) reinforce that cycles of cryopreservation and cell revival act as selection factors that favour the fast-growing populations and alter the original cellular performance of populations by fixing fast-growing cells as dominant populations.

Although the proliferation rates of CHO-S cell lines were improved with increasing generation number, this study confirms that the µ improvements were not always reflected in improvements in the peak of viable cell density or integral of viable cell density due to these growth parameters depend on the cellular responses to environmental insults such as hyper-osmolarity, toxic by-products and nutrient limitation during the stationary phase (Al-Rubeai and Singh 1998; Cotter and Alrubeai 1995). The inconsistent improvement behaviour with increasing generation number was more evident for the IVCD, where most of the clones at mid-generations (80 generations) exhibited the highest IVCD values, probably the notable improvement in IVCD at mid-generation was the result of overcoming the agitated conditions, which challenged the cells during the adaptation phase and led to the development of phenotypes with higher tolerance to the environmental stress, but particularly to the agitated cultivation. On the other hand, the observed decay in IVCD at late-generations (200 generations) may have resulted because the mechanism to tolerate or resist hostile conditions may have been altered or even lost in the late stages of the long-term culture since the clones did not undergo environmental stress in the whole evolution phase. Therefore, it can be suggested that the highly controlled environments experimented during the evolution phase (see chapter 3) may have resulted in decreases in the level of tolerance to environmental insults, in particular of those late-subpopulations.

Finally, analysing the intra-clonal variation it was possible to identify which clones exhibited the most stable phenotypes, being clones 2, 3, 4, 5, 9 and 14 the most stable populations and clones 1, 11, 12, 17, 20 and 22 those clones that exhibited higher

rates of variability over increasing generations, thus the most phenotypically unstable clones. On the other hand, the analysis indicated that clones 4, 7, 8, 10, 11 and 15 were those cell lines that in general exhibited better growth characteristic, such as elevated µ, VCD peak and higher IVCD on their early-, mid- and late-generations, whereas clones 9, 13, 16, 20, 21 and 22 in overall exhibited lower performances. By combining both parameters, stability and improved growth characteristics, clones 3, 4, 5, 10 and 14 were by far the clones that exhibited superior growth characteristics whereas clones 11, 13, 16, 17 and 22 showed poorer growth characteristics. The characterisation here shown was performed on the basis of the clones' growth performance (i.e., high proliferation rates, elevated VCD peaks, cumulative IVCD and small cell diameter) and growth stability measured as the variability along early-, mid- and late-subpopulations for all four growth parameters.

Chapter 5

POLY-FUNCTIONAL METABOLISM AMONG CHO-S CELL POPULATIONS DURING FED-BATCH CULTURE

Chapter 5

Poly-functional metabolism among CHO-S cell populations during fed-batch culture

This chapter introduces the procedures employed to analyse the global metabolism for 11 clonally-derived CHO-S cell lines at early-, mid- and late-generations under fed-batch regimen, corresponding to generations 0, 80 and 200, respectively, followed by assessments of the accumulated metabolism of glucose, lactate, glutamine and glutamate at exponential and stationary growth phases and the assessments of their specific consumption or production rates at three key time points of the fed-batch culture. Altogether, this methodology allows us to gain insight into metabolic dynamics within CHO cell populations during exponential and stationary growth phases to identify desirable metabolic performance in CHO-S populations.

5.1 Background

The understanding of cellular metabolic processes in CHO cells is crucial for developing optimal cell culture platforms for biologic production. The metabolism in CHO cells has been widely studied in the biotechnological industry to characterise the optimum metabolic flux that lead to optimised growth performance with elevated recombinant protein productivities (Altamirano et al. 2006; Young 2013). Unfortunately, the majority of this information remains as industrial secret and relatively little information about CHO metabolism is available, which has generated a poor understanding of how the metabolism in CHO cells is reflected in better biological processes. Studies of CHO metabolism have been challenging and labour-intensive due to the dynamic and complex interactions between intrinsic and extrinsic factors such as cellular complexity and environmental and phenotypic fluctuations in culture, resulting in constant bottlenecks for developing more efficient cell lines, better culture media and feeding strategies. In addition, coupling the mentioned drawbacks with the high cost and low analysis capacity of current technologies for cultivation and production process off-line monitoring, substantially have restricted the use of metabolic analysis in routine culture processes, in special at academic level.

It has been widely described that glucose and glutamine are the main carbon sources in mammalian cell lines for the production of energy and biomass (Burgess 2011). Being glucose the central nutrient for the glycolysis pathway and glutamine the

principal generator of anaplerotic intermediates to feed the TCA cycle (DeBerardinis et al. 2007; Young 2013). CHO metabolism is characterised by a high glucose and glutamine demand combined with elevated rates of by-products production (e.g., lactate and ammonium) (Altamirano et al. 2004; Lao and Toth 1997; Park et al. 2000; Zagari et al. 2013). This glucose and glutamine addiction is important in cancer cells because allows them to rapidly generate energy and biomolecules to maintain an active proliferation. However, when this behaviour is observed in biotechnological processes the effects are detrimental for the cells due to by-product accumulation along culture altering the cellular growth patterns and the productivity (Altamirano et al. 2004; Lao and Toth 1997; Park et al. 2000).

Lactate is the principal by-product obtained from the cultivation of CHO cells and other mammalian cell lines. It has been widely reported that CHO cells exhibit an unbalanced metabolism and incomplete oxidation of the carbon source (Ahn and Antoniewicz 2011; Altamirano et al. 2006; Kim and Lee 2007b; Martinez et al. 2013; Young 2013). This unbalance causes that a large proportion of the consumed glucose would be converted into lactate by lactate dehydrogenase (LDH), an enzyme that catalyses the production of lactate from pyruvate, thus increasing the lactate levels in culture which are detrimental for cell growth and protein production (Lao and Toth 1997; Ozturk et al. 1992; Zhao et al. 2013). For example, increasing the concentration of lactate by 55 mM was found to reduce cell growth by 50 % while levels above 20 mM also affect cell growth in CHO cells (Ozturk et al. 1992). These negative effects in cell performance are associated with increments in osmolarity (> 316 mOsm/kg) which results from alkali addition to control media pH) (Li et al. 2010; Luo et al. 2012; Xing et al. 2009; Zhu et al. 2005) and with the low energetic efficiency of cells which have preferred the lactate production over OXPHOS (Warburg 1956; Young 2013). Attempts for minimising this by-product accumulation to avoid their negative effects in cell culture have been widely performed thought genetic manipulation (e.g., down-regulating LDH and PDK) and non-genetic strategies (e.g., the use of alternative carbon sources), leading to significant reduction in ammonia and lactate accumulation (Dorai et al. 2009; Jeong et al. 2001; Paredes et al. 1999; Wlaschin and Hu 2007; Zhou et al. 2011), significant improvement in the growth performance such as VCD (Altamirano et al. 2004; Cockett et al. 1990; Park et al. 2000) and in specific increasing productivity and volumetric titters (Bollati Fogolin et al. 2004; Chen et al. 2001; Zhou et al. 2011).

Several studies have analysed the CHO metabolism using metabolic flux analysis (MFA) which allows us to determine the intracellular metabolic fluxes and metabolic changes within populations by using isotopic tracers such as ^{13}C-glucose and [13]C-

glutamine and analysing their distribution in intermediates or final metabolites of several metabolic pathways (Ahn and Antoniewicz 2013; Crown and Antoniewicz 2013; Goudar et al. 2010; Zamorano et al. 2010). For example, Altamirano et al. (2006) investigated the lactate metabolism in a producing-CHO cell line cultured using glucose and galactose as carbon sources, revealing that when both carbon sources were added cells supported better growth characteristics and switched their lactate metabolism from production to consumption. Similarly, multiple studies using MFA have characterised and described the cell behaviour along culture, identifying the principal metabolic flux within cells and then modelling this behaviour during culture processes (Altamirano et al. 2006; Goudar et al. 2010; Mulukutla et al. 2012).

However, the use of MFA is unpractical during cell line development because the number of relevant metabolites that would virtually need to be quantified is enormous, increasing the complexity of the data analysis and making it labour-intensive. Therefore, the metabolic balance analysis (MBA) is more widely used during routine cell culture and manufacturing processes. For this method, inputs (e.g., glucose, glutamine) and outputs (e.g., lactate, ammonia) are used to estimate metabolite concentrations and metabolic fluxes. In this chapter the metabolic analyses were based on the evaluation of three metabolites which are involved in energy and biomass production (i.e., glucose, glutamine and glutamate) and one metabolite resulted as by-product (i.e., lactate).

5.2 Chapter aims

In this chapter, I investigated three hypotheses (i) that the analysis of the glucose, lactate, glutamine and glutamate metabolism at exponential and stationary growth phases of a fed-batch culture would permit the identification and classification of cell lines with specific metabolic characteristic (ii) that the cell lines with elevated IVCD performance would share common metabolic patterns such as switching from lactate production to consumption and (iii) that clonal CHO-S cell lines with stable growth patterns over long-term culture (e.g., early- mid- and late-subpopulation) would conserve some metabolic traits. Thereby, I suggest that:

(i)   The inherent cellular heterogeneity present within the parental CHO-S population will permit the generation of clonally-derived cell lines with desired and relevant metabolic characteristics such as low lactate build-up.

(ii)   Over increasing generations, the clonally-derived CHO-S cell lines improved their glucose utilisation permitting them to reach higher proliferation rates.

(iii)   The clonally-derived CHO-S cell lines conserved some metabolic trails during exponential growth phase and then diverged significantly during the stationary growth phase.

The aim of this chapter is to reveal the optimal metabolic state among a panel of 11 clonally-derived cell lines with relevant industrial capabilities and understand the central carbon metabolism of the CHO cells during fed-batch experiments. Moreover, I aimed to study how the global IVCD performance observed during fed-batch cultivation is linked to optimal carbon source utilisation and how the metabolic state vary with increasing generation number (i.e., early, mid-, and late-subpopulations generated for each clone during a long-term culture regime, corresponding to generations 0, 80 and 200, respectively). Finally, I aimed to identify the optimal metabolic parameters which could permit the selection of subpopulations with enhanced and relevant phenotype and the optimisation of biopharmaceutical processes.

5.3 Chapter objectives

To address the chapter aims, the objectives of the work presented in this chapter were to:

i)   Examine the glucose, lactate, glutamine and glutamate metabolism for a set of 11 clonally-derived CHO-S cell lines at their early-, mid-, and late-subpopulations.

ii) Asses and compare the cellular metabolic status at exponential and stationary growth phases.

iii) Identify the key metabolites and metabolic events at exponential and stationary growth phases.

iv) Identify the effects of essential nutrient deprivation and the inhibitory effects of lactate accumulation on cell culture.

v)   Identify the potential correlation between metabolite consumption or production and growth phases.

5.4 Results

The introductory fed-batch experiments described in Chapter 4 demonstrated an important variability in growth characteristics (i.e., IVCD, peak VCD, µ and cell size) among CHO-S clones derived from the same parental line. To test the hypothesis that growth performance was related to the metabolic state of the clones and to evaluate if the metabolic behaviour was maintained in each individual clone with increasing generation number, a panel of 11 clonal CHO-S cell lines (clones 1, 2, 4, 6, 10, 11, 12, 15, 17, 19 and 22) that exhibited disparate specific growth characteristics was selected for further characterisation and as a start point classified on basis of phenotypic stability over the long-term cultivation (i.e., early, mid-, and late-subpopulations), overall growth performance (i.e., high IVCD, peak VCD and µ and small cell size) and their proposed potential (i.e., for recombinant protein production or cell line development) (Table 5-1).

The evaluation of the clone's metabolic performance was performed under fed-batch cultivation to investigate whether the observed variations in overall growth performance were related to metabolic differences along culture. For this experimentation, cell-free supernatant samples at days 2, 3, 5, 7, 9 and 11 were analysed for glucose, lactate, glutamine and glutamate concentrations using a Cedex bio-analyser. These analyses allowed the calculation of the specific metabolite production or consumption rates at different time points (i.e., growth phases) of the fed-batch culture (Figure 5-1). Specifically, measurements between days two and three ("day 3") denote the metabolic state at mid-exponential growth phase, measurements between days three and five ("day 5") represent the end-exponential growth phase, measurements between days five and seven ("day 7") belong to the early-stationary phase, measurements between days seven and nine ("day 9") represent the late-stationary phase and measurements between days nine and eleven ("day 11") belong to the death phase.

The analysis of these time points permitted to monitor the metabolic performance at key culture stages identified through VCD evaluations (Figure 5-1A). Being mid-exponential growth phase (day 3) when cells are more metabolically active as they synthesise biomolecules for their continuous and elevated proliferation rates and reflecting that the environments have no nutrient limitation. The end-exponential growth phase or deceleration growth phase (day 5) denotes the moment in which essential nutrients become limited (e.g., glutamine) or some by-products start to reach toxic levels (e.g., lactate) and thus cells start to reduce their proliferation rates. The early-stationary growth phase (day 7) indicates when cell reach their maximum viable cell

density and cease duplication or at least diminish it enough to balance cell death and proliferation, at this stage environmental stressors include depleted essential amino acids and elevated by-product and osmolarity levels, but cells remain metabolically active to maintain functionality. The late-stationary growth phase (day 9) represents the moment in which cells are subjected to higher environmental stressors such as hyper-osmolarity which causes important phenotypic changes and cell membrane damage. Finally, the death growth phase (day 11) starts when environmental stressors reach detrimental concentration able to trigger apoptosis or necrosis.

Table 5-1 Classification of selected cell lines for metabolic analysis according to stability and growth performance.

Clones	Phenotypic stability	Fitness of growth characteristics	Cell line potential
Parental	-	-	-
Clone 1	Low	Mid	Cell line development process
Clone 2	High	Mid	Protein production
Clone 4	High	High	Protein production
Clone 6	Mid	Mid	Cell line development process
Clone 10	High	High	Protein production
Clone 11	Low	High	Cell line development process
Clone 12	Low	Mid	Cell line development process
Clone 15	Mid	High	Protein production
Clone 17	Low	Low	Cell line development process
Clone 19	Mid	Mid	Cell line development process
Clone 22	Low	Low	Cell line development process

Clones were classified on basis of their observed fed-batch culture performance at three subpopulations (early-, mid- and late-subpopulations) generated from a long-term subculture regime, corresponding to generations 0, 80 and 200, respectively. Clones were grown in fed-batch culture in CD CHO media supplemented with 8 mM L-glutamine and maintained at 37°C, 170 rpm, under 5% (v/v) CO_2 atmosphere until culture viabilities dropped below 60%. During the culture 10% (v/v) CHO CD EfficientFeed™ was fed at days 3, 5, 7 and 9. For "phenotypic stability" classification the main consideration was the intra-clonal variation among subpopulations (chapter 3), whereas the "fitness of growth characteristics" classification was based on observed values for IVCD, peak VCD, specific growth rate and cell size (chapter 4).
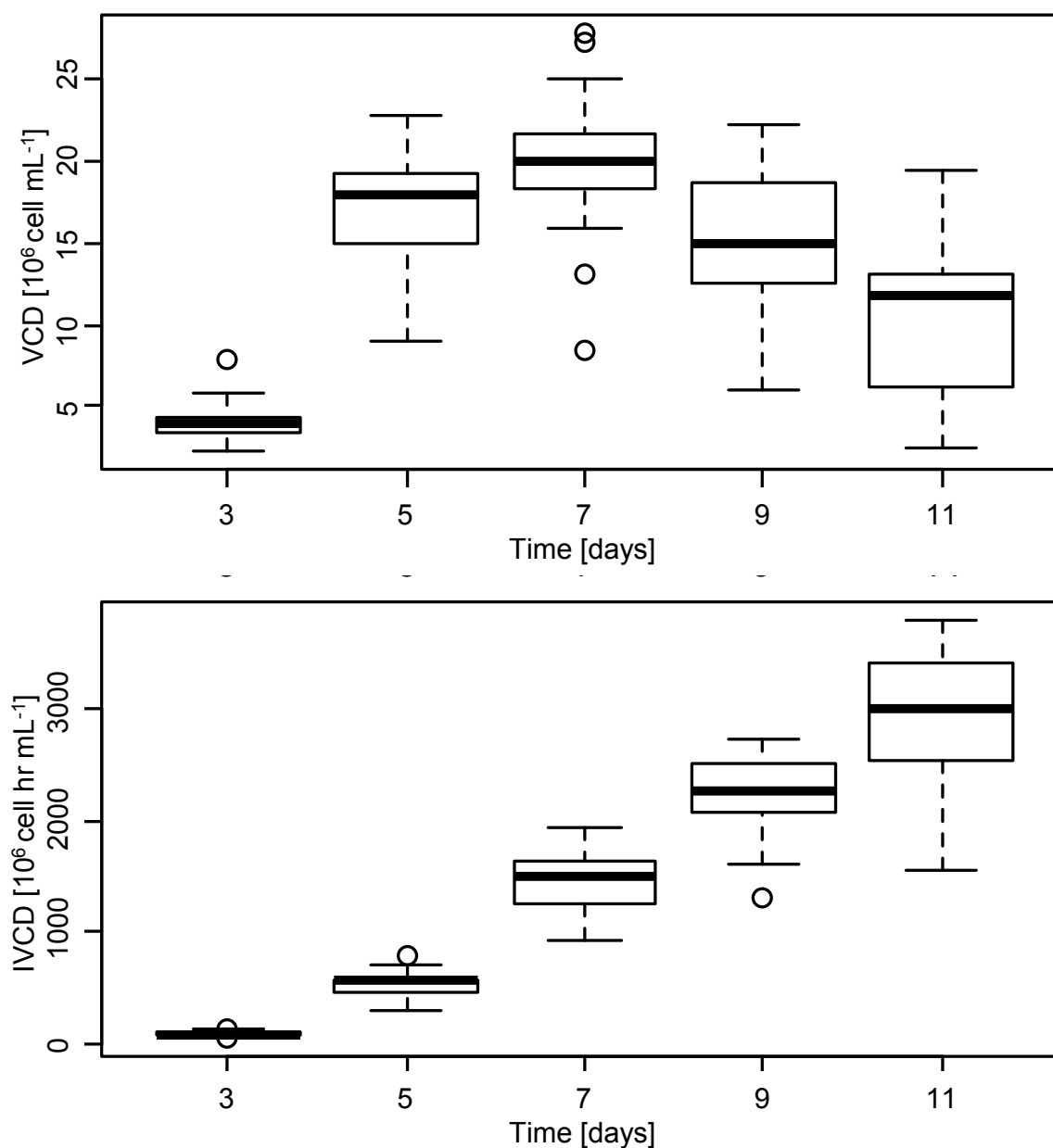
Figure 5-1 Viable cell density and integral of viable cell density patterns for 11 clonally-derived CHO-S cell lines during fed-batch culture. Cells were grown in fed-batch culture in CD CHO media supplemented with 8 mM L-glutamine and maintained at 37°C, 170 rpm, under 5% (v/v) CO_2 atmosphere until culture viabilities dropped below 60%, during the culture 10% (v/v) CHO CD EfficientFeed™ was fed at days 3, 5, 7 and 9. For each clone, early-, mid- and late-subpopulations generated from a long-term subculture regime, corresponding to generations 0, 80 and 200, respectively, were evaluated from duplicate cultures and grouped according to fed-batch culture time point. Viable cell density (A) and integral of viable cell density are presented (B). The bottom and top of the box represent the 25th and 75th percentiles, the line within the box the median, error bars indicate the 0th and 100th percentiles and circles are outliers.

The global growth performance analysis among clones in fed-batch cultures showed statistically significant differences between the selected time points of the Fed-batch culture and VCD (two-way ANOVA: $p < 0.0001$, F=23.4; Figure 5-1A), and IVCD (two-way ANOVA: $p < 0.0001$, F=1497; Figure 5-1B). Moreover, this analysis exhibited a low VCD and IVCD variability during the mid-exponential growth phase (day 3) and substantial increases in growth variability from day 5, suggesting that clones presented varied cellular responses when were exposed to elevated environmental stress.

To assess if the five time points (i.e., days 3, 5, 7, 8, 9 and 11) were sufficient to compare the metabolic performance of clones, the overall analysis of the specific rate for either consumption or production of the key metabolites was performed (Figure 5-2A-D), showing a significant differences along the culture for glucose (Figure 5-2A; two-way ANOVA, $p < 0.0001$, F=84.3), glutamine (Figure 5-2B; two-way ANOVA, $p < 0.0001$, F=536.4), lactate (Figure 5-2C; two-way ANOVA, $p < 0.0001$, F=509.7) and glutamate (Figure 5-2D; two-way ANOVA, $p < 0.0001$, F=46.0). The comparison between the culture's time points (i.e., days 3, 5, 7, 8, 9 and 11) showed significant differences in the specific metabolism between mid-exponential (Day 3) and the rest of the time points (Tukey's test: glucose, $p < 0.0001$; glutamine, $p < 0.0001$; lactate, $p < 0.0001$; glutamate, $p < 0.0001$), and differences between late-exponential growth phase (day 5) and the rest of the time points for glutamine metabolism (Tukey's test: $p < 0.0001$). Contrary, comparisons between stationary growth (days 7 and 9) and death growth (day 11) no showed significant differences. Finally, the ANOVA analysis also revealed that the age of the clones (i.e., 0, 80 or 200 generations) had no effect on the specific metabolite production or consumption rates at the different stages of the fed-batch culture.

This global analysis showed here was performed on per-cell basis to provide further information and compare each population and their respectively changes in metabolism over the culture. This allows us to identify that by using only three key fed-batch points i.e., mid-exponential, end-exponential and early-stationary growth phases, corresponding to day 3, 5 and 7, respectively, are enough to evaluate the specific metabolic rates across clones, therefore in the subsequent analyses these three growth phase points were analysed and compared.
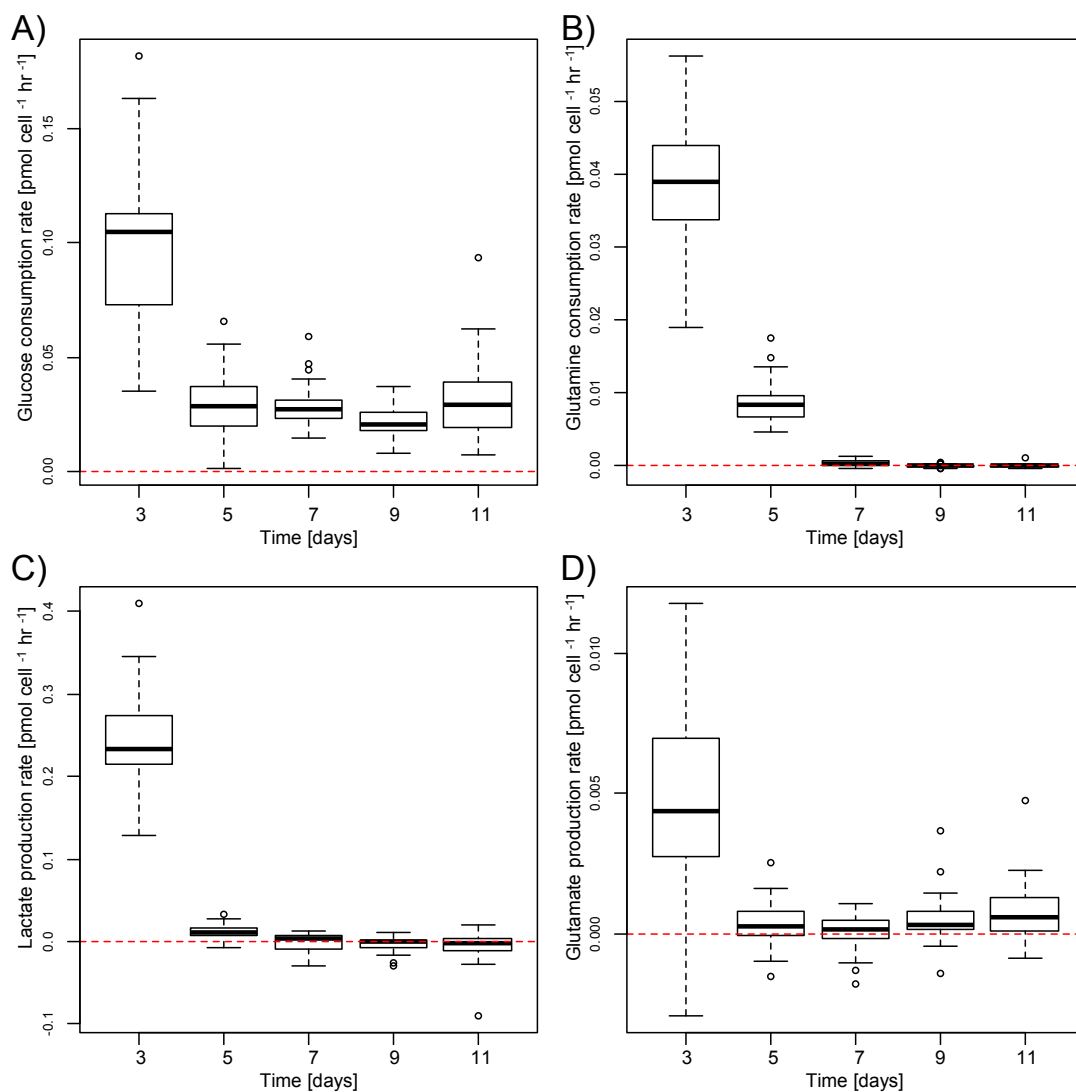
Figure 5-2 Analysis of the specific metabolic rate of glucose and glutamine consumption and lactate and glutamate production for 11 clonally-derived CHO-S cell lines during fed-batch culture. Cells were grown in fed-batch culture in CD CHO media supplemented with 8 mM L-glutamine and maintained at 37°C, 170 rpm, under 5% (v/v) CO_2 atmosphere until culture viabilities dropped below 60%, during the culture 10% (v/v) CHO CD EfficientFeed™ was fed at days 3, 5, 7 and 9. For each clone, early-, mid- and late-subpopulations generated from a long-term subculture regime, corresponding to generations 0, 80 and 200, respectively, were evaluated from duplicate cultures and grouped according to fed-batch culture time point. The specific metabolic rate of (A) glucose consumption, (B) glutamine consumption, (C) lactate production and (D) glutamate production were evaluated at mid-exponential, end-exponential, early-stationary, late-stationary and death growth phases (days 3, 5, 7, 9 and 11, respectively). The bottom and top of the box represent the 25th and 75th percentiles, the line within the box the median, error bars indicate the 0th and 100th percentiles and dots are outliers. Below red dotted line indicate a metabolic shift.

118

5.4.1 Effects of exponential and stationary growth phases during fed-batch culture on glucose consumption

To evaluate in detail the metabolic differences for glucose consumption between the exponential and stationary growth phases of the fed-batch culture, the accumulated uptake values were calculated and plotted (Figure 5-3A), showing significant differences in the cumulative glucose demand between both growth (two-way ANOVA, $p<0.0001$, F=157.5; Figure 5-3B), being between 1.9 and 6.1 fold changes higher the stationary demand. The comparison of each clone's individual glucose metabolism with respect to the parental population showed that clones increased their glucose demand during the stationary phase, probably because the clones exhibited higher peaks of VDC. Moreover, from the panel of 33 subpopulations, subpopulations C2-mid, C17-early and C17-mid exhibited similar levels of glucose uptake at both growth phases, suggesting a poor cell performance along the stationary phase. This hypothesis was verified by observing the IVCD data (data not shown) which indicated that these subpopulations exhibited a low IVCD. This data also shows that the subpopulations C17-early and C17-mid presented the highest glucose demand at exponential phase (Figure 5-3A), probably indicating that this subpopulations were more glycolysis-dependent during proliferation, however, this hypothesis must be analysed in conjunction with more metabolic parameters (see sections 5.4.2, 5.4.3 and 5.4.4).

To test any relationship between the cumulative glucose demand at both growth phases, a correlation analysis was performed (Figure 5-3C), showing a weak correlation between both growth phases (PPMCC r = -0.285, p-value > 0.05, n = 33). A similar analysis was performed using the suggested cell line potential use classification (i.e., cell line development or protein production processes; Table 5-1) showing no significant differences between both groups either at exponential (two-way ANOVA, $p>0.05$, F=0.43) or stationary (two-way ANOVA, $p>0.05$, F=0.02) growth phases. Therefore, this analysis clearly indicated that the analysis of glucose metabolism alone is not enough for identifying cell lines with improved characteristics.

The specific glucose consumption rates for all 11 clones at early, mid- and late subpopulations generated from a long-term culture regime (i.e., generations 0, 80 and 200, respectively) were analysed at three time points during the fed-batch culture, being these mid- exponential, end-exponential and stationary phases (Figure 5-4A). As expected, the specific glucose consumption rates, among and within clones, were highly variable (Figure 5-4A), showing significant differences between the growth phases (Figure 5-4B; two-way ANOVA, $p<0.001$, F=107.5).
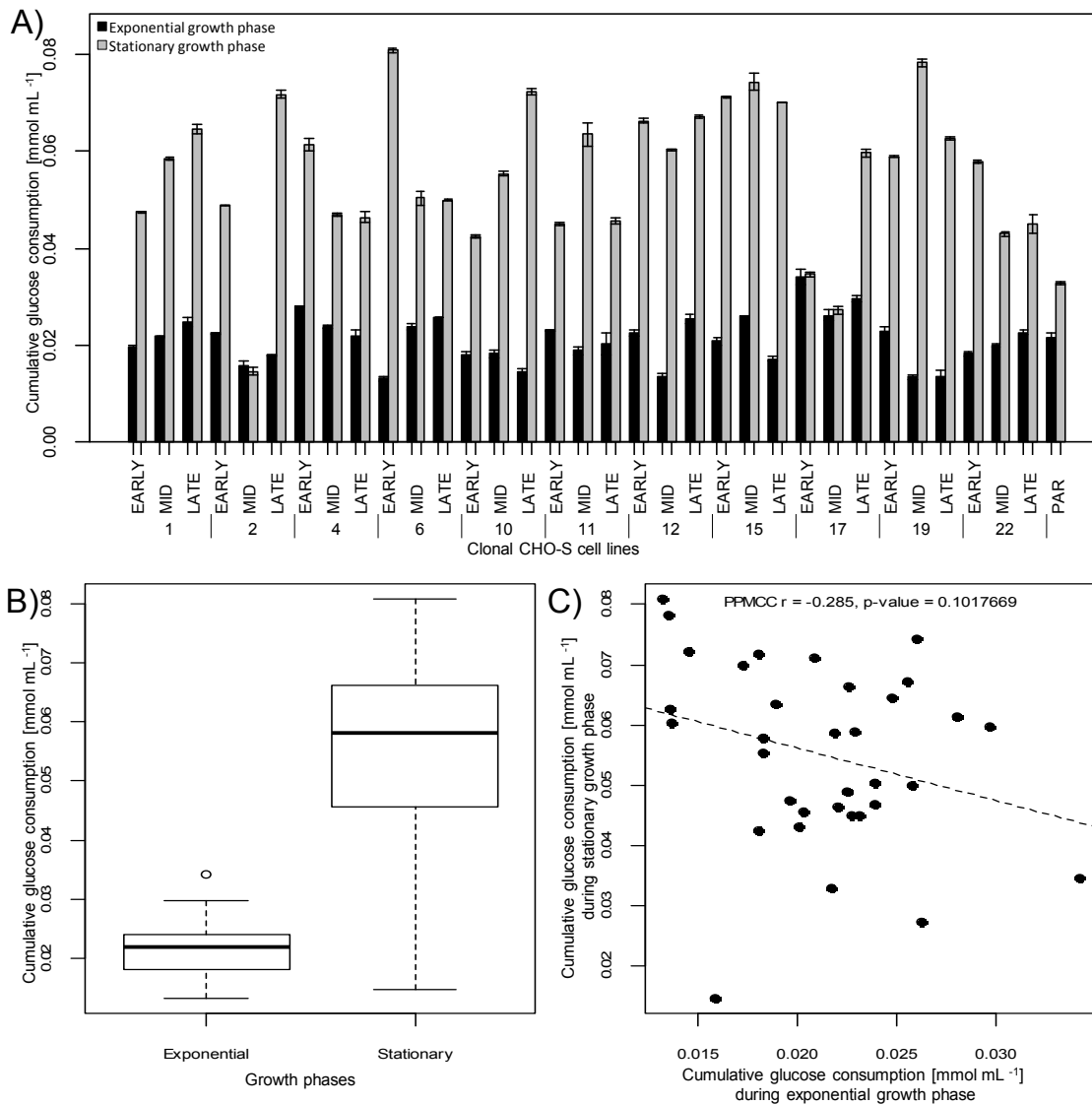
Figure 5-3 Comparison of glucose uptake metabolism during exponential and stationary growth phases of a fed-batch culture for 11 clonally-derived CHO-S cell lines. Cells were grown in fed-batch culture in CD CHO media supplemented with 8 mM L-glutamine and maintained at 37°C, 170 rpm, under 5% (v/v) CO_2 atmosphere until culture viabilities dropped below 60%, during the culture 10% (v/v) CHO CD EfficientFeed™ was fed at days 3, 5, 7 and 9. For each clone, early-, mid- and late-subpopulations generated from a long-term subculture regime, corresponding to generations 0, 80 and 200, respectively, were evaluated. (A) The cumulative glucose consumption at the exponential and stationary growth phases for the differently aged clonal subpopulations, (B) the global glucose consumption at the exponential and stationary growth phases for the differently aged clonal subpopulations and (C) the Pearson's correlation between the glucose consumption during stationary and exponential growth phases for the differently aged clonal subpopulations (PPMCC r = -0.285, p-value > 0.05, n = 33) are presented.
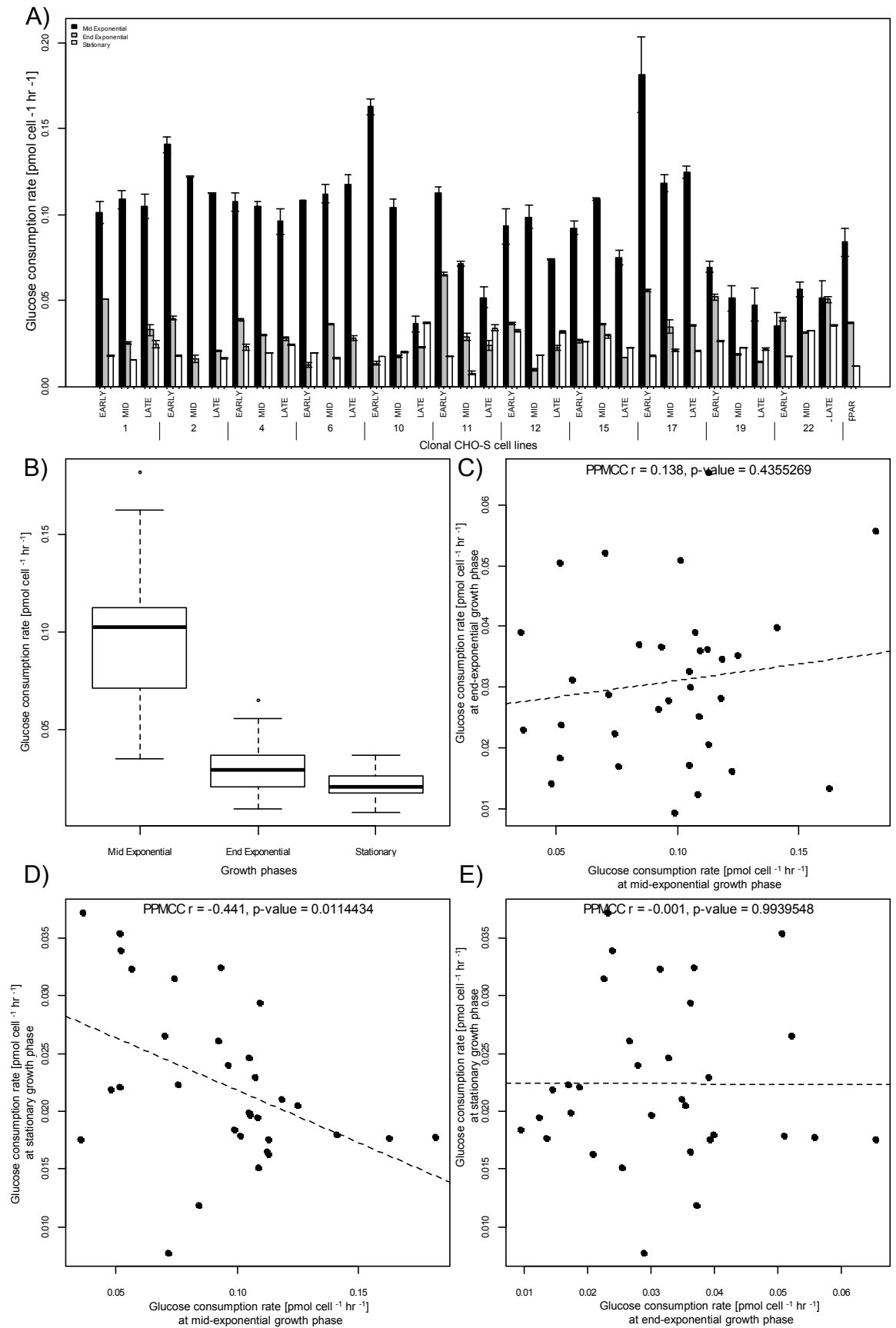
Figure 5-4 Analysis of the specific glucose consumption rate for 11 clonally-derived CHO-S cell lines during fed-batch culture. Cells were grown in fed-batch culture in CD

CHO media supplemented with 8 mM L-glutamine and maintained at 37°C, 170 rpm, under 5% (v/v) CO_2 atmosphere until culture viabilities dropped below 60%, during the culture 10% (v/v) CHO CD EfficientFeed™ was fed at days 3, 5, 7 and 9. For each clone, early-, mid- and late-subpopulations generated from a long-term subculture regime, corresponding to generations 0, 80 and 200, respectively, were evaluated. (A) Specific glucose consumption rates at the mid-exponential, end-exponential and stationary growth phases for the differently aged clonal subpopulations, (B) the global glucose consumption rates at the mid-exponential, end-exponential and stationary growth phases for the differently aged clonal subpopulations and the Pearson's correlation between (C) end-exponential and mid-exponential glucose consumption rates for the differently aged clonal subpopulations (PPMCC r = 0.138, p-value > 0.05, n = 33), (D) stationary and mid-exponential glucose consumption rates for the differently aged clonal subpopulations (PPMCC r = -0.441, p-value < 0.05, n = 33) and (E) stationary and end-exponential glucose consumption rates for the differently aged clonal subpopulations (PPMCC r = -0.001, p-value > 0.05, n = 33).

The data analysis presented in Figure 5-4B also indicated that during the mid-exponential growth phase clones were more metabolically active due to their energetic demands for cell biomass production. In contrast, clones at end-exponential growth phase notably reduced their glucose utilisation as they reduced their proliferation and clone at stationary growth phase reduced their glucose utilisation as they only need metabolic energy for their cellular maintenance. This significant reductions in glucose utilisation observed at end-exponential growth phase was the result of ceasing their proliferation and not related to glucose depletion as cultures always exhibited concentrations above 3 g L^{-1} at this time point (data not shown).

To identify if glucose consumption rates can be used to classify cell lines with desirable growth characteristics according with their potential for cell line development or protein production processes, clones were grouped and analysed on basis of the proposed cell line indication (Table 5-1), finding no differences between both groups at mid-exponential (two-way ANOVA, $p>0.05$, F=1.6), deceleration (two-way ANOVA, $p>0.05$, F=3.9) or stationary (two-way ANOVA: $p>0.05$, F=0.59) growth phases. This data confirms that individual cell lines with improved growth characteristics cannot be distinguished on basis of their glucose metabolism. Moreover, to identify any possible associations between the glucose rates at exponential and stationary phases, the Pearson's correlation analysis was performed (Figure 5-4C-E) showing only a significant negative correlation between mid-exponential and stationary growth phases (Figure 5-4D, PPMCC r = -0.441, p-value < 0.05, n = 33). Finally, the ANOVA analysis

revealed that the age of the clones (i.e., 0, 80 or 200 generations) only had an effect on the specific glucose consumption rates during the stationary growth phase (two-way ANOVA, $p<0.05$, F=2.95).

5.4.2 Lactate metabolism switched to net lactate consumption during stationary growth phase

The cumulative lactate production of the eleven clonally-derived CHO-S cell lines was evaluated and compared for the exponential and stationary fed-batch culture phases using differently aged subpopulations for each clone. A major finding was a shift in lactate metabolism, from production to consumption, during the stationary phase in at least one of the clones' subpopulations (i.e., generations 0, 80 or 200) (Figure 5-5A). Additionally, this analysis indicated significant differences in lactate metabolism between both the exponential and stationary phases (Figure 5-5B; two-way ANOVA: p<0.0001, F=214.6). However, this data did not reveal any relationship between the lactate metabolism at exponential and stationary phases (Figure 5-5C). Interestingly, the comparison between clones and the parental population showed that the majority of clones exhibited higher lactate accumulation during the exponential phase and that most of the clones had a notorious lactate shift from production to consumption. The analysis of the clone's cumulative lactate production according to the cell line classification presented in Table 5-1 (i.e., suitability for cell line development or protein production processes) did not show significant differences between both groups, indicating that the lactate metabolism cannot be implemented as a single culture parameter for differentiating cell lines that would be more suited for either cell line establishment or recombinant protein production.

The analysis of the specific lactate consumption/production rates showed significant differences along the growth phases of the fed-batch culture (Figure 5-6B; two-way ANOVA, $p<0.001$, F=610.5) with a prominent variability at mid-exponential growth, ranging between 0.13 and 0.41pmol cell^{-1} hr^{-1}. Additionally, this data showed two lactate metabolisms, the first at mid-exponential growth phase characterised by elevated levels of lactate production and the second at end-exponential and stationary growth phases characterised by a notable reduction in the lactate production and in some cases changing to lactate consumption.
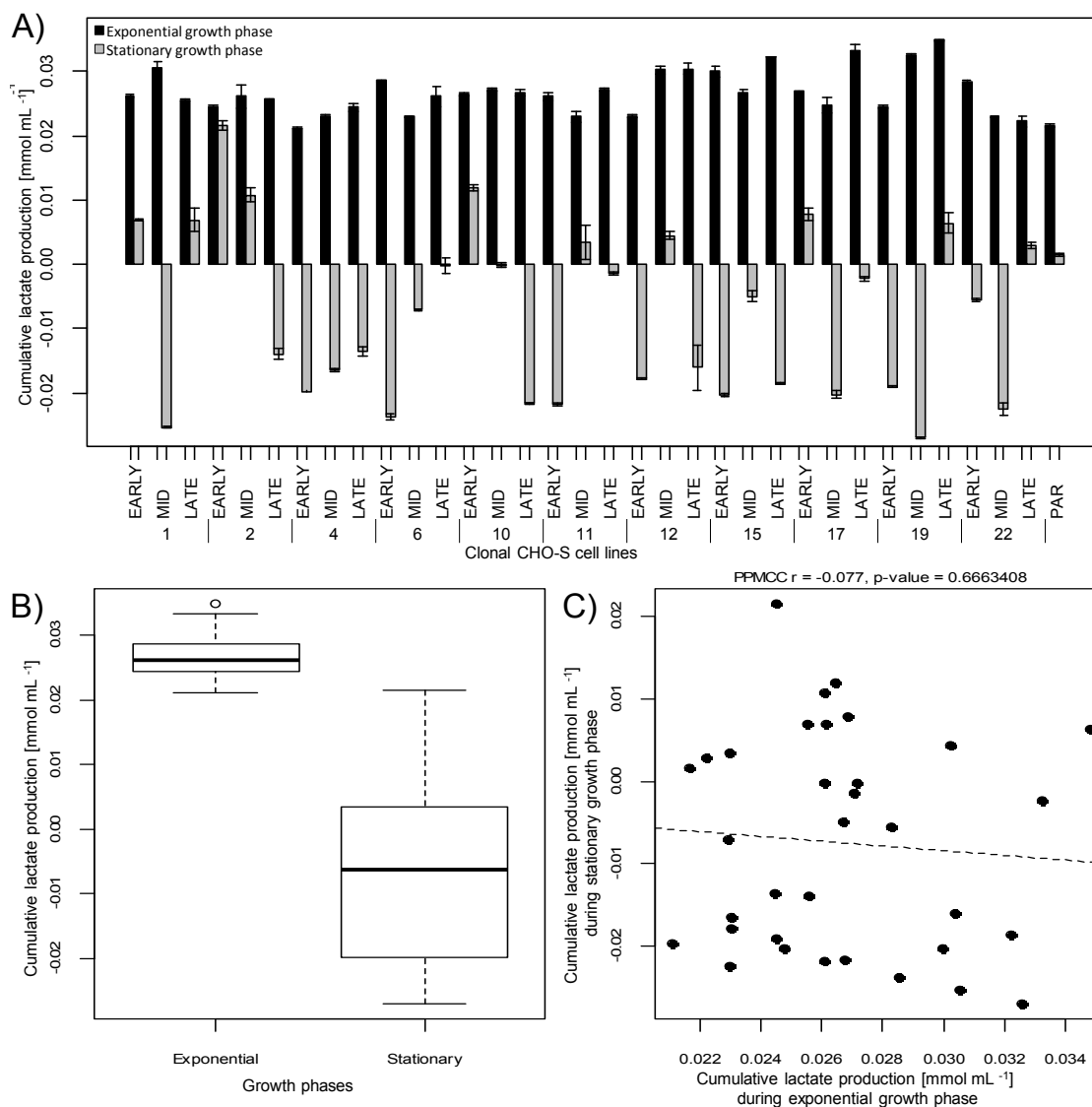
Figure 5-5 Comparison of lactate production metabolism during exponential and stationary growth phases of a fed-batch culture for 11 clonally-derived CHO-S cell lines. Cells were grown in fed-batch culture in CD CHO media supplemented with 8 mM L-glutamine and maintained at 37°C, 170 rpm, under 5% (v/v) CO_2 atmosphere until culture viabilities dropped below 60%, during the culture 10% (v/v) CHO CD EfficientFeed™ was fed at days 3, 5, 7 and 9. For each clone, early-, mid- and late-subpopulations generated from a long-term subculture regime, corresponding to generations 0, 80 and 200, respectively, were evaluated. (A) The cumulative lactate production/consumption at the exponential and stationary growth phases for the differently aged clonal subpopulations, (B) the global lactate metabolism at the exponential and stationary growth phases for the differently aged clonal subpopulations and (C) the Pearson's correlation between the lactate metabolism during stationary and exponential growth phases for the differently aged clonal subpopulations (PPMCC r = -0.077, p-value > 0.05, n = 33) are presented.
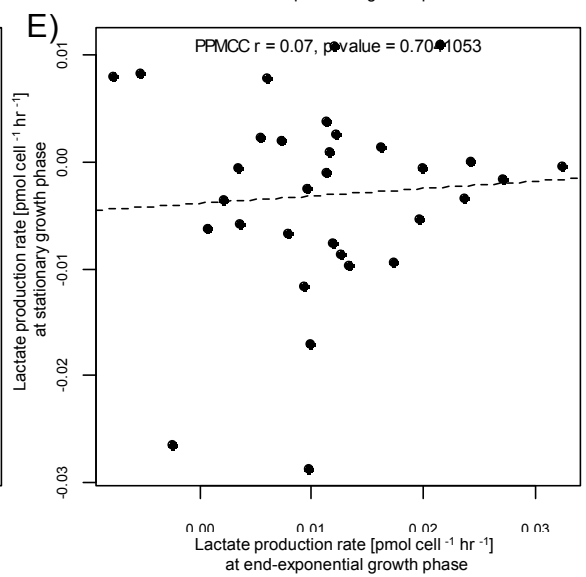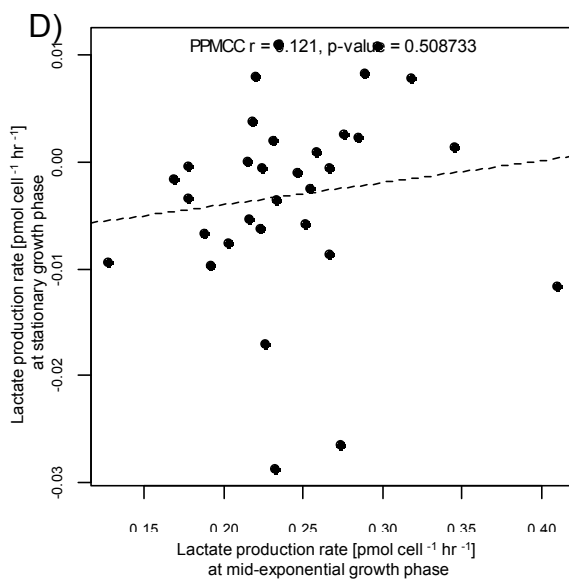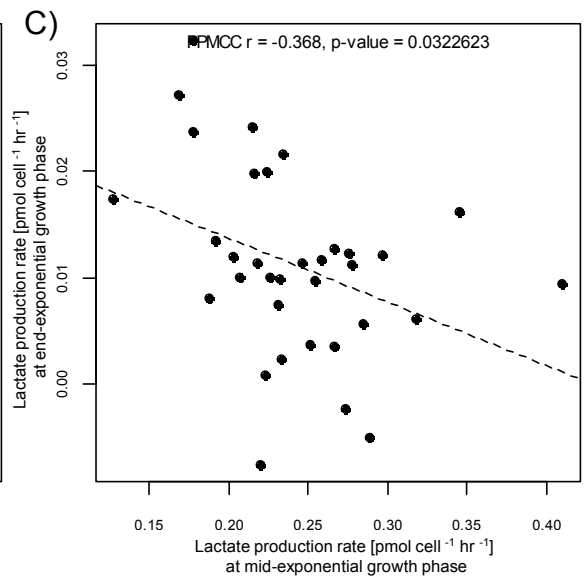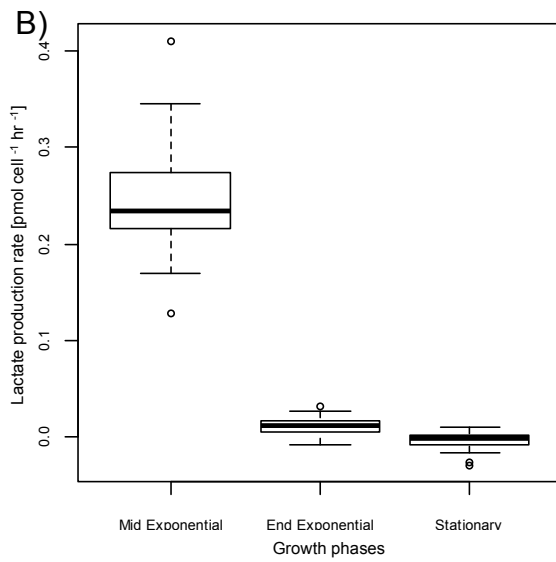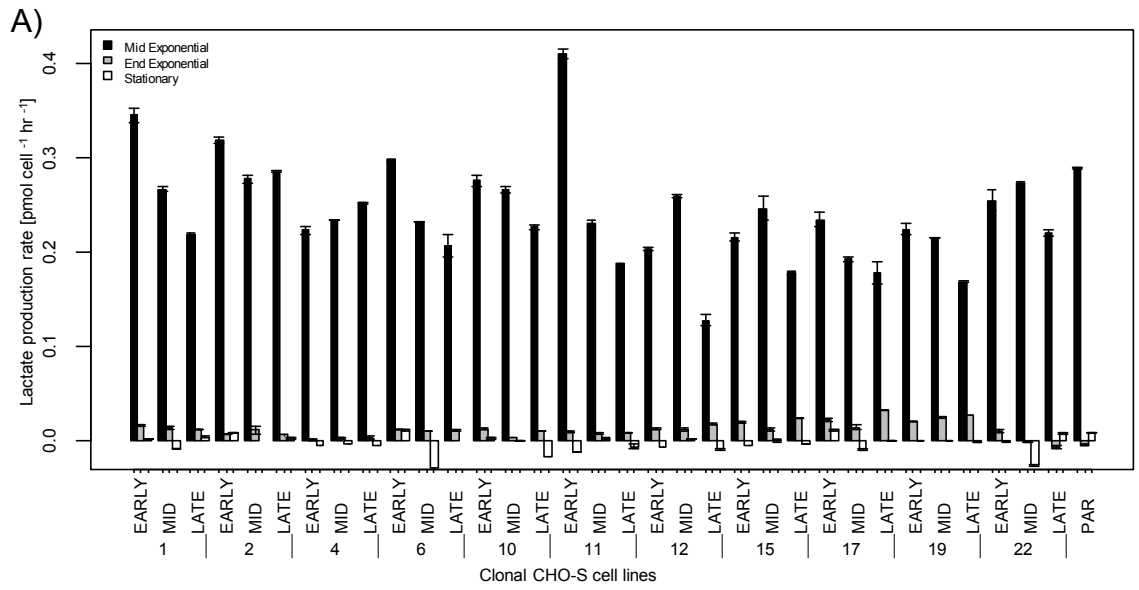
Figure 5-6 Analysis of the specific lactate consumption/production rate for 11 clonally-derived CHO-S cell lines during fed-batch culture. Cells were grown in fed-batch culture in CD CHO media supplemented with 8 mM L-glutamine and maintained at 37°C, 170 rpm, under 5% (v/v) CO_2 atmosphere until culture viabilities dropped below 60%, during the culture 10% (v/v) CHO CD EfficientFeed™ was fed at days 3, 5, 7 and 9. For each clone, early-, mid- and late-subpopulations generated from a long-term subculture regime, corresponding to generations 0, 80 and 200, respectively, were evaluated. (A) Specific lactate metabolic rates at the mid-exponential, end-exponential and stationary growth phases for the differently aged clonal subpopulations, (B) the global lactate metabolic rates at the mid-exponential, end-exponential and stationary growth phases for the differently aged clonal subpopulations and the Pearson's correlation between (C) end-exponential and mid-exponential lactate metabolic rates for the differently aged clonal subpopulations (PPMCC r = -0.368, p-value < 0.05, n = 33), (D) stationary and mid-exponential lactate metabolic rates for the differently aged clonal subpopulations (PPMCC r = 0.121, p-value > 0.05, n = 33) and (E) stationary and end-exponential lactate metabolic rates for the differently aged clonal subpopulations (PPMCC r = 0.07, p-value > 0.05, n = 33).

Moreover, the data presented in Figure 5-6A, seems to indicate that the clones reduced their lactate production rates during the mid-exponential growth phase of the fed-batch culture with increasing generation number (i.e., early, mid- and late subpopulations for each clone). In contrast, it was not possible to find special patterns for lactate metabolic rates at end-exponential and stationary growth phases of the fed-batch culture except for a significant decrease in production rates (Figure 5-6B; two-way ANOVA, $p<0.001$, F=41.59.5). This data may suggest an improvement in the link between glycolysis and TCA cycle. However, to support this hypothesis additional experiments such as glycolysis analysis are required (see chapter 6). Finally, no significant differences between lactate production rates for clones grouped according with desirable growth characteristics for protein production and cell line development (Table 5-1) were observed. Similarly, Pearson's correlations between the fed-batch culture stages did not show significant correlations between stationary and exponential growth phases, but a significant, negative correlation between mid- and end-exponential phases of the fed-batch culture was obtained for lactate production rate (PPMCC r = -0.368, p-value < 0.05, n = 33) (Figure 5-6C to E). In addition, the ANOVA analysis with respect to the age of the clones (i.e., 0, 80 or 200 generations) only reveals significant differences on the specific lactate consumption rates during the mid-exponential growth phase (two-way ANOVA, p<0.02, F=4.233).

5.4.3 Glutamine metabolism among clonally-derived CHO-S cell lines

In general, the cumulative glutamine consumption analysis for all 11 clones at early, mid- and late generations obtained from a long-term culture regime (i.e., generations 0, 80 and 200, respectively) exhibited significant differences between exponential and stationary growth phases of the fed-batch culture (Figure 5-7A and Figure 5-7B; two-way ANOVA: glutamine, $p<0.0001$, F=1848) with no significant correlation between both growth phases (Figure 5-7C, PPMCC r = -0.316, p-value > 0.05, n = 33). Moreover, no significant differences between cell lines with identified protein production and cell line development prospective capabilities (Table 5-1) were observed. The glutamine demand was characterised by an elevated glutamine utilisation at exponential growth phase, followed by a significant reduction at stationary phase (Figure 5-7A). This data also revealed that some subpopulations (4-early, 4-mid, 4-late, 6-mid, 6-late, 15-mid, 17-mid, 17-late, 19-late, 22-early and 22-late) seemed to slightly synthesise glutamine during the stationary phase, being more notorious in clone 4 for which all subpopulations exhibited the same glutamine behaviour. It is suggested that this apparent glutamine synthesis may result from their (i) low endogenous GS-activity which coupled with low glutaminolityc metabolism at the stationary phase led to increments in its concentration or (ii) resulted from media evaporation.

The analysis of the specific rates of glutamine consumption showed a gradual and significant reduction in the consumption rates at end-exponential growth phase along increasing generations for individual clones obtained from the long-term culture (i.e., early, mid and late subpopulations) (Figure 5-8A; two-way ANOVA: p<0.01, F=4.67) and also for the growth phases identified during the fed-batch culture (i.e., mid-exponential, end-exponential and stationary phases) (Figure 5-8B; two-way ANOVA: p<0.0001, F=398.7). The glutamine uptake reduction behaviour during fed-batch cultivation seems to be closely linked to biomass synthesis, indicating that glutamine was preferably used during cellular proliferation. Moreover, the drastic uptake decrease may be also associated to the glutamine availability in the culture media which was dramatically consumed during the mid-exponential growth phase and became limited, but not exhausted, at the end of the exponential phase (between 0.2 to 1.83 mmol L^{-1}, data not shown) and during the stationary phase (between 0.2 to 1.06 mmol L^{-1}, data not shown). In addition, this data analysis does not reveal any metabolic shift from consumption to production supporting the hypothesis that the apparent glutamine synthesis observed in Figure 5-7A resulted from media evaporation during the fed-batch culture.
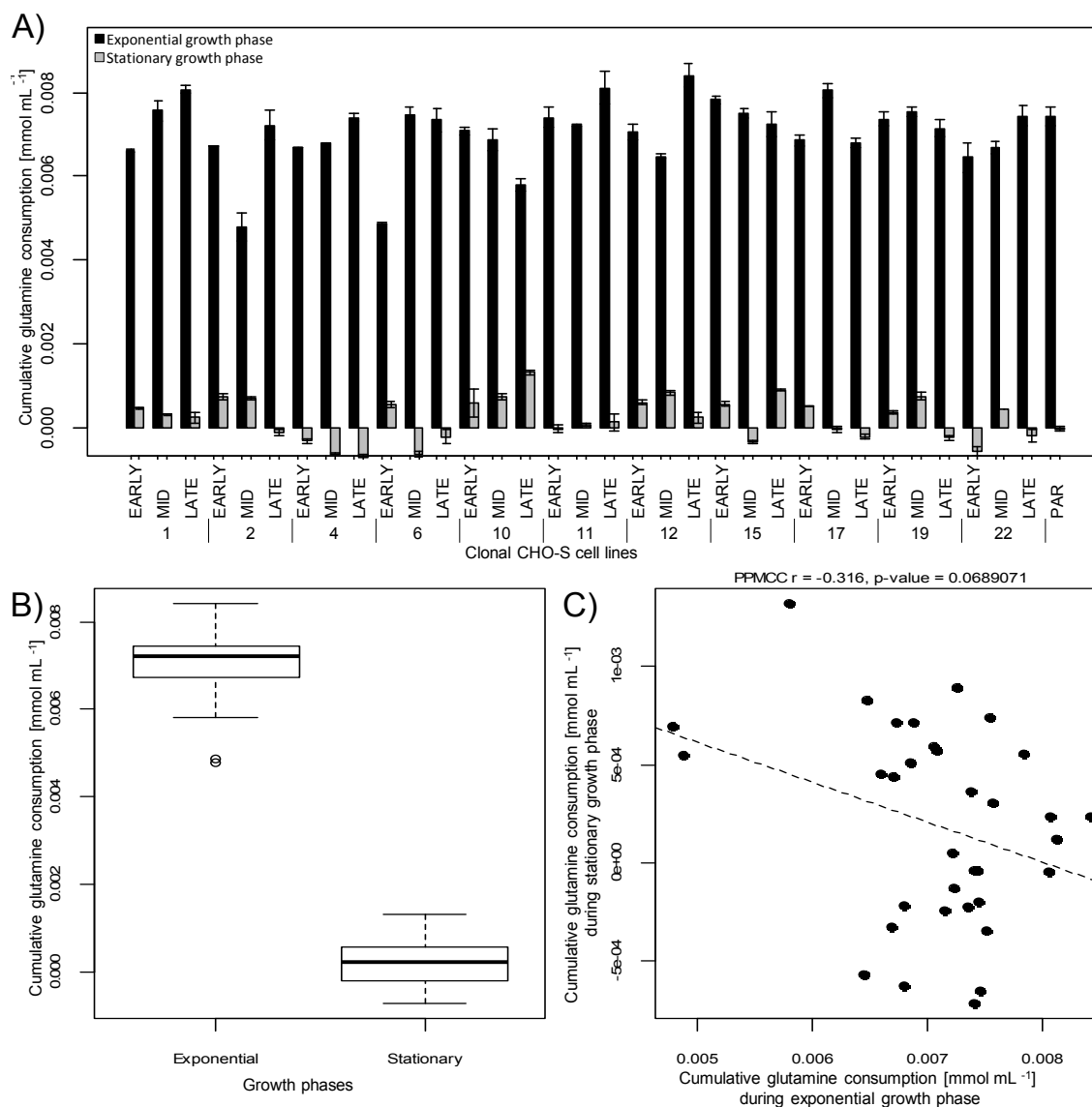
Figure 5-7 Comparison of glutamine uptake metabolism during exponential and stationary growth phases of a fed-batch culture for 11 clonally-derived CHO-S cell lines. Cells were grown in fed-batch culture in CD CHO media supplemented with 8 mM L-glutamine and maintained at 37°C, 170 rpm, under 5% (v/v) CO_2 atmosphere until culture viabilities dropped below 60%, during the culture 10% (v/v) CHO CD EfficientFeed™ was fed at days 3, 5, 7 and 9. For each clone, early-, mid- and late-subpopulations generated from a long-term subculture regime, corresponding to generations 0, 80 and 200, respectively, were evaluated. (A) The cumulative glutamine consumption at the exponential and stationary growth phases for the differently aged clonal subpopulations, (B) the global glutamine consumption at the exponential and stationary growth phases for the differently aged clonal subpopulations and (C) the Pearson's correlation between the glutamine consumption during stationary and exponential growth phases for the differently aged clonal subpopulations (PPMCC r = -0.316, p-value > 0.05, n = 33) are presented.
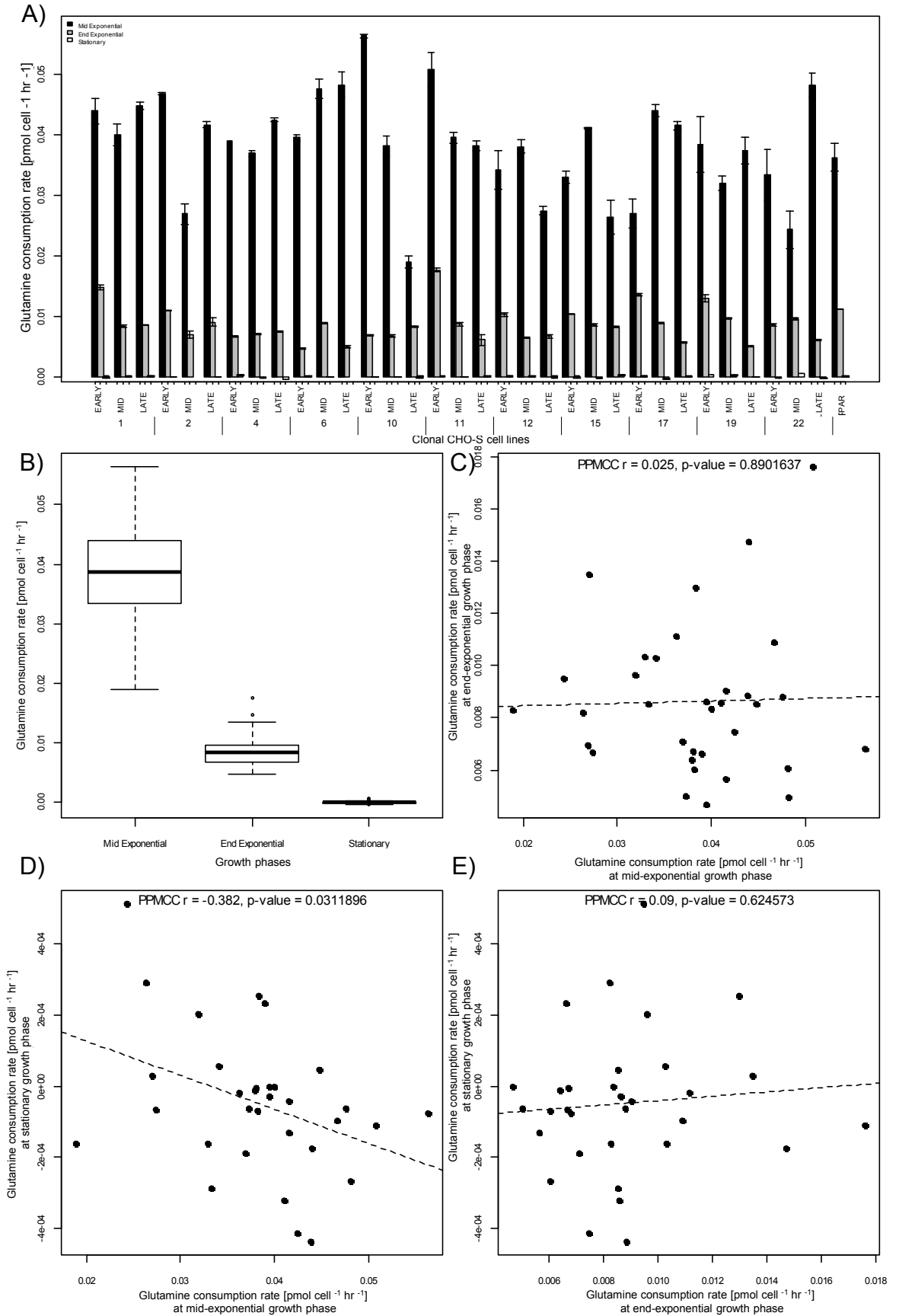
Figure 5-8 Analysis of the specific glutamine consumption rate for 11 clonally-derived CHO-S cell lines during fed-batch culture. Cells were grown in fed-batch culture in CD CHO media supplemented with 8 mM L-glutamine and maintained at 37°C, 170 rpm, under 5% (v/v) CO_2 atmosphere until culture viabilities dropped below 60%, during the culture 10% (v/v) CHO CD EfficientFeed™ was fed at days 3, 5, 7 and 9. For each clone, early-, mid- and late-subpopulations generated from a long-term subculture regime, corresponding to generations 0, 80 and 200, respectively, were evaluated. (A) Specific glutamine consumption rates at the mid-exponential, end-exponential and stationary growth phases for the differently aged clonal subpopulations, (B) the global glutamine consumption rates at the mid-exponential, end-exponential and stationary growth phases for the differently aged clonal subpopulations and the Pearson's correlation between (C) end-exponential and mid-exponential glutamine consumption rates for the differently aged clonal subpopulations (PPMCC r = 0.02, p-value > 0.05, n = 33), (D) stationary and mid-exponential glutamine consumption rates for the differently aged clonal subpopulations (PPMCC r = -0.382, p-value < 0.05, n = 33) and (E) stationary and end-exponential glutamine consumption rates for the differently aged clonal subpopulations (PPMCC r = 0.09, p-value > 0.05, n = 33).

Finally, the Pearson's correlation analysis (Figure 5-8C-E) exhibited a moderate negative correlation between the consumption rates at mid-exponential and stationary growth phases (Figure 5-8D; PPMCC r = -0.382, p-value < 0.05, n = 33), indicating that subpopulations with elevated glutamine dependence at mid-exponential phase rapidly exhaust the glutamine levels, making difficult its accessibility for stationary populations and thus triggering a low glutamine uptake at stationary phase.

5.4.4 Glutamate metabolism among clonally-derived CHO-S cell lines

Contrary to observations for the other metabolites, the glutamate metabolism did not exhibit significant differences between the exponential and stationary growth phases of the fed-batch culture when evaluating the panel of 11 clonally-derived CHO-S cell lines and their differently aged subpopulations (i.e., early, mid- and late subpopulations, corresponding to generations 0, 80 and 200, respectively) generated through long-term cultivation regime (Figure 5-9B; two-way ANOVA, *p*>0.05, F=2.698). However, the Pearson's correlation analysis exhibited a moderate positive correlation between glutamate accumulation at exponential and stationary growth phases (Figure 5-9C; PPMCC r = 0.385, p-value < 0.05, n = 33) and also exhibited significant

differences between exponential and stationary growth phases of the fed-batch culture (Figure 5 8A and Figure 5 8B; two-way ANOVA: glutamine, p<0.0001, F=1848).

The intra-clonal analysis of the accumulated glutamate showed that, in general, the accumulation trend was characterised by a constant increase in concentration at the exponential and stationary growth phases (Figure 5-9A). Interestingly, subpopulations C4-early, C4-mid, C4-late, C15-mid, C17-early and C17-late exhibited different metabolic characteristics for glutamate, being characterised by fast and efficient glutamate utilisation either in the exponential and/or in the stationary growth phases of the fed-batch culture. These results may indicate that the glutamine behaviour in these subpopulations probably resulted from an efficient intracellular assimilation and incorporation of this metabolite in to the TCA cycle (Nolan and Lee 2011).

Analysis of the specific metabolic rates for glutamate metabolism confirmed that C4-early, C4-mid and C4-late utilised the glutamate and avoided its accumulation at the end of the exponential growth phase and exhibited that C17-late used this metabolite during the mid-exponential and during the stationary phase. However, C17-early did not show signs of glutamate assimilation probably because the sampling points did not captured the right time due to a shifted uptake pattern, but it likely happened in a similar fashion as for C17-late (Figure 5-10A). Interestingly, the parental CHO-S cell line exhibited elevated rates of glutamate assimilation at mid-exponential growth phase, which avoided extracellular glutamate accumulation. This metabolic behaviour was noticeably different to the majority of the clones indicating that the isolated populations minimised or even lost this glutamate metabolism.

By comparing the glutamate production rates of all clones, notable differences between the fed-batch culture growth phases were observed (Figure 5-10B; two-way ANOVA, *p*<0.0001, F=59.97). Being the observed rates between mid-exponential and end-exponential phases significantly different, but not substantially different between end-exponential and stationary growth phases (Figure 5-10B). Contrary, the Pearson's correlation analysis between glutamate consumption rates at these three time points did not show any relationship between (Figure 5-10C to E). The ANOVA analysis with respect to the age of the clones (i.e., 0, 80 or 200 generations) only reveals significant differences during the mid-exponential growth phase (two-way ANOVA, p<0.02, F=4.233).
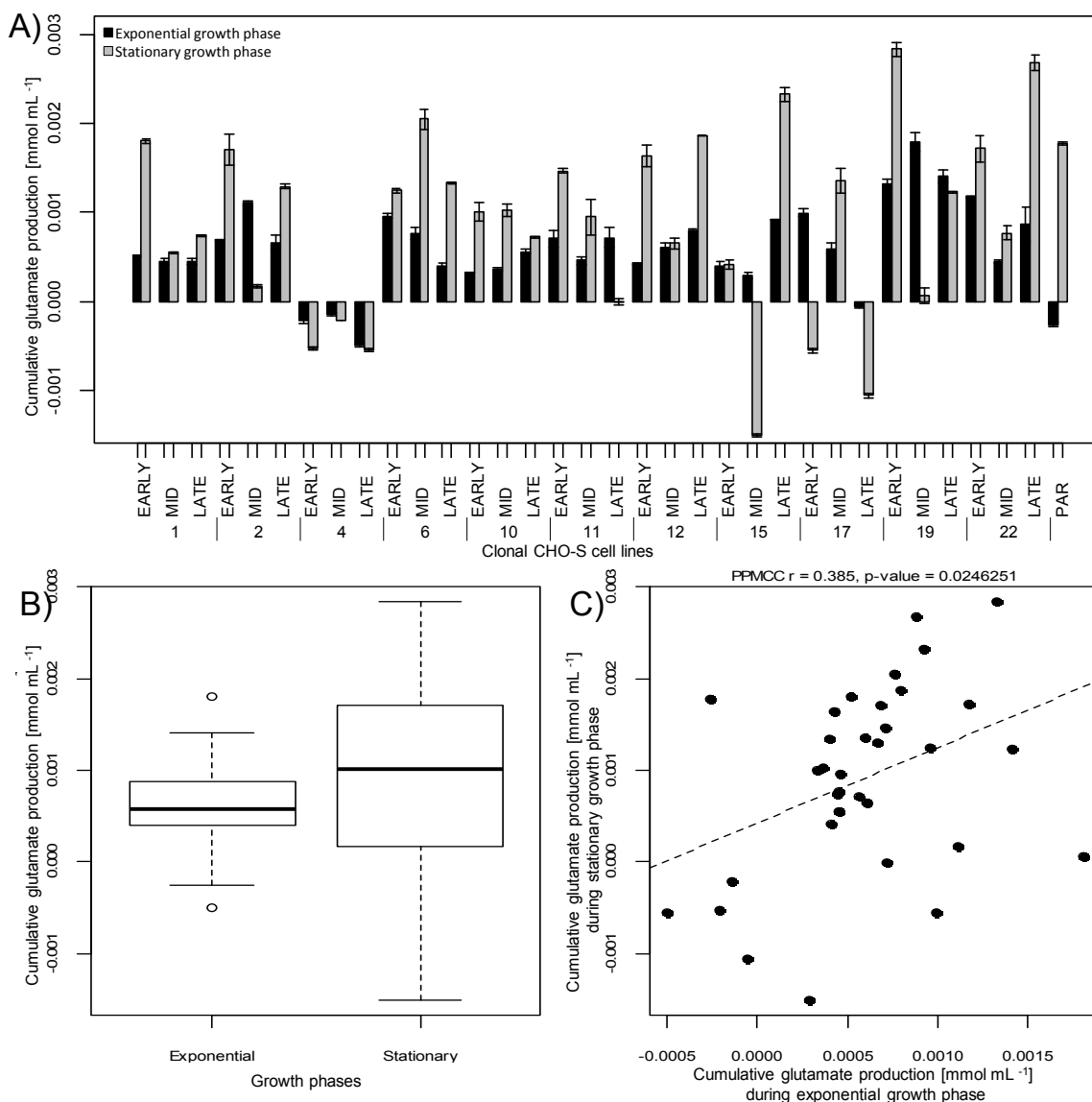
Figure 5-9 Comparison of glutamate metabolism during exponential and stationary growth phases of a fed-batch culture for 11 clonally-derived CHO-S cell lines. Cells were grown in fed-batch culture in CD CHO media supplemented with 8 mM L-glutamine and maintained at 37°C, 170 rpm, under 5% (v/v) CO_2 atmosphere until culture viabilities dropped below 60%, during the culture 10% (v/v) CHO CD EfficientFeed™ was fed at days 3, 5, 7 and 9. For each clone, early-, mid- and late-subpopulations generated from a long-term subculture regime, corresponding to generations 0, 80 and 200, respectively, were evaluated. (A) The cumulative glutamate metabolism at the exponential and stationary growth phases for the differently aged clonal subpopulations, (B) the global glutamate metabolism at the exponential and stationary growth phases for the differently aged clonal subpopulations and (C) the Pearson's correlation between the glutamate metabolism during stationary and exponential growth phases for the differently aged clonal subpopulations (PPMCC r = 0.385, p-value <0.05, n = 33).
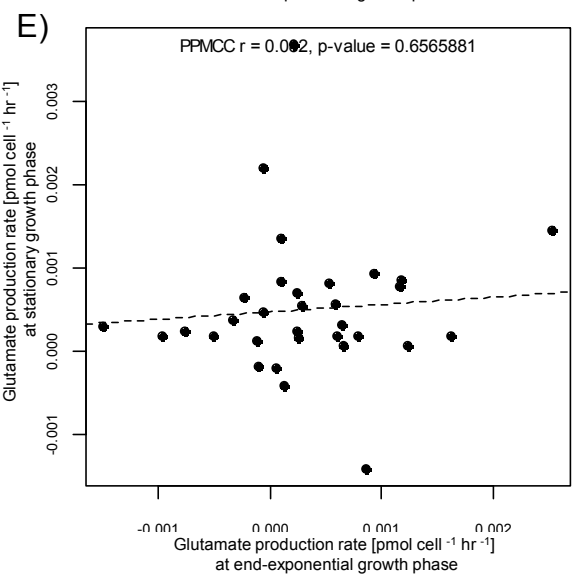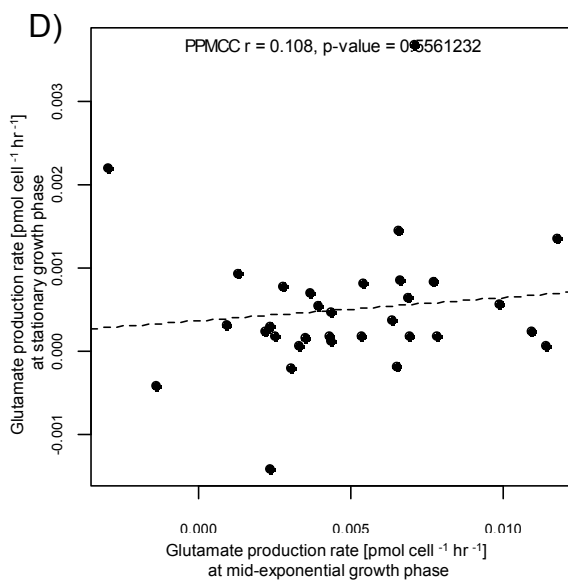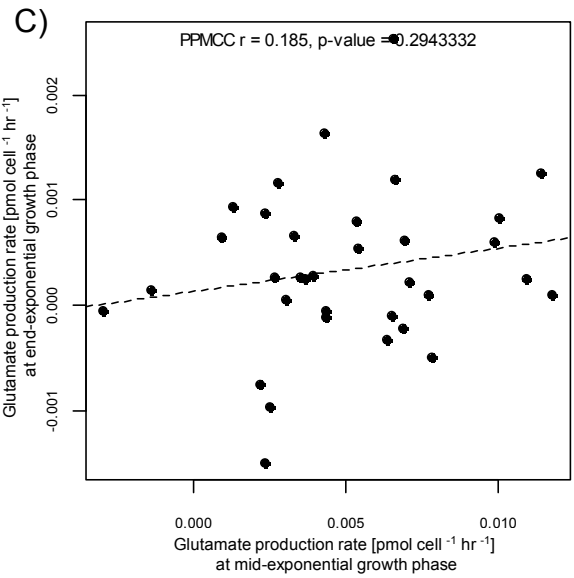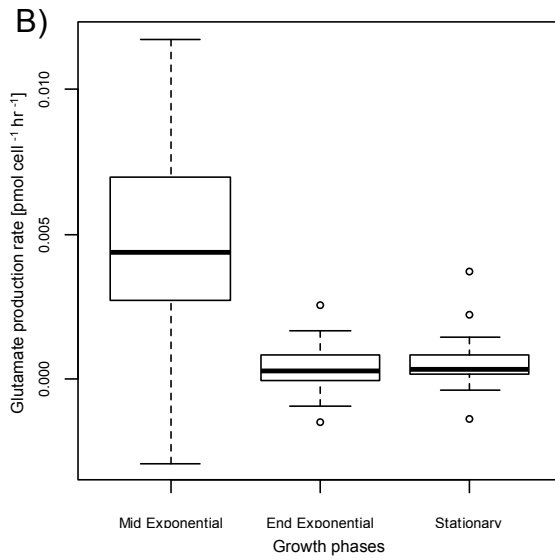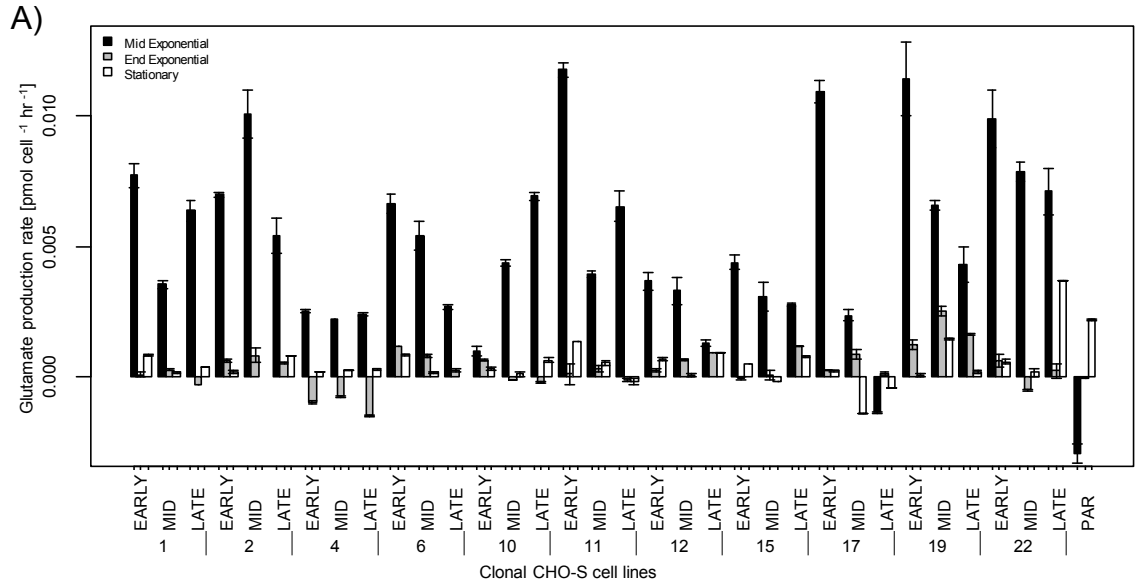
Figure 5-10 Analysis of the specific glutamate production rate for 11 clonally-derived CHO-S cell lines during fed-batch culture. Cells were grown in fed-batch culture in CD CHO media supplemented with 8 mM L-glutamine and maintained at 37°C, 170 rpm, under 5% (v/v) CO_2 atmosphere until culture viabilities dropped below 60%, during the culture 10% (v/v) CHO CD EfficientFeed™ was fed at days 3, 5, 7 and 9. For each clone, early-, mid- and late-subpopulations generated from a long-term subculture regime, corresponding to generations 0, 80 and 200, respectively, were evaluated. (A) Specific glutamate metabolic rates at the mid-exponential, end-exponential and stationary growth phases for the differently aged clonal subpopulations, (B) the global glutamate metabolic rates at the mid-exponential, end-exponential and stationary growth phases for the differently aged clonal subpopulations and the Pearson's correlation between (C) end-exponential and mid-exponential glutamate metabolic rates for the differently aged clonal subpopulations (PPMCC r = 0.185, p-value > 0.05, n = 33), (D) stationary and mid-exponential glutamate metabolic rates for the differently aged clonal subpopulations (PPMCC r = 0.108, p-value > 0.05, n = 33) and (E) stationary and end-exponential glutamate metabolic rates for the differently aged clonal subpopulations (PPMCC r = 0.082, p-value > 0.05, n = 33).

5.4.5 Growth and metabolic kinetics

To understand chances in the cell performance (i.e., IVCD), we plot the cumulative consumption or production of each metabolite over the fed-batch culture against the IVCD. These data revealed a strong correlation between IVCD and cumulative glucose consumption (r^2= 0.88, n=167, p < 0.0001, Figure 5-11A), cumulative metabolism of glucose and lactate combined (r^2= 0.84, n=167, p < 0.0001, Figure 5-11E), and lactate: glucose ratio (r^2= 0.66, n=167, p < 0.0001, Figure 5-11F). The Figure 5-11A indicates that cell growth and cell maintenance are closely linked to glucose consumption, whereas the glutamine, lactate and glutamate metabolism varies with culture progression (Figure 5-11B-D). The Figure 5-11H also exhibited a high lactate:glucose ratio (>2) during the early stage of the culture, leading us to hypothesised that glutamine provided elevated levels of NADPH for fatty acid biosynthesis, which also resulted in increased lactate production as the NADPH results from the malate conversion into pyruvate, and the latter is subsequently converted into lactate. Additionally, lactate:glucose ratios clearly indicates that proliferating cells (mid and end-exponential growth phase) present an elevated aerobic glycolysis, whereas stationary cells present a more efficient glucose oxidation probably linked to mitochondrial metabolism.
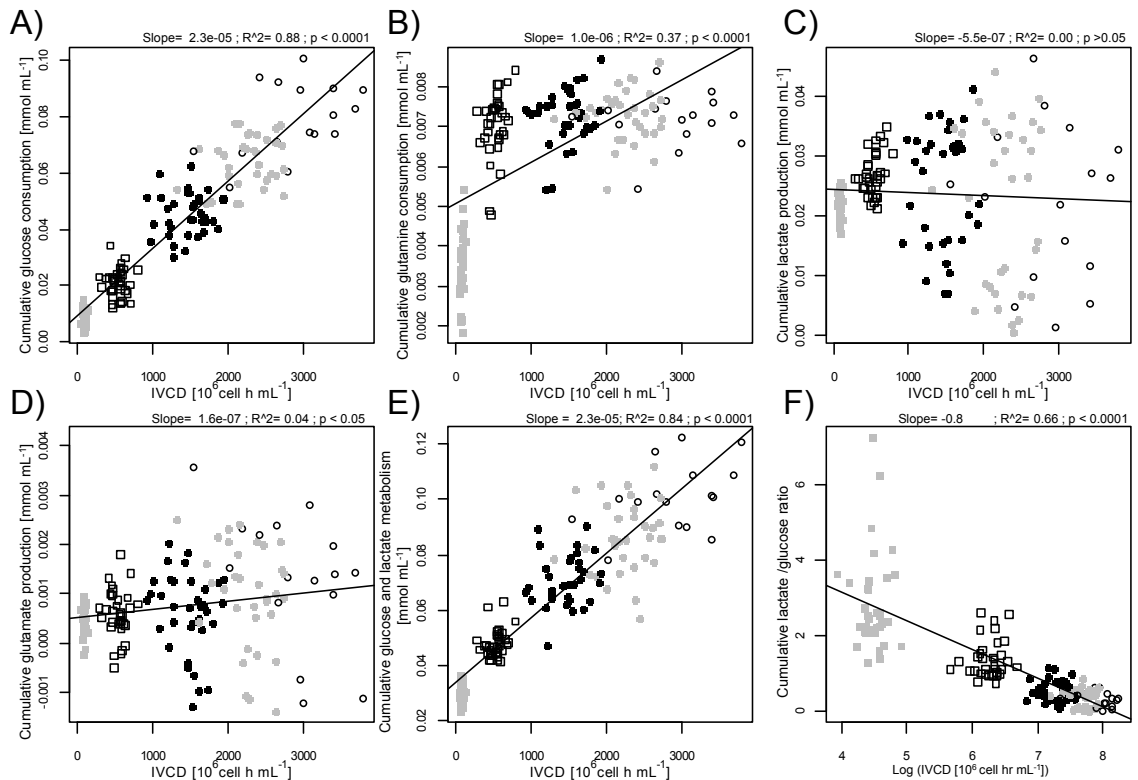
Figure 5-11 Analysis of the global specific metabolic rates for glucose, lactate, glutamate and glutamine for 11 clonally-derived CHO-S cell lines in fed-batch culture and their relation to IVCD. The cumulative consumption or production of indicated metabolites was plotted against integral of viable cell density. The slope values indicate the overall specific rates of consumption or production for 11 clones at early, mid- and late subpopulations. Correlations between (A) glucose consumption, (B) glutamine consumption, (C) lactate production and (D) glutamate production with IVCD are presented. Also, correlations between (E) the combined glucose and lactate metabolism and (E) lactate:glucose ratios with IVCD are shown. The grey and white squares represent the values generated at mid- and end-exponential growth phase for the clones through a fed-batch regime, respectively (i.e., day 3 and 5 of fed-batch, respectively). The black, grey and white circles represent the values generated at early- mid- and end-stationary growth phase generated for the clones through a fed-batch regime, respectively (i.e., day 7, 8 and 11 of fed-batch, respectively).

Specific metabolite rates at end-exponential growth phase

Specific metabolite rates at mid-exponential growth phase
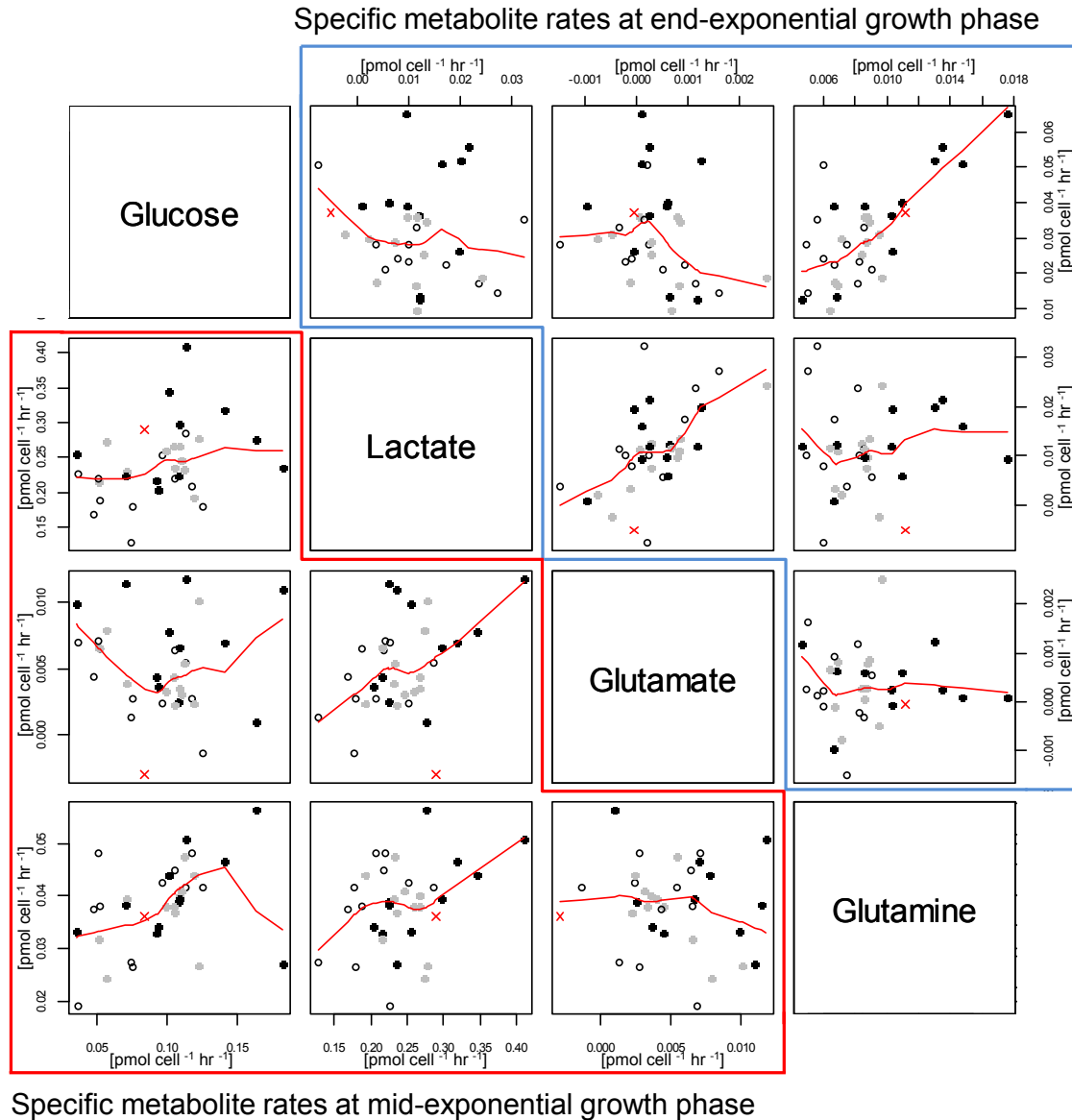
Figure 5-12 Relationship between the specific metabolic rates of glucose, lactate, glutamate and glutamine for 11 clonally-derived CHO-S cell lines during the mid-exponential and end-exponential growth phases of a fed-batch culture. The metabolic rate values inside the red and blue figures correspond to the values collected during the mid-exponential and end-exponential growth phases of the fed-batch, respectively. The black, grey and white circles represent the early, mid- and late-subpopulations generated for the clones through a long-term subculture regime, respectively (i.e., generations 0, 80 and 200, respectively). The red "x" represents the parental population.

The existence of correlations between specific metabolite consumptions during proliferation phase was evaluated by calculating the Pearson's correlation coefficient (Figure 5-12). The results exhibited moderate correlations between glucose and glutamine consumption (PPMCC $r = 0.41$, $n = 33$) and between glutamate and lactate metabolism (PPMCC $r = 0.39$, $n = 33$). The positive correlation between lactate accumulation and glutamate accumulation led us to hypothesise a negative deregulation of glutamate pyruvate transaminase, enzyme that catalyses the conversion of glutamate and pyruvate to alanine and α-KG (Mulukutla et al. 2012), which also suggest a low glutamate flux to feed the TCA cycle as a result of the elevated aerobic glycolysis observed at this growth phase. The positive correlation between glucose and glutamine consumption clearly indicated that both metabolites are closely related in proliferating populations. To validate this results, the Pearson's correlation coefficient at end-exponential growth were calculated (Figure 5-12), observing similar association between glucose and glutamine consumption (PPMCC $r = 0.72$, $n = 33$) and between glutamate and lactate production (PPMCC $r = 0.56$, $n = 33$), and thus confirming our hypotheses. Finally, no significant correlations were observed at stationary phase (Data not shown) indicating that cell metabolism varies in stationary cells.

5.5 General discussion

The cellular metabolism is crucial to understand the cell behaviour in each individual population, therefore several attempts have intended to characterise metabolic processes of CHO cell lines with varied growth and the expression characteristics to developing more efficient feeding strategies to increase the batch-to-batch consistencies and develop efficient mammalian cell cultures (Tsao et al. 2005; Zamorano et al. 2010). Most studies have been performed with the analysis of two or three populations with different cell features (i.e., elevated productivity, improved growth performance) due to the combination of the inherent variability between populations and processes, the poor knowledge on CHO cell metabolism, the intricate regulation of metabolic pathways and the cell-environment interactions, increase the complexity of the overall cellular characterisation.

The metabolic analysis performed in the present study was designed to characterise the metabolism of individual cell lines throughout increasing generations (i.e., early-, mid- and late-subpopulations corresponding to 0, 80 and 200 generations, respectively) and recognise the metabolic changes within cell lines at different stages

of the fed-batch culture. It can be suggested that cell lines with desirable phenotypic traits such as elevated growth performance and phenotypic stability during long-term sub-cultivation periods (see Table 5-1) may share some metabolic traits that would facilitate their identification and selection. However, the data presented here did not indicate any correlation or unique feature capable of identifying or distinguishing between the clonal CHO-S cell lines which previously were classified as optimal for protein production and cell line development. In fact, the data showed that clones were highly variable and suggested that each subpopulation (at early, mid- and late generations) must be considered as an individual CHO-S cell line with its own metabolic and phenotypic characteristic, even if they were generated from a common ancestor. Similar outcomes have reported that mammalian cell lines would diverge significantly throughout time as a result of their inherent phenotypic heterogeneity (Barnes et al. 2006; Chusainow et al. 2009; Kim et al. 1998).

The overall metabolic analysis among clones identified notable differences between stationary and exponential phases, being mainly associated with elevated carbon source utilisation (i.e., glucose and glutamine) at the exponential growth phase to generate energy and biomolecules for cellular proliferation. As expected, this data exhibited a strong "aerobic glycolysis" during the exponential growth phase, which is identified and characterised by extracellular lactate build-up as the result of incomplete glucose oxidation (Vander Heiden et al. 2009; Zhao et al. 2013). This inefficient, but fast glycolytic metabolism probably resulted from the up-regulation of key glycolytic enzymes (i.e., HK, PFK, PYK and LDHA) and glucose transporters (GLUT 1, GLUT 3 and GLUT 4) to promote the fast assimilation of glucose and its rapid conversion to lactate and the associated energy yield (Vander Heiden et al. 2009; Zhao et al. 2013). Similar data have been previously reported and associated to reductions in the pyruvate transport to the TCA cycle as the result of a down-regulation of the PDC complex (Kim et al. 2006; Young 2013; Zhou et al. 2011).

The reduction in specific glucose consumption along increasing generation number directly reduced lactate and glutamate metabolism, this data seems to indicate that populations tend to reduce their metabolic demand for biomass synthesis. Interestingly, the decline in glucose metabolism also favoured positively to the proliferation rates and therefore resulting in continuous improvements in the carbon source utilisation, and therefore reducing glucose uptake and lactate production (Warburg 1956; Young 2013). The metabolic analysis performed during the stationary growth phase exhibited notable decrements in glucose consumption compared with the exponential growth data. This metabolism was anticipated as cells ceased their

proliferation and reduced their energetic demand. This reduction in glucose demand was accompanied by a switch from lactate production to consumption for the majority of the clones or al leas by decreases in its synthesis. This metabolic switch has been widely documented as a desirable metabolic feature in cultures, because it reduces the lactate accumulation, eliminating its negative effects on cell growth (Lao and Toth 1997; Mulukutla et al. 2012; Ozturk et al. 1992; Zhao et al. 2013). Interestingly, the switch in lactate metabolism occurred when glutamine became limiting in medium, this seems to suggest that cells probably use this metabolite as an alternative source of carbon in absence of glutamine. Continuing with the comparison, the glutamine metabolism at exponential phase indicates that its assimilation exceeds the rate of glutamate assimilation into the TCA cycle, whereas the low levels of glutamate metabolism at stationary phase resulted from the glutamine depletion.

The particular analysis of clone 4, which was selected as a cell line that meets the desired characteristics for recombinant protein production given its stable phenotype over increasing generations, showed important metabolic characteristics at its three subpopulations (i.e., C4-early, C4-mid and C4-late, corresponding to generations 0, 80 and 200, respectively). The main differences between clone 4 and the rest of the clones were observed in the glutamate and lactate metabolism. Contrary to the majority of the clonal cell lines, the glutamate consumption observed in clone 4 was higher than its production. Taking into account that glutamate is produced from glutamine deamination, this data may suggest that the glutamine metabolism at end-exponential phase was actively couple with glutamate utilisation. This lead us to hypothesise that clone 4 exhibited higher fluxes in the TCA cycle or a high demand of NADPH for fatty acid biosynthesis. Moreover, this data also seems to indicate that glutamine was rapidly depleted and exhausted by the end of the exponential phase as the result of their high metabolism. To corroborate this hypothesis the raw data at day 5 of the fed-batch culture was analysed, which confirmed that the glutamine concentration at that time point was much lower than for the majority of the clones (< 0.46 mM). Interestingly, the lactate metabolism at stationary phase showed that clone 4 was the unique clonal CHO-S cell line that switched from production to consumption at its three subpopulations (i.e., C4-early, C4-mid and C4-late).

As described previously, clones were classified as "suitable for protein production" and "suitable for cell development process". Thus, in order to test if some metabolic traits were conserved among the clones who comprehend each group comparisons within them were performed. Unfortunately, our data reveals that clones included in each classification do not share any key metabolic characteristic, showing a

substantial level of metabolic heterogeneity among the populations and indicating that an a universal metabolic profile that would identify an specific growth performance cannot be developed, at least with only the global analysis of these four parameters (e.g., glucose, lactate, glutamine and glutamate). Using the same analogy, the metabolism along the long-term cultivation (i.e., early-, mid- and late subpopulations) indicated that in general clones at mid- and late-exponential growth phases tend to reduce their specific glucose consumption and specific lactate production over increasing generations, suggesting that populations reduce their metabolic demands for biomass synthesis, improve their carbon metabolism and minimise the media acidification, therefore improved metabolism resulted in higher proliferation rates.

After the fed-batch study execution, It was possible to identify that the age of the clones (i.e., generations 0, 80 and 200) play a fundamental role for the cell's metabolism by improving the carbon source usage over increasing generations, resulting in higher proliferation rates and lower rates of lactate acidification. In addition, it was identified significant differences in glucose, lactate, glutamine and glutamate metabolism between exponential and stationary growth phase, revealing that clones reduced their glycolytic phenotype (Warburg effect) and switched to a more efficient metabolism over the course of the culture. This hypothesis is supported by the evidences in lactate metabolism which showed notable reductions in the lactate: glucose ratio, therefore these data are a clear sign of the re-establishment of the TCA cycle and OXPHOS metabolism during stationary phase. Finally, this data showed that an elevated glutamine metabolism is required to maintain an active cell growth and that its near depletion promotes a switch from the lactate production to consumption and it defines the end of the exponential growth phase.

In this chapter, the fed-batch experiments were used with the main purpose of supplying optimal nutrients levels to the cell in order to investigate their metabolism. However, the strategy implemented always fed large quantities of glucose, causing a glucose excess during the whole fed-batch culture (data not shown). Opposite effects were observed with glutamine, being depleted at the end of the exponential phase as this metabolite was not supplied in the feeding strategy. As a result, the feeding strategy was non-ideal because did no supply optimal concentrations of both carbon sources, eliminating the possibility of controlling the cellular metabolism along fed-batch culture. Despite it, the results presented here an acceptable outcome considering the technical limitations such as the inability to real-time and online monitoring of the nutrient concentrations and the unknown formulation of the CHO CD EfficientFeed™ B. Other authors have studied cell lines in a similar fashion and their results have agreed

and disagreed with the ones presented here. This supports the idea that cell lines are open systems which constantly interact with their environment, that do not have consistent metabolic patterns and are not easy to predict. In the future, fed-batch cultures can be complemented with a supplementation of a defined formulation on basis of their growth and metabolic performance to control the glucose, glutamine and lactate concentration along the fed-batch culture. This future work can also be complemented with the analysis of other metabolites such as pyruvate and ammonia which could give an even more complete picture of the cell's metabolism.

Chapter 6

GLYCOLYTIC AND MITOCHONDRIAL METABOLISM AMONG CHO-S CLONAL DERIVATIVES

Chapter 6

Glycolytic and mitochondrial metabolism among CHO-S clonal derivatives

This chapter introduces the procedures employed to analyse the glycolytic and mitochondrial metabolism for a panel of clonally-derived CHO-S cell lines at early-, mid- and late-generations corresponding to generations 0, 80 and 200, respectively, during the exponential and stationary phase of a fed-batch regimen, followed by assessments of the four key glycolytic parameters and the six key mitochondrial parameters. Altogether, this methodology allows us to gain insight into metabolic dynamics within CHO cell populations during exponential and stationary growth phases.

6.1 Background

In the previous chapters it was demonstrated that the inherent phenotypic heterogeneity within CHO populations was responsible for generating a panel of 22 clonal CHO-S cell lines with significant differences in terms of cell growth performance (e.g., specific growth rate, IVCD, maximal VCD and cell size) and metabolism (e.g., glucose and glutamine consumption). Additionally, the glucose, lactate, glutamine and glutamate analyses described in chapter 5, exhibited that proliferating cell lines were more glycolytic during the exponential phase and also reveal that subpopulations switched to a more mitochondrial metabolism during the stationary growth phase. These findings permit to hypothesise that evaluating the glycolytic and mitochondrial performance during the stationary and exponential growth phase will increase our understanding of the metabolic behaviour observed in chapter 5.

As mentioned previously, glucose is the primary source of energy and a key molecule for living organisms. This molecule is transported across the cell membrane by glucose transporters (GLUTs), followed by its oxidation through glycolysis to generate two pyruvic acid molecules. At this stage, pyruvate can follow two pathways: (i) being reduced to lactic acid by the lactate dehydrogenase enzyme (LDH) under hypoxic conditions with a global production of two ATP molecules per glucose molecule or (ii) being oxidised into CO_2 through the TCA cycle to give NADH and $FADH_2$ which are subsequently coupled to OXPHOS to produce ATP (Adekola et al. 2012; Koopman et al. 2013). This complete glucose oxidation represents the optimal energetic

metabolism giving a global yield of up to 36 ATP molecules per glucose molecule (Gatenby and Gillies 2004; Koopman et al. 2013).

The conversion of pyruvate into lactate is a common metabolism called "aerobic glycolysis" observed in CHO cells, in which they prefer to use the glycolytic pathway as the main source of energy to fuel the cell metabolism even under aerobic conditions (Kim et al. 2006; Papandreou et al. 2006; Zhou et al. 2011). This metabolism plays an important role because the lactate production restores the levels of NAD+/NADH and this maintains the ATP production (Gatenby and Gillies 2004; Kim et al. 2006; Papandreou et al. 2006; Vander Heiden et al. 2009). However, during biological production processes (e.g., monoclonal antibodies manufacturing) the elevated lactate levels are detrimental for cells, reducing notably their cell growth performance and the protein production (Lao and Toth 1997; Ozturk et al. 1992; Zhao et al. 2013). Several studies have identified that this metabolism is the result of important metabolic and physiologic changes within cells, being the PDC inhibition by PDK activity one of the most important changes because its activity determines the route for pyruvate metabolism, either in the mitochondria or in the cytosol to form lactate, therefore PDC inhibition by PDK results in a subsequent reduction in the pyruvic acid flux from glycolysis to the TCA cycle (Diers et al. 2012; Kim et al. 2006; Young 2013; Zhou et al. 2011).

As mentioned above, the mitochondria respiration represents the more efficient cellular metabolism in terms of ATP production, comprising a set of biochemical reactions that transfer electrons from NADH and $FADH_2$ to O_2, through a series of enzymatic complexes (complex I, II, and III of the ETC) and electron carriers (ubiquinone/coenzyme Q and cytochrome c) yielding one water molecule and pumping protons to the IMS, which later are used to generate ATP through the action of the ATP synthase complex (complex IV) (Nicholls and Ferguson 2013). Despite being an efficient route, the mitochondria presents a natural proton leak, these protons then react with oxygen without producing ATP (Jastroch et al. 2010). This proton leak has been defined as a normal process within cells, representing around 20 to 30% of the mitochondrial respiration (Jastroch et al. 2010). However, elevated proton leak activity would denote potential mitochondrial membrane damage (Kokoszka et al. 2001).

For the above mentioned, the mitochondrion is an indispensable organelle for maintaining the cellular performance and needs to be evaluated during cell line development processes in other to generate cell lines with robust mitochondrial integrity. The mitochondrion consists of outer and inner double phospholipid membranes, intermembrane space and matrix, which together hold and coordinate the

indispensable metabolic pathways such as the TCA cycle, ETC and OXPHOS (Nelson and Cox 2013), regulate important physiological process such as apoptosis, cell division and cell growth (Bereiter-Hahn et al. 2008; Cadenas and Davies 2000), and maintain their functionality, integrity and communication with the cytosol (Detmer and Chan 2007; Gabriel et al. 2007; Vogtle et al. 2012). For the importance of the organelle for cellular regulation, it is not surprising that abnormal mitochondrial metabolism would result in apoptosis or in detrimental growth performances (Koopman et al. 2013; Valko et al. 2007). Consequently, in this study I analysed the glycolytic and the mitochondrial status in clonal CHO-S cell lines to identify glycolytic and respiratory parameters that will eventually lead us to design more efficient screening technologies for the selection of cell lines with improved growth characteristics (e.g., IVCD).

6.2 Chapter aims

In this chapter, I investigated four hypotheses (i) that cell lines with active proliferation rates prefer to use the glycolytic metabolism as the principal ATP source, (ii) that during the mid- and late-stage of the fed-batch culture cells restore the TCA cycle flux and increase their mitochondrial metabolism, (iii) that the mitochondrial integrity during the mid- and late–fed-batch culture is a key cellular parameter which dictates the overall longevity of the cells and (iv) that the analysis of the glycolytic and mitochondrial metabolism during the exponential and stationary growth phases would permit the identification of key metabolic features of cell lines with specific metabolic characteristic for cell line development or protein production processes. Thereby, I suggest that:

(i)   The clonally-derived CHO-S cell lines would exhibit significant metabolic differences in terms of glycolytic activity and mitochondria respiration.

(ii)   The clonally-derived CHO-S cell lines would exhibit elevated glycolytic activity during the early-stage of the fed-batch culture.

(iii)   The re-establishment of the mitochondrial activity among the clonally-derived CHO-S cell lines was responsible of reducing glucose demand and lactate accumulation during the late-stage of the fed-batch culture.

(iv)   The detrimental environmental conditions observed at mid- and late-stages of the fed-batch culture threaten the mitochondrial integrity, resulting in increases of proton leak across the IMM.

The aim of this chapter was to reveal the optimal metabolic state among clonally derived populations and understand the central carbon metabolism of the CHO cells during fed-batch experiments. Moreover, I aimed to study how the mitochondrial and glycolytic metabolisms during fed-batch cultivation are closely regulated. Finally, I aimed to identify the optimal glycolytic and mitochondrial parameters that could permit the selection of subpopulation with relevant phenotype.

6.3 Chapter objectives

To address the chapter aims, the objectives of the work presented in this chapter were to:

i) Characterise the glycolytic metabolism of a panel of 24 clonally-derived CHO-S subpopulations and a parental line during the exponential and stationary growth phases of fed-batch culture.

ii) Examine the four key glycolytic parameters (i.e., non-glycolytic acidification, glycolysis, glycolytic capacity and spare glycolytic capacity) during the exponential and stationary growth phases of fed-batch culture.

iii) Characterise the profiles of respiratory capacity of a panel of 35 clonally-derived CHO-S subpopulations and a parental line during the exponential and stationary growth phases of fed-batch culture.

iv) Examine the six key mitochondrial parameters (i.e., non-mitochondrial respiration, basal mitochondrial respiration, maximal respiration, spare respiratory capacity, ATP linked respiration and proton leak) at exponential and stationary growth phases.

v) Identify the potential correlation between the glycolytic parameters at exponential and stationary growth phases.

vi) Identify the potential correlation between the respiratory parameters at exponential and stationary growth phases.

6.4 Results

6.4.1 Analysis of the glycolytic activity function among clonal CHO-S cell lines during exponential and stationary growth phase

In the previous chapter (see chapter 5) the metabolism of 11 clonally-derived CHO-S cell lines at different ages was studied in fed-batch culture. The global metabolism among the clonally-derived CHO-S cell lines was characterised by elevated glucose and glutamine demand and important lactate build-up in proliferating cells during the exponential phase, this behaviour was subsequently replaced by a drastic reduction in the cell's glucose dependence and lactate accumulation during the stationary phase, and for some clones even a switch to lactate consumption was detected. The elevated glucose addiction and lactate accumulation observed during the early-stage of the fed-batch culture clearly evidenced a prominent glycolytic phenotype with an incomplete glucose oxidation, indicating that proliferating CHO cells preferred the aerobic glycolysis over OXPHOS to meet the energetic and biosynthetic demands for proliferation. On the other hand, a substantial reduction in glucose consumption and lactate accumulation at stationary growth phase evidenced significant changes in the glycolytic metabolism, suggesting that cells reactivated the glycolysis-TCA cycle link, which was minimised in proliferating cells, and therefore exhibited efficient glucose utilisation (i.e., lactate was not accumulated) coupled to OXPHOS to meet their metabolic demands.

To characterise the glycolytic metabolism among the differently aged clonally-derived CHO-S subpopulations, glycolysis was evaluated in triplicate at mid-exponential and stationary growth phases using the cell metabolic analyser Seahorse XF24 which measured the extracellular acidification rate. ECAR is as indicator of glycolysis as glycolytic cells present elevated rates of acidification resulted from the lactate production. During the test, cells were maintained in un-buffered DMEM media without glucose to exhaust the intracellular glucose, followed by a sequential treatment with (i) glucose (final concentration 10 mM) to induce glycolysis, (ii) oligomycin (final concentration 1.125 µM), an ATP synthase inhibitor which blocks OXPHOS and forces cells to rely on glycolysis to meet the energetic demands and thus discloses the maximal glycolytic capacity and (iii) 2-DG (final concentration 100 mM), a glycolysis inhibitor which stops the glycolytic metabolism and reveals the non-glycolytic acidification (Figure 6-1).

A)

Glycolytic activity at mid-exponential growth phase

B)

Glycolytic activity at stationary growth phase

Glycolysis   Glycolytic capacity   Glycolytic reserve   Non-Glycolytic acidification
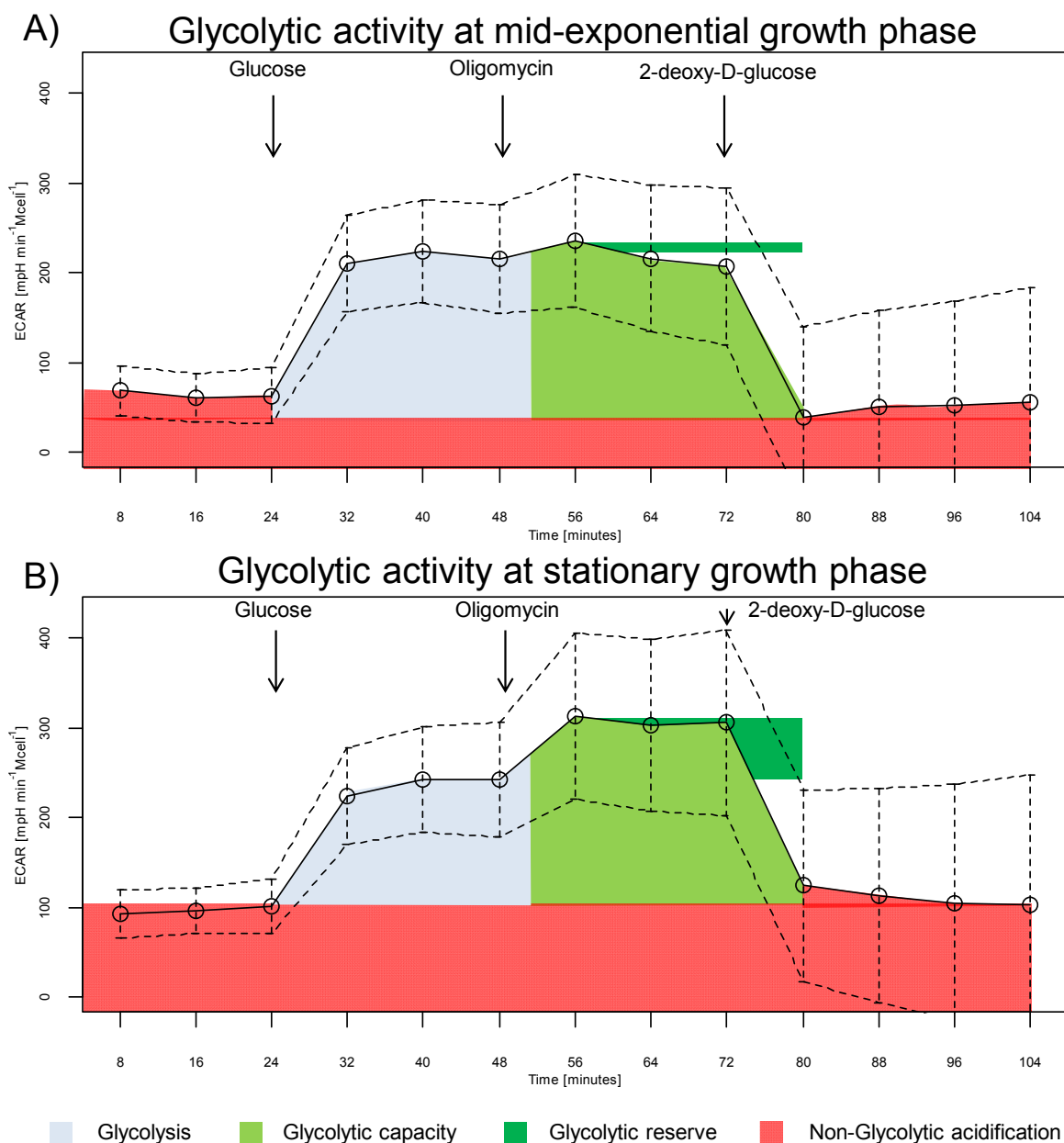
Figure 6-1 Global extracellular acidification rate (ECAR) profiles during the exponential and stationary growth phases for 24 clonally-derived CHO-S subpopulations and the parental line. For each clone, cell samples at (A) exponential growth phase (day 3) and (B) stationary growth phase (day 7) were harvested and analysed using the cell metabolic analyser Seahorse XF24. During the test cells were maintained in un-buffered DMEM and triplicate measurements of the basal ECAR were obtained, followed by triplicate measurements of ECAR after injection of each of the following compounds: glucose, oligomycin and 2-deoxy-glucose, used for glycolysis evaluation, maximal glycolytic capacity induction and non-glycolytic acidification evaluation, respectively. The circles represent the average for 24 differently aged clonal subpopulations and the superior and inferior dotted lines represent the SD.

For improving the glycolytic analysis, the concentration of oligomycin was optimised to ensure a complete inhibition of OXPHOS and also to reduce its toxic effects (e.g., cell death) during the test. The identification of the optimal oligomycin concentration was performed by testing seven different concentrations (i.e., 0, 0.25, 0.50, 0.75, 1.00, 1.125 and 1.25 µM) and measuring the basal OCR and ECAR before and after the oligomycin injection. The lower oligomycin concentration that supported the highest effects on OCR and ECAR was selected as the optimal concentration for glycolytic analysis.

In this section, the global glycolytic metabolism (i.e., glycolysis, glycolytic capacity, glycolytic reserve and non-glycolytic acidification) described in Figure 6-1 was analysed at exponential and stationary growth phases to give an insight into the varied glycolytic capabilities among clonal CHO-S cell lines. However, in subsequent sections a more detailed analysis is carried out (see sections 6.4.2 to 6.4.5). This global analysis was performed using 24 individual subpopulations, parental cell line included, with different accumulated generations originated from a long-term culture regime (i.e., generations 0, 80 or 200, corresponding to the early-, mid- or late- subpopulations of each clone), these clones were analysed and compared during the exponential and stationary phases. At first glance, it can be observed a significant difference between the glycolytic metabolism at stationary and exponential growth phases (Figure 6-1A-B), exhibiting that proliferating cells commonly utilised their glycolytic metabolism at their maximal capacity, whereas stationary growth phase cells used the glycolytic pathway below their maximal capacity (~ 63% of their maximal glycolytic capacity). This data clearly confirms that proliferating cells present an strong Warburg effect, this preferring the aerobic glycolysis over OXPHOS to meet their energetic and biosynthetic demands. Moreover, this data suggest that during the stationary phase cells switched to a more efficient energetic metabolism and relied more on OXPHOS. This hypothesis is supported by previous observations in the cellular metabolism among the clonal CHO-S cells (see chapter 5), which demonstrated that cells at stationary phase significantly reduced their glucose consumption and even switched from lactate production to consumption. Moreover, to corroborate this hypothesis the mitochondrial analysis is presented in sections 6.4.7 to 6.4.13.

The comparison between stationary phase and exponential phase revealed that subpopulations at stationary growth phase exhibited an increment in the non-glycolytic acidification (~ 125%, Figure 6-1A-B). This metabolic performance probably resulted from increments in the CO_2 production via the TCA cycle as cells switched from aerobic glycolysis to OXPHOS metabolism during the stationary growth phase. A similar

glycolytic behaviour was observed for the glycolytic capacity and glycolytic reserve which were enhanced up to 1.15 and 22.05 fold change compared with the exponential growth phase, respectively. Finally, the analysis of the basal glycolytic activity exhibited a contrary behaviour, characterised by reduction in the glycolytic flux during stationary phase (~ 25%). Together, this data strongly suggest that during stationary growth phase cells relied more on mitochondrial metabolism.

6.4.2 Non-glycolytic acidification

In cells, the glucose metabolism produces two types of acids: lactic acid which results from an incomplete glucose oxidation and carbonic acid which is generated from the complete glucose oxidation to CO_2 through the TCA cycle and then hydrated to carbonic acid (Newell et al. 1993). Therefore, the total extracellular acidification results from the glycolytic and the TCA cycle metabolism, as well as from the proton extrusion. To identify and compare the glycolytic metabolism among subpopulations, the inherent non-glycolytic acidification was identified and disregarded. This ECAR value was obtained through the complete inhibition of the glycolytic pathway by 2-DG (Figure 6-1). The residual ECAR observed after 2-DG injection was defined as non-glycolytic acidification and compared between subpopulations (Figure 6-2A). At first glance, significant differences between growth phases were observed (Figure 6-2B; two-way ANOVA, $p<0.0001$, F=105.6) with a moderate, but significant, correlation between the non-glycolytic acidification at the stationary and exponential growth phases (Figure 6-2C; PPMCC r = 0.407, p-value < 0.05, n = 25). Finally, the age of subpopulations (e.g., early, mid and late) did not exhibited an effect in the non-glycolytic acidification, either at exponential and stationary growth phase.

The comparison between growth phases showed that all the subpopulations significantly increased their non-glycolytic acidification at the stationary growth phase, ranging between 42% for C12-late and 880% for the parental population. On the basis of the metabolic analysis (see chapter 5) it can be suggested that the increase in the non-glycolytic acidification resulted from the activation of the OXPHOS metabolism at the stationary growth phase. An interesting finding was observed with the parental population, exhibiting the lowest non-glycolytic acidification at exponential phase, probably resulted from a strong Warburg effect with an elevated inhibition of the pyruvic acid flux into the TCA cycle. As a consequence, when the parental population stimulated its mitochondrial metabolism this was observed as a significant increment in

the non-glycolytic acidification, but in fact its stationary value was not superior to those observed in the other clones.
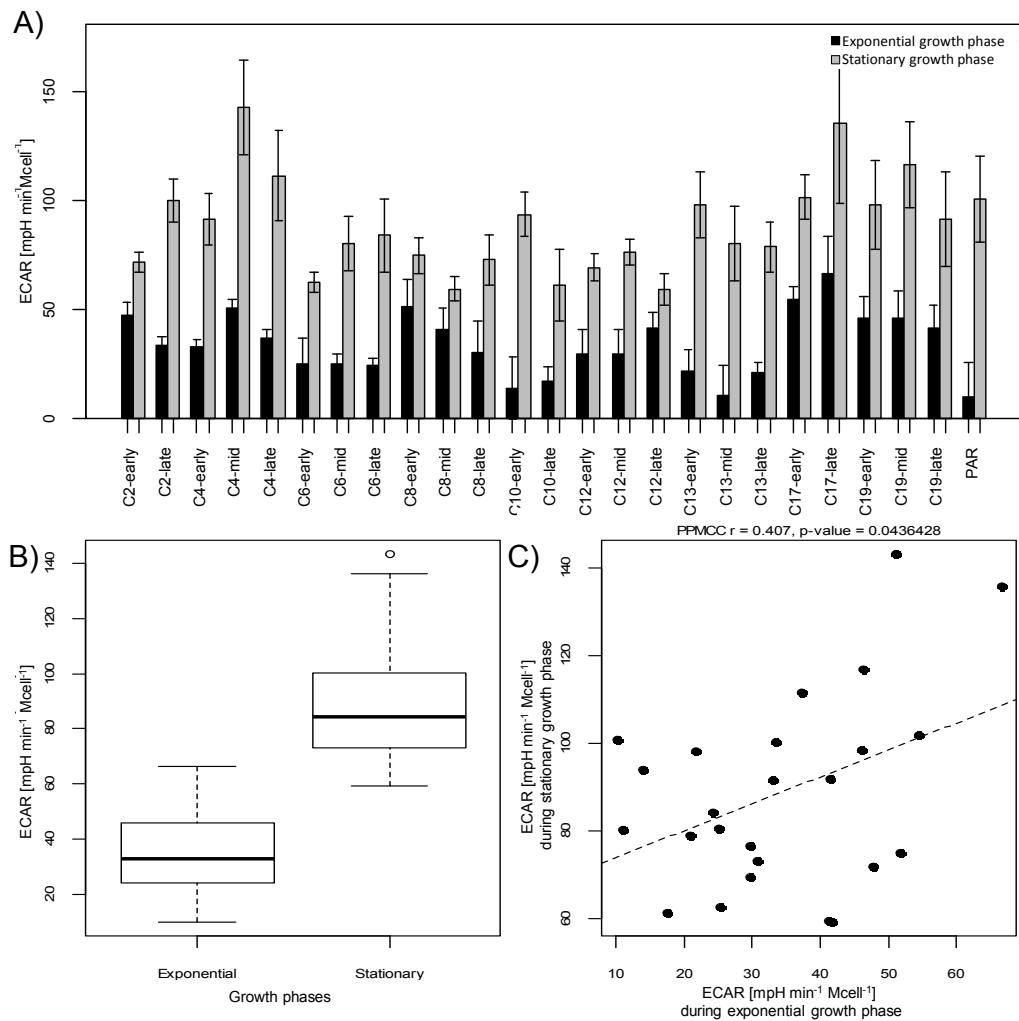
Figure 6-2 Analysis of the non-glycolytic acidification for 24 clonally-derived CHO-S subpopulations and the parental population during exponential and stationary growth phases. Cells were grown in fed-batch culture in CD CHO media supplemented with 8 mM L-glutamine and maintained at 37°C, 170 rpm, under 5% (v/v) CO_2 atmosphere until culture viabilities dropped below 60%, during the culture 10% (v/v) CHO CD EfficientFeed™ was fed at days 3, 5, 7 and 9. Early-, mid- and late-subpopulations generated from a long-term subculture regime, corresponding to generations 0, 80 and 200, respectively, were harvested and analysed using the cell metabolic analyser Seahorse XF24 at exponential (day 3) and stationary (day 7) growth phases. (A) Non-glycolytic acidification at exponential and stationary growth phases for the differently aged clonal subpopulations, (B) the global non-glycolytic acidification rates at the exponential and stationary growth phases and (C) the Pearson's correlation between the non-glycolytic ECAR at stationary and exponential growth phases for the differently aged clonal subpopulations (PPMCC r = 0.407, *p*-value < 0.05, n = 25).

151

6.4.3 Basal Glycolysis

The basal glycolysis represents the normal glucose metabolism under aerobic conditions without glucose limitation. To calculate this value, the glycolytic flux was first measured through glucose stimulation, which stimulates the glycolytic metabolism, and then the non-glycolytic acidification ECAR value was subtracted from the glucose treatment ECAR value. The comparison of the basal glycolysis at both exponential and stationary growth phases exhibited significant differences (Figure 6-3B; two-way ANOVA, $p<0.05$, F=4.3), being significant higher at stationary growth phase without any significant correlation between both growth phases (Figure 6-3C; PPMCC r = 0.176, p-value > 0.05, n = 25). This data also reveals that subpopulations tend to reduce their basal glycolysis over increasing generation at both growth phases with a significant variability between subpopulations with differences of up to 2.0 and 4.3 fold changes between lowest and highest ECAR activities for the exponential and stationary growth phases, respectively.

Analysing in detail the subpopulations, it can be observed that the majority of the clones reduced their glycolytic activity at the stationary phase, between 10 and 30%, whereas subpopulations C10-late, C13-early and C17-late did not present significant variations and C4-mid, C4-late, C10-early and C17-early increased their activity up to 28%. The observed reduction in basal glycolytic metabolism at stationary phase seems to be associated with the decreased or even interruption of cell growth. Contrary, the maintenance or increments of glycolic levels suggested that the predominance of a strong glycolytic metabolism for meeting the energetic demands for cell maintenance. A peculiar metabolism can be observed for C2-late which significantly increased its glycolytic metabolism by 133%, suggesting that the stationary cells still maintained a strong Warburg effect, but the lactate: glucose ratio (0.13 lactate moles produced per each glucose mole consumed) strongly reject this hypothesis.

A)

B)

C)

Figure 6-3 Analysis of glycolysis for 24 clonally-derived CHO-S subpopulations and the parental population during exponential and stationary growth phases. Cells were grown in fed-batch culture in CD CHO media supplemented with 8 mM L-glutamine and maintained at 37°C, 170 rpm, under 5% (v/v) CO_2 atmosphere until culture viabilities dropped below 60%, during the culture 10% (v/v) CHO CD EfficientFeed™ was fed at days 3, 5, 7 and 9. Early-, mid- and late-subpopulations generated from a long-term subculture regime, corresponding to generations 0, 80 and 200, respectively, were harvested and analysed using the cell metabolic analyser Seahorse XF24 at exponential (day 3) and stationary (day 7) growth phases. (A) Glycolytic metabolism at exponential and stationary growth phases for the differently aged clonal subpopulations, (B) the global glycolysis rates at the exponential and stationary growth phases and (C) the Pearson's correlation between the glycolytic ECAR at stationary and exponential growth phases for the differently aged clonal subpopulations (PPMCC r = 0.176, *p*-value > 0.05, n = 25).

6.4.4 Maximal glycolytic capacity

The inhibition of OXPHOS by oligomycin forces cells to generate all the ATP demanded to survive via aerobic glycolysis, revealing the glycolytic capacity. This maximum glycolytic capacity value was calculated by subtracting the non-glycolytic acidification ECAR value from the oligomycin treatment ECAR value. Gathering the maximum glycolytic metabolism for all clones and classifying it into exponential and stationary phases (Figure 6-4B) showed that the differences between both growth phases were statistically significant (two-way ANOVA, $p<0.05$, F=5.18) with moderate, but no significant positive correlation between the observed glycolytic capacity at both growth phases (Figure 6-4C; PPMCC r = 0.317, p-value > 0.05, n = 25). As expected, the comparison of glycolytic capacity among clones also exhibited a large variability, with up to 2.7 and 3.8 fold differences between the lowest and highest ECAR activities at exponential and stationary growth phases, respectively. Moreover, the observed increments in the maximal glycolytic fluxes at stationary phase may be the resulted of the glycolytic machinery accumulated along exponential phase, which was slightly reduce during the stationary phase, thus the latent glycolytic capacity allow to efficiently and quickly switch between mitochondrial and glycolytic metabolism

The glycolytic analysis over increasing generation showed a notable reduction in the maximal glycolytic capacity after 200 generation, confirming that the evolved sub-clones tend to reduce their glycolytic capacity over increasing generation. Moreover, the comparison among subpopulations revealed that the majority of the clones increased between 10 and 88% their glycolytic capacity from exponential to stationary phase, whereas six subpopulations (C6-early, C8-early, C8-late, C8-mid, C13-mid and C19-early) did not exhibit significant variations and only four subpopulations reduced their glycolytic capacity between 18 and 33% (C6-mid, C6-late, C12-late and C13-late). From the clones, subpopulations C2-late and C10-early exhibited a peculiar performance characterised by significant increments from exponential to stationary phase, 120 and 219%, respectively. Interestingly, subpopulation C2-late also showed a notable difference in the basal glycolytic metabolism between both growth stages, suggesting that C2-late up-regulated its glycolytic capacity at stationary phase to meet the energetic demands for cell maintenance. The further analysis of C2-late and C10-early also indicated that both cell lines (i) exhibited elevated rates of glucose consumption during exponential phase with an incomplete glucose oxidation allowing high levels of lactate and (ii) that both cell subpopulations not presented the a switch from lactate production to consumption (see chapter 5).
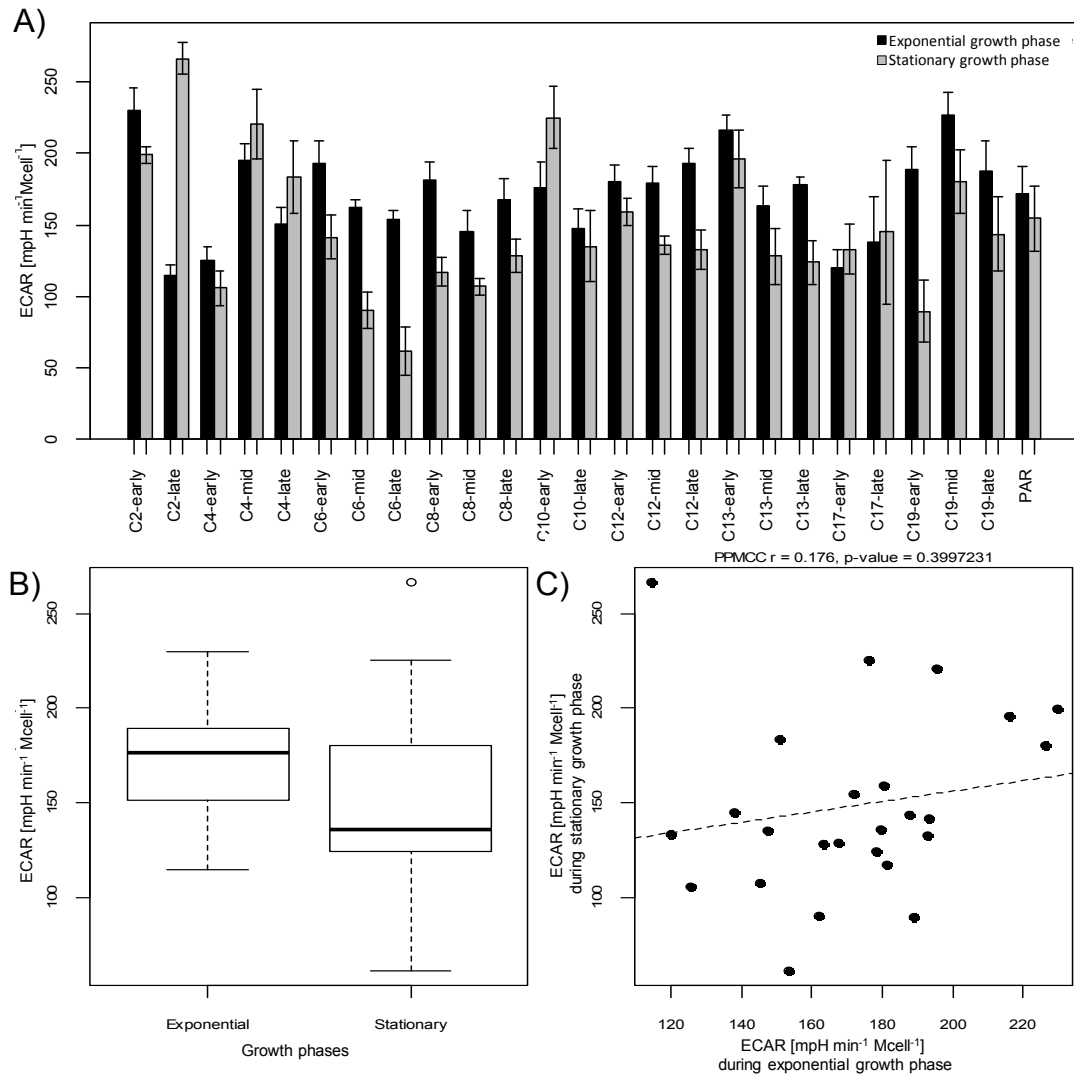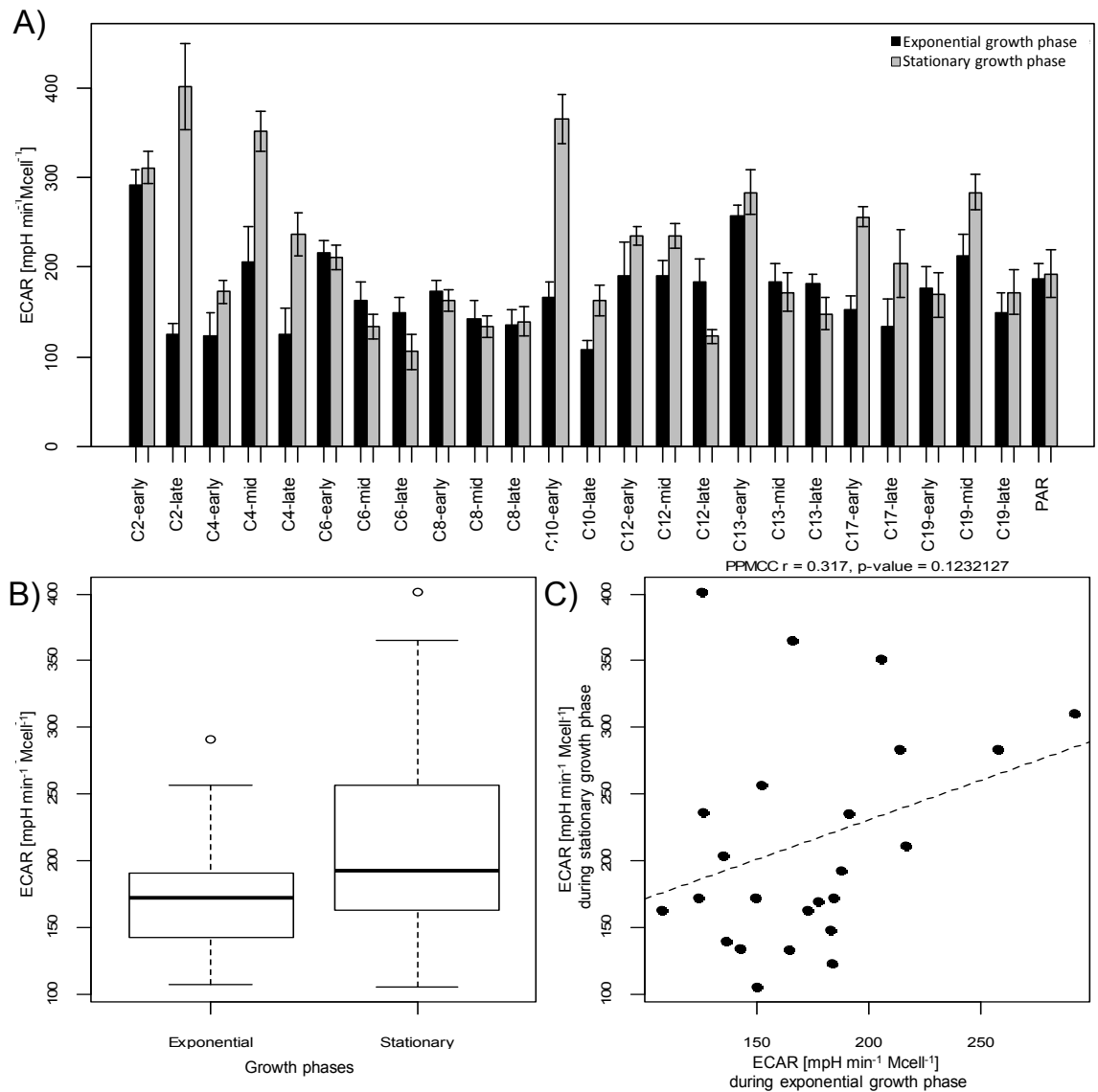
Figure 6-4 Analysis of the maximal glycolytic capacity for 24 clonally-derived CHO-S subpopulations and the parental population during exponential and stationary growth phases. Cells were grown in fed-batch culture in CD CHO media supplemented with 8 mM L-glutamine and maintained at 37°C, 170 rpm, under 5% (v/v) CO_2 atmosphere until culture viabilities dropped below 60%, during the culture 10% (v/v) CHO CD EfficientFeed™ was fed at days 3, 5, 7 and 9. Early-, mid- and late-subpopulations generated from a long-term subculture regime, corresponding to generations 0, 80 and 200, respectively, were harvested and analysed using the cell metabolic analyser Seahorse XF24 at exponential (day 3) and stationary (day 7) growth phases. (A) Maximal glycolytic capacity at exponential and stationary growth phases for the differently aged clonal subpopulations, (B) the global maximum glycolytic capacity rates at the exponential and stationary growth phases and (C) the Pearson's correlation between the maximal glycolytic capacity at stationary and exponential growth phases for the differently aged clonal subpopulations (PPMCC r = 0.317, *p*-value > 0.05, n = 25).

6.4.5 Glycolytic reserve capacity

The glycolytic reserve is the difference between glycolytic capacity and basal glycolysis rate, and it represents the metabolic cellular capacity to increase the ATP production through glycolysis under sudden circumstances in which OXPHOS, the TCA cycle and/or the ETC are inhibited or down-regulated. This disruptive mitochondrial performance is commonly found in cancer cells as the result of the environmental stressors (e.g., hypoxia and elevated extracellular lactate) and/or by metabolic changes within cells (e.g., Warburg effect), therefore this reserve capacity is needed to avoid detrimental effects such as cell death (Das 2013). At first glance, significant differences between growth phases were observed (Figure 6-5B; two-way ANOVA, $p<0.0001$, F=46.42), with a moderate, but not significant, correlation between the glycolytic reserved capacity at both growth phases (Figure 6-5C; PPMCC r = 0.476, p-value < 0.05, n = 25). The comparison of the age of subpopulations (e.g., early, mid and late) revealed a significant decrease the reserve capacity in the late subpopulations, these findings strongly correlate with the decreases in basal glycolysis and maximal glycolytic capacity, suggesting that late subpopulations were not able to maintain the its ATP demand by switching to glycolysis and thus cells arrested their cellular metabolism in order to reduce their energetics demands and avoid detrimental effects such as cell death.

The glycolytic reserve analysis also demonstrated a large variability between subpopulations, with important differences between subpopulations with the lowest and highest reserved activities, being up to 1.55 and 15 fold changes at exponential and stationary growth phases, respectively. This comparison also revealed that the majority of proliferating cells did not present a glycolytic reserve or this was too low as exponential cells normally utilised the glycolysis, at their maximal capacity, as the main source of energy (Figure 6-5A). A completely different pattern was observed on stationary growth phase, in which all the subpopulations (except 12-late) presented an elevated glycolytic reserve. This switch from non-glycolytic reserve to glycolytic reserve presence, from the exponential to the stationary phase, corroborated our hypotheses from chapter 5, stating that proliferating populations preferred the inefficient, but faster aerobic glycolysis over the OXPHOS as the main source of energy and those non-proliferating populations reduce their metabolic demand and switched from strong aerobic glycolytic to a more efficient OXPHOS metabolism.
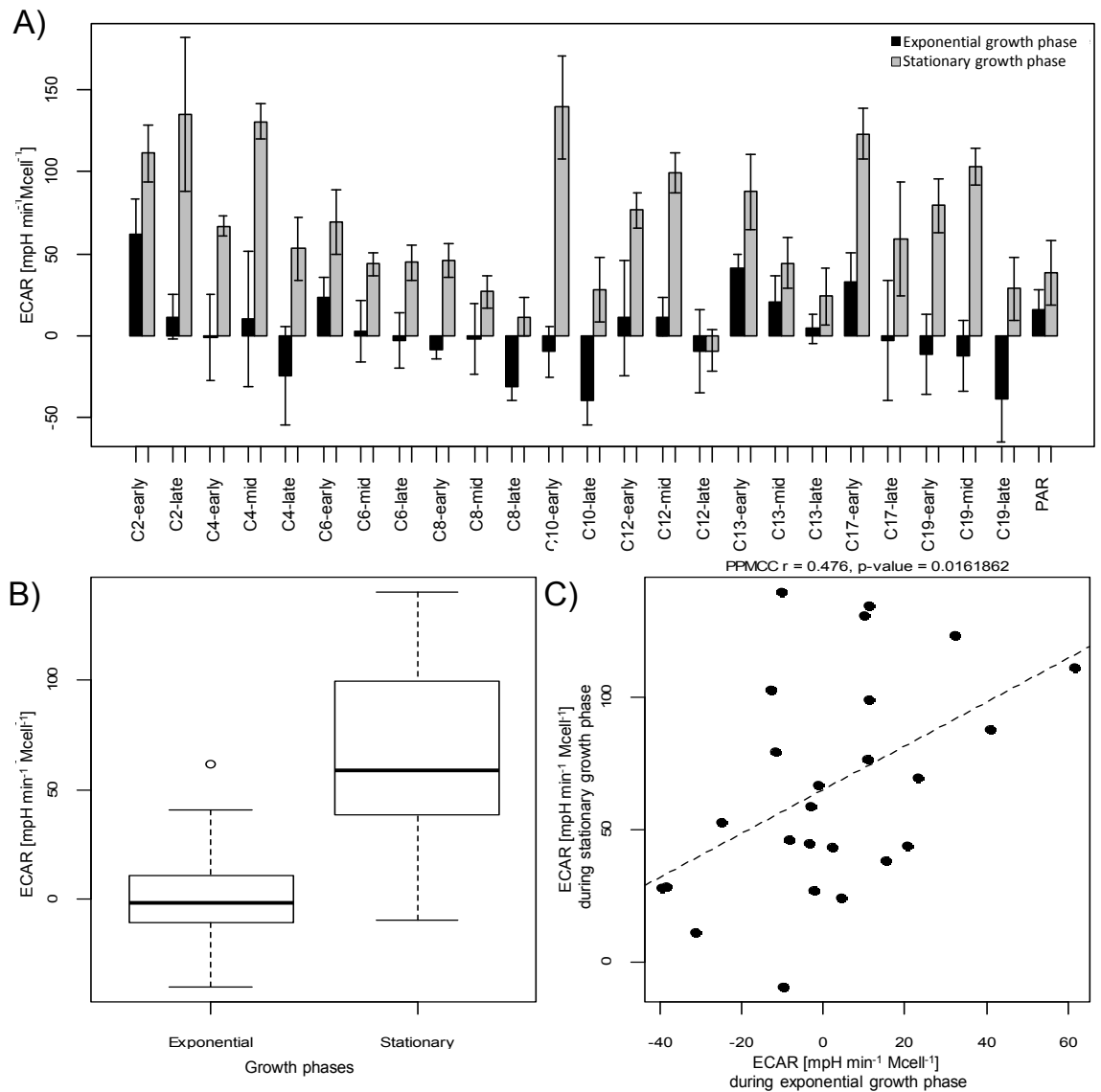
Figure 6-5 Analysis of the glycolytic reserve for 24 clonally-derived CHO-S subpopulations and the parental population during exponential and stationary growth phases. Cells were grown in fed-batch culture in CD CHO media supplemented with 8 mM L-glutamine and maintained at 37°C, 170 rpm, under 5% (v/v) CO_2 atmosphere until culture viabilities dropped below 60%, during the culture 10% (v/v) CHO CD EfficientFeed™ was fed at days 3, 5, 7 and 9. Early-, mid- and late-subpopulations generated from a long-term subculture regime, corresponding to generations 0, 80 and 200, respectively, were harvested and analysed using the cell metabolic analyser Seahorse XF24 at exponential (day 3) and stationary (day 7) growth phases. (A) Glycolytic reserve at exponential and stationary growth phases for the differently aged clonal subpopulations, (B) the global glycolytic reserve ECAR rates at the exponential and stationary growth phases and (C) the Pearson's correlation between glycolytic reserve ECAR at stationary and exponential growth phases for the differently aged clonal subpopulations (PPMCC r = 0.476, *p*-value < 0.05, n = 25).

6.4.6 Correlation in the glycolytic performance at exponential and stationary growth phases

In order to identify any relationship between the key glycolytic parameters presented above (sections 6.4.2 to 6.4.5), Pearson's correlation analyses were performed at both growth exponential and stationary phases (Figure 6-6). First, strong correlations between the glycolytic capacity and the basal glycolysis and between the glycolytic capacity and the glycolytic reserve were observed for the exponential growth phase data. However, no correlations between any of the parameters belonging to the glycolytic metabolism and the non-glycolytic metabolism were observed at this phase, suggesting that the elevated glycolytic phenotype in proliferating cells, also known as Warburg effect, strongly inhibited the PDH enzyme (Zhou et al. 2011) resulting in an inefficient shuttle of pyruvate into the TCA cycle, thus restricting carbonic acid production, which would normally acidify the media through non-glycolytic processes. I suggest that the Warburg effect in proliferating populations was responsible for the annulation of the potentially existing correlation between the glycolytic parameters and the non-glycolytic acidification. This hypothesis is supported by the fact that glucose metabolism normally produces acid molecules such as lactic acid through glycolysis and carbonic acid through the TCA cycle, in the last case causing the non-glycolytic acidification which should correlate with the glucose consumption (Newell et al. 1993).

To further support this hypothesis, the analysis of the stationary growth phase was performed in order to validate that cells with a restored pyruvic acid flux shuttle from glycolysis to the TCA cycle would exhibit an extent correlation between the glycolytic and non-glycolytic acidification. This analysis clearly demonstrates that both the parameters belonging to glycolysis and the non-glycolytic acidifications were correlated, supporting the hypothesis that the glycolytic and non-glycolytic acidification should exhibit some extent of correlation as the acid molecules results from the glucose metabolism. Moreover, It is important to emphasise that during the stationary phase cells re-established or at least increased their mitochondrial metabolism (see chapter 5) by increasing the pyruvate shuttle into the TCA cycle.

Finally, although the data here presented exhibits important correlations between glycolytic parameters when compared with the exponential and stationary phases, the comparisons made between both growth phases on sections 6.4.2 to 6.4.5 only showed modest correlations in non-glycolytic acidification and glycolytic reserve. This analysis strongly suggests that the glycolytic analysis performed at exponential growth phase cannot be employed to estimate their energetic metabolism on stationary phase, and vice versa, indicating a varied energetic demands that both growth phases.

Glycolytic activity at stationary growth phase
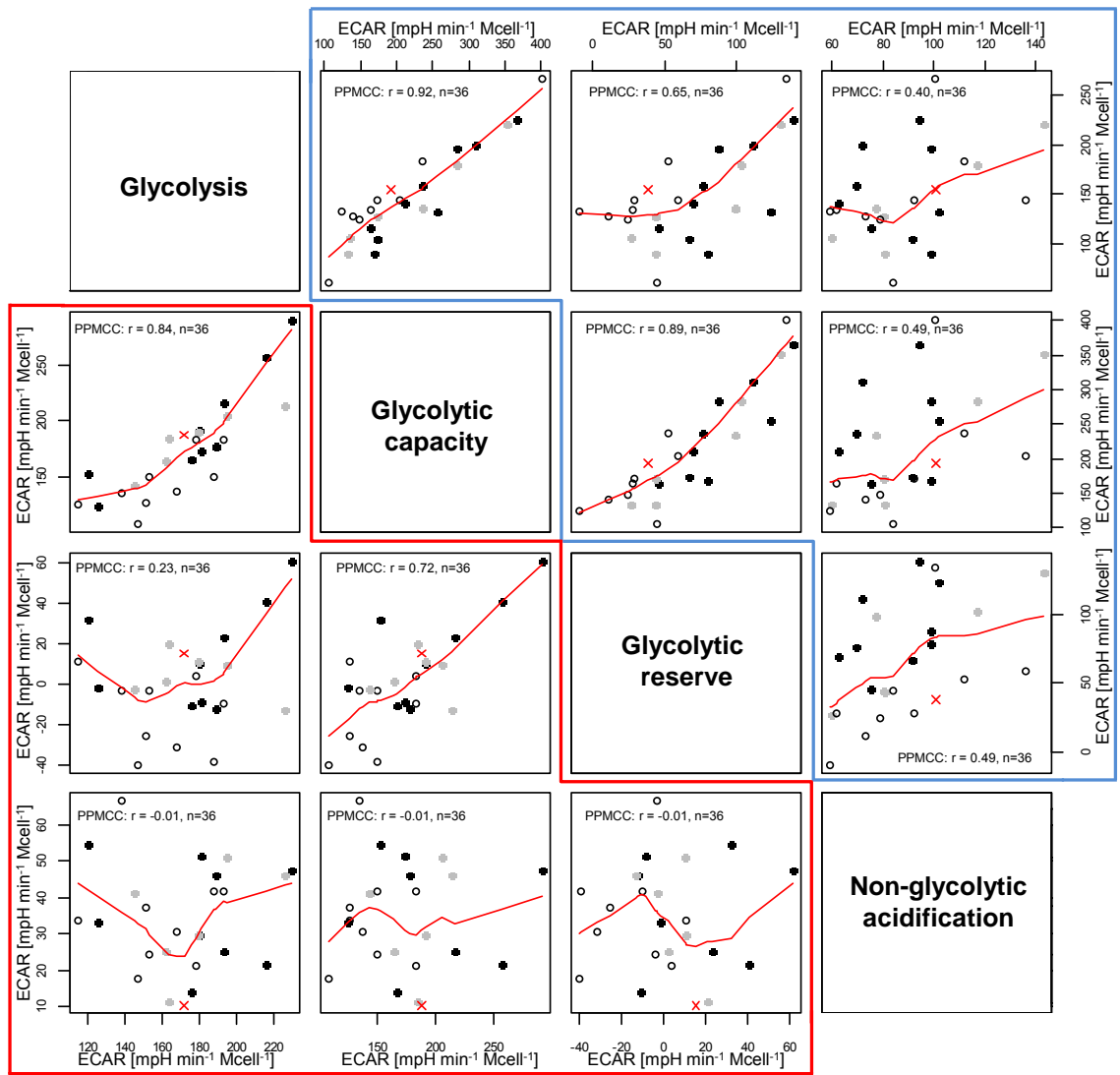
Glycolytic activity at mid-exponential growth phase

Figure 6-6 Pearson's correlation of the Global extracellular acidification rate (ECAR) profiles during the exponential and stationary growth phases for 24 clonally-derived CHO-S subpopulations and the parental line. The four key glycolytic parameters (i.e., non-glycolytic acidification, glycolysis, glycolytic capacity and spare glycolytic capacity) inside the red and blue figures correspond to the values collected during the exponential and stationary growth phases of the fed-batch, respectively. The black, grey and white circles represent the early, mid- and late-subpopulations generated for the clones through a long-term culture regime, respectively (i.e., generations 0, 80 and 200, respectively). The red "x" represents the parental population.

6.4.7 Analysis of the mitochondrial respiration among clonal CHO-S cell lines during exponential and stationary growth phase

In order to gain a major insight in the metabolic performance among the clonal populations, the mitochondrial oxidative capacity among clones, defined as respiration levels, were analysed in triplicate at mid-exponential and stationary growth phases using the cell metabolic analyser Seahorse XF24 which permits to quantify mitochondrial respiration by measurements of OCR. During the test, cells were maintained in un-buffered DMEM media to measure their basal oxygen consumption rates, followed by a sequential treatment with three mitochondrial inhibitors: (i) oligomycin (final concentration 1.0 µM) an ATP synthase inhibitor which blocks the ATP production and discloses the respiration non-associated to ATP, (ii) FCCP (final concentration 1.25 µM) a proton ionophore and ETC accelerator which depolarises the mitochondrial membrane potential and increases the cellular oxygen consumption revealing the maximal respiratory capacity and (iii) rotenone & antimycin A (final concentration 1.0 µM) inhibitors of ETC at complex I and III, respectively, which stop the mitochondrial respiration an exposes the non-mitochondrial OCR (Figure 6-7). For improving the mitochondrial metabolic analysis, the concentration of oligomycin, FCCP and rotenone & antimycin A were optimised to ensure a complete inhibition of its target and reduce their toxic effects during the test (e.g., cell death). For each inhibitor, the selection of the optimal concentration consisted in testing six different concentrations (i.e., 0, 0.25, 0.50, 0.75, 1.00 and 1.25 µM) and measuring the basal OCR and ECAR before and after the treatment. The lower concentration of each inhibitor that supported the highest effects on OCR and ECAR was selected as the optimal concentration for the mitochondrial analysis.

The previous metabolic studies performed among the clones (see chapter 5) demonstrated large differences in glucose metabolism among clones indicating an incomplete glucose oxidation. To evaluate if this metabolism was related to the mitochondrial dysfunction, comparisons among clones at exponential (Figure 6-7A) and stationary (Figure 6-7B) growth phases were performed, observing a large variability in the mitochondrial activity among clones along the test. This first part of the analysis consisted in evaluating the global mitochondrial performance for the clones, observing that in general they presented higher mitochondrial activity at stationary phase (up to 1.52 fold change using the global performance among the clones). This metabolic behaviour seems to be closely linked to biomass synthesis, suggesting that proliferating cells prefer to utilise glycolysis as the main source of energy (see 6.4.1).
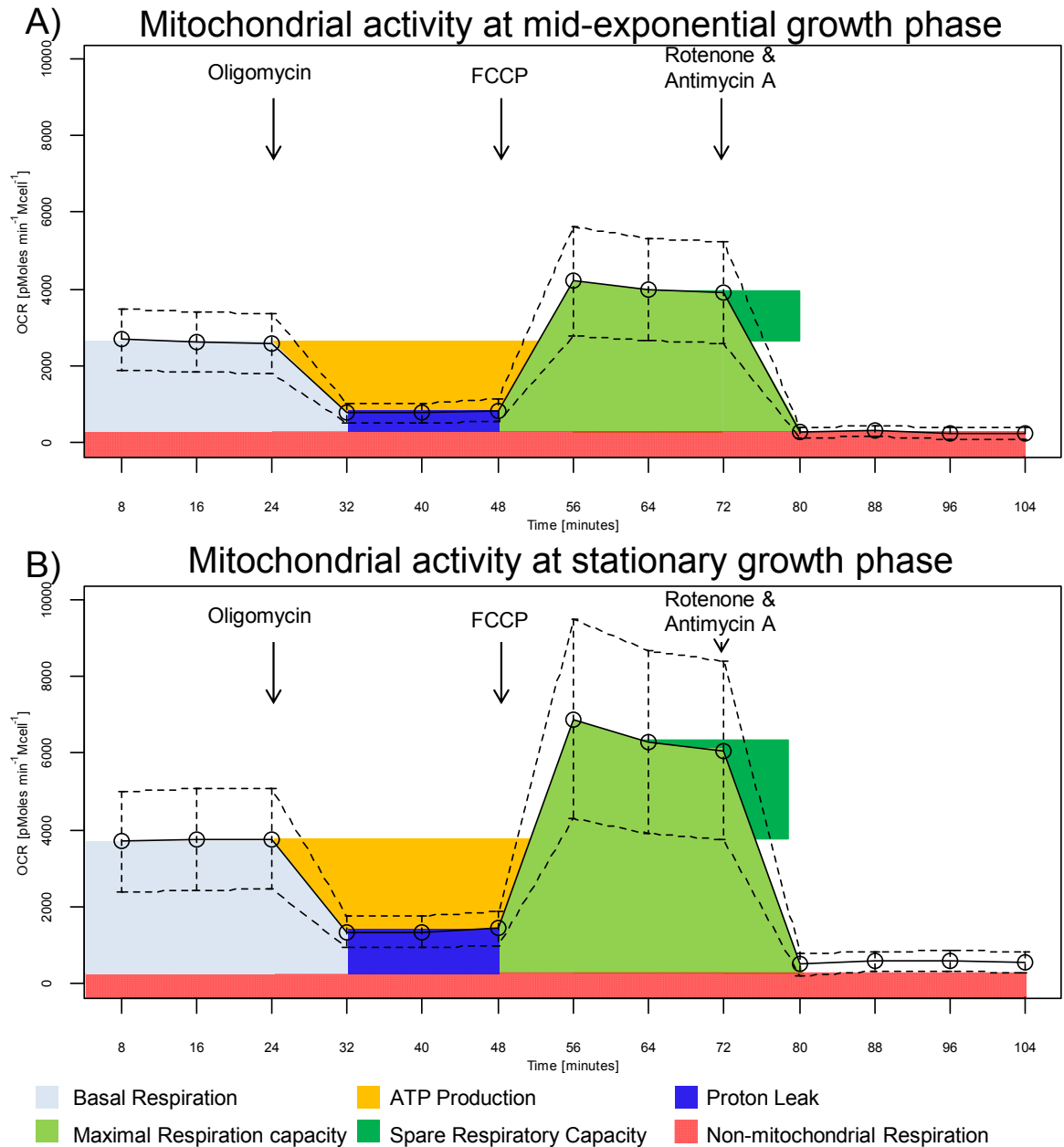
Figure 6-7 Global oxygen consumption rate (OCR) profiles during the exponential and stationary growth phases for 35 clonally-derived CHO-S subpopulations and the parental line. For each clone, cell samples at (A) exponential growth phase (day 3) and (B) stationary growth phase (day 7) were harvested and analysed using the cell metabolic analyser Seahorse XF24. During the test cells were maintained in un-buffered DMEM and triplicate measurements of the basal OCR were obtained, followed by triplicate measurements of OCR after injection of each of the following mitochondrial inhibitors: oligomycin, FCCP and rotenone & antimycin A, used for measuring the OCR resulted form the proton leak, the maximal respiratory capacity and the non-mitochondrial OCR, respectively. The circles represent the average of 35 differently aged clonal subpopulations and the superior and inferior dotted lines represent the SD.

Analysing the global data in detail, it is observed that stationary cells responded differently to the inhibitor treatments (Figure 6-7A-B), showing that in general cell at stationary phase increased their basal respiration and their oxygen consumption after the Oligomycin, FCCP and Rotenone & Antimycin A treatments when compared to OCR responses at exponential growth phase.

To analyse in more detail the mitochondria activity, the functional mitochondrial parameters (i.e., non-mitochondrial, basal, ATP linked, proton leak and maximal respiration, and the spare respiratory capacity) described in Figure 6-7 were calculated for both stationary and exponential growth stages and analysed in detail in the next sections (see section 6.4.8 to 6.4.13), but here the global behaviour among clones was analysed to identify the principal mitochondrial differences. Interestingly, clones increased all their respiratory parameters at stationary stage, from those non-related to mitochondrial activity (e.g., non-mitochondrial respiration) to those parameters associated with the mitochondria integrity (e.g., basal and maximal respiration, respiration coupled to ATP production and linked to proton leakage, and the spare respiratory capacity). In general, clones at stationary phase increased 34% their basal respiration, 55% the maximal respiration and 91% their spare respiratory capacity, as well as showed a 29% higher respiration associated to ATP production which suggested that clones depended less on aerobic glycolysis to survive (Figure 6-7B).

It can be observed that the significant increments in the spare respiratory capacity at stationary growth phase were the result of the notable improvement at the maximal respiration, which interestingly was 55% higher than for exponential cells. These differences between both growth phases may suggest that (i) proliferating cells present a down-regulated ETC pathway as they did not exhibit similar levels of OCR to those of the stationary cells when the respiration was uncoupled using FCCP or (ii) that cells increased the mitochondria content within the stationary phase in order to meet their energetic demands. Another important characteristic in mitochondrial metabolism was observed as a 50% increment in the OCR linked to proton leak from exponential to stationary growth phase. Proton leak is a respiratory measure that is not coupled to ATP production and an elevated leakage indicated that cells were more permeable to protons across the IMM, probably resulted from oxidative damage in the IMM (Kokoszka et al. 2001).

Together, this data exhibited that the mitochondrial metabolism at stationary growth phase was more active, suggesting that cells rely on aerobic glycolysis for meeting their ATP demands during proliferation and then switch to OXPHOS when they have reached the stationary growth phase. This hypothesis is corroborated as

they notably increased their respiratory activity associated with ATP production (Figure 6-7B). Additionally, the observed increments in proton leakage indicated a potential damage in mitochondrial membranes (i.e., mitochondrial inner membrane) during the stationary phase probably resulted from the high oxidative stress and by-product accumulation in the culture environment (Kokoszka et al. 2001).

6.4.8 Non-mitochondrial respiration

The total oxygen consumption within cells is the result of mitochondrial and non-mitochondrial activity. To identify and compare the mitochondrial functionality among cells it is important to identify and remove this inherent non-mitochondrial OCR activity. The non-mitochondrial respiration was assessed through the total inhibition of OXPHOS and the ETC by combining the effects of oligomycin, FCCP and rotenone & antimycin A (Figure 6-7). The residual OCR observed after the treatment was defined as non-mitochondrial respiration and compared between subpopulations (Figure 6-8A). At first glance, it was observed significant differences between growth phases (Figure 6-8B; two-way ANOVA, $p<0.0001$, F=40.36) with no significant correlation between the stationary and exponential growth phases (Figure 6-8C; PPMCC r = 0.025, p-value > 0.05, n = 36). This data also revealed significant differences between subpopulations with the lowest and highest OCR activities, being up to 24.5 and 10.5 fold changes at exponential and stationary growth phases, respectively.

Analysing in detail the subpopulations, it can be observed that the subpopulations tend to decrease their non-mitochondrial respiration in their late-stage of the long term-cultivation, whereas non-significant differences along the long-term were observed at stationary growth phase. This slightly reduction in non-mitochondrial activity observed on late-generations seems to be associated with a reduction in the cytosolic oxidase activity such as NADH oxidase, which under aerobic glycolysis is employed to restore the levels of NAD+/NADH and maintain the ATP production via glycolysis.

In Figure 6-8A is exhibited that 31 out of 35 subpopulations increased their non-mitochondrial respiratory activity from the exponential to stationary growth phase, with increments between 1.12 and 5.68 fold changes. From the remaining 5 subpopulations, C6-early and C12-mid had no significant differences between growth phases, whereas C8-early, C8-mid and C11-mid displayed significant decrements at stationary phase (up to 76%). An interesting behaviour was observed in clone 11 at mid-subpopulations, exhibiting the lowest levels at both stages. Although, at first glance this low activity may seem the result from an experimental error, the use of appropriate controls and the analysis repetition at separated days corroborated the findings.
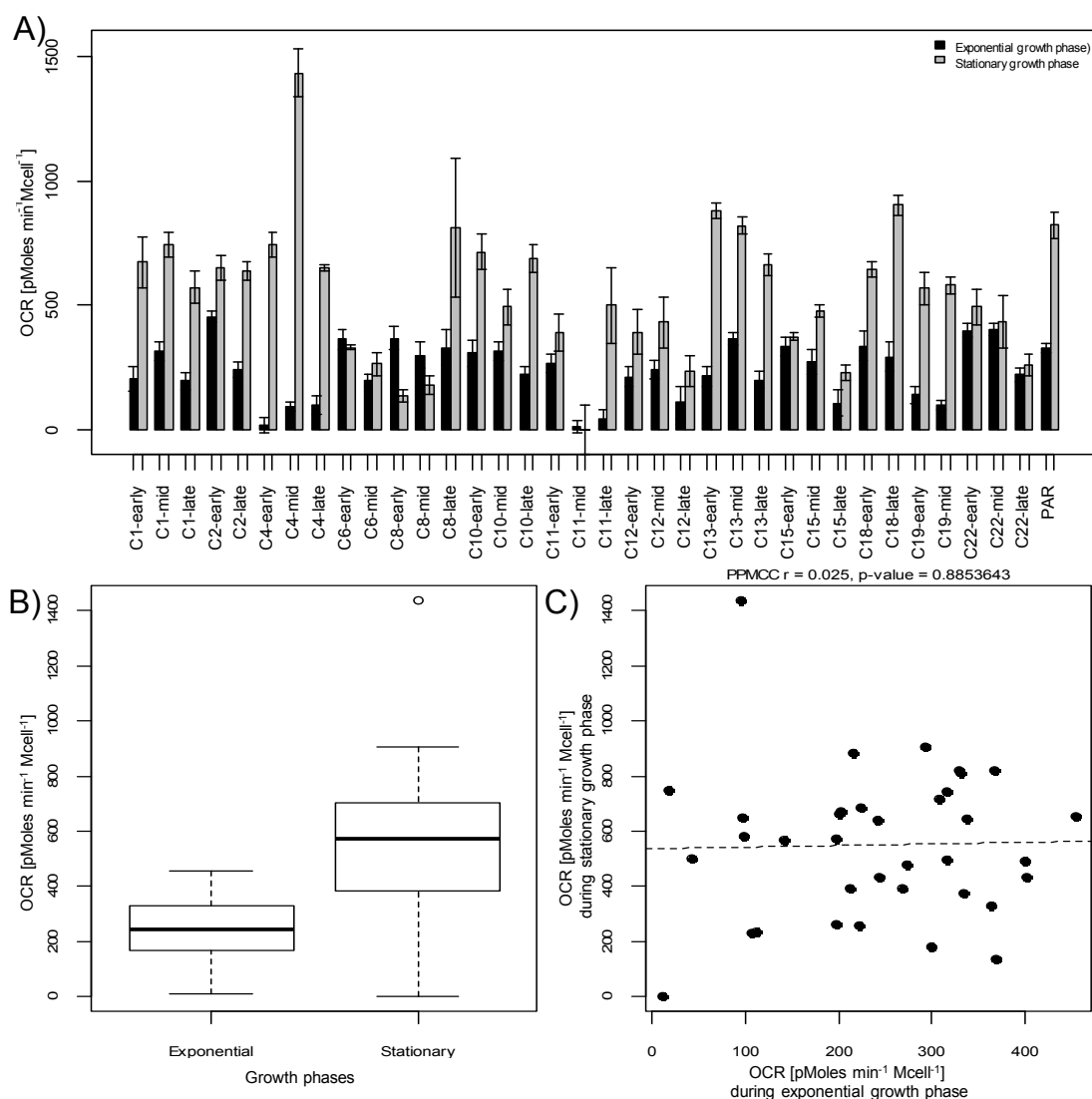
Figure 6-8 Analysis of the non-mitochondrial activity for 35 clonally-derived CHO-S subpopulations and the parental population during exponential and stationary growth phases. Cells were grown in fed-batch culture in CD CHO media supplemented with 8 mM L-glutamine and maintained at 37°C, 170 rpm, under 5% (v/v) CO_2 atmosphere until culture viabilities dropped below 60%, during the culture 10% (v/v) CHO CD EfficientFeed™ was fed at days 3, 5, 7 and 9. Early-, mid- and late-subpopulations generated from a long-term subculture regime, corresponding to generations 0, 80 and 200, respectively, were harvested and analysed using the cell metabolic analyser Seahorse XF24 at exponential (day 3) and stationary (day 7) growth phases. (A) The non-mitochondrial OCR at the exponential and stationary growth phases for the differently aged clonal subpopulations, (B) the global non-mitochondrial OCR at the exponential and stationary growth phases and (C) the Pearson's correlation between non-mitochondrial OCR at stationary and exponential growth phases for the differently aged clonal subpopulations (PPMCC r = 0.025, *p*-value > 0.05, n = 36).

The notable OCR variability among clones suggests significant differences in cytosolic oxidase activity. In fact, elevated activities of these oxidase families (e.g., 2-oxoglutarate dependent oxygenase and NADPH oxidases families) have been associated to cancer mechanisms as they catalyse oxidative reactions at proteomic and genomic level (Rose et al. 2011; Tarhonskaya et al. 2014), and also have been linked to elevated oxidative stress (Qutub and Popel 2008). Therefore, it can be suggested that the observed increment in non-mitochondrial activity at stationary phase was the result of the elevated cytosolic oxidase activity triggered from the environmental stress encountered at stationary phase.

6.4.9 Basal mitochondrial respiration

The basal mitochondrial respiration represents the normal mitochondrial status of cells as the result of the ATP production and the proton leak across the IMM. The analysis exhibited significant differences between exponential and stationary growth phases (Figure 6-9B; two-way ANOVA: $p<0.0002$, F=15.57) without any significant correlation between both growth phases (Figure 6-9C; PPMCC r = -0.072, p-value > 0.05, n = 36). The analysis of the age of subpopulations (e.g., early, mid and late) showed that over increased generations the cells tend to reduce their basal mitochondrial respiration. This findings seems to be closely related to the observed reductions in cellular content along increased generations, measured as cell diameter cell diameter (see chapter 4), resulting in lower the ATP requirements for cell biomass production and maintenance.

The mitochondrial activity data presented here can also be classified in three groups. The first including those subpopulations that decreased their basal respiration from the exponential to stationary growth phase (7 out of 36 subpopulations; C6-early, C8-early, C8-mid, C15-early, C15-mid, C15-late and C18-early), the second group characterised by subpopulations with no-significant changes (6 out of 36 subpopulations; C8-late, C12-early, C13-late, C18-late, C19-early and C19-mid) and the third group that account for the majority of the clones with significant improvements in basal respiration at the stationary phase ranging between 31% to up to 197% (Figure 6-9A). From this classification, groups one and two, but specially clones 8, 15 and 18 and 19 represent those subpopulations that probably rely on aerobic glycolysis along the culture, whereas clones from the group three suggest that they switched from aerobic glycolysis to mitochondrial metabolism at stationary phase.
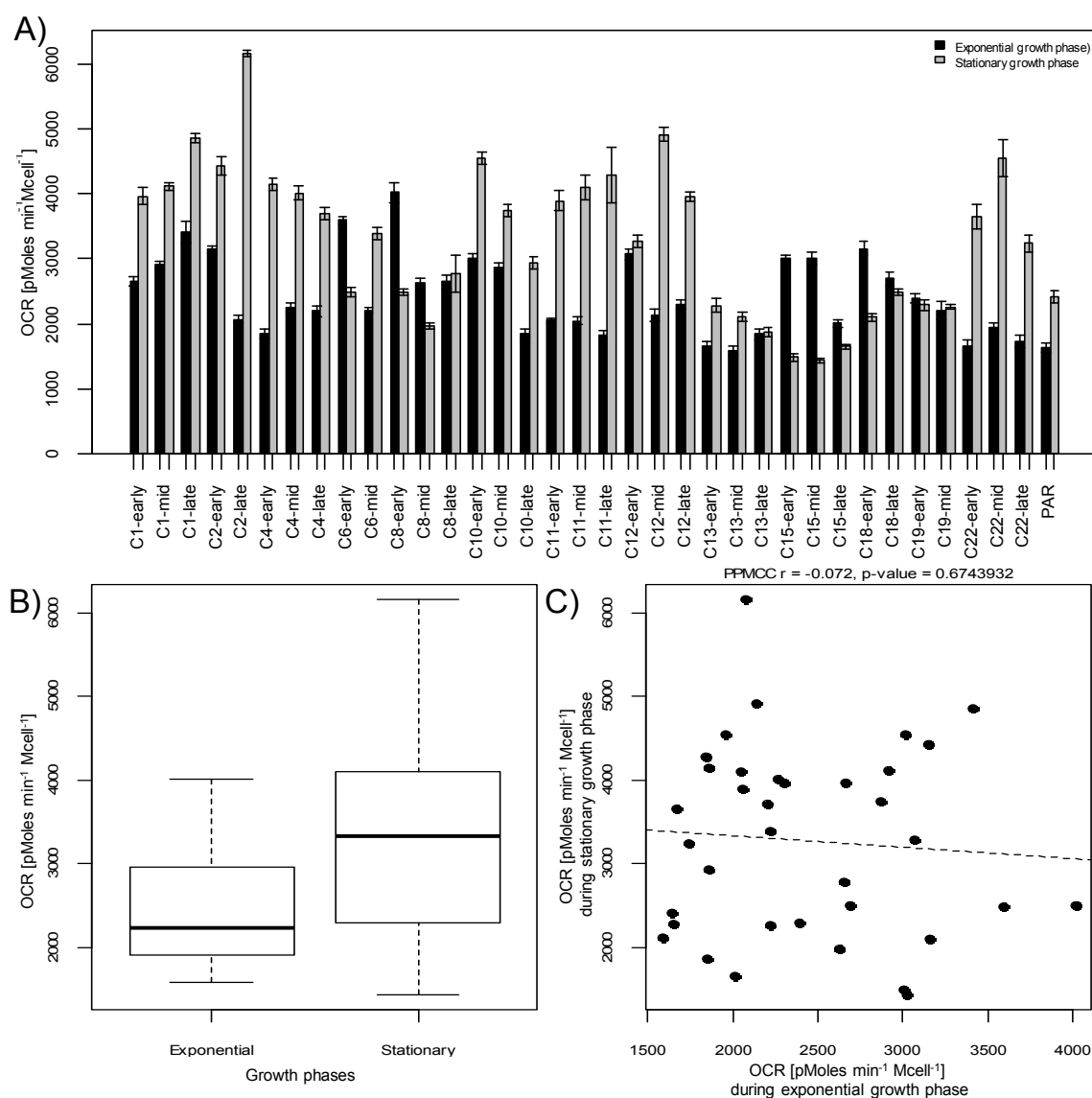
Figure 6-9 Analysis of the basal respiration activity for 35 clonally-derived CHO-S subpopulations and the parental population during exponential and stationary growth phases. Cells were grown in fed-batch culture in CD CHO media supplemented with 8 mM L-glutamine and maintained at 37°C, 170 rpm, under 5% (v/v) CO_2 atmosphere until culture viabilities dropped below 60%, during the culture 10% (v/v) CHO CD EfficientFeed™ was fed at days 3, 5, 7 and 9. Early-, mid- and late-subpopulations generated from a long-term subculture regime, corresponding to generations 0, 80 and 200, respectively, were harvested and analysed using the cell metabolic analyser Seahorse XF24 at exponential (day 3) and stationary (day 7) growth phases. (A) The basal respiration at the exponential and stationary growth phases for the differently aged clonal subpopulations, (B) the global basal respiration at the exponential and stationary growth phases and (C) the Pearson's correlation between the basal respiration OCR at stationary and exponential growth phases for the differently aged clonal subpopulations (PPMCC r = -0.072, *p*-value > 0.05, n = 36).

6.4.10 Proton Leak

The proton leak is a normal process in the mitochondria, studies estimate that proton leak represents around 20 to 30% of the mitochondrial respiration (Jastroch et al. 2010). However, elevated proton leak activity has been associated to damage in IMM resulted from ROS species (Kokoszka et al. 2001). To test for changes in the mitochondrial integrity of the clones from exponential to stationary growth phase, the OCR associated to proton leakage was calculated by subtracting the non-mitochondrial respiration from the OCR value resulted from the oligomycin treatment (Figure 6-10). This analysis showed significant differences along the growth phases (Figure 6-10B; two-way ANOVA, $p<0.0001$, F=20.5), exhibiting an increment in the proton leakage at stationary phase without any significant correlation between both growth phases (Figure 6-10C; PPMCC r = 0.185, p-value > 0.05, n = 36). The data also allowed us to measure the large variability at stationary phase, with up to 7.9 fold differences, between those subpopulations with the lowest and the highest OCR activities, corresponded to subpopulations C4-mid and C1-early, respectively.

Analysing in more detail the subpopulations, it can be observed that the subpopulations tend to reduce their proton leakage along the long term-cultivation whereas non-significant differences can be observed at stationary growth phase. The behaviour observed at exponential phase seem to indicate that populations tend to evolve a better mitochondrial function as low proton leakage means lower mitochondrial membrane damage and better strategies to alleviate the oxidative stress. Unfortunately, no changes in proton leakage was observed at stationary phase over increasing generation mainly because during the evolution process clones were not grown to reach this growth phase, thus they never encounter this common environmental stressor (e.g., nutrient depletion and high osmolarity) which could be resulted in elevated mitochondrial integrity at stationary growth phase.

The proton leak analysis also revealed that the majority of the cells tended to increase their proton leak activity at stationary phase, suggesting inferior mitochondrial membrane integrity probably resulted from the elevated environmental stress at stationary phase (e.g., lactate and ammonia build-up and high osmolarity). To test whether the proton leak activity was the result of an abnormal mitochondrial metabolism, OCR resulted from proton leakage was compared with the basal respiration. These comparisons indicated that during the exponential growth phase the OCR values for proton leakage represented between 15 and 30% of the basal mitochondrial respiration, being normal levels proton leak activity.
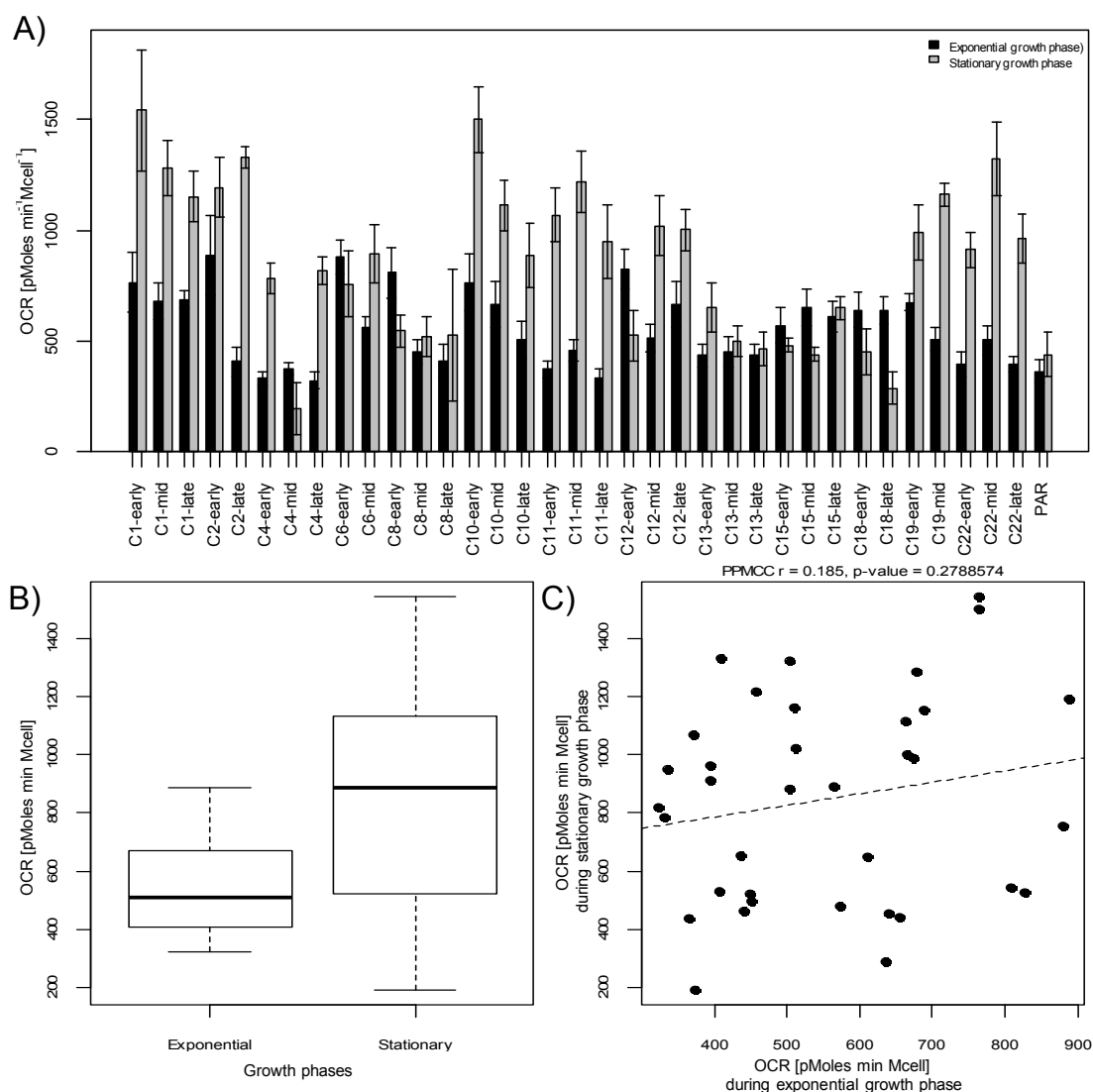
Figure 6-10 Analysis of the oxygen consumption activity resulted from proton leakages across the IMM for 35 clonally-derived CHO-S subpopulations and the parental population during exponential and stationary growth phases. Cells were grown in fed-batch culture in CD CHO media supplemented with 8 mM L-glutamine and maintained at 37°C, 170 rpm, under 5% (v/v) CO_2 atmosphere until culture viabilities dropped below 60%, during the culture 10% (v/v) CHO CD EfficientFeed™ was fed at days 3, 5, 7 and 9. Early-, mid- and late-subpopulations generated from a long-term subculture regime, corresponding to generations 0, 80 and 200, respectively, were harvested and analysed using the cell metabolic analyser Seahorse XF24 at exponential (day 3) and stationary (day 7) growth phases. (A) The proton leakage OCR activity at the exponential and stationary growth phases for the differently aged clonal subpopulations, (B) the global oxygen consumption associated to proton leakage at the exponential and stationary growth phases and (C) the Pearson's correlation between OCR values for proton leak at stationary and exponential growth phases for the differently aged clonal subpopulations (PPMCC r = 0.185, *p*-value > 0.05, n = 36).

A similar analysis was performed using the stationary growth data observing slightly increments in the contribution of the proton leak to the basal mitochondrial respiration. This finding seem to suggests a marginally reduction in the mitochondria integrity in the non-growing populations as the result of the elevated environmental stress found at this stages of the culture.

From the panel of 35 subpopulations, seven subpopulations (C1-Early, C1-Mid, C10-Early, C15-Early, C15-Late, C19-Early and C19-Mid) showed an abnormally proton leak activity at stationary phase which probably resulted from a severe mitochondrial damage. A contrary effect was observed in eight subpopulations (i.e., C4-mid, C6-early, C8-early, C12-early, C15-early, C15-mid, C18-early and C18-late) in which decreases their proton leakage activity at stationary phase, but from these subpopulations the C6-early, C8-early, C15-early, C15-mid and C18-early slightly increased their proton leak contribution to the basal respiration without reach abnormal levels.

6.4.11 ATP turnover

The ATP is the principal energetic molecule for biological reactions within organisms. It is generated by electrochemical proton gradient across the mitochondrial membrane, which is coupled to oxygen reduction in complex IV of the ETC, via OXPHOS (Koopman et al. 2013). The ATP turnover represents the OCR associated to ATP production, indicating the ATP activity within the cells at that specific moment. To evaluate the ATP capacity among cells, the OCR ATP turnover value was calculated by subtracting the proton leak OCR value from the basal respiration (Figure 6-11). The data showed significant differences between the exponential and stationary growth phases (Figure 6-11B; two-way ANOVA, $p<0.003$, $F=10.03$) without any significant correlation between both growth phases (Figure 6-11C; PPMCC $r = -0.052$, p-value $>$ 0.05, n = 36). Moreover, this data allowed us to measure the large variability at exponential and stationary phase being up to 2.8 and 4.9 fold changes, respectively, between those subpopulations with the lowest and the highest OCR activities (Figure 6-11A).

Further analysis, indicated that proliferating cells tend to reduce their OCR related to ATP activity along increasing generation clones, whilst no changes at stationary phase were observed. The findings at exponential phase may be the result of a decrease in ATP demands as along increasing generations cells reduced their cell volume.
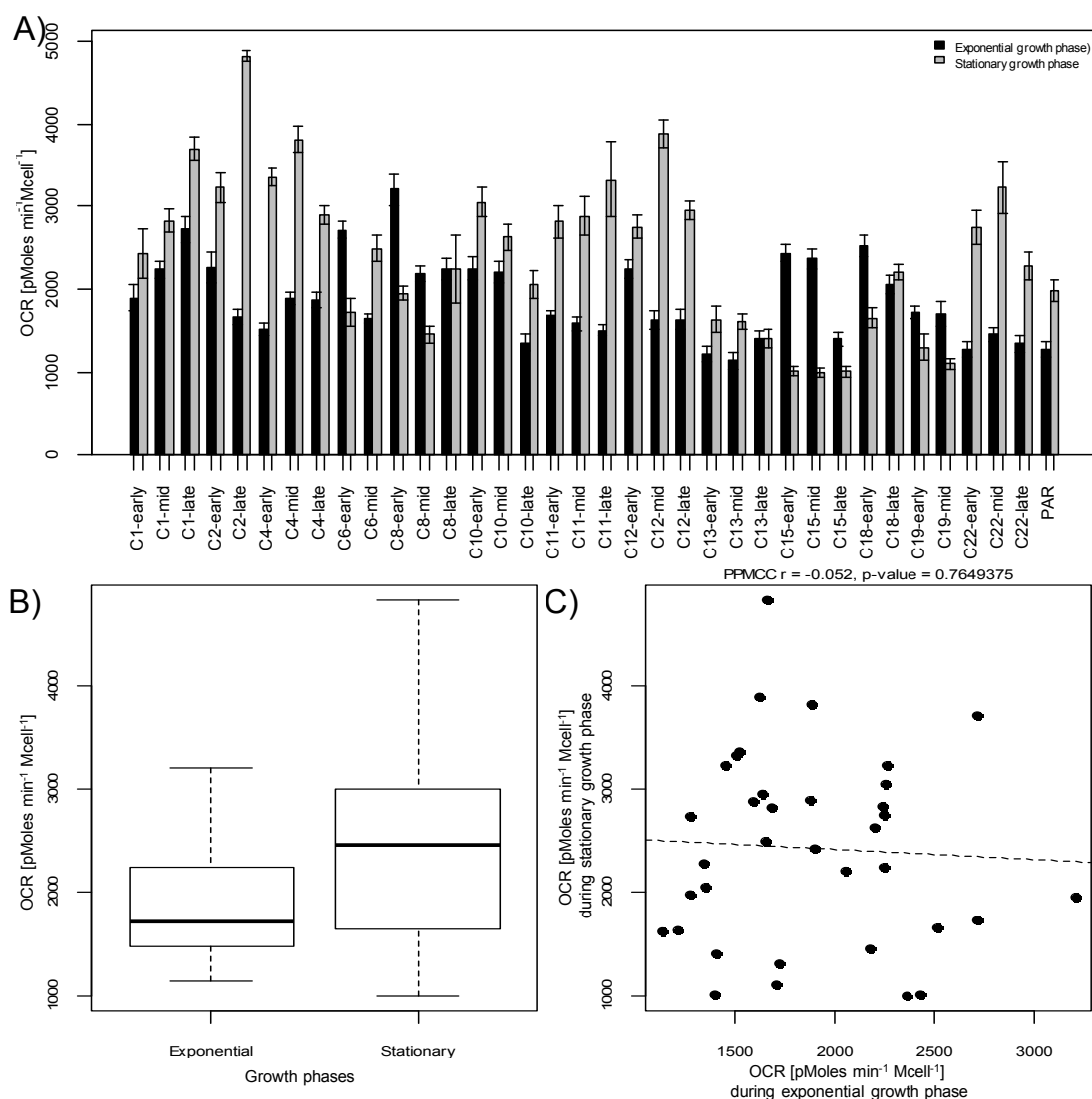
Figure 6-11 Analysis of the respiration activity associated to ATP production for 35 clonally-derived CHO-S subpopulations and the parental population during exponential and stationary growth phases. Cells were grown in fed-batch culture in CD CHO media supplemented with 8 mM L-glutamine and maintained at 37°C, 170 rpm, under 5% (v/v) CO_2 atmosphere until culture viabilities dropped below 60%, during the culture 10% (v/v) CHO CD EfficientFeed™ was fed at days 3, 5, 7 and 9. Early-, mid- and late-subpopulations generated from a long-term subculture regime, corresponding to generations 0, 80 and 200, respectively, were harvested and analysed using the cell metabolic analyser Seahorse XF24 at exponential (day 3) and stationary (day 7) growth phases. (A) The respiration associated to ATP activity at the exponential and stationary growth phases for the differently aged clonal subpopulations, (B) the global respiration associated to ATP production at the exponential and stationary growth phases and (C) the Pearson's correlation between the OCR's ATP production at stationary and exponential growth phases for the differently aged clonal subpopulations (PPMCC r = -0.052, *p*-value > 0.05, n = 36).

The significant increment in the OCR activity related to ATP production at stationary growth phase confirmed that the majority of the clones increased their ATP production via OXPHOS at stationary phase, between 19 and 190% compared with their exponential phase values, supporting the hypothesis that non-proliferating cells exhibited a switch from an inefficient aerobic glycolysis to an efficient mitochondrial metabolism. This analyses also showed that C8-late, C13-late, C18-late did not exhibit notable changes, whereas C6-early, C8-early, C8-mid, C15-early, C15-late, C15-mid, C18-early, C19-early and C19-mid reduced from 24 to 58% their OCR ATP turn over. These latter subpopulations were also associated with decreased basal respiration and with increments of proton leak contribution to the basal respiration, confirming that these cells may have mitochondrial damage.

6.4.12 Maximal respiration

The analysis of the maximal respiration represents the greatest mitochondrial capacity at that specific moment, it results from the depolarisation of the mitochondrial membrane potential by FCCP which induced an increase in cellular oxygen consumption maintaining the mitochondrial membrane potential (Desquiret et al. 2006; Park et al. 2002). To identify the maximal respiratory capacity among clones this value was calculated by subtracting the rotenone and antimycin A OCR value from the FCCP treatment OCR value (Figure 6-12). As expected this analysis exhibited significant differences between exponential and stationary growth phases (Figure 6-12B; two-way ANOVA, $p<0.0001$, F=26.97) with no significant correlation between them (Figure 6-12C; PPMCC r = -0.092, p-value > 0.05, n = 36). These comparisons also exhibited a large variability among clones, with up to 3.6 and 4.9 fold differences between the lowest and the highest OCR activity at exponential and stationary growth phases, respectively.

As observed in basal respiration, proton leak and ATP turnover, a negative trend was observed with increasing generation number, the reduction in the maximal respiratory capacity seems to be the result of a down-regulation of the mitochondrial activity, probably resulted from the activation of different isoforms of ETC proteins with an reduced activity (e.g., complex IV). Different authors have describe that long-term regulators of the OXPHOS modulate the maximal capacity by promoting the expression of different isoforms of mitochondrial proteins with varied activity (Desler et al. 2012), indicating that this mechanisms are essential for the setting of the maximal respiratory capacity.
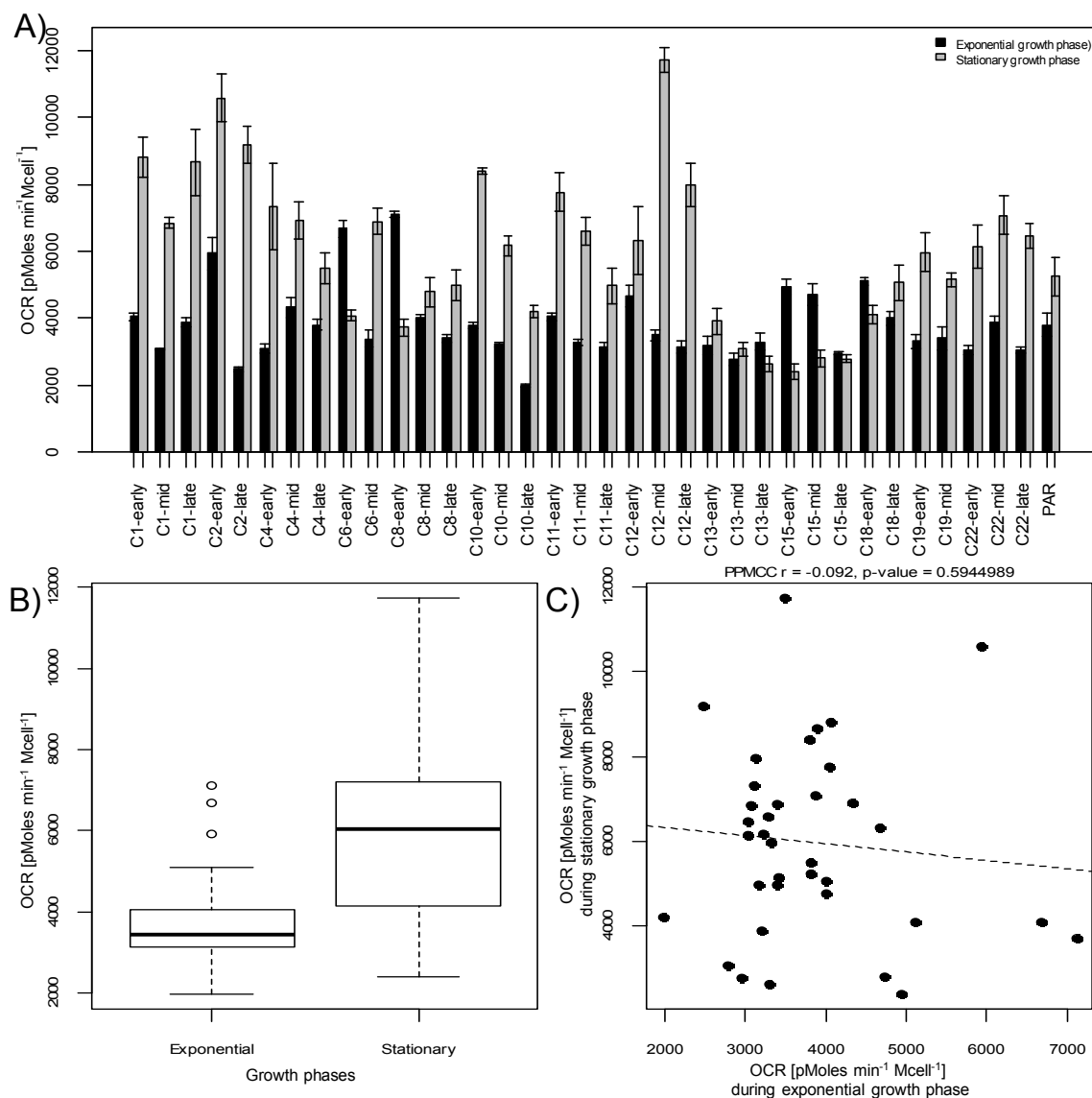
Figure 6-12 Analysis of the maximal respiration activity for 35 clonally-derived CHO-S subpopulations and the parental population during exponential and stationary growth phases. Cells were grown in fed-batch culture in CD CHO media supplemented with 8 mM L-glutamine and maintained at 37°C, 170 rpm, under 5% (v/v) CO_2 atmosphere until culture viabilities dropped below 60%, during the culture 10% (v/v) CHO CD EfficientFeed™ was fed at days 3, 5, 7 and 9. Early-, mid- and late-subpopulations generated from a long-term subculture regime, corresponding to generations 0, 80 and 200, respectively, were harvested and analysed using the cell metabolic analyser Seahorse XF24 at exponential (day 3) and stationary (day 7) growth phases. (A) The maximal respiration activity at the exponential and stationary growth phases for the differently aged clonal subpopulations, (B) the global maximal respiration at the exponential and stationary growth phases and (C) the Pearson's correlation between the maximal respiration activity at stationary and exponential growth phases for the differently aged clonal subpopulations (PPMCC r = -0.092, *p*-value > 0.05, n = 36).

172

The analysis of this variable was peculiar due to the large differences between exponential and stationary growth phases, before performing the mitochondrial assay, it was expected to obtain similar values at both stages due the short time-periods between this growth phases, but the measurements showed that clones notably increased their maximal mitochondrial machinery at the stationary phase. The significant differences at both growth phases may be linked to short and that long-term regulators of the OXPHOS which module the mitochondrial capacity by promoting the expression of different isoforms of mitochondrial proteins with varied activity (Desler et al. 2012). This analyses also showed that from the subset of subpopulations only C15-late not exhibited significant differences between both phases whereas C6-early, C8-early, C13-late, C15-early and C15-mid and C18-early revealed a notable decrease at stationary phase, between 19 and 51%. As observed with the previous parameters, these 6 subpopulations also had inferior mitochondrial performances at stationary phase, thus probably denoting mitochondrial membrane damage.

6.4.13 Spare respiratory capacity

Under diverse circumstances cells are continuously exposed to unpredictable metabolic and environmental stressors that demand an unexpected increase in their energetic levels to avoid detrimental effects such as cell death. The ability to respond satisfactorily to stressors has been associated with elevated reserve respiratory capacity, which is described as the additional ATP that can be generated by OXPHOS in case of metabolic stress (Desler et al. 2012). The calculation of the spare respiratory capacity or reserve respiratory capacity consisted in subtracting the basal respiration from the maximal respiration. This analysis revealed significant differences between subpopulations with up to 23.6 and 9.8 fold differences between the lowest and the highest OCR activity at exponential and stationary growth phases, respectively (Figure 6-13A). The data also showed significant differences between growth phases (Figure 6-13B; two-way ANOVA, $p<0.0001$, F=25.07) with no significant correlation between the behaviour at both growth phases (Figure 6-13C; PPMCC r = -0.029, p-value > 0.05, n = 36). The comparison of the age of subpopulations (e.g., early, mid and late) revealed a decrease the reserve respiratory capacity over increasing generations, which correlate with the decreases observed in maximal and basal respiration. This suggests that over course of the long-term cultivation cells reduced their capacity to sudden increase their energetic levels, thus decreasing the chances to avoid detrimental pathologies associates with aging and cell death.
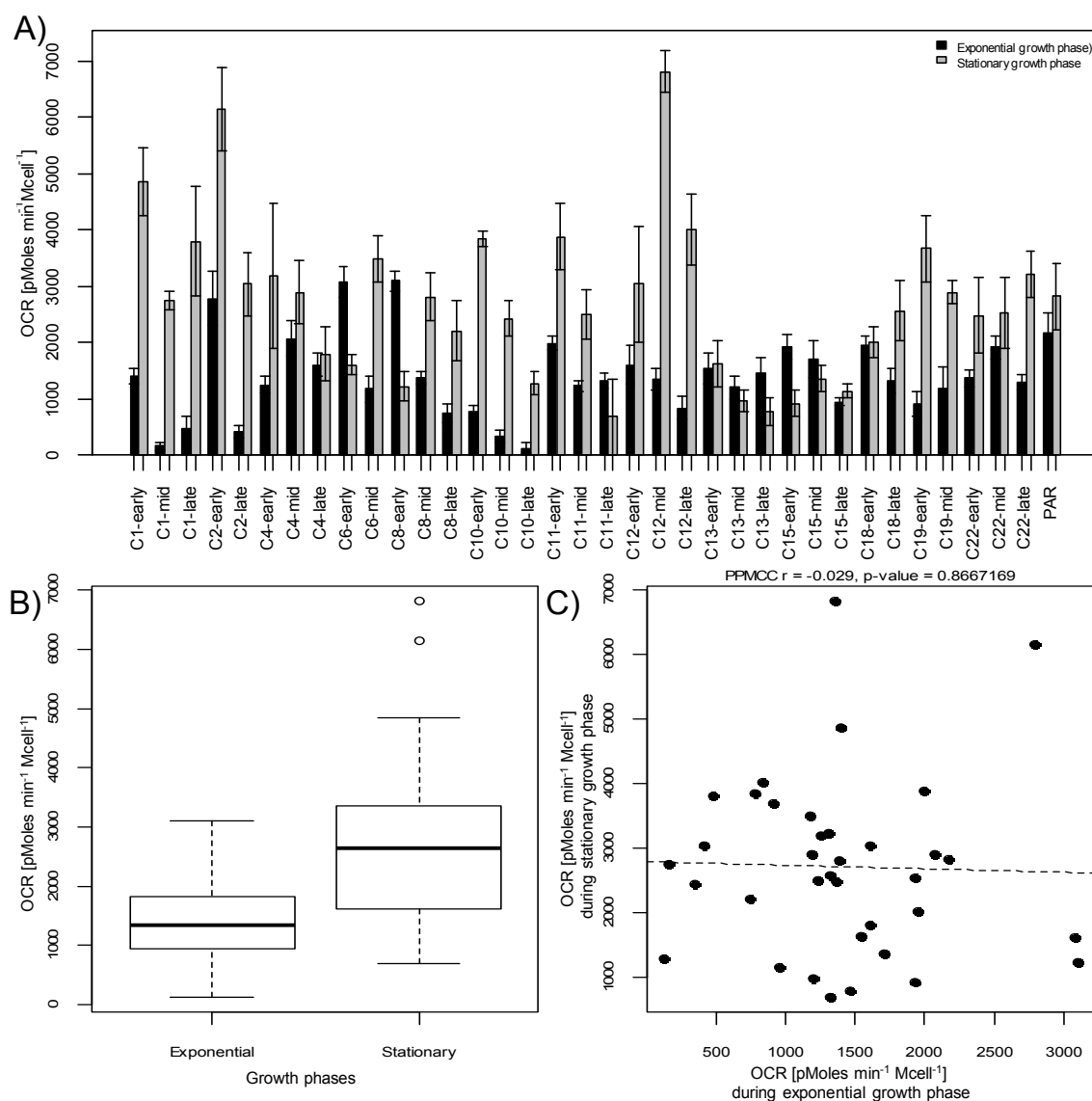
A)

B)

C)

Figure 6-13 Analysis of the spare respiratory capacity for 35 clonally-derived CHO-S subpopulations and the parental population during exponential and stationary growth phases. Cells were grown in fed-batch culture in CD CHO media supplemented with 8 mM L-glutamine and maintained at 37°C, 170 rpm, under 5% (v/v) CO_2 atmosphere until culture viabilities dropped below 60%, during the culture 10% (v/v) CHO CD EfficientFeed™ was fed at days 3, 5, 7 and 9. Early-, mid- and late-subpopulations generated from a long-term subculture regime, corresponding to generations 0, 80 and 200, respectively, were harvested and analysed using the cell metabolic analyser Seahorse XF24 at exponential (day 3) and stationary (day 7) growth phases. (A) The spare respiratory capacity at the exponential and stationary growth phases for the differently aged clonal subpopulations, (B) the global spare respiratory capacity at the exponential and stationary growth phases and (C) the Pearson's correlation between the spare respiratory capacity at stationary and exponential growth phases for the differently aged clonal subpopulations (PPMCC r = -0.029, *p*-value > 0.05, n = 36).

The observed reduction in spare respiratory capacity thorough the life span has been analysed by other authors, indicating the existence of long-term regulators on OXPHOS which contribute to functional alterations in the mitochondrion, in particular in complex IV, which results in elevated ROS activity and in decrements in the reserve respiratory capacity (Desler et al. 2012).

An interestingly findings observed between both growth phases was an increment in the reserve respiratory capacity. These increments resulted from the over expression of different isoforms of mitochondrial proteins with elevated activity (e.g., complex IV) during this growth phase allowing to increase their maximal respiratory capacity and thus in their spare respiratory capacity (Desler et al. 2012). From the panel of subpopulations, only C6-early, C8-early, C11-late, C13-late, C13-mid, C15-early and C15-mid subpopulations reduced their spare respiratory capacity. Interestingly, these subpopulations were previously associated with deficiency in the mitochondrial integrity and thus associated with mitochondrial dysfunctions.

Together, this data confirms that cells reactivate and improved their mitochondrial metabolism at the stationary growth phase, resulting in more efficient glucose utilization and in increments in the OXPHOS activity (see section 6.4.11). As mentioned previously, this behaviour resulted from increments of the TCA cycle flux caused by the switch from the initial aerobic glycolysis to mitochondrial metabolism (see chapter 5) and from the over expression of mitochondrial proteins with elevated activity. Moreover, this data seems to indicate that during the stationary growth phase cells presented a less efficient mitochondrial respiration characterised by higher rates of proton leakage activity (see section 6.4.10) due to elevated environmental stressor (e.g., osmolarity) which threaten the membrane integrity of mitochondria.

6.4.14 Correlation in the mitochondrial metabolism at exponential and stationary growth phases

To evaluate the existence of any correlations between the key mitochondrial parameters described above (sections 6.4.8 to 6.4.13), Pearson's correlation analyses were performed at exponential and stationary growth phases (Figure 6-14), exhibiting from moderate to strong correlations among the basal and maximal respiration and the proton leakage and ATP turnover activity at both growth phases. These correlations were expected as some calculations depend on each other or were calculated from a common factor, for example the basal glycolysis results from the sum of the proton leakage and ATP turnover activity.

Mitochondrial activity at stationary growth phase
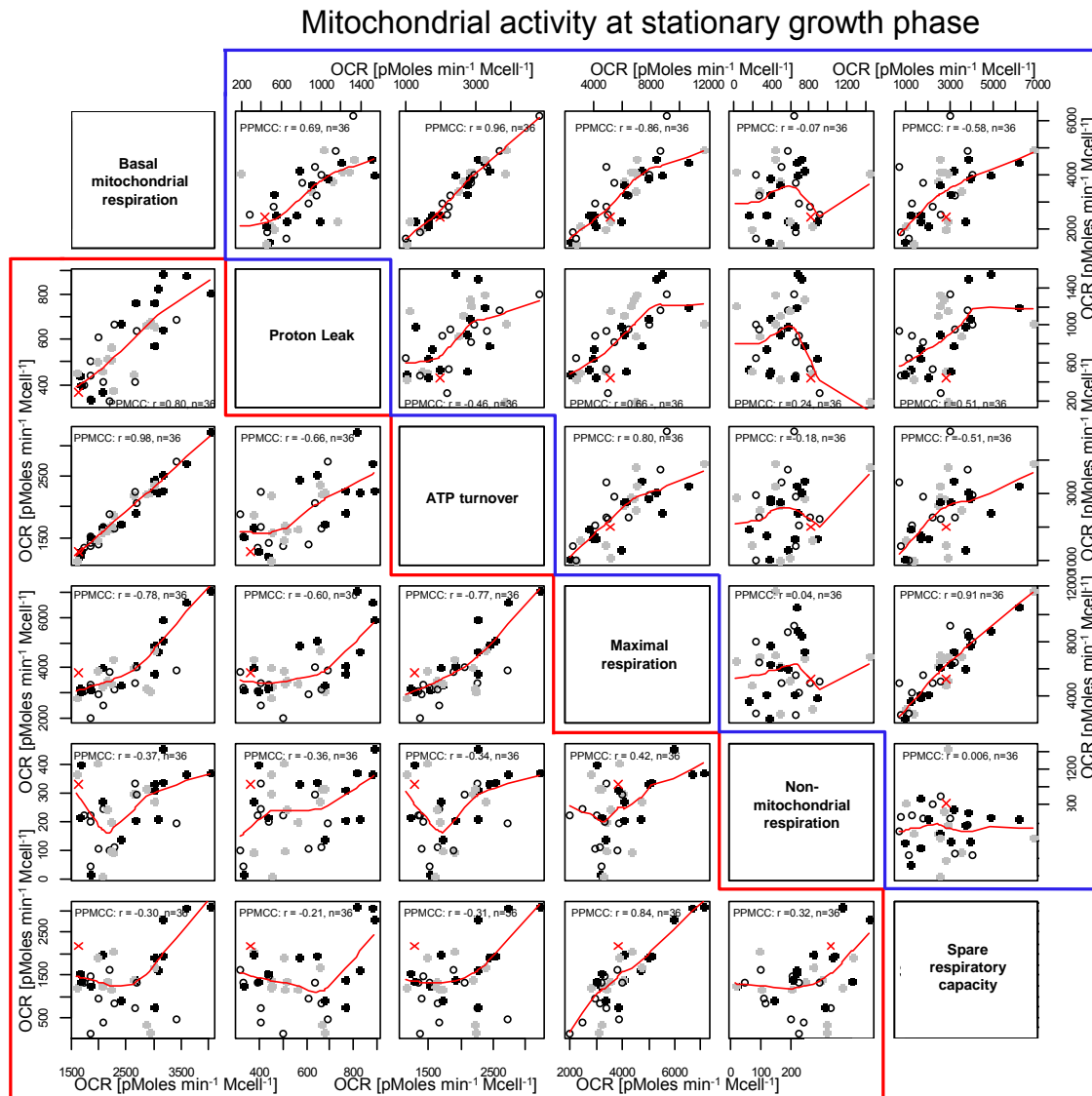
Mitochondrial activity at mid-exponential growth phase

Figure 6-14 Pearson's correlation of the global oxygen consumption rate (OCR) profiles during the exponential and stationary growth phases for 35 clonally-derived CHO-S subpopulations and the parental line. The six key mitochondrial parameters (i.e., non-mitochondrial respiration, basal mitochondrial respiration, maximal respiration, spare respiratory capacity, ATP linked respiration and proton leak) inside the red and blue figures correspond to the values collected during the exponential and stationary growth phases of the fed-batch, respectively. The black, grey and white circles represent the early, mid- and late-subpopulations generated for the clones through a long-term culture regime, respectively (i.e., generations 0, 80 and 200, respectively). The red "x" represents the parental population.

The Pearson's correlation analyses exhibited strong associations of the basal glycolysis with the proton leakage (PPMCC r= 0.80, n=36 and r= 0.69, n=36 at exponential and stationary growth phase, respectively; Figure 6-14), ATP turnover (PPMCC r= 0.98, n=36 and r= 0.96, n=36 at exponential and stationary growth phase, respectively; Figure 6-14) and Maximal respiration (PPMCC r= 0.78, n=36 and r= 0.86, n=36 at exponential and stationary growth phase, respectively; Figure 6-14) suggesting that subpopulations tend maintain some degree of proportion between the basal respiration and these parameters Moreover, the moderate and strong correlations at exponential growth phase between the spare respiratory capacity and the rest of the mitochondrial parameters was resulted from the enhancement in the OXPHOS activity at this growth phase. Finally, as we expected not significant correlation between the non-mitochondrial and mitochondrial parameters were observed.

Although important correlations within growth phases can be observed, the individual comparisons made between the values at exponential and stationary growth phases (see sections 6.4.8 to 6.4.13) not showed significant correlations, confirming that both growth phases exhibited a large differences in metabolism. This analysis strongly suggests that the mitochondria analysis performed at exponential growth phase cannot be employed to estimate their energetic metabolism on stationary phase, and vice versa, indicating significant differences in the energetic demands along cultivation.

6.4.15 Interaction of the main glycolytic and mitochondrial parameters associated with improved IVCD performance

To evaluate the IVCD performance with respect the mitochondrial and glycolytic activity, the Pearson's correlation analyses were performed using the exponential and stationary growth phase's values. For the glycolytic parameters, only the glycolytic reserve exhibited a negative correlation with IVCD performance at exponential growth phase (Figure 6-15C; PPMCC r= -0.431, n=25, $p < 0.05$), whereas no correlations at stationary growth phase were observed. On the other hand, the mitochondrial activity exhibited a weak, but significant positive correlation between the ATP turnover and IVCD performance during the exponential growth phase (Figure 6-15A; PPMCC r= 0.339, n=35, $p < 0.05$) and a negative correlation between basal respiration and IVCD performance during the stationary growth phase (Figure 6-15B; PPMCC r= -0.417, n=35, $p < 0.05$).
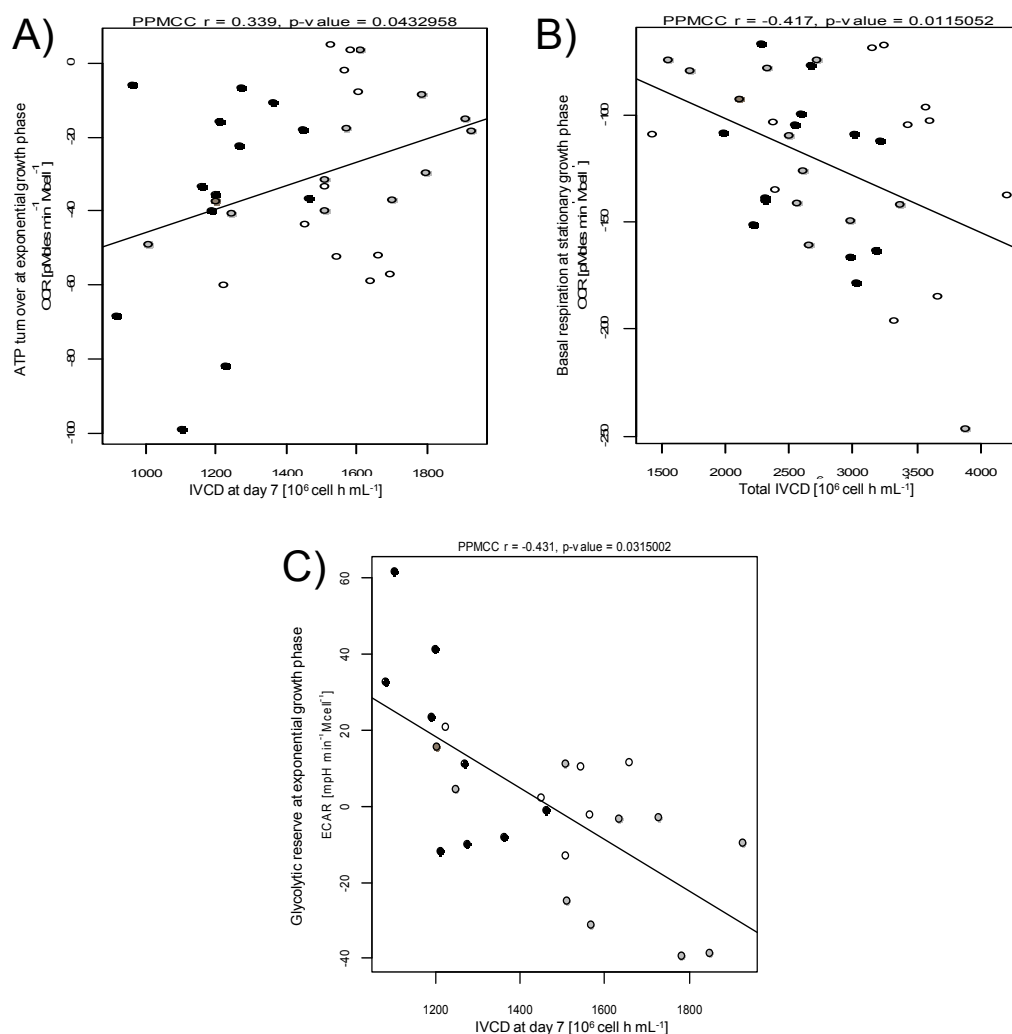
Figure 6-15 Interaction of the main glycolytic and mitochondrial parameters associated with improved IVCD performance for a panel of clonally-derived CHO-S cell lines. Cells were grown in CD CHO media supplemented with 8 mM L-glutamine and maintained at 37°C, 170 rpm and 5% (v/v) CO_2 atmosphere until culture viabilities dropped below 60%. During the culture 10% (v/v) CHO CD EfficientFeed™ was fed at days 3, 5, 7 and 9. Pearson correlations of the integral of viable cell density with (A) the ATP turnover, (B) basal mitochondrial respiration and (C) glycolytic reserve are shown. The black, grey and white circles represent clones at the early, mid- and late stages of the long-term subculture (i.e. generations 0, 80 and 200), respectively.

These parameters seem to indicate that the combination of an elevated OXPHOS activity and high aerobic glycolysis are desirable metabolic characteristics during the exponential growth phase, whereas a slow respiratory metabolism is required at stationary phase in order to reach superior IVCD performance. The elevated glycolytic and OXPHOS activity at exponential phase are essential to meet the energy

requirements and provide a large number of biomolecules for biomass production, on the contrary, a low respiratory, but efficient activity is important during stationary phase due to low mitochondrial activities mean low proton leakage and ROS production and thus a healthier mitochondrial membrane integrity (Kokoszka et al. 2001).

6.5 General discussion

The glycolytic analysis performed in this study permitted to identify the general glycolytic metabolism within CHO cell populations during the two principal growth stages of fed-batch culture (i.e., exponential and stationary growth phases). Revealing that during the exponential phase CHO-S cell lines relied on glycolysis to meet their energetic and metabolite requirements for biomass production, exhibiting a strong glycolytic phenotype characterised by elevated basal glycolytic activity near to the maximal capacity (representing approximately 98.1% of their maximal capacity) and no glycolytic reserve. These findings were validated by the metabolic analysis presented in chapter 5, in which cells exhibited an elevated glucose and glutamine consumption as well as high lactate: glucose ratio during the exponential stage. Together, this data clearly corroborated that during exponential growth phase populations had a strong aerobic glycolysis or "Warburg effect" metabolism, which is commonly defined as an abnormal metabolism due to the low energetic efficiency under aerobic environments (Gatenby and Gillies 2004; Warburg 1956). However, this inefficient glucose metabolism provides of a rapid source of energy and biomolecules for proliferation (Bartrons and Caro 2007; Vander Heiden et al. 2009; Zhao et al. 2013) which also has been commonly described in CHO populations (Ahn and Antoniewicz 2012; Young 2013) and other cancer cell lines (Amoedo et al. 2013; Vander Heiden et al. 2009).

Given the nature of the fed-batch strategy implemented in this study, the glucose levels along the culture were always elevated, therefore it can be suggested that the constant glucose availability was one of the key factor that promoted this glycolytic phenotype, as cells always encountered an unlimited amount of carbon source that could be easily assimilated. This hypothesis is supported by studies showing that most of the cancer cells exhibit elevated expression levels of key glucose transporters (e.g., GLUT 1, GLUT 3 and GLUT 4) which facilitate the constant incorporation of glucose into the cells and accelerate glycolysis (Adekola et al. 2012; Macheda et al. 2005). Given the similitudes of CHO cells with cancer cells, it is suggested that the abundance of glucose and the over-expression of the glucose transporters (e.g., GLUT1 and GLUT5) promoted this elevated glycolytic metabolism and the over-expression of

glycolytic enzymes (e.g., HK, PFK and PYK) and the LDH enzyme to rapidly restore the required NAD+/NADH levels (Kim et al. 2006; Papandreou et al. 2006; Vander Heiden et al. 2009; Zhou et al. 2011). On this basis, it can be suggested that this abnormal glycolytic metabolism can be reduced by maintaining low glucose levels during the whole cultivation. The cultivation strategy involving restricted glucose levels has been widely implemented in cell culture proving efficacy in terms of low glucose consumption and low lactate production (Altamirano et al. 2004; Cruz et al. 1999; Rodriguez et al. 2005; Wilkens and Gerdtzen 2011; Zhang and Robinson 2005).

The analysis of the glycolytic performance during the stationary growth phase clearly denotes notable increases in the glycolytic capacity, reductions in the basal glycolytic activity and increments in the non-glycolytic acidification (Figure 6-1). It is important to note the differences between these parameters, for example the glycolytic capacity represents the highest rate of glucose oxidation that cells can process under extreme circumstances, the basal glycolytic activity denotes the glucose utilisation at a specific time point, and the non-glycolytic acidification indicates the environmental acidification that is not associated with lactate acidification (i.e., aerobic glycolysis).

The reduction in the basal glycolysis at stationary phase resulted from a deceleration of the cell growth and the switch to OXPHOS, reducing their glucose demand as its oxidation is couple to the TCA cycle and release as CO2. This metabolic switch allows them to reduce the carbon uptake to maintain energetic demand. As the glucose oxidation become more efficient, it is tough that important glycolytic enzymes (e.g., HX, LDH and PFK) and glucose transporters (e.g., GLUT1) were strictly regulated to maintain normal ATP levels. When stationary cells were treated with rotenone, the OXPHOS activity was shut-down and cells were forced to increase the ATP production through glycolysis, revealing their previous glycolytic capacity. Interestingly, the disruption in the mitochondrial performance result in a higher glycolytic capacity, when compared with stationary growth phase, probably because cells re-activated the latent glycolytic machinery accumulated throughout the whole exponential growth phase which was also characterised for elevated enzymatic activities (Km). The reduction of basal glycolysis linked with increment in glycolytic capacity generated that non-proliferating cells exhibited a glycolytic reserve, indicating that non-proliferating populations are able increase significantly the ATP production via glycolysis under unexpected changes in the mitochondrial metabolism.

Reduction of glycolytic metabolism at stationary phase was accompanied with increases in the non-glycolytic acidification, which mainly resulted from the glucose oxidation to CO_2 via the TCA cycle, which was then converted into carbonic acid.

Therefore, this data indicated that cells did not reduce their ATP requirement and in fact confirmed the switch from an inefficient "aerobic glycolysis" to the efficient mitochondrial metabolism in terms of ATP production. Finally, despite the levels of ATP were not monitored, our previous metabolite analyses (e.g., low lactate: glucose ratio and high glutamate assimilation; see chapter 5) confirm that cells switched to a more efficient mitochondrial metabolism. A different metabolism was observed during the exponential growth phase, in which populations employ the aerobic glycolysis as the main source of ATP and intermediates for biomass synthesis, resulting in a lack of glycolytic reserved (~1.8% of the total glycolytic capacity) as they needs to consumed glucose at their maximal glycolytic capacity. In contrast, the switch to mitochondrial metabolism at stationary phase allowed them to reduce their basal glycolytic flux and this increase their glycolytic reserved capacity (~36% of the total glycolytic capacity).

In general, the glycolytic analysis revealed that cells exhibited a strong aerobic glycolysis during proliferation, as they required a rapid synthesis of a large number of biomolecules including DNA, lipids and proteins for cell division, and as they were grown in an abundance of glucose which provided an unlimited and readily available carbon source. The combination of these factors trigger a dynamic system which moulded their metabolism on response to the environment, therefore cells were able to up-regulate key proteins associated with the transport and metabolism of glucose (e.g., GLUT1, LDH and HK) and down-regulate other critical enzymes for the mitochondrial metabolism (e.g., PDC) to take advantage of the environment and maintain elevated levels of biomolecules (e.g., amino acids, nucleotides) (Dang 2012; Papandreou et al. 2006; Vander Heiden et al. 2009). On the other hand, during stationary growth phase the cell division is reduce and cells are subjected to environmental stress such as nutrient limitation (e.g., glutamine), elevated osmolarity and toxic levels of by-products (e.g., lactate and ammonia), therefore cells re-arranged their metabolism and reactivated the pyruvic acid mitochondrial flux towards the TCA cycle for producing energy and intermediates needed for cell maintenance, secondary metabolites production and for avoiding deleterious consequences.

The bioenergetics of mitochondrial metabolism was measured as basal mitochondrial respiration, maximal respiration, spare respiratory capacity, ATP related respiration and proton leak respiration, at the two principal growth stages of fed-batch culture (i.e., exponential and stationary growth phases), revealing that cells notably improved their mitochondrial metabolism at the stationary phase, but also disclosing a slightly reduction in the respiratory efficiency, which was observed as an increment in the proton leak across the IMM. These findings are strongly supported by the glycolytic

metabolism, in which exhibited that populations reduced their glycolytic activity and increased the non-glycolytic acidification during stationary growth phase (see sections 6.4.3 and 6.4.2, respectively). In addition, the metabolic analysis presented in chapter 5 confirmed that non-proliferating cells increased their TCA flux by increasing their glutamate metabolism and switching to the lactate consumption. Together this data supports the hypothesis that cells switched form aerobic glycolysis to OXPHOS during the stationary growth phase. Previous reports using CHO cells found increments in the mitochondrial activity during the transition from exponential to stationary growth phase (Sengupta et al. 2011; Tsao et al. 2005; Young 2013). For example, Sengupta et al. (2011) found that non-proliferating cells increased their pyruvate flux towards the TCA cycle during the stationary phase to meet their metabolic demands. In contrast, our findings also disagree with the studies reported by Ahn and Antoniewicz (2011) in which they showed that the TCA cycle activity remains similar during both growth phases, but in their study they employed an adherent CHO-K1 cell line, different media and fetal bovine serum and culture conditions; probably these cell culture and cell line differences defined the cellular metabolism in CHO-K1 populations.

Reductions in the respiratory efficiency were confirmed by the increments in the proton leak activity during the stationary phase. Although, it is important to note that the proton leakage OCR activity did not reveal abnormal levels for the majority of the clones (accounting for less than 30% of the basal respiration), this data clearly suggested that these increases were a result of the elevated oxidative stress and hyper-osmolarity which constantly threatened the mitochondria integrity. Previous studies have reported a close relation between ROS activity and proton leakage, for example, Kokoszka et al (2001) found that oxidative stress and ROS production increase the proton leakage activity across IMM in cell lines with low anti-oxidant responses, destroying the mitochondria membrane potential and triggering apoptosis. Therefore, this data suggests that the mitochondrial metabolism during the stationary phase became less efficient as they encountered hostile environmental conditions which gradually damaged the IMM. Taking this into consideration, this measurement can also be employed to select cell lines that may "potentially" tolerate elevated oxidative stress. Moreover, I suggest that the proton leak activity must be complemented with the measurement of the mitochondria membrane potential to monitor its integrity, and glutathione and ROS production to indicate the level of oxidative stress.

The mitochondrial analyses comparing both growth phases also exhibited that CHO-S populations tend to increase their maximal mitochondrial respiration during the

stationary growth phase. Our results suggest that the respiratory differences between proliferating and non-proliferating cells were mainly derived from short-term regulators of the OXPHOS which module the mitochondrial capacity by promoting the expression of different isoforms of mitochondrial proteins with enhanced activity (Desler et al. 2012), Alternatively, the metaboloepigenetics effects of key energy metabolites such as ATP, NAD+, SAM and acetyl-CoA may be responsible of rapid metabolic shift through the silencing processes as this molecules serve as essential co-factors for epigenetic mechanism and its relative abundance may modulate the energetic state of the cells (Donohoe and Bultman 2012). In addition, it can be suggested that the increments in maximal mitochondrial respiration could be resulted from an increase in the amount of mitochondrial content (e.g., mitochondria size and number) and not only resulted from the reactivation of the OXPHOS pathways with an elevates activity, although in this study the mitochondria content was not quantified, we can infer that the FCCP treatment can give an insight with respect to the mitochondria content within cells as this treatment discloses the maximal oxygen consumption per cell. However, FCCP treatment measure is not associated with the mitochondrial content, thus making these experiments insufficient to explain mitochondrial morphology. Therefore, I suggest that future works need to be complemented with direct or indirect measurements of mitochondrial mass (e.g., mitochondrial DNA content, complex I-V ETC protein quantity, citrate synthase activity).

In addition, the mitochondrial analysis during exponential phase revealed that an elevated aerobic glycolysis was not sufficient to meet the energetic demands needed for proliferation and consequently cells still relied on OXPHOS, but this respiratory activity was not supported solely by glucose as cells down-regulated the pyruvate shuttle into the TCA cycle. This OXPHOS activity resulted from the active glutamine metabolism which contributed with ATP via OXPHOS and with carbon molecules (e.g, citrate and amino acids) and energy molecules (NADH, FADH$_2$ AND NADPH) needed for biomass synthesis (e.g., amino acids, fatty acids and nucleotides). This hypothesis is supported with studied carried out by DeBerardinis et al. (2007) which revealed that the glutamine metabolism in glioblastoma cells contributed with significant NADPH levels via malic enzyme in the cytosol, which is the electron donor for fatty acid synthesis, and that NADPH production also increased the lactate level as this enzymatic reaction produces pyruvate that subsequently is converted into lactate by LDH enzyme. Our metabolic analysis agreed with this study by observing elevated glutamine consumption and elevated lactate: glucose ratios during the exponential phase (of up to 2.5 ratio for clone C19-late, meaning 2.5 lactate moles produced per

each glucose mole consumed, which exceeds the maximum possible coefficient for glucose metabolism from glycolysis), indicating that a large proportion of glutamine metabolism contributed to NADPH and lactate production. Finally, the proton leak activity resulted from exponential phase seems to indicate that proliferating populations present a better mitochondrial integrity as they were not exposed to nutritional and environmental stress (e.g., osmolarity and by-product accumulation).

Analysing the global effects, this data clearly corroborated that along the course of fed-batch culture subpopulations exhibited a dynamic metabolism characterised by an accelerated glycolytic metabolism, near to the maximal capacity, with large lactate accumulation, probably resulted from the PDC inhibition which ceased the glycolytic and the TCA cycle connection and promoted the pyruvic acid reduction to lactic acid, during the exponential phase (Kim et al. 2006; Papandreou et al. 2006; Vander Heiden et al. 2009; Zhou et al. 2011). To compensate the deficiency of pyruvic acid flux towards the TCA cycle, cells demanded elevated levels of glutamine assimilation to feed this pathway, but also to produce the electron donor NADPH and acetyl-CoA for fatty acid synthesis. The transition from exponential to stationary phase was characterised by metabolic rearrangements which involved the reestablishment of pyruvic acid flux towards the TCA cycle and thus improving the glucose metabolism and switching to a more efficient OXPHOS systems for ATP production. Along the stationary phase a decrement in the respiratory efficiency was observed, resulted from the severe environmental conditions (e.g., elevated osmolarity, nutrient depletion, ROS activity) which gradually threatened the mitochondrial integrity and reduced their respiratory efficiency.

In addition to the differences between growth phases our findings have demonstrated important changes in the glycolytic and mitochondrial metabolism over increasing generation, this is the first study using CHO cells models that have evaluated the energetic metabolism along time, our findings clearly indicate a reduction in the glycolytic and mitochondrial usage along increasing generation which is thought to result mainly from the optimisation in the ATP usage for cellular maintenance and cell decision. This behaviour seems to be associated with the reduction in cells size observed along the evolution phase which has implications on the demands of cellular biomass, or protein content, required proliferate. Therefore a low protein content phenotype resulting from a constant reduction in the cell size was enough to improve the ATP usage, enhance higher proliferation rates and reduce the glycolytic and mitochondrial metabolism. A similar behaviour can be observed on population at stationary growth phase in which cells showed significant changes in the glycolytic

metabolism but not in the mitochondrial metabolism over increasing generation. This metabolic phenotype on non-proliferation populations seems to support that populations optimised and reduced their energetic demands by reducing their glucose dependence and reutilising lactate, and thus improving the TCA cycle. Together, our traits seem to indicate that over increasing generation non-proliferation populations rely more on the mitochondrial metabolism to survive.

To conclude this chapter, the mitochondrial and glycolytic analysis with respect to IVCD performance at both growth phases revealed the desirable mitochondrial and glycolytic characteristic for reaching highest "cumulative cell time". Being the maintenance of an elevated OXPHOS activity (ATP turnover) coupled with an upregulated basal glycolytic rate (at their maximal glycolytic capacity) essential during exponential growth phase to support the enough energy and intermediates for proliferate, whereas a slow basal respiration during stationary growth phase is important to prevent oxidative stress and the uncoupled respiration to protect the mitochondria integrity and reduce a potential mitochondrial membrane damage, which already occurs from the hostile environmental conditions, reducing detrimental effects such as cell death. The evidences showed in chapter 5 hold that an elevated glutamine metabolism is needed in growing populations to feed the TCA cycle and maintain an active OXPHOS as the strong Warburg phenotype uncoupled the flux of pyruvic acid to the mitochondrial TCA cycle. Whether these metabolic phenotypes are essential feature of high growing cell lines prior producing recombinant proteins, it will be interesting complement this work by measuring the ATP, NAD+/NADH, oxidative stress and molecules such as pyruvate, citrate and acetyl-CoA throughout increasing generations.

Chapter 7

CONCLUSIONS AND FUTURE DIRECTIONS

Chapter 7
Conclusions and future directions

Selection of cell lines for manufacturing recombinant proteins usually involves multiple screening steps of transfected clones that would meet the industrial standards such as productivity and gene stability over extended culture periods, followed by their adaptation into industrial biotechnological processes. However, the early-stages of cell line development processes underestimate the importance of the cell growth performance and their contributions towards volumetric productivity. Therefore, the initial screening omits assessment of metabolic performances among isolated clones, reducing the potential of selecting clonal cell lines with optimal metabolic and growth behaviour for biotechnological processes. This research was done to present an alternative strategy to develop cell lines with industrial relevance (e.g., optimal growth and metabolic performance) by implementing a reverse cell line development strategy, consisting of harnessing the phenotypic heterogeneity within a non-transfected parental CHO-S population to isolate a panel of 22 clonally-derived CHO-S cell lines, followed by accelerating genetic drift to evolve the phenotypic traits of the isolates. This strategy permitted to generate a panel of 132 un-transfected CHO-S subpopulations with enhanced and varied metabolic and growth characteristics that can be selected on basis of their growth characteristics and/or metabolic performance to be employed for producing recombinant proteins under specific culture environments.

An important contribution of this study was the confirmation that the phenotypic heterogeneity within a donor Parental CHO population is an important source of phenotypic diversity that must be exploited to develop cell lines with improved metabolic and growth characteristics. This research project also confirmed that non-genetic engineering strategies can be used as alternative approaches to improve phenotypes and in fact these cell lines may exhibit higher phenotypic and metabolic stability than those genetically manipulated cell lines as they were not exposed to the random genomic insertion of constructs needed for enhancing the cell behaviour using blind genetic engineering strategies. However, this project was only the first stage of the proposed strategy which needs to be complemented with analysis of the cell lines' ability to incorporate exogenous genes, synthesise difficult-to-express recombinant proteins and evaluate their metabolism during protein production. Additionally, the importance of this panel of CHO-S cell lines is its usefulness in the evaluation of conserved genetic and epigenetic features that may permit to identify and trace cell lines and phenotypes over time, as well as to identify differential expression levels of

proteins that are reflected in superior and stable phenotypes (e.g., transcription factors, DNA repair enzymes and anti-apoptotic proteins).

In this study, the broad analysis of the phenotypic heterogeneity among clonally-derived CHO-S cell lines revealed significant metabolic differences among the isolated populations and the parental population which open the possibility of isolating cell lines with varied metabolite processing rates (e.g., glutamine, glucose, lactate and glutamate consumption/production rates), metabolic responses (e.g., shift to lactate consumption, reduced/increased glycolytic and OXPHOS activities) and cell growth performances (e.g., IVCD, μ, VCD peak). Therefore, it could be interesting to use enzymatic inhibitors to induce metabolic inhibition before and after cell cloning to examine the abundance of particular metabolic traits which are associated with high growing/producing phenotypes, for example lactate switch, short-term glycolysis and OXPHOS regulation. Similarly, the implementation of chemical inhibitors during the routine and prolonged cultivation would be desirable to promote the acquisition of beneficial and deleterious phenotypic characteristics that would fit with the culture environment. Furthermore, the employment of chemical inhibitors may be valuable to control the phenotypic plasticity limits along the different stages of the long-term culture (e.g., adaptation, early-evolution, mid- and late–evolution phase).

The overall long-term cultivation data has shown the effects of genetic drift as evolutionary process which firstly was characterised by a significant control in the level of phenotypic heterogeneity within the populations and then marked by a strongly selection of highly proliferative subpopulations. During the first stage, genetic drift notably reduced the elevated phenotypic variation within populations by removing subpopulations with low culture fitness and by minimising fluctuations in the culture environment that occurs as a consequence of the combination of heterogeneous metabolisms. Along the second stage, genetic drift favoured the dominance of fast-growing subpopulations after each successive cell passage by an indirect and random selection of subpopulations with elevated proliferation rates. It is important to mention that genetic drift had a positive effect by selecting fast-growing subpopulation, but also it is important to note that improvements in proliferation rates were not necessarily reflected as enhancements in IVCD and viable cell densities mainly because clones were not exposed to detrimental culture environments, such as nutrient exhaustion and by-product accumulation, which are commonly found during the measurement of this parameters. Therefore, it might be interesting to modify the subculture regimen during evolution strategy in order to enable the accumulation of harsh culture environments

which would permit the acquisition of cellular resistance to the environmental stressors commonly found at late-stages of fed-batch cultivation.

Cell revival revealed to possess strong genetic drift effects, in particular in subpopulations with low adaptability to the culture environment (e.g., subpopulations at generation 0) by selecting only those cells that resist the cryopreservation process and retain fitness to the culture environment, and by propagating them after each successive cell passage. The long-term cultivation implemented in this research did not consider the cryopreservation/cell revival cycles as evolutionary strategy, mainly because a repetitive cryopreservation/cell revival cycles would modify the growth profiles dramatically as each cycle generates substantial environmental stress that may increase the genetic instability within populations. Therefore, the evolutionary strategy chosen in this study was suitable to assess the acquisition of beneficial/detrimental genetic and phenotypic traits on proliferating populations under non-stress environments in order to prevent environmental changes that may increase the levels of genomic instability within populations. However, it would be interesting to evaluate a combination of a routine cryopreservation/cell revival cycles along the long-term cultivation in order to accelerate the evolutionary process, for example, by using different cryopreservation strategies and cryopreservation/cell revival schemes along a long-term cultivation in parental populations may be useful to identify and develop better evolutionary strategies.

The environmental conditions have an important role in the fixation of beneficial mutations, defining which phenotypic and metabolic characteristic must be conserved or improved. The long-term cultivation strategy presented here involved a routine sub-culture regimen using populations at mid-exponential growth phase, which was ideal for maintaining an active and continuous biomass production which resulted in constant improvements in proliferation rates over increasing generations. This subculture scheme indirectly contributed to the improvement of other growth characteristics such as VCD peak and IVCD, but these were not necessarily constantly improved along increasing generations as these parameters are defined by other culture environment characteristics that were not present in the long-term culture regime (e.g., hyper-osmolarity, ROS species and toxic by-products levels). Therefore, it could be interesting to evaluate the long-term cultivation in the presence of culture stressors (e.g., hyper-osmolarity, low nutrient availability, elevated toxic by-products concentrations, different culture formulation) (Prentice et al. 2007), alternative carbon sources (e.g., glutamate, galactose) (Altamirano et al. 2000) and low doses of

glycolytic and mitochondrial inhibitors (e.g., 2-DG, oligomycin) to investigate their potential effect in stationary growth phase parameters such as VCD peak and IVCD.

The constant phenotypic plasticity within CHO cells along the long-term cultivation corroborated that the inherent genetic instability within CHO cells cannot be eliminated. In fact, this work demonstrates that genetic instability is a latent threat that cannot be ignored as this behaviour can unexpectedly change the metabolic profile of a whole population in order to overcome and reach a maximum possible fitness in a given environment. Although CHO cells are well known for exhibiting a "mutator phenotype" (Barnes et al. 2006; Derouazi et al. 2006; O'Callaghan et al. 2010), the constant phenotypic changes cannot be attributed only to the inherent genetic instability as other mechanisms such as epigenetic events enable cells to continually adjust the gene expression according to the environment without modifying the DNA sequence (Chusainow et al. 2009; Flatscher et al. 2012; Sandoval and Esteller 2012). It could be interesting to evaluate the extent of genetic instability by analysing changes in the karyotype (Derouazi et al. 2006) or monitoring rate of mutations by using DNA microsatellite instability measurements. Alternatively, the epigenetic effects could be assessed by analysing changes in DNA methylation and histone modification through the inhibition of silencing processes via 5-aza-2--deoxycytidine, Valerio Acid, procaine and butyrate treatments (Kwaks and Otte 2006; Lyko and Brown 2005) and by analysing the methylation of cytosine nucleotides in the context of a CpG dinucleotide (Wippermann et al. 2014). To investigate this further the epigenetic activity within cells, it could be interesting to analyse key energy metabolites such as ATP, NAD+, SAM and acetyl-CoA as this molecules serve as essential co-factors for epigenetic mechanism and its relative abundance may modulate the energetic state of the cells (Donohoe and Bultman 2012)

The feeding strategy in fed-batch cultivation was optimised to promote an elevated global IVCD performance and increase cellular viability and culture longevity through a multi-day supplementation using a defined volume of CHO CD EfficientFeed™ B. The metabolic analyses suggest the importance of monitoring the principal carbon sources (e.g., glucose and glutamine) and by-product build-up (e.g., lactate and ammonia) during optimisation processes to avoid the exhaustion or accumulation of these metabolites and to meet individual metabolic demands based on the specific assessments of particular media components for each individual clone (Altamirano et al. 2000; Khattak et al. 2010; Wurm 2004). It would therefore be interesting to further improve the fed-batch strategy by controlling and maintaining the glucose and glutamine at low levels along fed-batch process (Altamirano et al. 2004;

Cruz et al. 1999; Rodriguez et al. 2005; Wilkens and Gerdtzen 2011; Zhang and Robinson 2005).

The metabolic assessments between exponential and stationary growth phases permitted to identify that proliferating cells required increased carbon source uptake (e.g., glutamine and glucose) for biomass biosynthesis (e.g., lipids, nucleotides and proteins), indicating that glucose is metabolised under aerobic glycolysis for supplying rapid ATP synthesis and maintaining the NAD+/NADH levels which is essential to continue with the elevated glycolytic activity. Additionally, glucose is fed to the pentose phosphate pathway to synthesised NADPH, a cofactor indispensable for lipid biosynthesis, and produce intermediates for the biosynthesis of nucleotides and aromatic amino acids (Gatenby and Gillies 2004; Kim et al. 2006; Papandreou et al. 2006; Vander Heiden et al. 2009). On the other hand, glutamine was employed to feed the TCA cycle produce energetic intermediates such as NADH and $FADH_2$ and citrate for ATP synthesis and fatty acid biosynthesis, respectively, as well as provide elevated levels of NADPH via cytosolic malic enzyme to ensure that a sufficient NADPH levels to performant biosynthetic pathways and protect against oxidative stress (DeBerardinis et al. 2007). It could be interesting to measure the PDH and a cytosolic malic enzyme activity to validate that glutamine was the principal carbon source for the mitochondrial metabolism and the important source of NADPH for biosynthesis, respectively. It would also remarkable to investigate whether the ability of the cells to produce NADPH is a key limiting step in proliferating populations.

Assessing the respiratory capacity of populations is fundamental to understanding cell metabolism and growth performance within populations. The mitochondrial and glycolytic analysis is of particular importance to measure the abnormal metabolism such as aerobic glycolysis, also known as Warburg effect along manufacturing process. This data revealed that the combination of an elevated OXPHOS activity and a strong aerobic glycolysis is essential to reach high μ and IVCD performance in proliferating populations. This metabolism seem to be contradictory as a strong aerobic glycolysis shut-downs the pyruvic acid flux towards the mitochondrial TCA cycle by inhibits the PDC enzyme and upregulating the LDH enzyme (Kim et al. 2006; Papandreou et al. 2006; Vander Heiden et al. 2009; Zhou et al. 2011), however this abnormal metabolism was the result of utilising both glucose and glutamine carbon sources, being the first used for feeding the aerobic glycolysis and the second for feeding the mitochondrial TCA cycle. To further elucidate these effects, it would be interesting to evaluate key glycolytic (i.e., HK, PFK and LDHA) and the TCA cycle (i.e.,

citrate) enzymes as well as the proteins involved in the electron transport chain (i.e., complex I, II and IV) (Koopman et al. 2013).

The assessment of mitochondrial activity at stationary growth phase is of particular importance to identify metabolic traits that may promote enhancements in the global IVCD performance, cellular viability and culture longevity. The extensive analysis of the glycolytic and mitochondrial metabolism showed that a low respiratory metabolism, but efficiently couple to ATP production is a desirable characteristic for attaining elevated IVCD on the late stage of fed-batch cultivation. These characteristic results from the importance of reducing the uncoupled mitochondrial respiration and its negative side effects such as oxidative stress that eventually would threaten the mitochondrial integrity and increase the proton and electron permeability across the IMM (Kokoszka et al. 2001). Consequently, a slow but efficient mitochondrial respiration is essential to minimise mitochondrial damage and ROS activity. It would be interesting to detect the oxidative stress within cells and evaluate the mitochondrial membrane potential to confirm these findings.

Testing proton leakage activity across the IMM enabled to identify that the mitochondrial respiration became less efficient at stationary growth phase, reducing the proportion of oxygen consumption associated to ATP production and increasing the proton leakage across the IMM. The latter is responsible for causing the collapse of the mitochondria membrane potential (MMP) that lead detrimental growth performances and apoptosis (Kokoszka et al. 2001). An inefficient respiratory activity also denotes potential mitochondrial damage probably resulted from increments in the rate of formation of mitochondrial superoxide and other forms of cellular oxidative stress. Therefore populations at stationary growth phase need to reduce their mitochondrial respiration to diminish detrimental consequences. To further support this finding, it would be interesting to analyse the MMP, ATP production, redox status of the cell and cellular oxidative stress along the course of fed-batch cultivation.

In this research there were a number of changes in cellular metabolism associated with the cell growth status, for example whether a cell line changes from exponential to stationary growth phase there are significant adjustments in the glycolytic and mitochondrial activity as well as in the glucose consumption within a cell. It is therefore possible to speculate that the rapid metabolic switch from an ineffective to efficient glucose metabolism is associated to potential epigenetic changes as there is a synergy between energy metabolism and of control gene expression. For example, analysing the relative abundance of key energy metabolites such as ATP, NAD+, SAM and acetyl-CoA could serve to identify potential gene silencing because their

abundance allows a cell to regulate its energetic because this molecules serve as essential co-factors for epigenetic mechanism that regulate DNA methylation, histone modifications and nucleosome position (Donohoe and Bultman 2012).

The results presented here strongly supports that the 132 subpopulations generated along the LDC and long-term subculture, corresponding to 22 clonally-derived CHO-S cell lines at subpopulations 0, 40, 80, 120, 160 and 200, are markedly different in terms of cellular growth and metabolism. The high phenotypic variability among subpopulations supports the notion that each subpopulation must be considered as an individual cell line as they evolved significant phenotypic and metabolic differences. These findings also remark the importance of a strict control in the passage number because underestimating it may mislead comparisons of cellular behaviour as aged cell lines may exhibited a very different metabolism to that found in the original cell bank .

The methodology outlined in this thesis generated a panel of 132 clonal CHO-S cell line that open the opportunity to gain major insight of the inherent phenotypic heterogeneity within of CHO populations. By using this panel, complex therapeutic proteins could be produced with efficacy by selecting, analysing and manipulating this broad spectrum of phenotypes. Moreover, this panel increase the chances of developing accurate prediction models of productivity, stability and cell growth performance which together would increase our understanding of the nature of relevant cell lines with desirable metabolic and growth phenotypes.

Bibliography

Bibliography

Adekola K, Rosen ST, Shanmugam M. 2012. Glucose transporters in cancer metabolism. *Curr Opin Oncol.* **24**(6):650-654.

Aggarwal S. 2008. What's fueling the biotech engine - 2007. *Nat Biotech.* **26**(11):1227-1233.

Ahn WS, Antoniewicz MR. 2011. Metabolic flux analysis of CHO cells at growth and non-growth phases using isotopic tracers and mass spectrometry. *Metab Eng.* **13**(5):598-609.

Ahn WS, Antoniewicz MR. 2012. Towards dynamic metabolic flux analysis in CHO cell cultures. *Biotechnol J.* **7**(1):61-74.

Ahn WS, Antoniewicz MR. 2013. Parallel labeling experiments with 1,2-C-13 glucose and U-C-13 glutamine provide new insights into CHO cell metabolism. *Metab Eng.* **15**:34-47.

Al-Rubeai M, Singh RP. 1998. Apoptosis in cell culture. *Curr. Opin. Biotechnol.* **9**(2):152-156.

Altamirano C, Illanes A, Becerra S, Cairo JJ, Godia F. 2006. Considerations on the lactate consumption by CHO cells in the presence of galactose. *J Biotechnol.* **125**(4):547-556.

Altamirano C, Paredes C, Cairo JJ, Godia F. 2000. Improvement of CHO cell culture medium formulation: Simultaneous substitution of glucose and glutamine. *Biotechnol Prog.* **16**(1):69-75.

Altamirano C, Paredes C, Illanes A, Cairo JJ, Godia F. 2004. Strategies for fed-batch cultivation of t-PA producing CHO cells: substitution of glucose and glutamine and rational design of culture medium. *J Biotechnol.* **110**(2):171-179.

Ames BN. 1983. Dietary carcinogens and anticarcinogens. Oxygen radicals and degenerative diseases. *Science* **221**(4617):1256-1264.

Amoedo ND, Valencia JP, Rodrigues MF, Galina A, Rumjanek FD. 2013. How does the metabolism of tumour cells differ from that of normal cells. *Biosci Rep.* **33**(6).

Arden N, Betenbaugh MJ. 2004. Life and death in mammalian cell culture: strategies for apoptosis inhibition. *Trends Biotechnol.* **22**(4):174-180.

Bae SW, Hong HJ, Lee GM. 1995. Stability of transfectomas producing chimeric antibody against the pre-S2 surface antigen of hepatitis B virusduring a long-term culture. *Biotechnol Bioeng.* **47**(2):243-251.

Baer CF, Miyamoto MM, Denver DR. 2007. Mutation rate variation in multicellular eukaryotes: causes and consequences. *Nat Rev Genet.* **8**(8):619-631.

Bailey LA, Hatton D, Field R, Dickson AJ. 2012. Determination of Chinese hamster ovary cell line stability and recombinant antibody expression during long-term culture. *Biotechnol Bioeng.* **109**(8):2093-2103.

Bandyopadhyay S, Mehta M, Kuo D, Sung M-K, Chuang R, Jaehnig EJ, Bodenmiller B, Licon K, Copeland W, Shales M and others. 2010. Rewiring of Genetic Networks in Response to DNA Damage. *Science* **330**(6009):1385-1389.

Barnes LM, Bentley CM, Dickson AJ. 2000. Advances in animal cell recombinant protein production: GS-NS0 expression system. *Cytotechnology.* **32**(2):109-123.

Barnes LM, Bentley CM, Dickson AJ. 2001. Characterization of the stability of recombinant protein production in the GS-NS0 expression system. *Biotechnol Bioeng.* **73**(4):261-270.

Barnes LM, Bentley CM, Dickson AJ. 2003. Stability of recombinant protein production in the GS-NSO expression system is unaffected by cryopreservation. *Biotechnol Prog.* **19**(1):233-237.

Barnes LM, Dickson AJ. 2006. Mammalian cell factories for efficient and stable protein expression. *Curr Opin Biotechnol.* **17**(4):381-386.

Bibliography

Barnes LM, Moy N, Dickson AJ. 2006. Phenotypic variation during cloning procedures: Analysis of the growth behavior of clonal cell lines. *Biotechnol Bioeng.* **94**(3):530-537.

Barrett S, Boniface R, Dhulipala P, Slade P, Tennico Y, Stramaglia M, Lio P, Gorfien S. 2012. Attaining Next-Level Titers in CHO Fed-Batch Cultures. *BioProcess International* **10**:56-62.

Bartrons R, Caro J. 2007. Hypoxia, glucose metabolism and the Warburg's effect. *J Bioenerg Biomembr.* **39**(3):223-229.

Beckman KB, Ames BN. 1997. Oxidative decay of DNA. *J Biol Chem.* **272**(32):19633-19636.

Beckman KB, Ames BN. 1999. Endogenous oxidative damage of mtDNA. *Mutat Res.* **424**(1-2):51-58.

Beckmann TF, Kramer O, Klausing S, Heinrich C, Thute T, Buntemeyer H, Hoffrogge R, Noll T. 2012. Effects of high passage cultivation on CHO cells: a global analysis. *Appl Microbiol Biotechnol.* **94**(3):659-671.

Benhar M, Dalyot I, Engelberg D, Levitzki A. 2001. Enhanced ROS production in oncogenically transformed cells potentiates c-Jun N-terminal kinase and p38 mitogen-activated protein kinase activation and sensitization to genotoxic stress. *Mol Cell Biol.* **21**(20):6913-6926.

Bereiter-Hahn J, Voeth M, Mai S, Jendrach M. 2008. Structural implications of mitochondrial dynamics. *Biotechnol J.* **3**(6):765-780.

Bergoglio V, Pillaire MJ, Lacroix-Triki M, Raynaud-Messina B, Canitrot Y, Bieth A, Gares M, Wright M, Delsol G, Loeb LA and others. 2002. Deregulated DNA polymerase beta induces chromosome instability and tumorigenesis. *Cancer Res.* **62**(12):3511-3514.

Bode BP. 2001. Recent molecular advances in mammalian glutamine transport. *J Nutrition.* **131**(9):2475S-2485S.

Bollati Fogolin M, Wagner R, Etcheverrigaray M, Kratje R. 2004. Impact of temperature reduction and expression of yeast pyruvate carboxylase on hGM-CSF-producing CHO cells. *J Biotechnol.* **109**(1-2):179-191.

Bonner WM, Redon CE, Dickey JS, Nakamura AJ, Sedelnikova OA, Solier S, Pommier Y. 2008. OPINION gamma H2AX and cancer. *Nat Rev Cancer.* **8**(12):957-967.

Burgess DJ. 2011. Metabolism: Choose your carbon source. *Nat Rev Cancer* **11**(2):81-81.

Cadenas E, Davies KJA. 2000. Mitochondrial free radical generation, oxidative stress, and aging. *Free Radic Biol Med.* **29**(3-4):222-230.

Cahill DP, Kinzler KW, Vogelstein B, Lengauer C. 1999. Genetic instability and darwinian selection in tumours. *Trends Cell Biol.* **9**(12):M57-M60.

Campos PRA, Wahl LM. 2009. The effects of population bottlenecks on clonal interference, and the adaptation effective population size. *Evolution* **63**(4):950-958.

Carlson B. 2011. Pipeline Bodes Well for Biologics Growth. *Gen Eng Biotechnol News* **31**(12):16-17.

Chandhok NS, Pellman D. 2009. A little CIN may cost a lot: revisiting aneuploidy and cancer. *Curr Opin Genet Dev.* **19**(1):74-81.

Chang DJ, Cimprich KA. 2009. DNA damage tolerance: when it's OK to make mistakes. *Nat Chem Biol.* **5**(2):82-90.

Chen KQ, Liu Q, Xie LZ, Sharp PA, Wang DIC. 2001. Engineering of a mammalian cell line for reduction of lactate formation and high monoclonal antibody production. *Biotechnol Bioeng.* **72**(1):55-61.

Chen PF, Harcum SW. 2005. Effects of amino acid additions on ammonium stressed CHO cells. *J Biotechnol.* **117**(3):277-286.

Christie A, Butler M. 1999. The adaptation of BHK cells to a non-ammoniagenic glutamate-based culture medium. *Biotechnol Bioeng.* **64**(3):298-309.

Chu L, Robinson DK. 2001. Industrial choices for protein production by large-scale cell culture. *Curr Opin Biotechnol.* **12**(2):180-187.

Chung MI, Lim MH, Lee YJ, Kim IH, Kim IY, Kim JH, Chang KH, Kim HJ. 2003. Reduction of ammonia accumulation and improvement of cell viability by expression of urea cycle enzymes in Chinese hamster ovary cells. *J Microbiol Biotechnol* **13**(2):217-224.

Chusainow J, Yang YS, Yeo YHM, Toh PC, Asvadi P, Wong NSC, Yap MGS. 2009. A Study of Monoclonal Antibody-Producing CHO Cell Lines: What Makes a Stable High Producer? *Biotechnol Bioeng.* **102**(4):1182-1196.

Cockett MI, Bebbington CR, Yarranton GT. 1990. High level expression of tissue inhibitor of metalloproteinases in Chinese hamster ovary cells using glutamine synthetase gene amplification. *Biotechnology (N Y)* **8**(7):662-667.

Coller HA, Coller BS. 1983. Statistical analysis of repetitive subcloning by the limiting dilution technique with
a view toward ensuringhybridoma monoclonality. *Hybridoma.* **2**(1):91-96.

Cotter TG, Alrubeai M. 1995. Cell-death (apoptosis) in cell-culture systems. *Trends Biotechnol.* **13**(4):150-155.

Crown SB, Antoniewicz MR. 2013. Publishing C-13 metabolic flux analysis studies: A review and future perspectives. *Metab Eng.* **20**:42-48.

Cruz HJ, Ferreira AS, Freitas CM, Moreira JL, Carrondo MJT. 1999. Metabolic responses to different glucose and glutamine levels in baby hamster kidney cell culture. *Appl Microbiol Biotechnol.* **51**(5):579-585.

Cruz HJ, Freitas CM, Alves PM, Moreira JL, Carrondo MJT. 2000. Effects of ammonia and lactate on growth, metabolism, and productivity of BHK cells. *Enzyme Microb Technol.* **27**(1-2):43-52.

Dang CV. 2012. Links between metabolism and cancer. *Genes Dev.* **26**(9):877-90.

Das KC. 2013. Hyperoxia decreases glycolytic capacity, glycolytic reserve and oxidative phosp horylation in MLE-12 cells andinhibits complex I and II function, but not complex IV in isolated mouse lung mitochondria. Plos One **8**(9).

Davies A, Greene A, Lullau E, Abbott WM. 2005. Optimisation and evaluation of a high-throughput mammalian protein expression system. *Protein Expr Purif.* **42**(1):111-121.

Davies SL, Lovelady CS, Grainger RK, Racher AJ, Young RJ, James DC. 2012. Functional heterogeneity and heritability in CHO cell populations. *Biotechnol Bioeng.* **110**(1):260-274.

De Bont R, van Larebeke NR. 2004. Endogenous DNA damage in humans: a review of quantitative data. *Mutagenesis.* **19**(3):169-185.

Deaven LL, Petersen DF. 1973. The chromosomes of CHO, an aneuploid Chinese hamster cell line: G-band, C-band, and autoradiographic analyses. *Chromosoma* **41**(2):129-144.

DeBerardinis RJ, Mancuso A, Daikhin E, Nissim I, Yudkoff M, Wehrli S, Thompson CB. 2007. Beyond aerobic glycolysis: Transformed cells can engage in glutamine metabolism that exceeds the requirement for protein and nucleotide synthesis. *Proc Natl Acad Sci USA.* **104**(49):19345-19350.

Demain AL, Vaishnav P. 2009. Production of recombinant proteins by microbes and higher organisms. Biotechnol Adv. **27**(3):297-306.

Derouazi M, Martinet D, Schmutz NB, Flaction R, Wicht M, Bertschinger M, Hacker DL, Beckmann JS, Wurm FM. 2006. Genetic characterization of CHO production host DG44 and derivative recombinant cell lines. *Biochem Biophys Res Commun* **340**(4):1069-1077.

Desler C, Hansen TL, Frederiksen JB, Marcker ML, Singh KK, Juel Rasmussen L. 2012. Is there a link between mitochondrial reserve respiratory capacity and aging? **J Aging Res 2012**.

Desquiret V, Loiseau D, Jacques C, Douay O, Malthiery Y, Ritz P, Roussel D. 2006. Dinitrophenol-induced mitochondrial uncoupling in vivo triggers respiratory adaptation in HepG2 cells. *Biochim Biophys Acta.* **1757**(1):21-30.

Detmer SA, Chan DC. 2007. Functions and dysfunctions of mitochondrial dynamics. *Nat Rev Mol Cell Biol.* **8**(11):870-879.

Diers AR, Broniowska KA, Chang CF, Hogg N. 2012. Pyruvate fuels mitochondrial respiration and proliferation of breast cancer cells: effect of monocarboxylate transporter inhibition. *Biochem J.* England. p 561-71.

Dinnis DM, Stansfield SH, Schlatter S, Smales CM, Alete DI, Birch JR, Racher AJ, Marshal CT, Nielsen LK, James DC. 2006. Functional proteomic analysis of GS-NS0 murine myeloma cell lines with varying recombinant monoclonal antibody production rate. *Biotechnol Bioeng.* **94**(5):830-841.

Donohoe DR, Bultman SJ. 2012. Metaboloepigenetics: Interrelationships between energy metabolism and epigenetic control of gene expression. *J Cell Physiol.* **227**(9):3169-3177.

Dorai H, Kyung YS, Ellis D, Kinney C, Lin C, Jan D, Moore G, Betenbaugh MJ. 2009. Expression of Anti-Apoptosis Genes Alters Lactate Metabolism of Chinese Hamster Ovary Cells in Culture. *Biotechnol Bioeng.* **103**(3):592-608.

Dreesen IAJ, Fussenegger M. 2011. Ectopic Expression of human mTOR Increases Viability, Robustness, Cell Size, Proliferation, and Antibody Production of Chinese Hamster Ovary Cells. *Biotechnol Bioeng.* **108**(4):853-866.

Durocher Y, Butler M. 2009. Expression systems for therapeutic glycoprotein production. *Curr Opin Biotechnol.* **20**(6):700-707.

Endo Y, Sawasaki T. 2006. Cell-free expression systems for eukaryotic protein production. *Curr Opin Biotechnol.* **17**(4):373-380.

Fan Y, Jimenez Del Val I, Müller C, Wagtberg Sen J, Rasmussen SK, Kontoravdi C, Weilguny D, Andersen MR. 2014. Amino acid and glucose metabolism in fed-batch CHO cell culture affects antibody production and glycosylation. *Biotechnol Bioeng.*

Fann CH, Guirgis F, Chen G, Lao MS, Piret JM. 2000. Limitations to the amplification and stability of human tissue-type plasminogen activator expression by Chinese hamster ovary cells. *Biotechnol Bioeng.* **69**(2):204-212.

Ferrer-Miralles N, Domingo-Espin J, Corchero JL, Vazquez E, Villaverde A. 2009. Microbial factories for recombinant pharmaceuticals. *Microb Cell Fact.* **8**(17):1-8.

Flatscher R, Frajman B, Schonswetter P, Paun O. 2012. Environmental heterogeneity and phenotypic divergence: can heritable epigenetic variation aid speciation? *Genet Res Int.* **2012**:698421-698421.

Friedberg EC. 2003. DNA damage and repair. *Nature* **421**(6921):436-440.

Friedberg EC. 2006. DNA Repair and Mutagenesis: ASM Press.

Friedberg EC, Aguilera A, Gellert M, Hanawalt PC, Hays JB, Lehmann AR, Lindahl T, Lowndes N, Sarasin A, Wood RD. 2006. DNA repair: From molecular mechanism to human disease. *DNA Repair.* **5**(8):986-996.

Fumarola C, La Monica S, Guidotti GG. 2005. Amino acid signaling through the mammalian target of rapamycin (mTOR) pathway: Role of glutamine and of cell shrinkage. *J Cell Physiol.* **204**(1):155-165.

Gabriel K, Milenkovic D, Chacinska A, Mueller J, Guiard B, Pfanner N, Meisinger C. 2007. Novel mitochondrial intermembrane space proteins as substrates of the MIA import pathway. *J Mol Biol.* **365**(3):612-620.

Garber K. 2006. Energy deregulation: Licensing tumors to grow. *Science* **312**(5777):1158-1159.

Gatenby RA, Gillies RJ. 2004. Why do cancers have high aerobic glycolysis? *Nat Rev Cancer.* **4**(11):891-899.

Bibliography

Gawlitzek M, Valley U, Wagner R. 1998. Ammonium ion and glucosamine dependent increases of oligosaccharide complexity in recombinant glycoproteins secreted from cultivated BHK-21 cells. *Biotechnol Bioeng.* **57**(5):518-528.

GEN. 2014. Biosimilars: 11 Drugs to Watch. The list. http://www.genengnews.com/insight-and-intelligenceand153/biosimilars-11-drugs-to-watch/77900135/: *Gen Eng News.*

Genzel Y, Ritter JB, Konig S, Alt R, Reichl U. 2005. Substitution of glutamine by pyruvate to reduce ammonia formation and growth inhibition of mammalian cells. *Biotechnol Progr.* **21**(1):58-69.

Gillies RJ, Verduzco D, Gatenby RA. 2012. Evolutionary dynamics of carcinogenesis and why targeted therapy does not work. *Nat Rev Cancer* **12**(7):487-493.

Gomord W, Chamberlain P, Jefferis R, Faye L. 2005. Biopharmaceutical production in plants: problems, solutions and opportunities. *Trends Biotechnol.* **23**(11):559-565.

Goodman M. 2009. Market watch: Sales of biologics to show robust growth through to 2013. *Nat Rev Drug Discov.* **8**(11):837-837.

Gordo I, Dionisio F. 2005. Nonequilibrium model for estimating parameters of deleterious mutations. *Phys Rev E.* **71**(3):4.

Gorfien SF, Paul W, Judd D, Tescione L, Jayme DW. 2003. Optimized nutrient additives for fed-batch cultures. *Biopharm international* **16**:34-41.

Goudar C, Biener R, Boisart C, Heidemann R, Piret J, de Graaf A, Konstantinov K. 2010. Metabolic flux analysis of CHO cells in perfusion culture by metabolite balancing and 2D C-13, H-1 COSY NMR spectroscopy. *Metab Eng.* **12**(2):138-149.

Greaves M, Maley CC. 2012. Clonal evolution in cancer. *Nature* **481**(7381):306-313.

Gresham D, Desai MM, Tucker CM, Jenq HT, Pai DA, Ward A, DeSevo CG, Botstein D, Dunham MJ. 2008. The Repertoire and Dynamics of Evolutionary Adaptations to Controlled Nutrient-Limited Environments in Yeast. *Plos Genetics.* **4**(12).

Ha M, Ng DWK, Li W-H, Chen ZJ. 2011. Coordinated histone modifications are associated with gene expression variation within and between species. *Genome Res.* **21**(4):590-598.

Hacker DL, De Jesus M, Wurm FM. 2009. 25 years of recombinant proteins from reactor-grown cells - Where do we go from here? *Biotechnol Adv.* **27**(6):1023-1027.

Hallatschek O, Hersen P, Ramanathan S, Nelson DR. 2007. Genetic drift at expanding frontiers promotes gene segregation. *Proc Natl Acad Sci USA.* **104**(50):19926-19930.

Hammill L, Welles J, Carson GR. 2000. The gel microdrop secretion assay: Identification of a low productivity subpopulation arising during the production of human antibody in CHO cells. *Cytotechnology.* **34**(1-2):27-37.

Heinrich C, Wolf T, Kropp C, Northoff S, Noll T. Growth characterization of CHO DP-12 cell lines with different high passage histories; 2011. *BMC Proc.* p P29.

Helleday T, Lo J, van Gent DC, Engelward BP. 2007. DNA double-strand break repair: From mechanistic understanding to cancer treatment. *DNA Repair.* **6**(7):923-935.

Henry O, Durocher Y. 2011. Enhanced glycoprotein production in HEK-293 cells expressing pyruvate carboxylase. *Metab Eng.* **13**(5):499-507.

Hiller A. 2009. Fast Growth Foreseen for Protein Therapeutics. *Genetic Engineering News.* **29**(1):18-18.

Hong JK, Cho SM, Yoon SK. 2010. Substitution of glutamine by glutamate enhances production and galactosylation of recombinant IgG in Chinese hamster ovary cells. *Appl Microbiol Biotechnol.* **88**(4):869-876.

Huang S. 2009. Non-genetic heterogeneity of cells in development: more than just noise. *Development* **136**(23):3853-3862.

.

Jackson AL, Loeb LA. 2001. The contribution of endogenous sources of DNA damage to the multiple mutations in cancer. *Mutat Res.* **477**(1-2):7-21.

Janke R, Genzel Y, Handel N, Wahl A, Reichl U. 2011. Metabolic Adaptation of MDCK Cells to Different Growth Conditions: Effects on Catalytic Activities of Central Metabolic Enzymes. *Biotechnol Bioeng.* **108**(11):2691-2704.

Jardon MA, Sattha B, Braasch K, Leung AO, Cote HCF, Butler M, Gorski SM, Piret JM. 2012. Inhibition of glutamine-dependent autophagy increases t-PA production in CHO Cell fed-batch processes. *Biotechnol Bioeng.* **109**(5):1228-1238.

Jastroch M, Divakaruni AS, Mookerjee S, Treberg JR, Brand MD. 2010. Mitochondrial proton and electron leaks. *Essays in Biochem.* **47**:53-67.

Jayapal KR, Wlaschin KF, Hu W-S, Yap MGS. 2007. Recombinant protein therapeutics from CHO cells - 20 years and counting. *Chem Eng Prog.* **103**(10):40-47.

Jeong DW, Kim TS, Lee JW, Kim KT, Kim HJ, Kim IH, Kim IY. 2001. Blocking of acidosis-mediated apoptosis by a reduction of lactate dehydrogenase activity through antisense mRNA expression. *Biochem Biophys Res Comm.* **289**(5):1141-1149.

Jones PA, Baylin SB. 2007. The epigenomics of cancer. *Cell.* **128**(4):683-692.

Jun SC, Kim MS, Hong HJ, Lee GM. 2006. Limitations to the development of humanized antibody producing Chinese hamster ovary cells using glutamine synthetase-mediated gene amplification. *Biotechnol Prog.* **22**(3):770-780.

Kaneko Y, Sato R, Aoyagi H. 2010. Evaluation of Chinese hamster ovary cell stability during repeated batch culture for large-scale antibody production. ***J Biosci Bioeng.*** **109**(3):274-280.

Kantardjieff A, Jacob NM, Yee JC, Epstein E, Kok Y-J, Philp R, Betenbaugh M, Hu W-S. 2010. Transcriptome and proteome analysis of Chinese hamster ovary cells under low temperature and butyrate treatment. *J Biotechnol.* **145**(2):143-159.

Khattak SF, Xing Z, Kenty B, Koyrakh I, Li ZJ. 2010. Feed Development for Fed-Batch CHO Production Process by Semisteady State Analysis. *Biotechnol Prog.* **26**(3):797-804.

Kim DY, Chaudhry MA, Kennard ML, Jardon MA, Braasch K, Dionne B, Butler M, Piret JM. 2013. Fed-batch CHO cell t-PA production and feed glutamine replacement to reduce ammonia production. *Biotechnol Prog.* **29**(1):165-175.

Kim HH, Joo H, Kim T, Kim E, Park SJ, Park JK, Kim HJ. 2009. The Mitochondrial Warburg Effect: A Cancer Enigma. *IBC* **1**:1-7.

Kim JW, Tchernyshyov I, Semenza GL, Dang CV. 2006. HIF-1-mediated expression of pyruvate dehydrogenase kinase: A metabolic switch required for cellular adaptation to hypoxia. *Cell Metabolism* **3**(3):177-185.

Kim NS, Kim SJ, Lee GM. 1998. Clonal variability within dihydrofolate reductase-mediated gene amplified Chinese hamster ovary cells: Stability in the absence of selective pressure. *Biotechnol Bioeng.* **60**(6):679-688.

Kim SH, Lee GM. 2007a. Differences in optimal pH and temperature for cell growth and antibody production between two Chinese hamster ovary clones derived from the same parental clone. *J Microbiol Biotechnol.* **17**(5):712-720.

Kim SH, Lee GM. 2007b. Down-regulation of lactate dehydrogenase-A by siRNAs for reduced lactic acid formation of Chinese hamster ovary cells producing thrombopoietin. *Appl Microbiol Biotechnol.* **74**(1):152-159.

Kim SH, Lee GM. 2007c. Functional expression of human pyruvate carboxylase for reduced lactic acid formation of Chinese hamster ovary cells (DG44). *Appl Microbiol Biotechnol.* **76**(3):659-665.

Kim T, Chung J, Sung Y, Lee G. 2001. Relationship between cell size and specific thrombopoietin productivity in chinese hamster ovary cells during dihydrofolate reductase-mediated gene amplification. *Biotechnol Bioprocess Eng.* **6**.

Klaunig JE, Kamendulis LM. 2004. The role of oxidative stress in carcinogenesis. *Annu Rev Pharmacol Toxicol.* **44**:239-267.

Bibliography

Klaunig JE, Kamendulis LM, Hocevar BA. 2010. Oxidative Stress and Oxidative Damage in Carcinogenesis. *Toxicol Pathol.* **38**(1):96-109.

Kokoszka JE, Coskun P, Esposito LA, Wallace DC. 2001. Increased mitochondrial oxidative stress in the Sod2 (+/-) mouse results in the age-related decline of mitochondrial function culminating in increased apoptosis. *Proc Natl Acad Sci USA.* **98**(5):2278-2283.

Koopman WJH, Distelmaier F, Smeitink JAM, Willems P. 2013. OXPHOS mutations and neurodegeneration. *Embo J.* **32**(1):9-29.

Kromenaker SJ, Srienc F. 1994. Stability of producer hybridoma cell lines after cell sorting: a case study. *Biotechnol Prog.* **10**(3):299-307.

Kumar S, McCarthy K, Francullo L, Crowe K, Heller-Harrison R, Wang W, Hiller G, Leonard M. A High Cell Density Approach to Fed-Batch Cell Culture for Production of Biopharmaceuticals; 2009; Dublin, Ireland, June 7-10, 2009. Springer. p 589-592.

Kurano N, Leist C, Messi F, Kurano S, Fiechter A. 1990. Growth-behavior of Chinese Hamster Ovary cells in a compact loop bioreactor. 2. Effects of medium components and waste products. *J Biotechnol.* **15**(1-2):113-128.

Kwaks THJ, Otte AP. 2006. Employing epigenetics to augment the expression of therapeutic proteins in mammalian cells. Trends in Biotechnology 24(3):137-142.

Kyriakopoulos S, Polizzi KM, Kontoravdi C. 2013. Comparative analysis of amino acid metabolism and transport in CHO variants with different levels of productivity. *J Biotechnol.* **168**(4):543-551.

Lai T, Yang Y, Ng SK. 2013. Advances in Mammalian cell line development technologies for recombinant protein production. *Pharmaceuticals (Basel)* **6**(5):579-603.

Laken HA, Leonard MW. 2001. Understanding and modulating apoptosis in industrial cell culture. *Curr Opin Biotechnol.* **12**(2):175-179.

Lange SS, Takata K, Wood RD. 2011. DNA polymerases and cancer. *Nat Rev Cancer.* **11**(2):96-110.

Lao MS, Toth D. 1997. Effects of ammonium and lactate on growth and metabolism of a recombinant Chinese hamster ovary cell culture. *Biotechnol Prog.* **13**(5):688-691.

Lauc G, Essafi A, Huffman JE, Hayward C, Knezevic A, Kattla JJ, Polasek O, Gornik O, Vitart V, Abrahams JL and others. 2010. Genomics Meets Glycomics-The First GWAS Study of Human N-Glycome Identifies HNF1 alpha as a Master Regulator of Plasma Protein Fucosylation. *Plos Genetics* **6**(12).

Leader B, Baca QJ, Golan DE. 2008. Protein therapeutics: A summary and pharmacological classification. *Nat Rev. Drug Discov.* **7**(1):21-39.

Lee YY, Yap MGS, Hu WS, Wong KTK. 2003. Low-glutamine fed-batch cultures of 293-HEK serum-free suspension cells for adenovirus production. *Biotechnol Prog.* **19**(2):501-509.

Legmann R, Melito J, Belzer I, Ferrick D. Analysis of glycolytic flux as a rapid screen to identify low lactate producing CHO cell lines with desirable monoclonal antibody yield and glycan profile; 2011. *BioMed Central Ltd.* p P94.

Lengauer C, Kinzler KW, Vogelstein B. 1998. Genetic instabilities in human cancers. *Nature.* **396**(6712):643-649.

Levine B. 2005. Eating oneself and uninvited guests: Autophagy-related pathways in cellular defense. *Cell* **120**(2):159-162.

Lewis NE, Liu X, Li Y, Nagarajan H, Yerganian G, O'Brien E, Bordbar A, Roth AM, Rosenbloom J, Bian C and others. 2013. Genomic landscapes of Chinese hamster ovary cell lines as revealed by the Cricetulus griseus draft genome. *Nat Biotechnol.* **31**(8):759-+.

Li F, Vijayasankaran N, Shen A, Kiss R, Amanullah A. 2010. Cell culture processes for monoclonal antibody production. *Mabs* **2**(5):466-479.

LifeTechnologies. 2007. FreeStyle™ CHO-S Cells [User Manual]. Manuals. http://tools.lifetechnologies.com/content/sfs/manuals/FreeStyle_CHO-S_Cells_man.pdf: *Invitrogen Corporationn.* p Catalog nos. R800-07.

Liu X, Liu J, Wright TW, Lee J, Lio P, Donahue-Hjelle L, Ravnikar P, F. W. 2010. Isolation of Novel High-Osmolarity Resistant CHO DG44 Cells After Suspension of DNA Mismatch Repair.: *BioProcess International.* p 68–76.

Loeb LA. 1989. Endogenous carcinogenesis: molecular oncology into the twenty-first century-presidential address. *Cancer Res.* **49**(20):5489-5496.

Loeb LA. 2001. A mutator phenotype in cancer. *Cancer Res.* **61**(8):3230-3239.

Lum JJ, Bauer DE, Kong M, Harris MH, Li C, Lindsten T, Thompson CB. 2005. Growth factor regulation of autophagy and cell survival in the absence of apoptosis. *Cell* **120**(2):237-248.

Luo J, Vijayasankaran N, Autsen J, Santuray R, Hudson T, Amanullah A, Li F. 2012. Comparative metabolite analysis to understand lactate metabolism shift in Chinese hamster ovary cell culture process. *Biotechnol Bioeng.* **109**(1):146-156.

Lyko F, Brown R. 2005. DNA methyltransferase inhibitors and the development of epigenetic cancer therapies. *J Natl Cancer Inst.* **97**(20):1498-1506.

Macheda ML, Rogers S, Best JD. 2005. Molecular and cellular regulation of glucose transporter (GLUT) proteins in cancer. *J Cell Physiol.* **202**(3):654-662.

Martinez VS, Dietmair S, Quek L-E, Hodson MP, Gray P, Nielsen LK. 2013. Flux balance analysis of CHO cells before and after a metabolic switch from lactate production to consumption. *Biotechnol Bioeng.* **110**(2):660-666.

Matasci M, Baldi L, Hacker DL, Wurm FM. 2011. The PiggyBac transposon enhances the frequency of CHO stable cell line generation and yields recombinant lines with superior productivity and stability. *Biotechnol Bioeng.* **108**(9):2141-2150.

Matasci M, Hacker DL, Baldi L, Wurm FM. 2008. Recombinant therapeutic protein production in cultivated mammalian cells: current status and future prospects. *Drug discovery today. Technologies* **5**(2-3):e37-42.

Maynard S, Schurman SH, Harboe C, de Souza-Pinto NC, Bohr VA. 2009. Base excision repair of oxidative DNA damage and association with cancer and aging. *Carcinogenesis.* **30**(1):2-10.

McGivan JD, Bungard CI. 2007. The transport of glutamine into mammalian cells. *Frontiers in Bioscience* **12**:874-882.

McKown RL. 2002. Development of biotechnology curriculum for the biomanufacturing industry. *J ISPE.* **22**(3):1-6.

Meleady P. 2007. Proteomic profiling of recombinant cells from large-scale mammalian cell culture processes. *Cytotechnology.* **53**(1-3):23-31.

Merlo LMF, Pepper JW, Reid BJ, Maley CC. 2006. Cancer as an evolutionary and ecological process. *Nat Rev Cancer* **6**(12):924-935.

Michor F. 2005. Chromosomal instability and human cancer. Philosophical Transactions of the Royal Society B-Biological Sciences 360(1455):631-635.

Miller EC. 1978. Some current perspectives on chemical carcinogenesis in humans and experimental animals: Presidential Address. *Cancer Res.* **38**(6):1479-1496.

Mulukutla BC, Gramer M, Hu WS. 2012. On metabolic shift to lactate consumption in fed-batch culture of mammalian cells. *Metab Eng.* **14**(2):138-149.

Negrini S, Gorgoulis V, Halazonetis T. 2010. Genomic instability - an evolving hallmark of cancer. *Nat Rev Mol Cell Biol.* **11**(3):220-228.

Nelson DL, Cox MM. 2013. Lehninger Principles of Biochemistry: W.H. Freeman.

Newell K, Franchi A, Pouyssegur J, Tannock I. 1993. Studies with glycolysis-deficient cells suggest that production of lactic acid is not the only cause of tumor acidity. *Proc Natl Acad Sci USA.* **90**(3):1127-1131.

Nicholls DG, Ferguson S. 2013. Bioenergetics: Elsevier Science. 419 p.

Nijsten MWN, van Dam GM. 2009. Hypothesis: Using the Warburg effect against cancer by reducing glucose and providing lactate. *Med Hypotheses.* **73**(1):48-51.

Nolan RP, Lee K. 2011. Dynamic model of CHO cell metabolism. *Metab Eng.* **13**(1):108-124.

Nowell PC. 1976. Clonal evolution of tumor-cell populations. *Science.* **194**(4260):23-28.

O'Callaghan PM, James DC. 2008. Systems biotechnology of mammalian cell factories. *Brief FuncT Genomic Proteomic.* **7**(2):95-110.

O'Callaghan PM, McLeod J, Pybus LP, Lovelady CS, Wilkinson SJ, Racher AJ, Porter A, James DC. 2010. Cell line-specific control of recombinant monoclonal antibody production by CHO cells. *Biotechnol Bioeng.* **106**(6):938-951.

Ozturk SS, Riley MR, Palsson BO. 1992. Effects of ammonia and lactate on hybridoma growth, metabolism, and antibody production. *Biotechnol Bioeng.* **39**(4):418-431.

Page MJ. 1988. Expression of foreign genes in Mammalian cells. *Methods Molr Biol.* **4**:371-84.

Papandreou I, Cairns RA, Fontana L, Lim AL, Denko NC. 2006. HIF-1 mediates adaptation to hypoxia by actively downregulating mitochondrial oxygen consumption. *Cell Metabolism* **3**(3):187-197.

Paques F, Haber JE. 1999. Multiple pathways of recombination induced by double-strand breaks in Saccharomyces cerevisiae. *Microbiol Mol Biol Rev.* 63(2):349-+.

Paredes C, Prats E, Cairo JJ, Azorin F, Cornudella L, Godia F. 1999. Modification of glucose and glutamine metabolism in hybridoma cells through metabolic engineering. *Cytotechnology* **30**(1-3):85-93.

Park HS, Kim IH, Kim IY, Kim KH, Kim HJ. 2000. Expression of carbamoyl phosphate synthetase I and ornithine transcarbamoylase genes in Chinese hamster ovary dhfr-cells decreases accumulation of ammonium ion in culture media. *J Biotechnol.* **81**(2-3):129-140.

Park KS, Jo I, Pak YK, Bae SW, Rhim H, Suh SH, Park SJ, Zhu MH, So I, Kim KW. 2002. FCCP depolarizes plasma membrane potential by activating proton and Na+ currents in bovine aortic endothelial cells. *Pflugers Arch.* **443**(3):344-352.

Pastwa E, Neumann RD, Mezhevaya K, Winters TA. 2003. Repair of radiation-induced DNA double-strand breaks is dependent upon radiation quality and the structural complexity of double-strand breaks. *Radiat Res.* **159**(2):251-261.

Pavelka N, Rancati G, Li R. 2010. Dr Jekyll and Mr Hyde: role of aneuploidy in cellular adaptation and cancer. *Curr Opin Cell Biol.* **22**(6):809-815.

Pelicano H, Carney D, Huang P. 2004. ROS stress in cancer cells and therapeutic implications. *Drug Resist Updat.* **7**(2):97-110.

Pilbrough W, Munro TP, Gray P. 2009. Intraclonal protein expression heterogeneity in recombinant CHO cells. *Plos One.* **4**(12):e8432.

Pochini L, Scalise M, Galluccio M, Indiveri C. 2014. Membrane transporters for the special amino acid glutamine: structure/function relationships and relevance to human health. *Frontiers in chemistry* **2**:61-61.

Polakova S, Blume C, Zarate J, Mentel M, Jorck-Ramberg D, Stenderup J, Piskur J. 2009. Formation of new chromosomes as a virulence mechanism in yeast Candida glabrata. *Proc Natl Acad Sci USA.* **106**(8):2688-2693.

Pray L. 2008. Eukaryotic genome complexity.: *Nat Edu.* p 96.

Prentice HL, Ehrenfels BN, Sisk WP. 2007. Improving performance of mammalian cells in fed-batch processes through "bioreactor evolution". *Biotechnol Prog.* **23**(2):458-464.

Pörtner R. 2007. Animal Cell Biotechnology: Methods and Protocols: Humana Press.

Qutub AA, Popel AS. 2008. Reactive oxygen species regulate hypoxia-inducible factor 1 alpha differentially in cancer and ischemia. *Mol Cell Biol.* **28**(16):5106-5119.

Redwan E-RM. 2007. Cumulative updating of approved biopharmaceuticals. *Human Antibodies.* **16**(3-4):137-158.

Reinhart D, Kaisermayer C, Damjanovic L, Kunert R. 2013. Benchmarking of commercially available CHO cell culture media for antibody production. *BMC Proc.* **7**(Suppl 6):13.

Rodriguez J, Spearman M, Huzel N, Butler M. 2005. Enhanced production of monomeric interferon-ss by CHO cells through the control of culture conditions. *Biotechnol Prog.* **21**(1):22-30.

Rose NR, McDonough MA, King ONF, Kawamura A, Schofield CJ. 2011. Inhibition of 2-oxoglutarate dependent oxygenases. *Chem Soc Rev.* **40**(8):4364-4397.

Ryall B, Eydallin G, Ferenci T. 2012. Culture History and Population Heterogeneity as Determinants of Bacterial Adaptation: the Adaptomics of a Single Environmental Transition. *Microbiol Mol Biol Rev.* **76**(3):597-625.

Sandoval J, Esteller M. 2012. Cancer epigenomics: beyond genomics. *Curr Opin Genet Dev.* **22**(1):50-55.

Schmitt MW, Venkatesan RN, Pillaire M-J, Hoffmann J-S, Sidorova JM, Loeb LA. 2010. Active Site Mutations in Mammalian DNA Polymerase delta Alter Accuracy and Replication Fork Progression. *J Biol Chem.* **285**(42):32264-32272.

Schofield MJ, Hsieh P. 2003. DNA mismatch repair: Molecular mechanisms and biological function. *Annual Rev Microb.* **57**:579-608.

Schumpp B, Schlaeger EJ. 1992. Growth study of lactate and ammonia double-resistant clones of HL-60 cells. *Cytotechnology.* **8**(1):39-44.

Selmecki A, Gerami-Nejad M, Paulson C, Forche A, Berman J. 2008. An isochromosome confers drug resistance in vivo by amplification of two genes, ERG11 and TAC1. *Mol Microbiol.* **68**(3):624-641.

Sengupta N, Rose ST, Morgan JA. 2011. Metabolic Flux Analysis of CHO Cell Metabolism in the Late Non-Growth Phase. *Biotechnol Bioeng.* **108**(1):82-92.

Shackleton M, Quintana E, Fearon ER, Morrison SJ. 2009. Heterogeneity in Cancer: Cancer Stem Cells versus Clonal Evolution. *Cell.* **138**(5):822-829.

Silander OK, Tenaillon O, Chao L. 2007. Understanding the evolutionary fate of finite populations: The dynamics of mutational effects. *Plos Biology* **5**(4):922-931.

Sinacore MS, Drapeau D, Adamson SR. 2000. Adaptation of mammalian cells to growth in serum-free media. *Mol Biotechnol.* **15**(3):249-257.

Singer B, Kusmierek JT. 1982. Chemical mutagenesis. *Annual Rev Biochem.* **51**:655-693.

Stich M, Manrubia SC, Lazaro E. 2010. Variable Mutation Rates as an Adaptive Strategy in Replicator Populations. *Plos One* **5**(6).

Stock C, Schwab A. 2009. Protons make tumor cells move like clockwork. Pflugers Archiv-European Journal of Physiology 458(5):981-992.

Sunley K, Tharmalingam T, Butler M. 2008. CHO cells adapted to hypothermic growth produce high yields of recombinant beta-interferon. *Biotechnol Prog.* **24**(4):898-906.

Susin SA, Lorenzo HK, Zamzami N, Marzo I, Snow BE, Brothers GM, Mangion J, Jacotot E, Costantini P, Loeffler M and others. 1999. Molecular characterization of mitochondrial apoptosis-inducing factor. *Nature* **397**(6718):441-446.

Takata M, Sasaki MS, Sonoda E, Morrison C, Hashimoto M, Utsumi H, Yamaguchi-Iwai Y, Shinohara A, Takeda S. 1998. Homologous recombination and non-homologous end-joining pathways of DNA double-strand break repair have overlapping roles in the maintenance of chromosomal integrity in vertebrate cells. *EMBO J.* **17**(18):5497-5508.

Tarhonskaya H, Rydzik AM, Leung IKH, Loik ND, Chan MC, Kawamura A, McCullagh JSO, Claridge TDW, Flashman E, Schofield CJ. 2014. Non-enzymatic chemistry enables 2-hydroxyglutarate-mediated activation of 2-oxoglutarate oxygenases. *Nat Commun.* **5**.

Bibliography

Thompson SL, Bakhoum SF, Compton DA. 2010. Mechanisms of Chromosomal Instability. *Curr Biol.* **20**(6):R285-R295.

Tjio JH, Puck TT. 1958. Genetics of somatic mammalian cells. II. Chromosomal constitution of cells in tissue culture. *J Exp Med.* **108**(2):259-268.

Torsvik A, Stieber D, Enger PO, Golebiewska A, Molven A, Svendsen A, Westermark B, Niclou SP, Olsen TK, Chekenya Enger M and others. 2014. U-251 revisited: genetic drift and phenotypic consequences of long-term cultures of glioblastoma cells. *Cancer Med.* **3**(4):812-824.

Tsao YS, Cardoso AG, Condon RGG, Voloch M, Lio P, Lagos JC, Kearns BG, Liu Z. 2005. Monitoring Chinese hamster ovary cell culture by the analysis of glucose and lactate metabolism. *J Biotechnol.* **118**(3):316-327.

Underwood PA, Bean PA. 1988. Hazards of the limiting-dilution method of cloning hybridomas. *J Immunol Methods.* **107**(1):119-128.

Valko M, Leibfritz D, Moncol J, Cronin MTD, Mazur M, Telser J. 2007. Free radicals and antioxidants in normal physiological functions and human disease. *Int J Biochem Cell Biol.* **39**(1):44-84.

van Berkel PHC, Gerritsen J, Perdok G, Valbjorn J, Vink T, van de Winkel JGJ, Parren PWHI. 2009. N-linked glycosylation is an important parameter for optimal selection of cell lines producing biopharmaceuticalhuman IgG. *Biotechnol Prog.* **25**(1):244-251.

van der Valk J, Brunner D, De Smet K, Svenningsen AF, Honegger P, Knudsen LE, Lindl T, Noraberg J, Price A, Scarino ML and others. 2010. Optimization of chemically defined cell culture media - Replacing fetal bovine serum in mammalian in vitro methods. *Toxicol Vitro.* **24**(4):1053-1063.

Vander Heiden MG, Cantley LC, Thompson CB. 2009. Understanding the Warburg effect: the metabolic requirements of cell proliferation. *Science* **324**(5930):1029-33.

Vander Heiden MG, Chandel NS, Li XX, Schumacker PT, Colombini M, Thompson CB. 2000. Outer mitochondrial membrane permeability can regulate coupled respiration and cell survival. *Proc Natl Acad Sci USA.* **97**(9):4666-4671.

Venkatesan RN, Bielas JH, Loeb LA. 2006. Generation of mutator mutants during carcinogenesis. *DNA Repair* **5**(3):294-302.

Vives J, Juanola S, Cairo JJ, Godia F. 2003. Metabolic engineering of apoptosis in cultured animal cells: implications for the biotechnology industry. *Metab Eng.* **5**(2):124-132.

Vogtle FN, Burkhart JM, Rao S, Gerbeth C, Hinrichs J, Martinou JC, Chacinska A, Sickmann A, Zahedi RP, Meisinger C. 2012. Intermembrane Space Proteome of Yeast Mitochondria. *Mol Cell Proteomics* **11**(12):1840-1852.

Walsh G. 2004. Second-generation biopharmaceuticals. *Eur J Pharm Biopharm.* **58**(2):185-196.

Walsh G. 2010a. Biopharmaceutical benchmarks 2010. *Nat Biotechnol.* **28**(9):917-924.

Walsh G. 2010b. Post-translational modifications of protein biopharmaceuticals. Drug Discovery Today 15(17-18):773-780.

Walsh G. 2014. Biopharmaceutical benchmarks 2014. *Nat biotechnol.* **32**(10):992-1000.

Walsh G, Jefferis R. 2006. Post-translational modifications in the context of therapeutic proteins. *Nat Biotechnol.* **24**(10):1241-1252.

Warburg O. 1956. On the origin of cancer cells. *Science* **123**(3191):309-314.

Webb BA, Chimenti M, Jacobson MP, Barber DL. 2011. Dysregulated pH: a perfect storm for cancer progression. *Nat Rev Cancer* **11**(9):671-677.

Webster DE, Thomas MC. 2012. Post-translational modification of plant-made foreign proteins; glycosylation and beyond. *Biotechnol Adv.* **30**(2):410-418.

Wilkens CA, Gerdtzen ZP. 2011. Engineering CHO cells for improved central carbon and energy metabolism. *BMC Proc.* **5**(8):120.

Wippermann A, Klausing S, Rupp O, Albaum SP, Buentemeyer H, Noll T, Hoffrogge R. 2014. Establishment of a CpG island microarray for analyses of genome-wide DNA methylation in Chinese hamster ovary cells. *Appl Microbiol Biotechnol.* **98**(2):579-589.

Wise DR, Thompson CB. 2010. Glutamine addiction: a new therapeutic target in cancer. *Trends Biochem Sci,* **35**(8):427-433.

Wlaschin KF, Hu WS. 2007. Engineering cell metabolism for high-density cell culture via manipulation of sugar transport. *J Biotechnol.* Netherlands. p 168-76.

Wong CH. 2005. Protein glycosylation: New challenges and opportunities. *J Org Chem.* **70**(11):4219-4225.

Wong DCF, Wong KTK, Goh LT, Heng CK, Yap MGS. 2005. Impact of dynamic online fed-batch strategies on metabolism, productivity and N-glycosylation quality in CHO cell cultures. *Biotechnol Bioeng.* **89**(2):164-177.

Worton RG, Ho CC, Duff C. 1977. Chromosome stability in CHO cells. *Somatic Cell Genet.* **3**(1):27-45.

Wuest DM, Harcum SW, Lee KH. 2012. Genomics in mammalian cell culture bioprocessing. *Biotechnol Adv.* **30**(3):629-638.

Wurm FM. 2004. Production of recombinant protein therapeutics in cultivated mammalian cells. *Nat Biotechnol.* **22**(11):1393-1398.

Wurm FM. 2013. CHO Quasispecies -Implications for Manufacturing Processes. *Processes* **1**(3):296-311.
.

Xing ZZ, Kenty BN, Li ZJ, Lee SS. 2009. Scale-Up Analysis for a CHO Cell Culture Process in Large-Scale Bioreactors. *Biotechnol Bioeng.* **103**(4):733-746.

Xu X, Nagarajan H, Lewis N, Pan S, Cai Z, Liu X, Chen W, Xie M, Wang W, Hammond S and others. 2011. The genomic sequence of the Chinese hamster ovary (CHO)-K1 cell line. *Nat Biotechnol.* **29**(8):735-U131.

Yang M, Butler M. 2000. Effects of ammonia on CHO cell growth, erythropoietin production, and glycosylation. *Biotechnol Bioeng.* **68**(4):370-380.

Yoon SK, Hwang SO, Lee GM. 2004. Enhancing effect of low culture temperature on specific antibody productivity of recombinant Chinese hamster ovary cells: Clonal variation. *Biotechnol Prog.* **20**(6):1683-1688.

Yoshikawa T, Nakanishi F, Itami S, Kameoka D, Omasa T, Katakura Y, Kishimoto M, Suga K. 2000. Evaluation of stable and highly productive gene amplified CHO cell line based on the location of amplified genes. *Cytotechnology.* **33**(1-3):37-46.

Young JD. 2013. Metabolic flux rewiring in mammalian cell cultures. *Curr Opin Biotechnol.* **24**(6):1108-1115.

Zagari F, Jordan M, Stettler M, Broly H, Wurm FM. 2013. Lactate metabolism shift in CHO cell culture: the role of mitochondrial oxidative activity. *New Biotechnology* **30**(2):238-245.

Zamorano F, Wouwer AV, Bastin G. 2010. A detailed metabolic flux analysis of an underdetermined network of CHO cells. *J. Biotechnol.* **150**(4):497-508.

Zhang JY, Robinson D. 2005. Development of animal-free, protein-free and chemically-defined media for NSO cell culture. *Cytotechnology* **48**(1-3):59-74.

Zhang L, Shen H, Zhang YX. 2004. Fed-batch culture of hybridoma cells in serum-free medium using an optimized feeding strategy. *J Chem Technol Biotechnol.* **79**(2):171-181.

Zhao Y, Butler E, Tan M. 2013. Targeting cellular metabolism to improve cancer therapeutics. *Cell Death Dis.* **4**:e532.

Zhou BBS, Elledge SJ. 2000. The DNA damage response: putting checkpoints in perspective. *Nature.* **408**(6811):433-439.

Zhou M, Crawford Y, Ng D, Tung J, Pynn AFJ, Meier A, Yuk IH, Vijayasankaran N, Leach K, Joly J and others. 2011. Decreasing lactate level and increasing antibody production in Chinese Hamster Ovary cells (CHO) by reducing the

expression of lactate dehydrogenase and pyruvate dehydrogenase kinases. *J Biotechnol.* **153**(1-2):27-34.

Zhu MM, Goyal A, Rank DL, Gupta SK, Boom TV, Lee SS. 2005. Effects of Elevated pCO2 and Osmolality on Growth of CHO Cells and Production of Antibody-Fusion Protein B1: A Case Study. *Biotechnol Prog.* **21**(1):70-77.